Identification and characterization of genetic markers and metabolic pathways controlling net feed efficiency in beef cattle

Presented by

Madan Bhaskar Naik

01/09/2008

A thesis submitted in partial fulfilment of the award
of Ph.D. in the Discipline of Agriculture and Animal Science
at
The University of Adelaide, Australia

TABLE OF CONTENTS

ABSTRACT

Net feed intake or residual feed intake is the feed intake of an animal after adjustment for its average weight and weight gain while on the feed test. High net feed efficiency (NFE) animals have a low net feed intake, so the aim is to select animals that have high net feed efficiency in order to reduce the 70% expenditure for feed costs. Thus far, very few studies have been undertaken on beef cattle to identify genetic markers for NFE and to understand the molecular genetics of feed intake regulation and energy balance. Therefore, in an attempt to identify genes and metabolic pathways controlling feed efficiency in beef cattle, three different experimental approaches were taken herein: a) linkage and linkage disequilibrium quantitative trait loci (QTL) mapping for net feed intake in Limousin x Jersey animals, b) mitochondrial oxidative phosphorylation enzyme assays in high and low NFE cattle, and c) 2-dimensional fluorescent gel electrophoresis (DIGE) proteomics analysis of mitochondrial proteins.

For the cattle QTL mapping, the results from a previous trial were utilized. In the trial, a double back-cross design was employed using two extremely divergent *Bos taurus* breeds [Jersey (J) dairy breed and Limousin (L) beef breed]. These breeds are known to differ in many traits including carcass composition, fat colour, marbling, body size, and meat tenderness. Three first cross (F1=X) sires were mated to pure Jersey or pure Limousin cows, creating in total 366 XJ and XL backcross progeny (range 120-156 progeny per sire). The amount of feed consumed each day during the 70-100 day test was recorded electronically for each animal. Feed intake data were processed by calculating the least-square means for each animal over the test period. The data for net feed intake were analysed using a QTL half-sib interval-mapping model. The interval linkage analysis of whole genome detected six suggestive QTL (BTA 1, 6, 8, 9, 16, and 20) segregating for NFE. Of these 6 QTL, 4 NFE QTL (BTA 1, 6, 16, and 20) were homeologous to QTL for NFE observed in full-sib F2 families of mouse selection lines (Fenton 2004). After the NFE data were re-analysed for outliers, a QTL on BTA11 was re-ranked and placed in the top 4 NFE QTL in terms of size of effect and statistical support, whereas the QTL on BTA 6 and BTA 16 had less support. Since the QTL on BTA 9 was not independent of growth, only 4 QTL (BTA 1, 8, 11 and 20) were targeted for further study herein. These NFE QTL were cross-validated in Angus NFE selection line animals in collaboration with

Department of Primary Industries (DPI), Victoria by microsatellite linkage mapping. Two of the QTL on BTA 8 and 20 were confirmed and three other minor QTL on BTA 1, 11, and 20 were detected in the Angus animals.

Based on this background information, a comparative genome mapping study was undertaken to identify candidate genes. Using the human and bovine genome Ensembl databases, 205 NFE candidate genes underlying the 4 major QTL regions (BTA 1, 8, 11, and 20) were identified and 61 were sequenced in the mapping F1 Limousin x Jersey mapping sires. In these 61 genes, 308 SNPs were discovered, of which 27 were potentially functional SNPs changing the amino acids. 84 SNPs were selected for genotyping and used for fine mapping the 4 QTL and for SNP association studies with NFE. From the positions of the analyses, the 4 NFE QTL were refined and 27 candidate SNPs in 20 genes showed strong association with NFE in the Limousin x Jersey animals.

A ParAllele whole genome scan with a bovine 10K SNP chip was also performed on a subset of the Angus NFE selection line animals by DPI Victoria. 100 ParAllele SNPs had significant association with NFE in the Angus selection line animals. These ParAllele SNPs were tested in the Limousin x Jersey animals and 16 ParAllele SNPs were significantly associated with NFE. Four of these SNPs were located in the NFE QTL on BTA 1, 11 and 20.

Based on the candidate genes underlying the 4 NFE QTL, 8 potential metabolic pathways contributing to NFE were identified. These metabolic pathways included mitochondrial oxidative phosphorylation and glucose turnover. Therefore, to determine if these specific pathways are indeed involved in net feed efficiency, oxidative phosphorylation enzyme assays and mitochondrial protein profiling were conducted on progeny from the Angus Trangie NFE selection line animals. Liver and skeletal muscle samples were obtained from extreme high and low NFE animals with an average phenotypic difference of 3 kg net feed intake per day.

Using these liver and muscle samples, mitochondria were prepared and assessed. The mitochondrial preparations were assayed for enzyme activity of 3 complexes (Complex I, II and IV) involved in oxidative phosphorylation. The enzyme activities were measured spectrophotometrically and analysed by regression analysis. The

activity of the liver mitochondrial Complex I was found to be significantly decreased in the high NFE animals compared to the low NFE animals ($p<0.0001$). The Complex II and IV activities were increased in the high NFE cattle, but the differences were not statistically significant.

Using the mitochondrial preparations, 2-D polyacrylamide gel electrophoresis differential gel electrophoresis (2-D PAGE DIGE) was used to generate a mitochondrial protein profile for the high and low NFE Angus cattle. An ontological analysis based on the differentially expressed proteins (>1.5 fold difference) in the high *vs.* low NFE cattle unambiguously identified a total of 27 proteins in 6 physiologically different groups. The mitochondria proteomics results also confirmed the involvement of oxidative phosphorylation in net feed intake regulation. Eleven oxidative phosphorylation complex subunit proteins were found to be differentially expressed between the high and low NFE animals. Other differentially expressed proteins included six stress-related proteins, seven energy production and glucose turnover proteins, two protein turnover and nitrogen balance enzymes, and two proteins involved in mitochondrial DNA and protein biosynthesis. Four of the differentially expressed proteins were found in the NFE QTL regions.

The results of these experiments provide a better understanding of the relationship between variation in feed efficiency and cellular energy production mechanisms in beef cattle. The proteomics and mitochondrial enzyme assay results suggest that energy metabolism and homeostasis may not be an efficient process in low NFE cattle. Lastly, a set of candidate SNPs are now available for the further validation as markers for selection of NFE in cattle breeding programs.

LIST of TABLES

List of Figures

List of figures (continuation)

List of figures (continuation)

APPENDIX

List of Tables in appendix

List of Figures in appendix

ABBREVIATIONS

ß-LPH	lipotropin beta
℃	degree celcius
2D	2-dimensional
2-D DIGE	2-D differential gel electrophoresis
5-HT	5-hydroxytryptamine
AA1	aspartate aminotransferase 1
ACAD	acyl-CoA dehydrogenase
ACTH	adrenocorticotrophin
ADG	average daily gain
ADP	adenosine diphosphate
AGTR1	angiotensin receptor 1
AHSG	alpha-HS-glycoprotein
AMPK	adenine monoposphate-activated protein kinase
ANOVA.	analysis of variance
ANT	adenine nucleotide translocators
APS	ammonium persulphate
ASS	argininosuccinate synthase
AST	aspartate aminotransferase
ATP	adenosine triphosphate
Bc1	bovine mitochondrial cytochrome 1
BLASTN	bovine Ensembl genome nucleotide sequence using the basic local alignment search tool
bp	base pairs
BVA	biological variation analysis
C1-THF synthase	C-1-tetrahydrofolate synthase C
CART	cocaine- and amphetamine-regulated transcript protein precursor
CAT	carnitine palmitoyltransferase isoenzyme
cDNA	complementary deoxyribonucleic acid

CHAPS	3-[(3-cholamidopropyl)dimethylammonio]-2-hydroxy-1-propanesulfonate
cM	centiMorgan
CoA	coenzyme A
COX	cytochrome c oxidase
CPT	carnitine palmitoyltransferase isoenzyme
CSF	cerebrospinal fluid
CTSB	cathepsin B
Cy	cyanine dyes
D(3)	dopamine receptor 3
DB	decylubiquinone
DCIP	dichloroindophenol
DFI	daily feed intake
DIA	data image analysis
DMF	dimethylformamide
DNA	deoxyriboneuclic acid
dNTP	deoxyribonucleotide triphosphate
DTNB	5'- dithiobis-2-nitrobenzoic acid
DTT	dithiothreiotol
EBV	estimated breeding value
EDTA	ethyl diamine tetracetic acid
EMA	eye muscle area
ERK	extracellular signal-regulated kinases
ES	eating sessions
ET	eating time
ExPASY	expert protein analysis system
$FADH_2$	flavin adenine dinucleotide (reduced)
FP	fluorescence polarization
FSHR	follicle stimulating hormone receptor
FST	follistatin precursor

g	gram
GABA	g-aminobutyrate
GDH1	glutamate dehydrogenase1
GDP	guanosine di-phosphate
GH	growth hormone
GHF	growth hormone factor
GHR	growth hormone receptor
GLUT	glucose transporter
GSH	conjugate glutathione
GSTs	glutathione-s-transferases
GTP	guanosine tri-phosphate
HBP	hexosamine biosynthesis pathway
HCCA	α-cyano-4-hydroxycinnamic acid
HSA	human chromosome
HSCW	hot carcass weight
HTR	hydroxytryptamine receptor
ICAT	isotope coded affinity tag technique
IEF	isoeletric focusing
IGF	Insulin like growth factor
IL1 beta	interleukin 1 beta
IL12A	interleukin 12 A
IMF	intra-muscular fat
IMVS	Institute of Medical and Veterinary Science
IPG	immobilized pH gradient
IRS	insulin receptor substrate
JAK	janus activated kinase
KCN	potassium cyanide
kDa	kiloDalton
kg	kilogram

KH_2PO_4	potassium phosphate monobasic
KSP	kidney-specific protein partial
LCFA	long chain fatty acid
LOD	log of odds
LPL	lipoprotein lipase
m	mass
MALDI	matrix-assisted laser desorption / ionisation
MALDI-TOF	matrix-assisted laser desorption/ionization-time of flight
MAP	microtubule-associated protein -1B
MAPK	ras-mitogen-activated protein kinase
MAS	marker assisted selection
Mb	megabase
$MgSO_4$	magnesium sulphate
ml	millilitre
MMWT	metabolic body weight
MOWSE	molecular weight search
mP	millipolarisation
MPCK	mitochondrial phosphoenolpyruvate carboxykinase
MS	mass spectrometry
mtDNA-	mitochondrial DNA
mTOR	mammalian target of rapamycin
MW	molecular weight
NAD^+	nicotinamide adenine dinucleotide (oxidised)
NADH	nicotinamide adenine dinucleotide phosphate (reduced)
NaOH	sodium hydroxide
NCBI	National Center for Biotechnology Information
NFE	net feed efficiency
NFI	net feed intake

ng	nanogram
nmol/mg/min	nanomoles / milligram / minute
NSW	New South Wales
NTS	nucleus tractus solitarius
NZ	New Zealand
O_2^-	molecular oxygen
OD	optical density
Oligo	oligonucleotide
OMIM	Online Mendelian Inheritance in Man
OSCP	oligomycin sensitivity-conferring protein
OX-PHOS	oxidative phosphorylation
PAGE	polyacrylamide gel electrophoresis
PCR	polymerase chain reaction
PEPCK2	phosphoenolpyruvate carboxykinase 2 isoform 1 precursor isoform
PGC-1α	peroxisome proliferator-activated receptor-gamma coactivator-1
PI	Phosphatidylinositol
pI	isoelectric point
PIK3R1	phosphatidylinositol 3-kinase P-85 -alpha subunit
Pit-1	pituitary-specific positive transcription factor 1
PMSF	phenyl methyl sulfonyl fluoride
PNOC	nociceptin
POMC	pro-opiomelanocortin
POUF	growth hormone secretagogue receptor type
PPARα	peroxisome proliferator-activated receptor-alpha
ppm	parts per million
PRKAA1	5'-AMP-activated protein kinase- alpha 1
PRL	prolactin

PRLR	prolactin receptor precursor
QTL	quantitative trait loci
RCR	respiratory control ratio
RNA	ribonucleic acid
ROS	reactive oxygen species
SD	standard deviations
SE	standard error
SDS-PAGE	sodium dodecyl sulphate–polyacrylamide gel
SELDI-TOF	surface-enhanced laser desorption/ionization-time of flight
SHB	Src homology 2 domain containing
SLC2A2	glucose transporter 2
SNP	single nucleotide polymorphism
SST	somatostatin precursor
STAT	signal transducer and activator of transcription
TAMRA	tetramethyl-6-carboxyrhodamine
TCA	tricarboxylic acid
TDI-FP	template-directed dye-terminator incorporation with fluorescence polarization detection
TE	Tris-ethyline di-amine tetra-acetic acid
TEK	tyrosine kinase
TEMED	N,N,N',N'-tetramethylethanediamine
TFA	trifluoroacetic acid
TGF	transforming growth factor
Tm	melting temperature
TNF	tumor necrosis factor
TOF	time-of-flight
TRIS-HCl	TRIS hydrochloride
tRNA	transfer RNA
UMPS	uridine monophosphate synthetase

USDA	United States Department of Agriculture
UTR	untranslated region
UV	ultra violate
V-ATPase	vacuolar ATP synthase
VLDL	very low-density lipoprotein
z	charge
µL	microliter
pmol	picomole

DECLARATION

I certify that this thesis contains no material which has been accepted for the award of any other degree or diploma in any university or other tertiary institution and, to the best of my knowledge and belief, contains no material previously published or written by another person, except where due reference has been made in the text. I give consent to this copy of my thesis, when published in the University Library, being available for loan and photocopying.

Madan B Naik
1/09/2008

DEDICATION

To my respected parents specially Papa, loving wife, Chitra, Kalpana mavshi, Aai, Guru Datta

and

all "true" scientists who never been recognised for their research.

ACKNOWLEDGMENTS

First of all, I sincerely would like to thank to my supervisor Professor Cynthia Bottema for offering PhD scholarship, her technical guidance, offering exposure to local and international scientific community and tremendous support throughout my candidature. I really appreciated for her patience, painstaking efforts and time spent to check my thesis meticulously, which helped me to learn technical scientific writing. I also admire for her quick problem-solving nature, and lively and caring approach towards every student which helps to develop a secure and comfortable environment while working in the laboratory. I am glad to mention that she fulfilled my definition of 'the ideal supervisor, administrator and teacher' criteria, which I was seeking before starting my doctorate program.

I would also like to thank my co-supervisor Dr Wayne Pitchford for his help in analysing statistical data and valuable suggestions in thesis proof-reading. My doctorate research and scholarship was fully supported by Co-operative Research Centre for Beef and Cattle Quality of Australia, without whom my doctorate research was not possible. My sincere thanks to different organisations for providing international travel scholarships during my candidature including the Welcome-Unilever Trust for attending Days of Molecular Medicine conference in Cambridge, 2004; the International Society of Animal Genetics for attending the 2004 ISAG conference at Tokyo, Japan and the Australian Federation of University Women for attending the ISAG 2006 in Brazil.

This large research project was made possible because of technical assistance from many different people. I would like extend my sincere thanks to Bozena Kruk for her great help in the genotyping and DNA sequencing; Dr Zibby Kruk for his huge help in organising sample collection from abattoir; Dr Scott Foster for generating the marker linkage map with CRI-MAP and assisting in fine mapping data analysis; Arthur Mangos and team at the DNA Sequencing Centre, Institute of Medical and Veterinary Science (IMVS) for the DNA sequencing, Dr Mike Goddard and his research team (Dannielle Hulett, Helen McPartlan, Dr Ben Hays and Lakshmi Krishnan) from the Department of Primary Industries, Victoria for the genotyping using SNPlex technology, providing the Angus QTL and SNP whole genome scan data, the cross-validation of our SNP data on their Angus animals; and Dr Chris Bagley and Dr Megan Retallick, Proteomics Facility, Molecular Biosciences for helping to conduct

the proteomics experiments. Special thanks is extended to Dr Chris Bagley for resolving my technical queries and advice on conducting proteomic experiments.

Besides this, I am also thankful to Andrew Egarr (for his help in thesis formatting), Dr Brian Siebert, Dr Graham Webb and the doctorate students Rugang Tian, Lei Chang, Ali Koshkoih for lovely discussions.

My special thanks to Lawrence Burk for in depth technical discussions on aeronautical & automobile engineering, remote sensing and international politics which made my stay comfortable in Roseworthy campus. My cosy stay in Roseworthy Campus would not be possible without mentioning the names of Lesley Menzel, Pat Sheean, Jane Copland, and especially for Audrey Stratton for making the taxi service available to all Roseworthy residents.

I am highly indebted to Aai, Kalpana mavshi, Mr Nandakumar Pottdar, Padmaja Pottdar, and Nagesh Pednekar for their special contribution in my life. I am also very much grateful to Professor Jogdeo for his contribution in introducing logic and analytical thinking into my life. I am particularly thankful for answering all my basic fundamental mathematical queries and clarifying all the mathematical formulas and their applications in everyday life in the context to statistics. I shall always appreciate the continuous showering of valuable technical knowledge. His passion for mathematics and statistics always inspired me and he is another professor in my "*ideal professor* "list.

I am also sincerely thankful to Varsha Pawar, Minal Pednekar, Lalita Mavshi, all Kaka's and other Mavshi's and Naik family (Swati, Neela, Lata, Sanjay, and Tai) for unconditional support, love, and encouragements throughout my life.

For my whole life, I will always be obligation to my parents, specially to my father, for their support from all directions during my education; I do not have any words that can express my gratitude.

Finally, of course my very special thanks to my loving wife, Chitra, who always ensures I receive special intensive cosy care. I also appreciate her great help in

thesis table preparation, reference checking and formatting. Your best food recipes, discussing medical cases, and your care are truly amazing.

Chapter 1
Introduction and review of literature

1.1 Introduction

The cost of feed is considered the most important variable in commercial animal farming operations and has significant economic implications on the profitability of beef production. The majority of farming expenditure goes towards feed costs. A mature animal uses 70-75% of the energy received from feed to maintain total body mass. The remainder of the energy is used for production, including growth, pregnancy, and lactation (Gregory, 1972; Montano-Bermudez *et al* 1990; Johnston, 2002). Maintenance energy can be defined as the energy required to sustain an animal's tissues without changes in body mass (Evan, 2001). Reducing the maintenance energy of animals will make the herd more efficient, and therefore, has the potential to increase profitability due to lower feed requirements. Koch (Koch *et al* 1963) introduced the term residual feed intake (RFI) in the context of selecting animals with lower requirements for maintenance energy. RFI is the difference between actual feed intake and expected feed intake for the maintenance of body weight. RFI is also referred to as net feed intake (NFI) and is phenotypically independent of body weight and gain. Residual feed intake, hence, acts as a measure of net feed efficiency (NFE). The net feed efficiency of an animal depends on the ability of the animal to consume less feed per kg weight gain by improving the utilisation of nutrients and energy from the feed for maintenance and growth. Net feed efficiency is opposite in sign, but equal in magnitude to net feed intake, such that animals with low net feed intake are said to have high net feed efficiency.

A 5% improvement in net feed efficiency could have an economic impact four times greater than a 5% improvement in average daily gain (Basarab, 2002). After recognising the potential of reducing feed costs by measuring NFI, substantial progress have been made in the poultry, pig, cattle and sheep industries to address NFE as a trait because the cost of feed and accurate feed measurements are easily quantified. Archer *et al* (1999) have shown that selection for net feed efficiency provides an opportunity to significantly reduce feed costs in cattle breeding programs. Many other studies have come to the same conclusion (Koch *et al* 1967; Herd *et al* 1997; Archer *et al* 1998, 1999; Arthur *et al* 2001a; Johnston, 2002; Arthur *et al* 2004).

1.2 Evidence of variation in maintenance energy requirements of cattle

In cattle, maintenance energy requirements vary with body weight, breed, sex, age, season, temperature, physiological state, and nutrition. Armsby and Fries (1911) reported the first comparison between beef cattle for energy efficiency. They found that "scrub" steers utilised energy less efficiently than "good" beef animals. Koch *et al* (1963) found that the differences in both weight maintained and weight gained affected the feed requirements in growing cattle. Reports on the nutritional requirements of beef cattle by the USA National Research Council (updated in 2000) included research studies showing differences in energy requirements or efficiency of energy utilisation among several breeds of

Bos taurus cattle between the period of 1970-1990. These studies also included a comparison of maintenance energy requirements between *Bos taurus* and *Bos indicus* cattle, which revealed that *Bos indicus* cattle are 10% more efficient in terms of maintenance energy requirements.

The compiled results from last ten years of Beef CRC projects conducted in Australia by Arthur *et al* (2004) also demonstrated variation in feed utilisation efficiency. Direct comparisons between the studies are difficult because of the differences in methods and breed diversity. However, these studies on the differences in maintenance energy between and within cattle breeds serve to document that considerable variation exists.

1.3 Net feed efficiency as a genetic trait

There is now considerable evidence that net feed efficiency in cattle, pigs, poultry and mice is moderately heritable (0.08-0.44) (Table 1.1) (Arthur *et al* 2001b, 2001c, 2001d, 2004; Basarab 2002; Herd *et al* 2003; Robinson and Oddy, 2004, Pitchford, 2004). In beef cattle, heritability estimates for NFE range from 0.14 (± 0.12) to 0.41 (± 0.07) (Archer *et al* 1997; Fan *et al* 1997) (Table 1.1). Given the genetic variation in net feed intake, there is scope to improve net feed efficiency by genetic selection using NFI as a measure. The research suggests that the reducing cost of beef production through genetic selection of high NFE animals should be possible by decreasing feed intake without affecting growth performance (Arthur *et al* 2004).

However, Archer *et al* (1999) raised concerns about the heritability estimates of NFE based on phenotypic regression in cattle. Korver *et al* (1991), Jensen *et al* (1992) and Fan *et al* (1995) also reported contradictory genetic correlations between phenotypic NFE with production traits in cattle. Korver *et al* (1991) found no genetic correlations between NFE with growth rate (r = -0.08) or with body weight (r = 0.03). However, Jensen *et al* (1992) found a genetic correlation of 0.32 between NFE and average daily gain, and Fan *et al* (1995) reported NFE was genetically and phenotypically correlated with production traits, such as growth rate and fertility.

These discrepancies are partly due to the difficulty and expense of measuring feed intake on sufficient numbers of cattle to estimate the genetic variation accurately in a given breed. The discrepancies in the genetic NFE estimates from different studies can be a result of the limited data, which leads to biased heritability and correlation estimates. Therefore, it is very difficult to predict the true magnitude of the genetic correlations of NFE with other traits in beef cattle.

Few heritability estimates have been determined for maintenance energy requirements. Those for weight and energy equilibrium have been high (.71 to 39) (Taylor *et al* 1986; Carstens *et al* 1987b; Hotovy *et al* 1991). Hotovy *et al* 1991 measured the genetic variation in maintainance energy expenditures between and within identical twin pairs of beef cattle. Variation within twin pairs was less than the variation between pairs *($p < .05$)* for maintenance requirements and fasting heat production *($p < .005$)*, suggesting the presence of strong genetic component for NFE in beef cattle. This result is in agreement with Carstens et al. (1987b), who discussed the advantage of using monozygous twins for measurement of maintenance heat production due to the significant twin pair effect for NFE. Selection of individuals in a beef herd with a desired level of heat production appears to be possible, assuming that there is an additive component to the measured genetic variance. Selection of cows with lower energy expenditures below or near maintenance could decrease total feed costs in the herd and (or) decrease a cow's susceptibility to nutritional and other environmental stresses.

NFE calculated from genotypic regression is genetically independent of production (growth, body weight and lactation) and therefore, would be a better indicator of genetic variation of net feed efficiency rather than phenotypic regression. However, there are no published data for net feed intake calculated from genotypic regression.

There is even less certainty about existence of genetic variation in the efficiency of lactating cattle. Heritability estimates for NFE in dairy cattle range from 0.36 (± 0.17) (Jakobsen *et al* 2000), 0.22 (± 0.11) (Korver *et al* 1991), 0.19 (± 0.12) (van Arendonk *et al* 1991), 0.16 (Ngwerume and Mao 1992), 0.05 (Veerkamp *et al* 1995) to 0.0 (Svendsen *et al* 1993) (Table 1.1).

In other species, the ranges are similar. In poultry, there are estimates of 0.12 (Bordas *et al* 1992) and 0.62 (Luiting and Urff 1991a). In pigs, the estimates range from 0.18 (Von Felde *et al* 1996) to 0.38 (Mrode and Kennedy 1993) (Table 1.1). In mice, heritability estimates range from 0.16 (Hastings *et al* 1997) to 0.28 (Nielsen *et al* 1997a) (Table 1.1). Three projects have used the mouse as a model for NFE selection: one at the University of Edinburgh, UK (Hastings *et al* 1997; Bunger *et al* 1998); a second at the University of Nebraska, USA (Nielsen *et al* 1997a, 1997b); and a third at the University of Adelaide, Australia (Archer and Pitchford 1996; Hughes *et al* 1998). All 3 groups have clearly demonstrated that NFE is moderate heritability in mice and NFE can be improved by selection, resulting in differences between the lines of 17-33% depending on the number of generations of selection. The overall evidence from heritability estimates from different species indicates that genetic variation in net feed efficiency exists in most species (Archer *et al* 1999) and net feed efficiency can be improved with selection.

Table 1.1 Heritability estimates for net feed efficiency in different species (adapted from Pitchford, 2004)

Species	Physiological state	No. of Animals	Heritability	Reference
Beef cattle	Growing	1324	0.28 ± 0.11	Koch *et al* (1963)
Beef cattle	Growing males	534	0.14 ± 0.12	Fan *et al* (1997)
Beef cattle	Growing	966	0.41 ± 0.07	Archer *et al* (1997)
Beef cattle	Growing	540	0.16 ± 0.08	Herd and Bishop (2000)
Beef cattle	Weaner bulls	792	0.32 ± 0.04	Arthur *et al* (2001 b)
Beef cattle	Yearling bulls	397	0.25 ± 0.10	Arthur *et al* (2001 d)
Beef cattle	Grown	1529	0.18	Robinson and Oddy (2004)
Dual purpose cattle	Growing	235	0.27 ± 0.23	Brelin and Brannang (1982)
Dairy cattle	Growing males	650	0.08 ± 0.05 to 0.36 ± 0.17	Jensen *et al* (1992), Jakobsen *et al* (2000)
Dairy cattle	Growing females	417	0.22 ± 0.11	Korver *et al* (1991)
Dairy cattle	Lactating heifers	360	0.19 ± 0.12	van Arendonk *et al* (1991)
Dairy cattle	Lactating cows	247	0.16	Ngwerume and Mao (1992)
Dairy cattle	Lactating cows	353	0	Svendsen *et al* (1993)
Dairy cattle	Lactating cows	204	0.05	Veerkamp *et al* (1995)
Pigs	Growing boars	7562	0.30, 0.33, 0.38	Mrode and Kennedy (1993)
Pigs	Growing boars	3188	0.18	Von Felde *et al* (1996)
Poultry	Laying hens	704	0.42 to 0.62	Luiting and Urff (1991a)
Poultry	Laying hens	Realised	0.12, 0.21, 0.28	Bordas *et al* (1992)
Poultry	Laying hens	-	0.27	Tixier-Boichard *et al* (1995)
Poultry	Cockerels	-	0.33	Tixier-Boichard *et al* (1995)
Mice	Growing	1000	0.27 ± 0.06	Archer *et al* (1998)
Mice	Growing	500	0.24 ± 0.08	Archer *et al* (1998)
Mice	Growing	Realised	0.16, 0.23, 0.27	Hastings *et al* (1997)
Mice	Growing	Realised	0.28 ± 0.003	Nielsen *et al* (1997a)
Mice	Growing	Realised	0.27 ± 0.02, 0.26 ± 0.03	Hughes *et al* (1998)

1.4 Measurement of feed intake and efficiency

Direct measurement of net feed intake with the currently available technology is very laborious, expensive and uneconomical for producers. At present, there are 3 approaches available for the measurement of NFI: centralised testing facilities, on-farm testing facilities and on pasture.

1.4.1 Centralised testing facilities

In centralised testing facilities, animals are maintained for a given length of time and feed intake is measured electronically. Generally, in Australian testing systems, after 3 weeks of adjustment to the

feeding system, animals spend 70 days in the testing station with *ad lib* access to feed (Kearney *et al* 2004). Each animal has an electronic ear tag that registers a unique number when it enters the feeding box. The feed intake and body weight for that particular animal is automatically downloaded and processed by the system. Total feed intake is calculated based on the difference between the weight of the feed bin before and after eating. Besides this reading, the electronic system also records the number of feeding sessions, the time spent feeding every day, and the time spent eating per session (Fenton, 2004). Although this electronic system allows a high level of control over the testing period and has relatively few errors, the cost is over AUD $500 per animal. Therefore, usually only a subset of animals from a herd is tested.

1.4.2 On farm testing

The on-farm testing system involves establishing on-farm facilities for the measurement of NFI. Feed intake can be measured by keeping records of the feed provided to animals in individual pens. Although such facilities can reduce the cost for farmers, it is difficult for farmers to operate for large numbers of animals. Moreover, accurate measures of weight must be recorded. Therefore, farmers need a low-cost automated system, which is currently unavailable. The advantage of such facilities is that more animals could be tested for feed intake nationally and the total costs would be lower than central testing (Archer *et al* 1999).

1.4.3 On pasture

Measurement of feed intake on pasture is based on providing markers, such as chromium oxide, to animals at a constant, known dosage with intra-ruminal controlled-release devices to dispense the marker. The marker is then measured in the faeces. However, this technology has limited accuracy and is not adequate for comparing feed intake between individual animals (Herd *et al* 1996).

1.5 Selection for high net feed efficiency (NFE)

1.5.1 Effects of selection for NFE on carcass traits

Several studies have reported associations between net feed efficiency and carcass quality traits. Five years of data from post-weaning selection of Angus cattle for NFE at Trangie (NSW, DPI), showed NFE is positively genetically correlated (r = 0.69) with daily feed intake (DFI) in cattle (Arthur *et al* 2001a, b; Archer *et al* 1998; Herd *et al* 1997; Archer and Barwick 2001; Richardson *et al* 2001). Selection for decreased NFI results is associated with increases in weight (7% heavier) and a reduction in daily feed intake (1.2 kg/day). Hence, efficiency appears to be achieved by the animals being genetically able to eat less whilst not reducing growth. Preliminary evidence from ultrasound scans of the subcutaneous fat on these Trangie Angus cattle suggested that selection of net feed efficiency may alter body composition (Richarsdon *et al* 2001, Arthur *et al* 1997). Steer progeny from high NFE parents had less

whole-body fat and whole-body protein than progeny of low NFE parents. It was estimated that these differences contributed to 5% of the genetic variation in net feed efficiency. Arthur *et al* (2001a) found the subcutaneous fat depth measured over the 12th /13th rib and rump fat depths at the end of the post-weaning test for feed intake were positively correlated with net feed intake in beef cattle ($r_{genetic}$ = 0.17, $r_{genetic}$ = 0.06, respectively). The genetic correlations between NFI and measures of fatness tend to be slightly positive. Richardson *et al* (2001) also reported that high NFE animals have a greater ratio of bone and total internal organs as a proportion of final live weight than low NFE animals.

The fat depth results were supported by McDonagh *et al* (2001) in preliminary correlation estimates between NFE and a range of beef quality attributes in a cross bred population of Angus and British *Bos taurus* crossbred steers. High NFE steers had less fat over the rib and rump than low NFE steers. However, there were no differences between the animals in terms of carcass weight, dressing percentage, eye muscle area, intramuscular fat percentage, marbling scores, meat colour or fat colour. There was 13% higher calpastatin activity in the *Longissimus dorsi* in the high NFE animals. Theoretically, this could negatively affect meat tenderness in low NFE animals. However, there were no differences in the tenderness measurements of shear force and compression in the *Longissimus dorsi* muscle samples.

Differences in body composition have been also reported as being related to variation in net feed intake in other species. In chickens, Luiting (1990) reported genetic and phenotypic correlations of body fat traits with net feed intake that ranged from -0.40 to 0.45. A high NFE chicken line contained 3.4% more fat than the low NFE line. Mice NFE selection line experiments conducted by three different research groups found 6-50% difference in fatness depending on the age of measurement (Hastings *et al* 1997; Bunger *et al* 1998; Nielsen *et al* 1997a, 1997b; Archer and Pitchford 1996; Hughes *et al* 1998 and Hughes and Pitchford 2004a). Hughes (2003) found efficient animals were 23% fatter than less efficient mice after seven generations of selection. These findings are consistent with those of Bishop and Hill (1985) and Nielsen *et al* (1997a).

1.5.2 Selection response for NFE

At the Trangie Agricultural Research Centre, 2,128 Angus bulls and heifers were evaluated for post-weaning NFI between 1993-1999. Using these data, the Breedplan program for the Angus Society of Australia generated estimated breeding values (EBVs) for NFI that ranged from -1.41 to +1.14 kg/day (10% difference), with accuracies as high as 87% (Herd *et al* 2003). NFI EBV records on 579 Hereford and Poll Hereford animals showed a range of EBV from -0.63 to + 0.90 kg/day (Australian Hereford Society, 2002). The benefit of estimating breeding values for NFI is related to the cost of feeding. If a

bull has an NFI EBV of -0.6 and another bull has an NFI EBV of +0.4, after adjusting for weight and gain of the progeny, the progeny of the first bull will eat 0.5 kg/day less feed than the progeny of the second bull. After 5 years of post-weaning selection at Trangie (NSW, DPI), the data from the divergent Angus cattle NFI selection lines showed average selection differentials of -0.54 ± 0.18 kg/day and 0.70 ± 0.17 kg/day per year for the low and high lines, respectively. An average annual divergence rate in NFI of 0.21 kg/day was achieved between the lines with a realised heritability of 0.33 (Arthur *et al* 2001, Herd *et al* 2003).

In another study, researchers at the University of Alberta, Lacombe Research Centre in Canada conducted a selection experiment in cattle with 148 steers from five genetic strains for daily feed intake, growth rate and NFI. Steers grew an average of 1.52 kg/day and had average dry matter intakes of 8.5 kg/day. Individual animals varied in NFI from an efficient -1.95 kg/day to an inefficient +1.82 kg/day. This represented a difference in actual feed intake of 3.77 kg/day between the most and least efficient steers. This variation in NFI represented a difference of USD $45.69 in feed costs (assuming feed costs of USD $0.10/kg) during the 120-day test period. This translates to a cost savings of approximately $333 million annually based on the 2.4 million feedlot cattle industry in Alberta. The benefit to cow-calf and seed stock producers is unknown, but was estimated to be at least as high (Basarab, 2003). Another study has estimated that efficient steers will produce 21% less methane than less efficient steers because of their lower feed intake (Okine *et al* 2001).

1.5.3 Negative consequences of selection for NFE

Three independent studies in mice (Nielsen *et al* 1997b; Rauw *et al* 2000; Hughes and Pitchford 2004b) and pigs (Estany *et al* 2002) showed a negative effect of high NFE on ovulation rate and subsequently on litter size. In poultry, the reports are contradictory. Morrison *et al* (1997) reported higher hatching rates in high efficiency hens, whereas in Hagger (1994) reported a negative correlation with egg number. Bordas *et al* (1992) did not observe any effect on egg number in their high efficient line. Thus far, no reports are available in cattle on the effect of NFE selection on fertility.

1.5.4 Major challenges for selection of NFE

The cost associated with the electronic measurement of cattle feed intake in testing facilities is the major barrier to industry adoption and there is not an economical alternative for commercial farmers or most stud breeders. Besides the cost, however, there are other limiting factors associated with testing stations including the capacity of testing, availability of measurement equipment, disease quarantine barriers to cattle movement, and the scheduling of testing (Herd *et al* 2003).

To avoid the high cost of feed intake measurements, the use of genetic markers associated with NFE would be a reasonable option for selection. These markers could be DNA markers or phenotypic biomarkers measured in the blood or urine. Several studies have shown that insulin-like growth factor-1 (IGF1) circulating levels is moderate heritability (r = 0.34-0.43) and positively genetically associated with feed efficiency, growth and carcass traits (intramuscular fat %, P8 fat, rump and rib fat depth) in beef cattle (Johnston *et al* 2001; 2002; Herd *et al* 2002a). Therefore, IGF1 has been used as an early life measure for the genetic improvement of finishing growth rate and carcass fat traits. Currently, IGF1 is being used for the commercial mass screening of pigs to improve feed efficiency and reduce carcass fatness. However, there is growing evidence that the relationship between IGF1 and feed efficiency in cattle is not as strong (R. Herd, personal communication).

Quantitative trait loci mapping has been used to identify chromosomal regions associated with NFE to develop better genetic DNA markers. A genetic DNA test for feed efficiency is an ideal solution for the selection of highly efficient animals as it will reduce the generation interval and costs since animals can be selected at younger age. Understanding the genetic basis and physiological mechanisms of feed efficiency may also open other avenues for increasing NFE.

1. 6 NFE QTL experiments

Publications on the molecular mechanisms regulating food intake, energy balance and obesity in humans and mice has increased dramatically over the past few years. The mouse has been an important model for the dissection of complex traits, such as feed intake, with the identification of quantitative trait loci (QTL), genes and metabolic pathways related to these traits (Pomp 1997; Robinson *et al* 2000; Brockmann and Bevova 2002; Fenton 2004). Fenton (2004) reported 9 NFE QTL in high and low mouse lines divergently selected for NFE over eight generations, many of which have been confirmed in other mouse studies (Table 1.2). For one of these QTL (MMU1), Pomp *et al* (2007) confirmed the feed efficiency QTL and found another QTL for feed intake adjusted for body weight in the same region. This QTL (on MMU1) also overlaps with a QTL for heat loss identified by Moody *et al* (1998, 1999). Another of the NFE QTL in mice on MMU11 overlaps with a suggestive NFE QTL from Moody *et al* (1999) and Pomp *et al* (2006). Two other NFE QTL identified by Fenton (2004) on MMU5 and MMU14 are located in the same regions as 2 NFE QTL identified in mice by Elo *et al* (2002) (Table 1.2).

Table 1.2 NFE QTL in mice (Fenton 2004)

NFE QTL (Mouse chromosome)	Supporting evidence from other mouse studies	Supporting evidence from poultry studies	Supporting evidence from cattle study
1	Moody *et al* (1998, 1999) for heat loss; Pomp *et al* (2007) at 21cM and 57cM		Fenton 2004
5	Elo *et al* (2002)	Van Kaam *et al* (1999); Tuiskula-Haavisto *et al* (2002); De Koning *et al* (2003)	Fenton 2004
11	Moody *et al* (1999); Pomp *et al* (2006)		
13			Fenton 2004
14	Elo *et al* (2002)		
15		Van Kaam *et al* (1999); Hensen *et al* (2005); Minvielle *et al* (2005)	
16			Fenton 2004

Of these 9 NFE QTL, 4 QTL (MMU1, 5, 13 and 16) in mice were also homeologous with cattle NFE QTL (BTA16, 6, 20 and 1 respectively) (Fenton 2004). Two mouse NFE QTL from the Fenton (2004) study were homeologous to QTL in poultry (Van Kaam *et al* 1999). The first QTL on MMU5 was homeologous to the QTL reported separately by Tuiskula-Haavisto *et al* (2002) and De Koning *et al* (2003) for feed intake on chromosome 4 in broiler chickens. The second QTL on MMU15 is homeologous to a QTL identified by Van Kaam *et al* (1999) for feed intake on chicken chromosome 1 (GGA01). This particular QTL was confirmed by Hensen *et al* (2005) at the same position in chicken and Minvielle *et al* (2005) in Japanese quail.

In pigs, there have been 2 studies conducted for selection for net feed efficiency, but the response to several generations of selection was not significant (Jungst e al. 1981; Webb and King 1983). In sheep, after 32 years of divergent selection for weaning weight, there were no differences found in NFE between Merino lines (Herd *et al* 1993).

So far, 68 and 168 chromosomal regions or QTL have been identified for energy balance in humans and animal models (mouse, poultry), respectively (Elo 2003). Map positions of candidate genes in mouse and the QTL generally overlap with each other. Of the candidate genes for energy balance, 93% have at least one identified QTL within 20 cM distance (Elo 2003). However, none of the QTL have been characterised at the DNA level or are supported by other molecular studies.

An interesting observation reported by Elo (2003) concerned the redundancy of metabolic energy metabolic pathways. The redundancy was discovered when enzymes that were thought to be unique and have a fundamental role in metabolism were "knocked-out" in animal models. The "knockout" animals had normal phenotypes despite lacking key enzymes or proteins. The normal phenotypes were a result of redundancy due to either the presence of a gene duplicate that has the same function ("gene family buffering") or due to the presence of alternate pathways that can achieve a similar function ("pathway buffering"). Thus, many pathways have been identified that have more than one mechanism

to produce the same phenotype by the expression of a completely different set of genes (Smith *et al* 2000; Osuga *et al* 2000). For example, glucose-6-phosphate can be derived from different metabolic sources such as xylulose 5-phosphate or erythrose 4-phosphate in the pentose phosphate pathway or from glycogen in the glycogenolysis pathway. Mechanisms involved in energy balance appear to be controlled by redundant metabolic pathways, and therefore, there will be many identified QTL for energy balance in different species. Thus, the effectiveness of the QTL approach for identifying genes underlying complex traits, like energy balance or net feed efficiency, can be questioned. Therefore, it is important to accompany QTL mapping with appropriate physiological, molecular and biochemical studies to provide a sound list of potential candidate genes.

1.7 Physiological components affecting feed efficiency

Understanding the various physiological components affecting the utilisation of nutrients and maintenance energy is important in order to identify candidate genes and to predict the possible outcomes of selection for efficient animals. Moreover, these indicators may be useful for manipulating favourable metabolic pathways to increase efficiency with very little relative cost.

1.7.1 Physical activity

Several researchers have reported strong associations between the level of physical activity and variation in feed efficiency since energy expenditure during locomotion can be very high relative to expenditure at rest. Moruppa *et al* (1990), Hughes *et al* 1997, Bunger *et al* (1998), Mousel (1998) and Fenton (2004) reported that efficient mice were half as active as inefficient animals. Mousel (1998) and Richardson *et al* (2000) found approximately a 10% and 10.5% difference in feed intake due to physical activity between selection lines of mouse and cattle, respectively. Luiting *et al* (1991) reported that 79% of the genetic variation in high and low NFE chickens could be due to the activity. They found efficient chickens spent only 18% of daily heat production on physical activity in comparison to 28% in efficient chickens (Luiting *et al* 1994).

1.7.2 Digestion and absorption

Digestible energy is the difference between gross energy and energy lost in the faeces. Digestible energy, as a proportion of gross energy, may vary from 30% for mature, weathered forage to nearly 90% for processed, high quality cereal grains (NRC 2000). Digestible energy is the combination of metabolisable energy, urinary energy and gaseous energy. The main source of gaseous energy is microbial fermentation in ruminants (NRC 2000). Kahn *et al* (2000) reported variation in the efficiency of microbial protein production in the rumen of different animals. Microbial fermentation also results in heat

production. Thus, digestible energy extracted from the feed may vary between the animals. Richardson *et al* (1996) found a 1% dry matter digestibility difference between high and low efficiency bulls and heifers could account for a 14% difference in NFE. In dairy cows, Adams and Belyra (1987) found that selection for high milk yield is associated with improvement in feed absorption. Unfortunately, intake was not measured in this study.

1.7.3 Heat increment of feeding

The heat increment of feeding is defined as the energy expenditure associated with the digestion and assimilation of food (Lee 2003). For example, greater heat production occurs if acetate is metabolised instead of propionate (Lee 2003). Ferrell and Jenkins (1998) reported that increased heat increment of feeding was correlated with high feed intake and heavier visceral organ weights in cattle. The heat increment of feeding is also linked with digestion, gastrointestinal passage, protein, and fat accretion in the body tissues. It is normal practice to feed cattle low-fibre rations during hot weather. Feeding more concentrates at the expense of fibrous ingredients increases the energy density of rations, and thus, reduces the heat increment of feeding (West 1999). Experiments in dairy cattle have indicated that a high percentage of grain in the diet (61.8, 51.8 and 31.8% of dry matter in the diet for early, mid and late lactation) resulted in lower milk yield and milk fat, lower dry matter intake and lower feed efficiency in multiparous cows (Tessmann *et al* 1991).

1.7.4 Visceral organs

Of all the tissues in the body, the visceral organs have the largest impact on maintenance energy requirements. In ruminants, the liver and intestinal tract use 70% of the maintenance energy (Ferrell and Jenkins 1985 and Ruppert *et al* 2002). Early *et al* (1990) reported a higher protein turnover in visceral tissues than in skeletal muscles, which could account for the high energy expenditure. The size of the visceral organs also contributes to the amount of energy expenditure. Studies showed that on a high plane of nutrition, sheep and cattle have increased viscera weights (liver, pancreas, small intestine) as a proportion of body weight, and this is associated with an increased energy requirement (Ferrell and Jenkins 1985, Burrin *et al* 1990, Ruppert *et al* 2002). In the context of feed efficiency, smaller and lighter viscera should make animals more energy efficient. However, Fenton (2004) did not find any significant differences in visceral organs in relation to net feed efficiency in mice.

1.7.5 Proton leakage

Brown adipose tissue is a specialised form of adipose tissue that plays an important role in thermogenesis. The energy derived from metabolic fuels is dissipated in a process that is facilitated by

proton leakage, thereby releasing heat. Proton leakage occurs during the movement of protons across the mitochondrial inner membrane, and happens spontaneously or is mediated by uncoupling proteins (UCPs) (Krauss *et al* 2005). This proton movement across membranes dissipates the proton motive force and represents an energetic inefficiency. Regulation of proton leakage is mediated by UCPs. Of the few UCPs that have been identified and related to the regulation of energy expenditure and heat production, UCP1 is expressed in brown adipose tissue, UCP3 in muscles and UCP2 in all other tissues (Jezek *et al* 1998). UCP2 and UCP3 may have roles in influencing maintenance energy requirement as they are linked to the proton-conductance pathways in mitochondria (Fleury *et al* 1997). Raimbault *et al* (2001) observed significant differences in high NFE and low NFE lines of chickens for the avian homologues of UCP2 and UCP3. However, Kolath *et al* (2006) found no relationship in levels of UCP2 and UCP3 and maintenance energy in Angus beef cattle. The gene expression of UCP2 is influenced by catecholamines (such as norepinephrine) (Thomas and Palmitter, 1997), thyroid hormones (Obregon *et al* 1996), peroxisome proliferation activating enzyme (Aubert *et al* 1997) and leptin (Zhou *et al* 1997).

UCPs also play a role in controlling superoxide production, and therefore, the production of reactive oxygen species (ROS) (Echtay *et al* 2002). Thus, the inefficient UCP-dependent proton leakage is associated not only with heat production but also with increased oxidative stress due to high levels of ROS, which can affect maintenance energy requirements. Increases in ROS production will induce the anti-oxidant metabolic pathways involving catalase, superoxide dismutase, glutathione peroxidise, and glutathione S transferase. Therefore, one can postulate that high net feed efficient animals will show less oxidative stress in comparison to low NFE animals.

Several experiments indicated high NFE selection mice lines have lower heat production (13-39%) (Hastings *et al* 1997; Bunger *et al* 1998; Nielsen *et al* 1997a, 1997b; Archer and Pitchford 1996; Hughes *et al* 1998). Nielsen and McDonald (2006) reported a 20.6% difference in heat loss and 15% variation in net feed intake in mice selected for heat loss for 15 generations. These heat loss differences could be generated from biochemical inefficiencies due to increased proton leakage.

1.7.6 Susceptibility to stress

In response to stressful conditions, there is an increase in the level of glucocorticoids, which stimulates the sympathetic nervous system. This, in turn, increases the blood glucose level and there is a characteristic change in the pattern of white blood cells (e.g. neutrophils, lymphocytes, basophils) as part of stress management. Richardson *et al* (2002) reported changes in the haematological profile of cattle under stress, with higher levels of glucocorticoids (cortisol), increased levels of neutrophils, and lower levels of lymphocytes in less efficient Angus steers compared to more efficient Angus steers. It is,

therefore, hypothesized that efficient steers are less susceptible to stress in comparison to inefficient steers. Increase stress susceptibility in low NFE animals would contribute to significant energy wastage.

In order to identify the differences in metabolites in response to stress, Richardson *et al* (2004) conducted a study on blood and urine for metabolic differences in Angus steers divergently selected for NFE. At weaning, there were phenotypic correlations between the concentrations in plasma of beta-hydroxy-butyrate (r =0.55; p<0.001), aspartate aminotransferase (r = 0.34; P<0.001), urea (r = 0.26; P<0.1), and total plasma protein (r = 0.26; P<0.1) and NFI. As measured at the start of the feedlot NFI test, the plasma levels of glucose, creatinine and aspartate aminotransferase were correlated with NFI over the experiment (r = 0.40, -0.45 and 0.43, respectively, P<0.05), providing evidence of phenotypic associations with NFI.

Of these metabolites, beta-hydroxy-butyrate in ruminants is predominantly derived from rumen butyrate production; only in fasting it is derived from endogenous ketogenesis of amino acids and fat. Urea, aspartate aminotransferase and total plasma protein are indicators of increased amino acid catabolism and protein turnover in the less efficient animals. Urea, in particular, is a product of ammonia absorption and protein degradation (Cameron 1992). Urea was positively correlated with genetic and phenotypic measures of net feed intake in steers (Richardson *et al* 2004), positively correlated with backfat in sheep (r = 0.24, Clarke *et al* 1996), and negatively correlated with lean growth in sheep (r = -0.50, Clarke *et al* 1996). Creatinine levels are positively associated with muscle mass in sheep (r = 0.35, Clarke *et al* 1996), negatively associated with fat depth in sheep (r = -0.44, Clarke *et al* 1996), and negatively associated with steer net feed intake (Richardson *et al* 2004). This would suggest greater muscle mass and possibly lower fat content in the more efficient steers. Therefore, differences in the metabolites are in agreement with the body composition results discussed earlier. The findings of Nockels (1994), where there was an increase in metabolites such as cortisol, glucose, aspartate aminotransferase, urea and creatinine in cattle under stress, were also corroborated by the Richardson *et al* study (2004).

1.7.7 Physiological components and NFE: Conclusion

Compiling the results from several research studies on the relationship between different physiological components and net feed intake, the differences in digestion contribute 10%, body composition 5%, feeding patterns 2%, protein turnover, tissue metabolism and stress 37%, heat increment of feeding 9%, and physical activity 10% to net feed efficiency (Richardson and Herd 2004) (Figure 1.1). Based on this distribution, it can be said that stress, thermogenesis and protein turnover are major factors in determining feed efficiency and controlling maintenance energy in cattle.

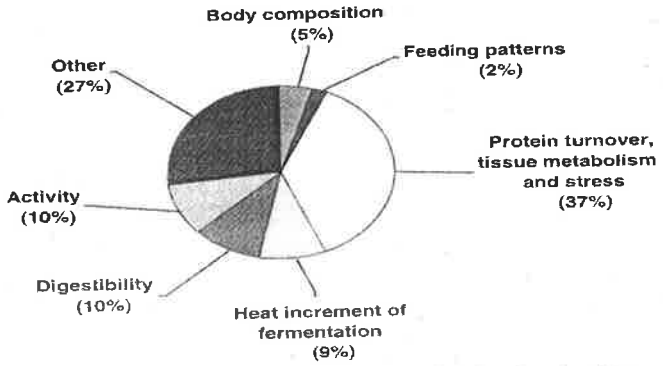

Figure 1.1 Percent contribution of different physiological components of net feed efficiency in beef cattle. (Figure adapted from Richardson and Herd 2004.)

1.8 Molecular mechanisms of energy expenditure and its regulation

In the context of the physiological components involved in feed efficiency, mitochondrial oxidative phosphorylation and proton leakage are likely to play prominent roles in the regulation of maintenance energy and feed intake. In order to identify genetic DNA markers for net feed efficiency, it is important to understand the molecular basis of energy expenditure and its regulation.

Energy enters an organism as food and exits the organism mainly through heat and faecal matter. Energy is released from food as a result of combustion to carbon dioxide and water. This is accomplished by enzymatically controlled mitochondrial oxidative phosphorylation in which a portion of the energy content of food is converted to ATP (Figure 1.2). Energy stored in the form of ATP is then used to perform the biological work within the cell. While much of the energy content of food is converted to ATP, a significant portion is lost as heat. This is due to the fact that in order for reactions to go forward, they need to be thermodynamically favourable (i.e., move from a state of higher energy to a state of lower energy). As a result, the conversion of fuel to ATP results in significant amounts of energy being released in the form of heat. Similarly, energy is also lost in the form of heat when ATP is used within the cell (Lowell 2002).

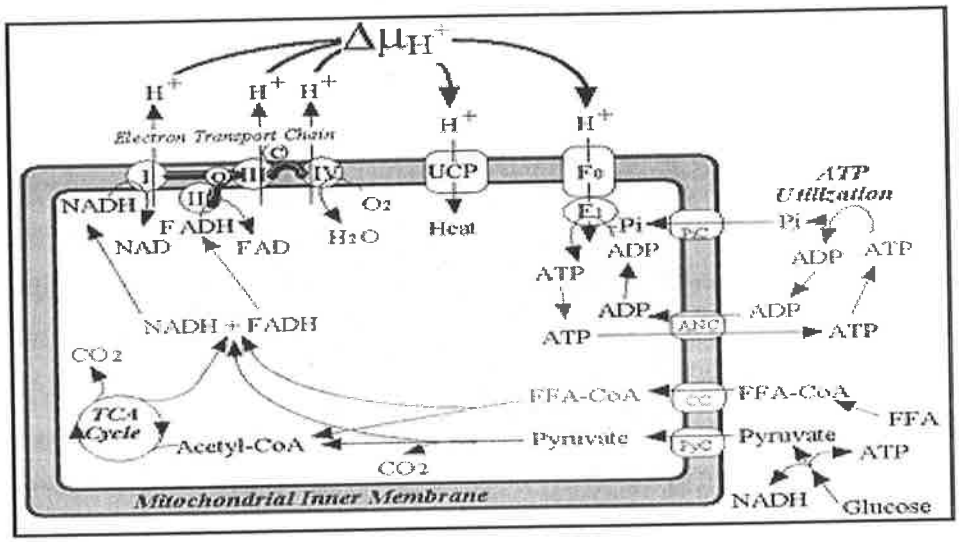

Figure 1.2 Step-by-step conversion of fuel into ATP. Free fatty acids (FFAs) and glucose are oxidized generating NADH and FADH2 which donate electrons to the electron transport chain. Ubiquinone (Q) shuttles electrons from both complexes I and II to complex III while cytochrome C (C) shuttles electrons from complex III to complex IV. Molecular oxygen (O_2) is the terminal electron acceptor. Protons are pumped out by complexes I, III and IV of the electron transport chain, creating a proton electrochemical potential gradient. Protons may re-enter the mitochondrial matrix via F0F1 ATP synthase, with energy being used to generate ATP from ADP and Pi. Proton re-entry via ATP synthase depends upon the availability of ADP which is generated in the cytosol from reactions utilizing ATP. Protons may also re-enter via uncoupling proteins (UCP), with energy being released in the form of heat. Abbreviations: ANC = adenine nucleotide carrier; CC = carnitine carrier; complex I = NADH-ubiquinone oxidoreductase; complex II = succinate:ubiquinone oxidoreductase; complex III = ubiquinone-cytochrome-c oxidoreductase; complex IV = cytochrome-c oxidase; PiC = phosphate carrier; PyC = pyruvate carrier. This figure was adapted from Lowell *et al* (1993).

1.8.1 Coupled energy metabolism reactions

The reactions involved in oxidative phosphorylation are tightly coupled. This has great significance for the regulation of energy expenditure (Rolfe and Brown 1997). For a given molecule of fuel, a fixed amount of NADH and FADH is generated, which in turn results in a fixed number of protons being pumped out of the mitochondrial matrix by the electron transport chain. These protons re-enter the mitochondrial matrix via ATP synthase (F0F1 ATPase), resulting in a fixed number of ATP molecules being created. A fixed number of ATP molecules are then used to perform a fixed amount of biological work.

If problems arise during the pumping of ions across the plasma membrane, there will be an increase in energy expenditure. Defects in the mitochondrial coupling between nutrient oxidation and oxidative phosphorylation can lead to proton leakage. Such mechanisms are referred to as "futile cycling". These pathways are called "futile" because there is no other effect than the expenditure of ATP (or some other form of metabolic energy) (Lowell, 2002). Consequently, such pathways can be responsible for increased maintenance energy requirements of animals. Muscle relaxation, proton leakage, protein degradation and dephosphorylation can all create "futile cycles". There has been much interest in the possible role of futile cycles in regulating energy expenditure. These cycles are characterised as a set of

opposing, non-equilibrium reactions catalyzed by different enzymes that act simultaneously with at least one of the reactions driven by ATP hydrolysis. The results of such cycles are that ATP energy is depleted, heat is produced, and no net substrate-to-product conversion is achieved.

One dramatic, pathological example of a futile cycle in pigs is the condition known as malignant hyperthermia, which is due to a mutation in the skeletal muscle ryanodine receptor (Denborough 1998), a calcium release channel of the sarcoplasmic reticulum. Abnormal calcium release by the mutant ryanodine receptor is triggered by anaesthesia and/or stress, and leads to increased pumping of calcium back into the sarcoplasmic reticulum, a process which consumes large amounts of ATP. The consumption of ATP, in turn, leads to an increase in all the steps of fuel combustion which precede the synthesis of ATP. The net result is a large increase in energy expenditure.

High net feed efficient animals would be expected to have tightly controlled mitochondrial coupling and very little proton leakage with less futile energy production. Whereas in low net feed efficient animals, there may be more proton leakage and ultimately, energy crisis will develop as a result of less ATP production through mitochondrial oxidative phosphorylation. An energy crisis situation will further increase the pressure on the mitochondrial oxidative phosphorylation pathway to generate more energy.

1.8.2 Substrate cycles

Substrate cycling is a set of opposing, nonequilibrium reactions catalyzed by different enzymes which act simultaneously with at least one of the reactions driven by ATP hydrolysis. The results of such cycles are that ATP energy is depleted and heat is produced. Examples of substrate cycling are gluconeogenesis and the glycolysis pathways as well as the triacylglyceride and fatty acid pathways (Rabkin and Blum 1985). Rates of substrate cycling may be increased many-fold in association with hypermetabolic states resulting from severe burns, cold exposure, hyperthyroidism, or acute exercise. Substrate cycling is higher in the liver than in most other tissues. Rabkin and Blum (1985) estimated the activity of five substrate cycles: 1) glucose / glucose-6-phosphate, 2) glycogen / glucose-6-phosphate, 3) fructose-6-phosphate / fructose 1, 4) 6-biphosphate, phosphoenolpyruvate / pyruvate / oxaloacetate, and 5) acetate / acetyl CoA. These five substrate cycles contributed 26% of the resting metabolic rate in liver. Newsholme (1980) estimated 50% of the contribution of adult human total daily energy expenditure could come from the phosphofructose-fructose biphosphate cycle if fully active. He concluded that stimulation of such cycles could result in the conversion of significant amounts of chemical energy into heat.

1.8.3 Protease systems and protein turnover

Protein synthesis contributes 15-18% of the standard metabolic rate (Waterlow, 1984). Webster *et al* (1978) predicted that protein synthesis and associated aspects of protein metabolism accounts for approximately 50% of heat production. The net energy costs of protein degradation are not clear but many researchers claim that this process is a significant energy sink (Siems *et al* 1982). Literature estimates suggest that the energy costs of protein turnover contribute about 20-25% towards maintenance energy expenditure (Pym and Tomas 1990; Reeds *et al* 1998). Both the intracellular protease systems (including the lysosomal, the Ca $^{2+}$- dependent, and the ATP/ubiquitin-dependent systems) (Baracos *et al* 1995) and extracellular matrix proteases contribute to the protein turnover of animal, and therefore, may be linked to maintenance energy requirements and efficiency of growth.

The expression of the intracellular muscle proteases calpain (μ-calpain and m-calpain large subunits) and ubiquitin are down-regulated during feed restriction, whereas the expression of the calpain inhibitor, calpastatin, is unchanged (Murdoch *et al* 2003). Gene expressions of calpain and ubiquitin have been found to be correlated to heat production and nitrogen intake (Murdoch *et al* 2003). For the extracellular proteolytic systems, a positive correlation has been observed between the gene expression of the cytokine-regulated urokinase-type-plasminogen-activator (uPa), tissue metallopeptidase inhibitor 3 (TIMP-3), matrix metallopeptidase 2 (MMP-2) and membrane type 3-anchored matrix metalloproteinase (MT3-MMP) with nitrogen intake, average daily gain and heat production (Murdoch *et al* 2003). In addition, excretion of the amino acids 3-methy-histidine (3-MH) and hydroxyproline in urine and heat production have been found to be positively correlated (Murdoch *et al* 2003). These 2 amino acids are indicators of myofibrillar protein breakdown (Murdoch *et al* 2003).

McBride and Kelly (1990) found that the Na^+K^+ATPase-linked ion transport system contributes 5.7-12.4% towards ruminant whole-body energy expenditure. They suggested that protein turnover is highly correlated with Na^+K^+ATPase linked ion pumping because ionic homeostasis and amino acid transport are ancillary processes of protein synthesis. As much as 25% of the energy required for protein synthesis in pigs has been attributed to Na^+K^+ATPase activity (Adeola *et al* 1989). Therefore, it is possible that ion transport systems can contribute to variation in net feed efficiency as well.

Variation in protein metabolism has been shown to accompany genetic selection for growth and feed efficiency traits in cattle (Oddy 1999, Fenton 2004). Tatham *et al* (2000) also found a positive relationship between NFE and protein turnover. They found that low efficiency cattle had a high plasma creatinine:urea ratio, which is an indicator of high turnover of creatine phosphate in the muscle. These findings have been confirmed in other species such as poultry (Pym 1990; Tomas *et al* (1988, 1991); Gabarrou *et al* (1997). McDonagh *et al* (2001) found a 13% difference in calpastatin activity in efficient steers after one generation of selection for divergent NFE in beef cattle. Calpastatin prevents muscle

protein degradation by the calpain system. Therefore, since the more efficient animals had higher calpastatin activity, these results support the conclusions of the other protein turnover reports. The combined studies indicate a positive association of low maintenance requirements in animals with either an increase in fatness or a decrease in protein degradation and turnover.

Murdoch *et al* (2003) reported that for the ATP-ubiquitin dependent proteolytic system, the ubiquitin gene was down-regulated during periods of less protein turnover ($p<0.001$) and its expression showed a positive correlation with the average heat production, suggesting energy saving during feed restriction. Feed restriction studies by Lovetto *et al* (2006) showed a significant reduction in heat production due to a decrease in protein turnover in pigs. Another interesting observation reported by this group is that protein deposition was more energetically efficient than lipid deposition in restricted feeding experimental trials on pigs. A reduction in protein turnover (and thus, a reduction in energy expenditure) seems to be the most plausible explanation for this observation. The reduced urinary nitrogen loss during feed restriction may also suggest a decrease in protein turnover (Lovatto *et al* 2006). These observations, in general, indicate that genetic differences in any of the proteases systems are likely to affect efficiency.

1.9 Regulation of energy expenditure and food intake

1.9.1 Role of the sympathetic nervous system in energy expenditure

The primary efferent pathway regulating energy expenditure is believed to be the sympathetic nervous system. Stimulation of the sympathetic nervous system increases secretion of catecholamines from adrenal glands, which act on adrenergic receptors. Catecholamines infiltrate thermogenic target tissues like brown adipose (Himms-Hagen 1989), skeletal muscles and liver (Murdoch *et al* 2003).

Gazzola (1993) used rats as a functional model for the control of energy expenditure via the sympathetic nervous system using an alpha-adrenoceptor agonist and antagonist. The model has been confirmed in cattle (Gazzola *et al* 1995). The pathway consists of pre-synaptic, inhibitory α_2-adrenoceptors, a sympathetic synapse (or neuromuscular junction), and post-synaptic α_1-adrenoceptors. α_2-Adrenoceptors-selective agonists decrease sympathetic activity, and therefore, the lower metabolic rate by reducing the tonic release of noradrenaline. α_1-Adrenoceptors-selective antagonists reduce sympathetic activity by blocking the activation of the α_1-adrenoceptors by noradrenaline (Ruffolo 1987).

Murdoch *et al* (2003) reported that beta adrenergic receptors, when stimulated by agonists, mediate increases in energy expenditure in ruminants by 30-40% in various tissues, which can be reversed by beta blocking agents (Miaron *et al* 1997). Activation of α_2-adrenergic receptor subtypes reduces energy expenditure and therefore, maintenance energy requirements in cattle by 12-20% in thermoneutral and

cold environments (Miaron *et al* 1995), whereas blocking the α_2-adrenergic receptor increases energy expenditure (Hidari *et al* 1991). In addition, administration of beta-adrenergic receptor agonists leads to a marked increase in energy expenditure (Himms-Hagen, 1989). In human studies, epinephrine infusion causes a 25% increase in energy expenditure (Simonsen *et al* 1992).

Animals treated with various blockers of the sympathetic nervous system, as well as mice lacking norepinephrine and epinephrine due to the knockout of the dopamine beta hydroxylase gene, have impaired brown fat function and are unable to maintain body temperature during cold exposure (Thomas and Palmiter 1997). UCP1 proteins are important mediators of the sympathetically-regulated thermogenesis in brown adipose tissue. The molecular mediators of thermogenesis in skeletal muscle, however, are presently unknown although UCP3 is active in muscle.

Peroxisome proliferator-activated receptor-gamma coactivator-1 (PGC-1) expression in brown adipocytes is induced by increased activity of the sympathetic nervous system, an effect mediated by beta-adrenoreceptors (beta-ARs). PGC-1 binds to and increases the activity of many factors affecting transcription, including peroxisome proliferator-activated receptor-gamma, the thyroid hormone receptor and the retinoic acid receptor; all of which are involved in thermogenesis (Puigserver *et al* 1998). PGC-1 also binds to and increases the activity of a number of transcription factors involved in mitochondrial biogenesis (Puigserver *et al* 1999).

Mice lacking beta-adrenoceptors, which mediate the thermogenic effects of norepinephrine and epinephrine, show diminished thermogenesis and susceptibility to obesity. On the other hand, mice lacking stearoyl-CoA desaturase 1 (SCD1) (which catalyzes the rate limiting step of the synthesis of monounsaturated fatty acids) activate the adenine monophosphate activated kinase (AMPK) pathway and show enhanced thermogenesis (Dobrzyn *et al* 2004). It is hypothesized that beta-adrenergic control of thermogenesis might be mediated via repression of the SCD1 gene. In mice lacking beta-adrenoceptors, the gene expression of SCD1 is elevated in the liver, skeletal muscle and white adipose tissue (Dobrzyn *et al* 2004). An elevated level of skeletal muscle SCD1 would cause the desaturation of *de novo* lipogenesis products and divert them away from mitochondrial oxidation. This would inhibit substrate cycling between *de novo* lipogenesis and lipid oxidation, thereby leading to a state of suppressed thermogenesis (Mainieri *et al* 2006). However, it was found that elevated SCD1 transcript levels in the tissues of mice lacking beta-adrenoceptors is not a direct effect of blunted beta-adrenergic signalling. Therefore, beta-adrenergic control of SCD1 repression is unlikely to be the primary effector in sympathoadrenal regulation of thermogenesis. As potential avenues for controlling energy expenditure, approaches that target both SCD1 and the molecular effectors of thermogenesis under beta-adrenergic control might be more effective than targeting SCD1 alone (Mainieri *et al* 2006).

The studies suggest that it may be possible to reduce maintenance requirements by manipulating the sympathetic nervous system and its receptors or by identifying animals that naturally express these receptors to a greater or lesser degree.

1.9.2 Role of the brain in energy expenditure

The brain has the capacity to detect alterations in environmental temperatures and diet through neural circuits that activate the efferent pathways controlling energy expenditure (Lowell *et al* 1999) (Figure 1.3). Neurons in the arcuate nucleus of the hypothalamus express proopiomelanocortin (POMC) and control diet-induced thermogenesis. The arcuate POMC neurons are activated by leptin (Elmquist *et al* 1999; 2001). POMC is processed in these neurons to form alpha-melanotroph stimulating hormone (alpha-MSH) (Figure 1.3). The melanocortin-4 receptor (MC4R) located in the paraventricular nucleus of hypothalamus is the likely mediator of alpha-MSH effects during sympathetically-driven diet-induced thermogenesis. In support of this supposition, MC4R gene knockout mice are obese (Huszar 1997) and have impaired diet-induced thermogenesis (Butler *et al* 2001).

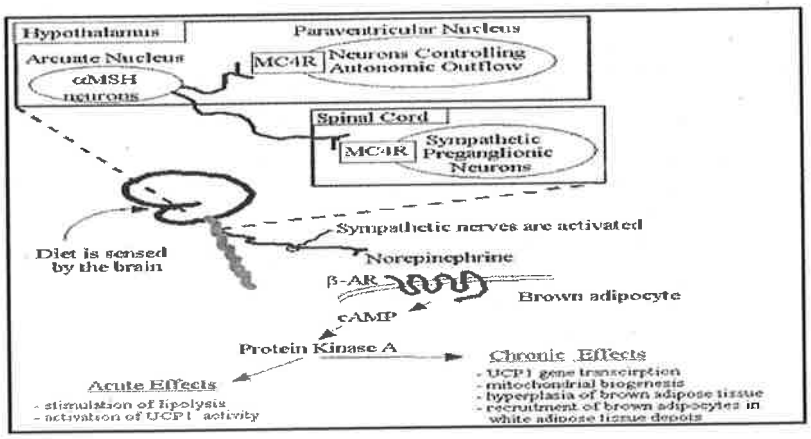

Figure 1.3 Central and efferent pathways regulating energy expenditure. Diet and cold are sensed by the brain. Alpha-melanotroph stimulating hormone (αMSH) neurons in the arcuate nucleus of the hypothalamus contributes in diet-induced thermogenesis. αMSH neurons project to neurons in the paraventricular nucleus of the hypothalamus controlling sympathetic outflow, as well as to sympathetic preganglionic neurons located in the intermedial lateral column of the spinal cord. Melanocortin-4-receptors (MC4Rs) situated in hypothalamus are likely to play an important role in thermogenesis. These pathways lead to increased activity of sympathetic nerves which release norepinephrine, activating beta-adrenoreceptor (ßARs). This has acute and chronic effects on brown adipocytes which promote increased thermogenesis. UCP: Uncoupling proteins; cAMP: cyclic adenine monophosphate Figure adapted from Lowell *et al* (1999).

The other neural pathways through which the central serotonergic systems regulate food intake and body weight are not fully elucidated. Serotonin, via action by the serotonin1B receptors (5-HT(1B)Rs) (core components of the central circuitry controlling body weight homeostasis), modulates the endogenous release of both agonists and antagonists of the melanocortin receptors (Heisler *et al* 2006). Serotonin-induced hypophagia requires downstream activation of melanocortin 4 receptors, but not melanocortin 3 receptors. Therefore, melanocortin receptors are responsible for the serotonergic

regulation of energy balance. Centrally-administered melanocortin agonists stimulate oxygen consumption, inhibit basal insulin release, and alter glucose tolerance. Furthermore, plasma insulin levels are increased in the young lean MC4-R knockout (MC4-RKO) mouse and impaired insulin tolerance takes place before the onset of detectable hyperphagia or obesity. Therefore, the central melanocortin system regulates not only energy intake and expenditure, but also processes related to energy partitioning, as indicated by the effects on insulin release and peripheral insulin responsiveness (Fan *et al* 2000).

1.9.3 Hormonal regulation of feed intake

The hypothalamus receives information relevant to energy balance through metabolic, neural and hormonal signals induced mainly from the visceral organs including the liver, pancreas, visceral adipose tissues, and gastrointestinal tract (Table 1.4). These visceral organs have specialised cell types that have developed highly specific fuel-sensing mechanisms (Seeley and York 2005). This helps to regulate homeostasis in the body (Considine 2000). Disorders in these essential homeostatic mechanisms lead to increased feed intake and energy expenditure. Many papers have been published that characterise the hypothalamic neuronal networks, neuropeptide transmitters, and circulating peptides, which act as energy sensors and send signals to the brain regarding the energy status of the body (Morton *et al* 2006, Stanley 2005, Baile and Della-Fera 2001, Robinson *et al* 2000, Schwartz *et al* 2000) (Figure1.4).

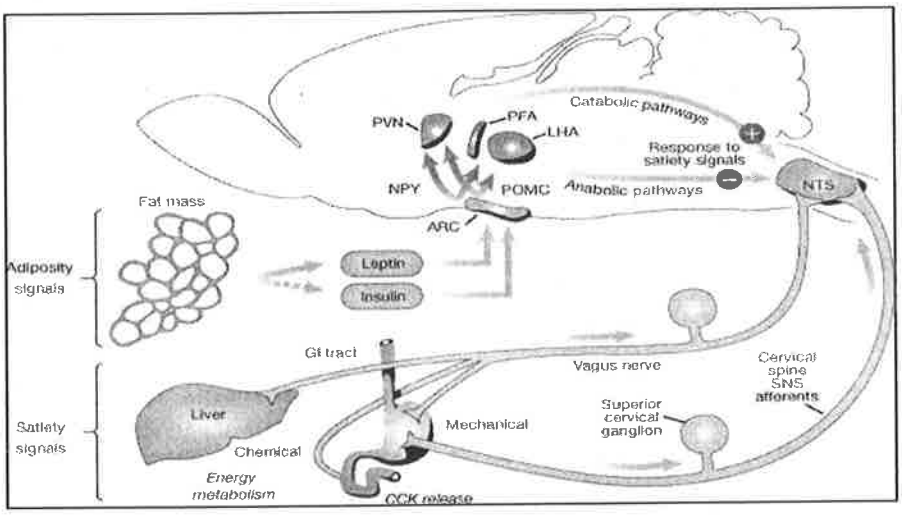

Figure 1.4 Neuroanatomical model of pathways of fuel sensors. Fuel sensor signals (like leptin, insulin, and cholecystokinin (CCK)) are secreted from adipose tissue, pancreas and intestine and interact with central autonomic circuits regulating feed intake. PVN: paraventricular nucleus; NPY: neuropeptide Y; ARC: arcuate nucleus; LHA: lateral hypothalamic area; PFA:Perifornical area; NTS: nucleus tractus solitarius; POMC: prooipmelanocortin. (Figure adapted from Schwartz *et al* 2000.)

1.9.3.1 Insulin

Pancreatic hormones, such insulin, pancreatic polypeptide, glucagon and amylin, contribute to glucose homeostasis and food intake regulation (Table 1.4). Among these hormones, insulin has a significant role in terms of glucose homeostasis. Insulin enters the brain from the blood and acts to reduce energy intake. Insulin is positively correlated with long-term energy balance. Plasma insulin concentrations depend upon the peripheral insulin sensitivity, which in turn, is related to total body fat stores and fat distribution, with visceral fat being the key determinant (Porte *et al* 2002). Secretion of insulin is stimulated by glucose and amino acids but not dietary fat.

Little or no insulin is synthesized within the brain (Woods and Seeley 2000). However, insulin receptors are found in many areas of the brain, but are localized in the hypothalamic nuclei, which regulates feeding behaviour. Insulin is transported into the central nervous system across the blood brain barrier by an active, saturable process, and also gains access through the circumventricular organs. Administration of insulin directly into the brain of rodents decreases food intake. In contrast, increased peripheral insulin levels in the absence of feeding results in hypoglycemia, which is a stimulus for food intake (Woods and Seeley 2000). Insulin release (both basal and in response to food intake) increases as body fat increases, in order to maintain glucose homeostasis in the presence of insulin resistance (Considine 2000).

Insulin modifies the supply of nutrients by a direct vasodilatory effect that increases blood flow (Wray-Cahen *et al* 1995) and decreases the arterial metabolite concentrations of glucose (Prior *et al* 1984), amino acids (Huntington and Prior, 1985) and non-esterified fatty acids (Wray-Cahen *et al* 1995). This decrease is due to the inhibition of hepatic gluconeogenesis, coupled with the inhibition of lypolysis and stimulation of lipogenesis in the adipose tissues. Insulin stimulates glucose metabolism by increasing glucose transport rate via vasodilatation and glucose transporter 4 (GLUT4) translocation. Insulin also stimulates the oxidation and recycling of lactate (Wray-Cahen *et al* 1995) and storage as glycogen. Insulin enhances uptake of other nutrients such as acetate. Insulin increases muscle energy requirements by increasing amino acid transport and protein synthesis (Lobley, 1991). Rapid growth and leaness of domestic mammals are generally associated with an enhanced insulin sensitivity of muscles and more glycolytic muscle energy metabolism (Oddy, 1993; Oddy *et al* 1995). A decrease in insulin sensitivity of skeletal muscles induces an increase in basal insulin plasma levels concomitant with a decrease in carcass growth and elevated carcass adiposity (Hocquette *et al* 1998). Insulin insensitivity could be a contributing factor to less efficiency in animals due to reduced glycolysis activity and energy production. Highly efficient animals could be expected to have increased rates of glycolysis in comparison to low efficiency animals.

1.9.3.2 Leptin

There are several adipose tissue hormones, including adiponectin and resistin, that are part of the insulin pathway, and therefore, involved in glucose homeostasis (Table 1.3). However, leptin is arguably one of the most important adipose tissue hormones with regards to feed intake.

Leptin is the product of the *ob* gene and is expressed mainly in adipocytes (Zhang *et al* 2002), but also at low levels in the gastric epithelium (Bado *et al* 1998) and placenta (Masuzaki *et al* 1997). Circulating leptin levels reflect both energy stores and acute energy balance. The rate of insulin-stimulated glucose uptake in adipocytes is a key factor linking leptin secretion to body fat mass. Although the mechanism is not clear, it may involve the glucose flux through the hexosamine pathway (Wang *et al* 1998). The decrease in serum leptin with fasting provides a signal to the central nervous system that food intake has not recently occurred, and in part, initiates the complex response of the body to restore energy stores (Flier and Flier 1998). Leptin also increases heat production through signalling the oxidation of fatty acids (Murdoch *et al* 2003). Studies have found associations between serum leptin concentration with carcass adipose depots and carcass characteristics of beef cattle (Minton *et al*, 1998; Geary *et al*, 2003).

Leptin inhibits the activity of orexigenic NPY/AgRP neurons and reduces expression of the neuropeptide and agouti-related protein NPY/AgRP (Elias *et al* 1998). On the other hand, leptin activates anorectic pro-oipmelanocortin / cocaine- and amphetamine-regulated transcript neurons, which affects food intake behaviour (Stanley *et al* 2005).

Table 1.3: Pancreatic and adipose tissue hormones in feed intake regulation

Protein	Contribution in feed intake regulation
Adiponectin (ADIPOQ)	Adiponectin is expressed in adipocytes, and is an excellent candidate gene for marbling in cattle because its product, adiponectin, modulates lipid and glucose metabolism in insulin-sensitive tissues (Chadran *et al* 2003). Adiponectin increases the sensitivity of hepatocytes to insulin, either through a direct action or indirectly by lowering circulating lipids (Saltiel 2001).
Resistin	Resistin is produced by adipose tissue and appears to increase insulin resistance. Circulating resistin is increased in obese rodents and decreased after weight loss in humans. Overexpression of a dominant negative form of resistin shows increased adiposity in mice with elevated leptin and adiponectin levels, as well as enhanced glucose tolerance and insulin sensitivity (Steppan *et al* 2001).

Pancreatic polypeptide	Pancreatic polypeptide is produced from the periphery of the Islets of Langerhans but are also secreted by the pancreas and distal gastrointestinal tract (Robinson *et al* 2000).Plasma pancreatic polypeptide is elevated by ghrelin, motilin and secretin and by gastric extension (Stanley *et al* 2005) and is inversely proportional to adiposity (Uhe *et al* 1992). Pancreatic polypeptide administration in mice decreases food intake, energy expenditure, and improves insulin resistance (Asakawa *et al* 2003).
Glucagon	Glucagon is secreted by the pancreatic α-cells and decreases meal size. The primary function of glucagon is the regulation of glucose homeostasis (Bray 2000).
Amylin (islet amyloid polypeptide, IAPP)	Amylin is synthesized in the pancreatic β-cells, also is expressed in the endocrine cells of the gut, visceral sensory neurons and hypothalamus (Reidelberger 2001). Amylin is a potent inhibitor of gastric emptying and hence, food intake (Woods and Seeley 2000).

1.9.4 Hypothalamic regulation of feed intake

The central nervous system regulates energy balance through the neuropeptides, neurotransmitters and specialised glucose sensing neurons that guide the control of food intake (and energy expenditure as discussed above). The hypothalamic ventromedial nucleus was found to be essential for leptin regulation of energy balance (Dhillion *et al* 2006). Insulin and leptin sensing arcuate nucleus neurons co-express neuropeptide Y and agouti-related proteins, which are the neuropetides that stimulate food intake. Expression of neuropeptide Y and the agouti-related proteins through their respective neurons are inhibited by leptin, insulin and PYY_{3-36}, whereas they are stimulated by ghrelin (Flier 2004). Nonadrenaline is co-localised with neuropeptide Y in the arcuate nucleus of hypothalamus. Injection of nonadrenaline into the paraventricular nucleus region of hypothalamus increases food intake (Leibowitz *et al* 1984). Nonadrenaline acts as an anabolic effector in the central nervous system control of energy homeostasis.

Adjacent to these neurons, other neurons express pro-opiomelanocortin (POMC), the polypeptide precursor for melanocortins, such as α-melanocyte stimulating hormone (α-MSH). POMC exerts its effects by binding to members of the melanocortin receptor family (MC3R and MC4R), and thereby, POMC decreases food intake and favours weight loss (Fan *et al* 1997). POMC neurons are stimulated by leptin but inhibited by the neighbouring neuropeptide Y and agouti-related protein neurons (Cowley *et al*, 2001) (Figure 1.5). Sinsuke *et al* (2006) recently found a new satiety molecule in the hypothalamus, called nesfatin-1. It is also associated with melanocortin signalling in the hypothalamus.

In addition to these hormones, there are a series of opioids and nonopioids produced by the hypothalamus that affect food intake. These include serotonin, dopamine, growth hormone, somatostatin and endorphins.

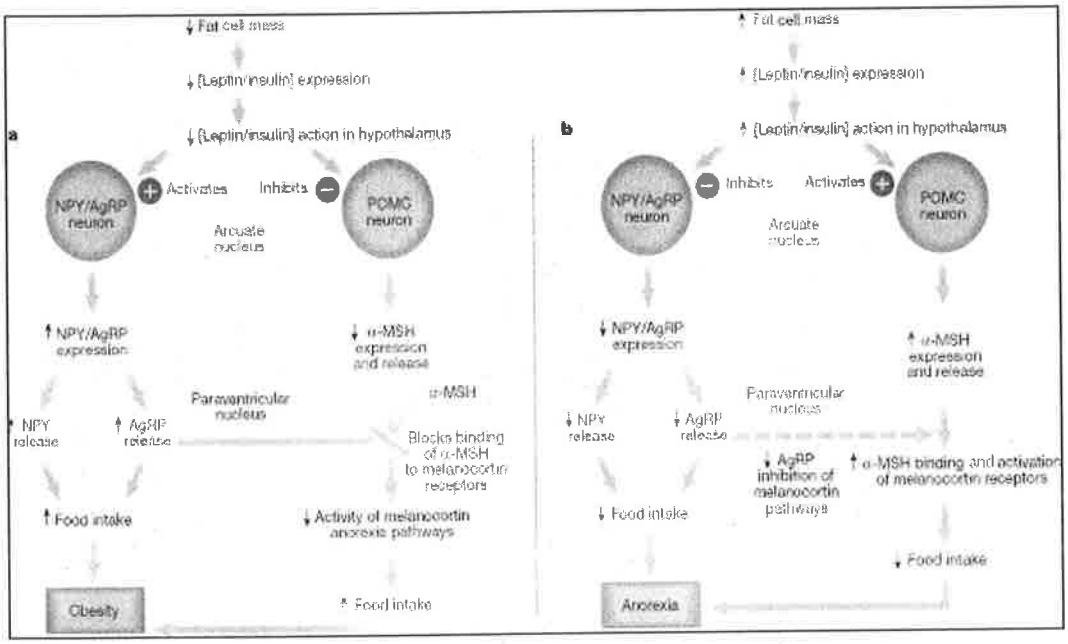

Figure 1.5: Role of the arcuate nucleus of the hypothalamus in food intake regulation and adiposity signalling. a. Effect of reduced level of leptin/insulin expression activates orexigenic neuropeptide Y/agouti-related protein neurons and simultaneously inhibits pro-opiomelanocortin (POMC) neurons, which increases food intake and obesity. b. Increased activity of leptin/insulin in the arcuate nucleus stimulates the pro-opiomelanocortin pathway and inhibits neuropeptide Y/agouti-related protein expression, which reduces food intake and encourages anorexia. NPY: Neuropeptide Y; AgRP: Agouti related protein; α-MSH: Alpha-melanocortin stimulating hormone. (Adapted from Schwartz *et al* 2000.)

1.9.4.1 Serotonin

Serotonin may directly influence the melanocortin pathway in the arcuate nucleus via 5-hydroxytryptamine (5-HT) receptors (Halatchev *et al* 2004). At least 14 5-HT receptor subtypes are expressed in the central nervous system, but their functions have not been yet defined. However, it is known that 5-HT_{2C} receptor null mice have increased plasma insulin and leptin levels, and reduced feed intake (Robinson *et al* 2000).

1.9.4.2 Dopamine

The dopaminergic system is also integral part of controlling feeding behaviour. Dopamine signalling is thought to be mediated by D_1 and D_2 receptors (Kuo 2002). D_2 receptors are expressed in the pituitary and regulate prolactin release. This implies a role of D_2 receptor in the regulation of pituitary hormones by dopamine (Robinson *et al* 2000).

1.9.4.3 Growth hormone

Growth hormone increases the intensity of energy-requiring metabolic pathways in muscles, mainly protein synthesis, as well as muscle protein degradation in ruminants (Pell and Bates, 1987). Exogenous administration of growth hormone in cattle and sheep causes increased body weight gain (10-18%), greater lean carcass (5-10%), decreased lipid accretion (10-20%), and improved feed efficiency (9-20%) (Kopchick and Cioffi, 1991). In the *little* mice model, which has a genetic deficiency in growth hormone production, there is a dramatic decrease in body weight and skeletal growth, and a marked increase in the percentage of body fat (Donahue and Beamer 1993). These changes in body composition occur without any change in food intake in terms of kcal consumed per gram of body weight. C57 hg/hg (high growth) mice have a mutation that increases in body size, but the mice are not obese. They show increased growth rate up to 50% accompanied by a higher energetic efficiency and/or lower maintenance requirements (Bernier 1986).

1.9.4.4. Somatostatin

Somatostatins (SST), also known as somatotropin-release inhibiting factors (SRIFs), are a family of cyclopepides that have an inhibitory action on the secretion of hormones such as growth hormone, insulin and glucagon. Somatostatin affects carbohydrate and lipid metabolism through the action of growth hormone, and affects muscle and bone growth via the action of insulin-like growth factor-1 (Melmed *et al* 1996).

Somatostatin is a one of the neurotransmitter modulators of upper gastrointestinal secretion, sensation, and motility. Intestinal mechanosensitive afferents are modulated by somatostatin (Su *et al* 2001). Somatostatin affects many other gastrointestinal functions, including secretion and absorption, which are involved in the regulation of feed intake. Somatostatin also inhibits secretion of the orexigenic hormone, ghrelin (Barken *et al* 2003), and so leads to appetite suppression.

1.9.4.5 Opioid system

It is known that the hypothalamic opiates, such as beta-endorphin, dynorphin A and enkephalins, promote phagia (Levine and Billington 1989). The opioid peptide genes include pro-opiomelanocortin (POMC), ß-endorphin, dynorphin, enkephalin, QFQ nociceptin, endorphin-1 and endorphin-2. There are 4 opioid receptors that have been identified and shown to be involved in food regulation: μ (MOR, OPR-3), □ (KOR, OPR-2), δ (DOR, OPR 1), and nociceptin (ORL-1) (Robinson *et al* 2000). Extensive evidence from clinical studies and mouse experiments suggest that opiate receptor antagonists, especially the μ- and □-antagonists, decrease food intake (Morely 1987). The microinjection of beta-endorphin and opiate agonists that bind to the μ-receptor subtype stimulate feeding. Neurons producing

the two enkephalin pentapeptides, methionine-enkephalin (met-ENK) and leucine-enkephalin (leu-ENK), are widely distributed in the hypothalamus. Although enkephalins are ineffective on their own, long-acting analogs stimulate feeding, possibly involving the δ-receptor subtype (Levine and Billington 1989). Central injection of the third hypothalamic opioid, dynorphin A 1–17, derived from the precursor prodynorphin, stimulates feeding by activating the κ-opiate receptor subtype. Dynorphin-producing cells are also found in various regions of the hypothalamus, including the arcuate nucleus and paraventricular nucleus (Levine and Billington 1989).

1.9.4.6 Other neuropeptides

Other neuropeptides, such as the corticotrophin-releasing hormone (CRH), thyrotropin-releasing hormone (TRH), cocaine- and amphetamine-regulated transcript (CART), interleukin-1ß (IL1ß), urocortin, oxytocin and neurotensin, are among the growing list of anorexigenic peptides that promote negative energy balance and act as catabolic effector signalling molecules. In contrast, melanocyte stimulating hormone (MSH), hypocretin 1 and 2, galanin and nonadrenaline are orexigenic peptides that promote increased energy intake (Schwartz *et al* 2000). CRH causes anorexia in mice and activates the sympathetic nervous system, in addition to its role as a major regulator of the hypothalamic-pituitary-adrenal axis (Bray *et al* 1990). TRH reduces food intake, in addition to stimulating the thyroid axis (Kow and Pfafff 1991). Oxytocin reduces food intake, in addition to regulating uterine function (Verbalis *et al* 1995). Two peptides, hypocretins 1 and 2, are exclusively expressed in neurons within the lateral hypothalamus; the region of the brain long known to be an important contributor to feeding behaviour (de Lecea 1998).

1.10 Satiety signals from the gastrointestinal tract

The major determinant of meal size is the onset of satiety, a biological state induced through neurohumoral stimuli during food ingestion by the gastrointestinal tract mechano- and chemosensitive receptors and conveyed to the hypothalamus, which leads to meal termination. The onset of satiety involves several set of pathways in response to satiety signals (Woods *et al* 1998).

1.10.1 Gastrointestinal mechanoreceptors and chemoreceptors

During food ingestion, increased levels of glucose, ketones, fatty acids, and hormones (e.g. glucagon-like peptide 1) cause the responsive neurons to terminate feed intake. Satiety information generated during the course of a meal is conveyed to the hindbrain via the vegal nerve by means of afferent fibres in the vagus nerve and by afferent fibres passing into the spinal cord from the upper gastrointestinal tract. The satiety-inducing signals are released because of the mechano-chemical stimulation of the

stomach and gastrointestinal tract. Humoral signals (such as cholecyctokinin) are released from the endocrine secretory cells lining the intestinal mucosa during food ingestion and from the neural input of the liver due to energy metabolism. This information converges in the nucleus tractus solitarius, which is an area of the caudal brainstem that integrates sensory information from the gastrointestinal tract and abdominal viscera (eg liver) and the taste information from the oral cavity (Figure 1.4, 1.5) (Schwartz *et al* 2000).

1.10.2 Gastrointestinal hormones

In addition to the mechano- and chemoreceptors, the entry of nutrients into the stomach and intestine elicits the release of several gastrointestinal hormones (e.g. gherlin and enterostatin), the majority of which act to inhibit food intake (Schwartz *et al* 2000) (Table 1.4, Appendix I). These hormones are synthesized in the gut and signal the central nervous system through vagal or sympathetic afferents and the circulation system (Figure 1.6). Circulating hormones gain access to the central nervous system via the circumventricular organs, which are specific areas of the brain where the blood brain barrier is porous. The median eminence and arcuate nucleus of the hypothalamus contain receptors for many of these circulating hormones and factors, and hence, regulate food intake. In addition, many of the gastrointestinal peptides and their receptors are also synthesized in the brain and act there as neurotransmitters to regulate food intake (Considine, 2002).

Table 1.4 Gastro-intestinal peptides regulating food intake (adapted from Considine 2002)

Peptide	Stimulus	Site of Production	Site of Action	Effect on Food Intake
Cholecystokinin (CCK)	protein and fat	small intestine, brain	vagal afferents	decrease
Glucagon-like Peptide 1 (GLP-1)	nutrients, gut hormones, gut neural signals	ileum/colon	Gastric mucosa, brain	decrease
Ghrelin	fasting	stomach	brain	increase
Apolipoprotein A-IV	fat absorption	intestine/liver	brain	decrease
Enterostatin	fat	stomach/intestine	vagal afferents	decrease
Bombesin	food ingestion	gastric mucosa	vagal afferents, brain	decrease

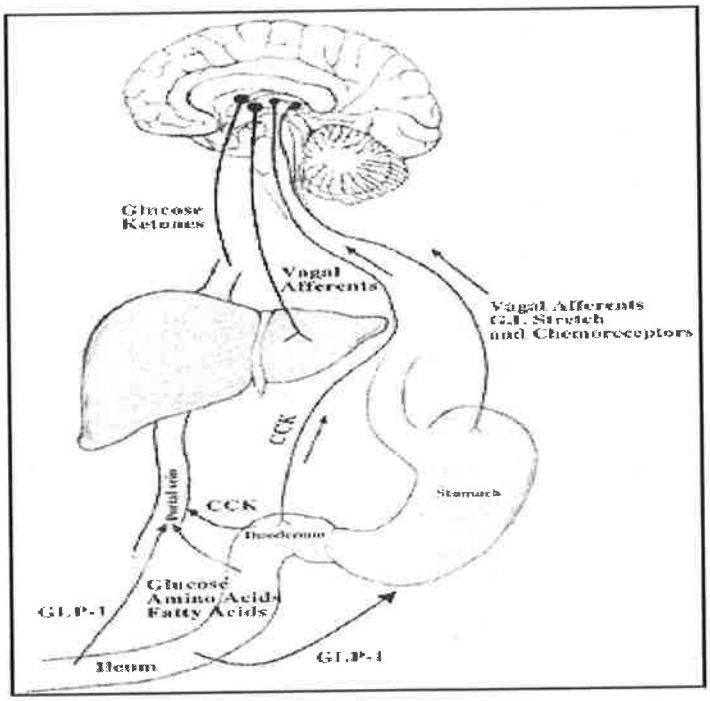

Figure 1.6 Gastrointestinal signals regulate food intake. The majority of signals from the gastrointestinal tract (GI) tract regulate the size of individual meals. Mechanoreceptors quantify the stretch of the stomach, and chemoreceptors are activated by nutrients in the gastrointestinal tract. These receptors transmit information via the vagal and sympathetic afferents to the hindbrain nuclei. This information is then transmitted to the hypothalamus and other forebrain structures for integration with additional signals regulating food intake. Vagal afferents from the liver signal the presence of specific nutrients. Glucose and ketones act as signals to the central nervous system directly via the responsive neurons in the hypothalamus. Gastrointestinal hormones such as cholecyctokinin (CCK) bind receptors in the liver to activate vagal afferents, or access the central nervous system (CNS) via the circulation. Thus provides satiety information to the nucleus tractus solitarius region of hypothalamus. Other hormones such as glucagon-like peptide 1 (GLP-1) inhibit feeding by slowing gastric emptying. (Figure adapted from Considine 2002).

1.10.3 Nutrient related signals

Changes in nutrient availability and body weight induce adaptive responses in food intake behaviour and in metabolic pathways that are optimised for the energy balance set point. According to Neel's (1999) hypothesis of "thrifty genotypes", the ability to efficiently store energy from an occasional feast represents a survival mechanism in human ancestral societies with limited supplies of food. In other words, animals have developed efficient nutrient sensing metabolic pathways to utilise nutrients to maintain energy balance and metabolic homeostasis by complex regulatory mechanisms without any adverse effects on growth and development. Among the known nutrient sensing pathways are the long chain fatty acyl-CoA pathway, the mammalian Target of Rapamycin (mTOR) and the hexosamine biosynthesis pathway.

1.10.3.1 Role of long chain fatty acyl-CoA

Long chain fatty acyl-CoA (LCFA-CoA) and malonyl-CoA are integral to the nutrient sensing mechanisms. Increased intra-cellular LCFA-CoA indicates an abundance of nutrients, while the enzyme AMP-activated protein kinase (AMPK) is a sensor of nutrient insufficiency. When cells experience a critical drop of fuel availability, this is reflected by the AMP/ATP ratio and AMPK is activated. AMPK increases LCFA-CoA substrate oxidation to replenish ATP levels, which contributes to the orexigenic effect.

The carnitine palmitoyltransferase (CPT1) enzyme controls the transfer of LCFA-CoA to the mitochondria for beta-fatty acid oxidation to generate more energy. Malonyl CoA is both an intermediate in the *de novo* synthesis of long chain fatty acids and an inhibitor of carnitine palmitoyltransferase (CPT1) in the AMPK pathway. Malonyl CoA levels change in response to alterations in cellular fuel availability and energy expenditure (Ruderman *et al* 2003) (Figure 1.7).

Any defects in the function of the enzymes involved in the AMPK and beta-fatty acid oxidation pathways could contribute to an energy crisis irrespective of nutrient excess. Such defects would increase feed intake due to an inability to induce early satiety signals and terminate feed intake. Therefore, it can be hypothesised that high net feed efficient animals should have relatively higher adenosine monophosphate activated kinase activity and mitochondrial beta-fatty acid oxidation in comparison to low net feed efficient animals.

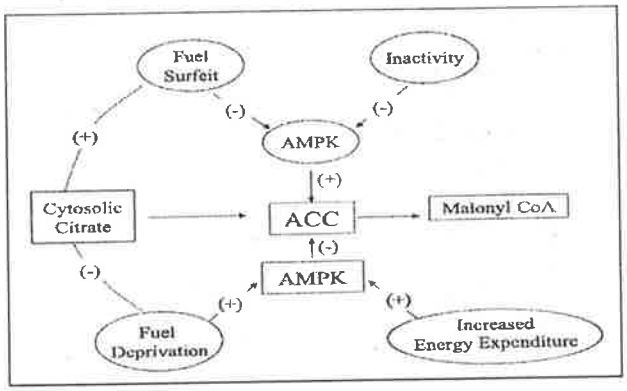

Figure 1.7 Role of AMPK and acetyl Co-A carboxylase (ACC) in food intake regulation. Changes in fuel availability and energy expenditure lead to alterations in the cytosolic concentration of citrate, ACC and the activity of the adenine mono-phosphate-activated kinase (AMPK). AMPK phosphorylates and inhibits ACC, which affects levels of malonyl CoA and the rate of fatty acid oxidation. (Figure adapted from Ruderman *et al* 2003).

1.10.3.2 Mammalian Target of Rapamycin pathway

The mammalian Target of Rapamycin (mTOR) protein is a serine-threonine kinase that regulates the cell cycle and growth by sensing changes in energy. In peripheral cells, the mammalian mTOR signalling pathway integrates nutrient signals with the hormonal signals (Sabatini *et al* 1994). This pathway stimulates protein synthesis. In mouse experiments, Denice *et al* (2001) observed that high cellular levels of ATP increases mTOR signalling and that mTOR itself acts as an ATP sensor. Like AMPK, mTOR is regulated by intracellular AMP/ATP ratios. AMPK activity is increased during fuel deficit and is inhibited by leptin and insulin (Andersson *et al* 2004). Such activation of AMPK leads to the inhibition of the nutrient-sensing enzyme activities of mTOR (Cota 2006). Thus, AMPK and mTOR have overlapping and reciprocal functions (Figure1.8). Although the interrelationship between AMPK and mTOR is reciprocal, mTOR activity may be increased in high net feed efficient animals relative to low net feed efficient animals due to the early signals indicating satiety and sufficient energy.

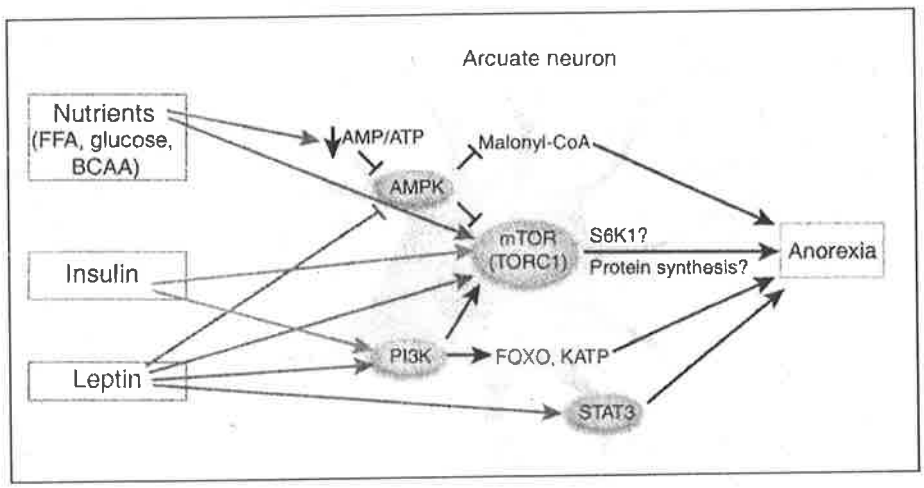

Figure 1.8 Relationship of the mammalian Target of Rapamycin (mTOR) and the adenine mono-phosphate-activated kinase (AMPK). Major classes of anorectic signals in the hypothalamus include nutrients such as free fatty acids (FFA), a glucose, leucine and other branched amino acids (BCAA), and hormones such as insulin and leptin. BCAA activates signalling through the TOR complex (TORC1). The regulation of cellular malonyl coenzyme-A levels is mediated by AMPK in parallel with AMPK effects on mTOR. In addition to the regulation of TROC1 through the inhibition of AMPK, insulin and leptin also control TROC1 via phosphatidylinositol 3-kinase (PI3K). Regulation of forkhead transcriptional factor subfamily box (FOXO)-dependent transcription and ATP- dependent potassium channels (KATP) also contributes to PI3K dependent anorexia. Although the mediators of TROC1-dependent anorexia are not clear, S6K1 and downstream events such as protein synthesis are likely to be involved. (Figure adapted from Kahn and Myers, 2006).

1.10.3.3 Hexosamine biosynthesis pathway

Marshall *et al* (1991) suggested a glucose fuel sensing mechanism that is dependent on the hexosamine biosynthesis pathway. This pathway is activated in response to excess glucose. The

metabolism of glucose by the hexosamine biosynthesis pathway represents only 1-3% of the total glucose metabolism but generates a cellular satiety signal that leads to reduced food intake and decreased glucose uptake by insulin-sensitive cells. The surplus glucose is converted into uridinediphosphoglucose-*N*-acetyl-glucosamine (UDP-GlcNAc) via glucosamine 6-phosphate (GlcN-6P). Nutrient excess (increased level of plasma glucose or long chain fatty acid-Coenzyme A) activates the hexosamine biosynthesis pathway. This pathway blocks the glycolysis and shunts substrates towards glucosamine 6-phosphate (GlcN-6-P) by converting fructose-6-phosphate. This reaction is catalased by the rate-limiting enzyme glutamine:Fru-6-P aminotransferase (GFAT) (Figure 1.9). Glucosamine 6-phosphate is further converted to uridine diphosphate-N-acetylglucosamine (GlcNAc) (UDP-GlcNAc), which is the main substrate for the glycosylation of the key regulatory proteins in the insulin signal transduction cascade (Heart *et al* 2000) and the transcriptional regulatory proteins of oxidative phosphorylation (Liu *et al* 1998). Excess glucose is also diverted to glycogen formation.

The hexosamine biosynthesis pathway not only senses high concentrations of glucose-derived fuels but also functions as a general sensor of nutrient availability and nutrient partitioning. If there is an alteration in the glucose transport due to insulin resistance, the nutrient excess signal from the hexosamine biosynthesis pathway cannot induce an early signal of satiety and feed intake termination. Hence, net feed efficiency in animals is likely to be affected by perturbation in nutrient sensing pathways. In high net feed efficient animals, therefore, an early increase in glucosamine 6-phosphate may be expected in comparison to low net feed efficient animals.

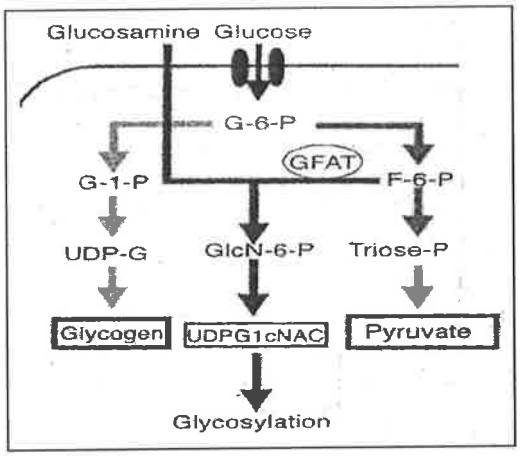

Figure 1.9 Hexosamine biosynthesis nutrient sensing pathway. Following glucose entry into cell through the glucose transport system, based on energy needs, the glucose is converted into glycogen, glucosamine 6-phosphate (GlcN-6-P) or fructose-6-phospate (F-6-P). F-6-P is either oxidised further through the mitochondrial citric acid cycle by conversion to pyruvate as a part of glycolytic pathway or used in the synthesis of glycogen. Conversion of F-6-P into glucosamine 6-phosphate is controlled by the rate-limiting enzyme, glutamine:Fru-6-P aminotransferase (GFAT). UDP-GlcNAc: uridine diphosphate (UDP)-N-acetylglucosamine (GlcNAc). (Figure adapted from Ravussin 2002.)

1.11 Summary

The regulation of food intake and energy expenditure is a complex process. Multiple biological circuitries participate in the integration of signals from very different sources, including the hypothalamus, gastrointestinal tract, liver, pancreas, and adipose tissues. These metabolic pathways have been studied extremely in rodents and humans in an attempt to control food intake and body weight. The experimental results have shown varying degrees of success in controlling feed intake without proportional changes in body weight. However, it is clear that it is possible to select for net feed efficiency wherein feed intake is reduced without affecting body weight. The difficulty is that many pathways can potentially be made more "efficient" and lead to increased NFE. Therefore, identifying candidate genes is problematic without detailed knowledge of energy homeostasis and regulation.

1.11.1 Gaps in NFE research

There has been some research on selection for net feed efficiency and heritability estimates of components related to net feed intake in cattle, poultry and mice. However, the genetic variation in net feed efficiency within breeds of beef cattle has not been accurately quantified. There are also no reports available on the genetics of feed efficiency in the context of different diets (e.g. roughage *vs.* concentrates, supplementing with feed additives). More data are required to generate accurate correlations between carcass composition (e.g. fat percent), meat quality traits (e.g. tenderness, marbling) and NFE. Since a major concern is the potentially undesirable genetic relationship between NFE with fertility, the relationship between post-weaning net feed efficiency and mature cow efficiency, reproduction and maternal traits needs to be explored (Archer *et al* 1999).

Moreover, very few efforts have focused on identifying genes controlling net feed efficiency. Several NFE QTL have been identified in different species, but most of these have not been confirmed. In fact, for beef cattle, no large linkage mapping studies have been reported for net feed efficiency. Even if NFE QTL are mapped in cattle, the selection of candidate genes for further study is complicated by the lack of a well-annotated bovine genome database and the complex nature of the physiology behind feed efficiency. A more thorough understanding of the underlying metabolic processes in energy expenditure that directly affect feed efficiency needs to be developed.

1.11.2 Objectives of the study herein

The major aim of this research project is to find molecular markers or genes and related metabolic pathways controlling net feed efficiency in beef cattle. The literature analysis identified many candidate pathways controlling energy metabolism that may be involved with NFE. These pathways include

adenine monophosphate-activated kinase (AMPK), oxidative phosphorylation, beta-oxidation, glucose turnover, stress regulation, growth regulation and protein turnover. Amongst these pathways, mitochondrial oxidative phosphorylation is one of the most likely sources of variation in net feed efficiency based on the literature. Due to metabolic redundancy or buffering, however, it is possible that different metabolic pathways play pivotal roles in net feed efficiency in different breeds and this needs to be investigated in detail.

1.11.3 Strategy

To address the aim of this project, three approaches were undertaken: QTL mapping, oxidative phosphorylation enzyme assays and mitochondrial proteomics.

A. Linkage and linkage disequilibrium mapping

Candidate genes from the metabolic pathways potentially controlling feed intake and energy balance were identified within 6 cattle NFE QTL by homeologous human-cattle comparative mapping. Single nucleotide polymorphisms (SNPs) were found in the candidate genes by sequencing the genomic DNA from the QTL mapping sires. Four of the identified quantitative trait loci (QTL) were confirmed by linkage mapping these SNPs in 3 Limousin-Jersey mapping families. The candidate gene SNPs were also validated by association studies in the Limousin-Jersey mapping progeny. The results of the fine mapping and association studies were verified in an Angus cattle population selected for NFE.

B. Oxidative phosphorylation biochemical enzyme assays

The activities of mitochondrial oxidative phosphorylation enzyme complexes in high and low net feed efficiency animals from Angus NFE selection progeny were measured. The results were used to confirm the role of oxidative phosphorylation in net feed efficiency.

C. Proteomics of mitochondria

Global mitochondrial protein expression differences between in high and low net feed efficiency animals were identified by 2-dimensional differential gel electrophoresis (DIGE) using samples from Angus NFE selection progeny. The results were used to cross-validate the candidate gene list and to predict metabolic pathways likely to be involved in NFE.

Chapter 2

Materials and methods

2.1 QTL mapping of net feed efficiency in beef cattle

Quantitative trait loci (QTL) mapping experiments were conducted in two different cattle populations: Davies mapping herd population (Limousin x Jersey) and Trangie Angus NFE selection line families at Discipline of Agriculture and Animal Science, University of Adelaide and Department of Primary Industry (DPI) at Victoria, respectively. The QTL mapping experiment conducted at Adelaide was performed in two parts: 1) whole genome QTL mapping using microsatellite markers and 2) fine mapping within the identified NFE QTL using SNP marker. The first part was completed separately by Michelle Fenton (2001-2004).

2.1.1 Cattle QTL mapping experimental design: Davies mapping herd

The Davies Cattle Gene Mapping project was established with the intention of identifying DNA markers for QTL affecting beef carcass composition and meat quality and to study the mode of inheritance of important carcass related traits. The project comprised a double back-cross design using two extreme *Bos taurus* breeds [the Jersey (J) dairy breed and Limousin (L) beef breed] (Morris *et al*, 2000). These breeds are known to differ in many traits including carcass composition, fat colour, marbling, body size and meat tenderness (Cundiff *et al*, 1986). Jersey cattle were crossed with Limousin to produce F1 progeny. Three pairs of first-cross (F1=X) half brothers were generated, with one of each pair used for mating in Australia and the other used for mating in NZ to both pure Jersey (J) and pure Limousin (L) dams, creating in total 784 three-quarter XJ and XL backcross progeny (range 120-156 progeny per sire) (Figure 2.1). In Australia, 366 calves were bred by natural mating over three breeding seasons (1997, 1998, and 1999) and reared on their dams in the one location (Martindale, South Australia). Calves were grown out on pasture until approximately 28 months of age and then finished on grain for at least 6 months as part of an intensive feed efficiency trial (age at slaughter was 34-40 months). In total, 210 purebred Limousin and Jersey dams were used to generate the Australian backcross progeny.

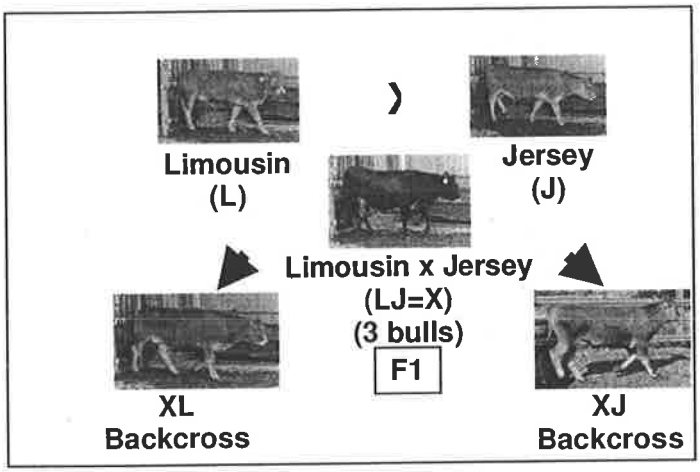

Figure 2.1: Backcross design for genetic mapping in cattle

In New Zealand, 418 calves were born over two years (1996-1997). They were grown out on pasture without grain concentrates and slaughtered at 24-28 months of age. Approximately 300 traits have been measured in the two locations, ranging from carcass composition, behaviour, biochemical traits to feed intake and efficiency. The New Zealand progeny were not measured for feed intake because they were finished on grass and will not be discussed further.

2.1.2 Net feed efficiency phenotyping

There were 80 animals in the first cohort (1996 heifers and steers) which were measured for feed intake at the Tullimba Research Feedlot located in Armidale, New South Wales. The following two years (1997 and 1998) of cattle, the heifers and steers were measured separately. These four cohorts were measured at the Struan Research Feedlot located in Naracoorte, South Australia.

Both feedlots utilised Ruddweigh electronic feeders. Cattle in a feeding pen were tagged with electronic ear tags that produce a signal for a unique number. Feed intake was calculated as the weight of the food after feeding subtracted from weight of the feed before feeding commenced and summed for each day. Also the time taken feeding (ET), the number of feeding sessions (ES) per day and body weight were recorded on a daily basis. Different parameters contributing to NFE such as daily feed intake, metabolic mid-weight, maintenance requirement, gross efficiency and eating rate were also calculated individually for each animal.

The data were analysed by calculating the least-squares means for each animal over a test period. Day was included in the model to allow for weather, personnel, time of feeding and any other factors that could affect the intake of all cattle. Average daily gain was calculated as the regression coefficient (slope) of weight against day of test. Net feed intake was calculated after modelling daily feed intake for metabolic body weight (MMWT) and average daily gain while on the feed intake test (Table 2.1). Although feed intake figures in NFE experiment are not adjusted for DM%, it is close to 100% DM, because animals were on a dry feedlot diet.The initial equation used to calculate daily feed intake (DFI) included the main effect of cohort and interactions between MMWT and ADG (equation 2.1).

Table 2.1: Summary of phenotypic data for the Australian Davies cattle (Fenton, 2004)

Trait	Total number of animals	Mean	CV%	Min.	Max.
MWt (Kg)	324	625.6	13	382.6	824.3
MMWt ($Kg^{0.73}$)	324	109.7	10	76.8	134.5
ADG (Kg/day)	324	0.94	61	-1.43	2.35
ADG (Kg/day)	324	12.94	17	6.37	18.95
NFI (Kg/day)	324	0.05	14	-5.04	7.23

Cohort was defined as the combination of year of birth (1996-1998) and sex (heifer or steer). However, both interaction terms and cohort were not significant. Thus, a simple model comprising only MMWT and ADG was used (equation 2.2). It should be noted that this simple model inflated the phenotypic variance.

DFI = Cohort + MMWT + ADG + Cohort.MMWT + Cohort. ADG + NFI (Equation 2.1)

DFI = Cohort + MMWT + ADG + ε (Equation 2.2)

where, DFI is daily feed intake (g feed/day), ADG is average daily gain (g body weight/day), MMWT is the metabolic mid-weight (g average body weight$^{0.73}$), NFI is the net feed intake and ε is the residual error term for NFI (Fenton, 2004). Net feed efficiency is the same as net feed intake but opposite in direction since animals that eat less are more efficient.

2.1.3 Marker linkage maps

CRI-MAP (Green *et al*, 1990) was used for analysis of the pedigrees to detect any errors in the genotyping of the cattle mapping experiments and to confirm marker order in the linkage maps. Non-Mendelian inheritance was detected when CRI-MAP was used for analysis of pedigree and genotype data file (*.Gen file). However, errors in genotyping do not always lead to non-Mendelian inheritance (the perceived error rate is less than the true error rate) so once the linkage map was built and confirmed with the published map (Bovine ArkDB; http://texas.thearkdb.org/browser?species=cow ; accessed 20th January 2002), the *chrompic* function of CRI-MAP was used. The *chrompic* function finds the maximum likelihood estimates of the recombination fractions of the specified locus order. These estimates were then used to find the particular phase for each sire family and the grand-paternal and grand-maternal phases (Green *et al* 1990). *Chrompic* also gives the number of recombination events. Any individuals with double or triple recombination events were carefully examined for genotyping or pedigree errors, as double recombinants are unlikely when markers are spaced at 20cM intervals (Fenton, 2003).

The *all* function of CRI-MAP was used to build the linkage map. Markers were added one at a time with a LOD score of >3, starting with the markers with the most informative meioses. The *all* function finds $\log_{10}$ likelihoods for all loci orders that result from placing the inserted loci in all possible positions. Those orders with an associated $\log_{10}$ likelihood of less than 3 were eliminated (Green *et al*, 1990). The flips (2-60) function was then used to determine if the fixed marker order was correct.

2.1.4 Microsatellite genotyping

Approximately 150 micro-satellite markers were genotyped for each animal across all autosomes (sex chromosomes not genotyped) using radioactive polyacrylamide gel electrophoresis (PAGE). Each gel was independently scored twice. There were 3-9 markers typed per chromosome for all 29 autosomes, at approximately 20cM intervals. In the half-sib design utilised, sires were all classified as being "AB". Thus, progeny would either inherit an "A" or "B" from the sire and another allele from the dam. Consequently, the genotypes in the progeny were AA, AB, AC, or BC where "C" = any other allele (Figure 2.2). If progeny were AB, then they were not informative for the analysis because it is not clear which allele they received from the sire (A or B).

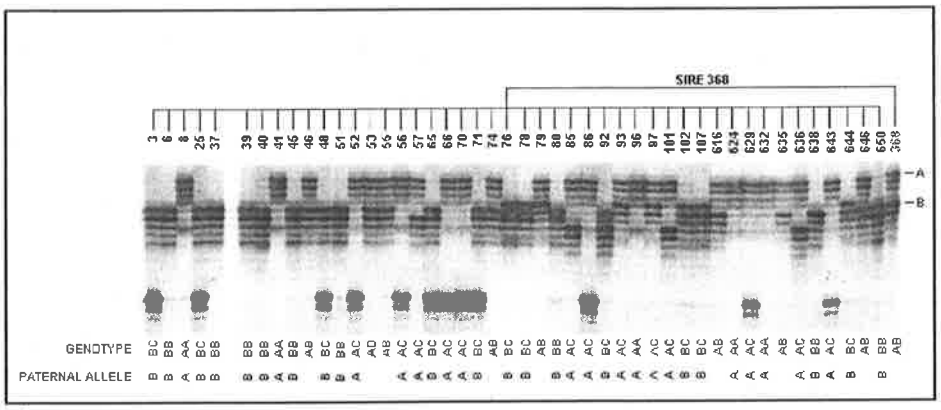

Figure 2.2 Example of genotyping of animals by radioactive PAGE

The *all* function of CRI-MAP (Green *et al*, 1990) was used to construct the marker linkage map as described before. The final linkage maps were compared with the MARC97 bovine genome linkage maps for conserved order and distance (Bovine ArkDB; http://texas.thearkdb.org/browser?species=cow; accessed 2nd January 2002). The MARC97 map marker locations were used for the microsatellite linkage analysis.

2.1.5 QTL analysis

Linkage maps were produced using CRIMAP to confirm the order of the markers and evaluate the data for multiple recombinants. Genotype probabilities were calculated using "QTL Express" (Seaton *et al* 2002; http//qtl.cap.ed.ac.uk; accessed November 2002) for every 1 cM interval on each chromosome. Animals were assigned a value of either 0 (which represents an A allele) or 1 (which represents a B allele) or 0.5 if uninformative. The genotype probability was then calculated between 0.5 and 1, depending on the level of confidence. Phenotypes were regressed against the genotype probabilities for every chromosome using "Haley and Knott regression" (Haley and Knott, 1992). Cohort (combination of sex and breed) and breed of dam (Jersey or Limousin) were included as factors in the model and the regression was nested within sire. Additional models that included two QTL or QTL by breed of dam interactions were also tested for a number of traits.

2.1.6 Threshold values

Experiment-wise threshold values were calculated according to Lander and Kruglyak (1995). Suggestive linkage was defined as $p<0.05$ for a genome-wide test, where one false positive was expected in 20 genome scans. To satisfy this criterion an F statistic of greater than 7.77 was required for tests across three sires. Significant linkages was defined as $p<0.001$ for a genome-wide test, where one false positive was expected in 1000 genome scans. Significant linkages occurred for individual sires when the F statistic was greater than 9.4.

2.1.7 Single nucleotide polymorphisms (SNP) experiments

2.1.7.1 Selection of candidate genes for SNP detection

Based on preliminary QTL analysis results, a fine mapping approach was undertaken to refine and confirm the NFE QTL locations. In this approach, candidate genes controlling the feed intake regulation and energy turnover were identified based on human-cattle comparative genome mapping. Then single nucleotide polymorphism (SNP) variants were found by DNA sequencing the sires for the candidate genes. Selected informative SNPs were genotyped in the Davies mapping population and another QTL analysis was performed.

2.1.7.2 Genomic DNA purification

Cattle blood was collected in ACD-solution A vacutainers (*Becton-Dickinson*) from a jugular vein using an 18 gauge needle (*Terumo*). Blood was mixed thoroughly to prevent clotting and stored at -20ºC for long term storage. Genomic DNA was extracted by phenolic / chloroform extraction method and stored in 1ml TE buffer (pH 8).

2.1.7.3 DNA concentration

The DNA quality was checked by Shimadzu UV-160 spectrophotometer with 0.5 ml quartz glass cuvettes to obtain the optical density ratio (260/280) between 1.6-1.8. Measurement of optical density (OD) was performed at 260 nm and 280 nm by using water as a control. DNA was only used if the OD ratio was between 1.6 - 2.0 (Sambrook *et al*, 1989).

2.1.7.4 Primer design

The bovine DNA sequences were used for designing primers to amplify regions of genes by PCR. Primers were designed for the promoters, 5' UTR, exons and 3' UTR for every selected candidate gene with *Primer3* software and tested against *OLIGO 4.04* software to avoid hairpin structures and primer dimer formation and to minimize the GC content. Oligonucleotides were synthesized by *GeneWorks*, Australia.

2.1.7.5 Optimisation of PCR conditions

Conditions for all primer sets were optimised and the genomic DNA from the three Davies F1 sires 361, 368 and 398 was amplified. PCR reactions were conducted on Omnigene Thermal Cycler with satellite attachments (*Hybaid*) and a Palm Cycler (*Corbett Research*). PCR conditions were optimised for each primer to obtain a single expected size product without any spurious amplicon. 25 µl reactions were performed in 96-well Thermoquick PCR plates with the following reagents.

PCR components	Volume	Final Concentration / µl
10x PCR buffer minus Mg containing 20mM Tris-HCL (pH 8.4), 50 mM KCL	2.5 µl	1X
dNTP (1.25 mM each of dTTP, dGTP dATP and dCTP)	2.5 µl	0.5 mM each
Forward primer (25, 5, 2.5 µM)	1 µl	1 - 0.1 µM
Reverse primer (25, 5, 2.5 µM)	1 µl	1 - 0.1 µM
Magnesium chloride (25 mM)	varies	1.5 - 3 mM
Taq DNA polymerase (0.5 U)	1 µl	0.02 U
Template DNA (100 ng)	1 µl	4 ng
Autoclaved distilled water to a final volume of 25 µl		

Reactions were overlaid with mineral oil (*Sigma*) and amplified under the following conditions:

Calibration factor: 500

Simulated tube control

Step 1 (Initial denaturation and enzyme activation): 1 cycle

95°C for 11 minutes (for *AmpliTaq Gold* DNA polymerase enzyme)

95°C for 4 minutes (for Gibco*Taq* DNA polymerase enzyme)

Step 2: 35 cycles

94°C for 1 minute (denaturation step)

T_A = 70°C - 62°C / 60°C - 50°C / 55°C - 45°C for 1 minute (primer annealing)

72°C for 1 minute (primer extension)

Step 3 (final primer extension): 1 cycle

72°C for 10 minutes

The reactions were stored at 4°C until electrophoresis. In step 2, three touch-down programs were used in combination with varying PCR primer concentrations (25 pmol, 12.5 pmol, 5 pmol, 2.5 pmol) or magnesium concentration (1.5 mM, 2 mM, 2.5 mM, 3 mM) for quick PCR optimisation. Two different DNA polymerase enzymes were used for PCR optimisation; A*mpliTaq Gold (Perkin Elmer Applied Biosystem)* for hotstart PCR and Gibco*Taq (Invitrogen)*.

2.1.7.6 Gel electrophoresis

After optimisation, the desired PCR amplified products were confirmed by running 1-5 µl of the product with a standard molecular size *pGEM marker* (51 bp-2,645 bp) on 2% agarose (P*rogen*) gels by electrophoresis *(Biorad).* Agarose gels were run on 1x TAE buffer (Appendix III 1.1) in a 'wide mini-sub cell' electrophoresis unit *(Biorad)* for 40 min – 1 hr at 90 volts depending on expected amplicon size. The gels were stained with ethidium bromide (0.5 µg/ml) for 10 min and photographed under UV illumination (312 nm) using a Gel-Documentation 1000 system *(Biorad).* The images were captured using *Quantity One 1.0.1* software (*Biorad*) and printed on a *Hewlett Packard 890CXI Inkjet printer.*

2.1.7.7 Automated DNA sequencing

For sequencing, four reactions using optimised PCR conditions were combined for column purification (QIAquick PCR purification columns, *Qiagen*) to remove unincorporated primers and dNTPs. The column eluted PCR product was concentrated in a 60ºC oven for 30 min up to 20 µl. Gel electrophoresis was repeated with 1 µl of the concentrated product to confirm the quality of the PCR product and to quantify the amount of product (30-100 ng) as recommended by the manufacturer's *BigDye* terminator cycle sequencing protocol (*PE Applied Biosystems*).

BigDye terminator cycle sequencing reactions were performed in thin-walled 0.5 ml PCR tubes (Eppendorf). 10 µl sequencing reactions were conducted using 4 µl of the BigDye terminator ready reaction mix, 1 µl of 25 pmol of primer, 1µl of DNA (30-100 ng) and 4 µl of PCR water. Reactions were overlaid with a drop of mineral oil (Sigma) and placed in pre-heated DNA Cetus Thermocycler (*PE Applied Biosystems*) with the following conditions:

25 cycles: 96°C for 30 sec, 50°C for 15 sec, 60°C for 4 min; then held at 4°C.

Cycle sequencing reactions were precipitated by ethanol-sodium acetate reagents according to the manufacturer's protocol (*PE Applied Biosystems*). Sequencing reactions were carefully transferred to another 1ml centrifuge tube (without oil) containing ethanol/salt mix to precipitate the sequencing fragments and remove excess ddNTPs. Reactions were air-dried and sent to the Institute of Medical and Veterinary Science (IMVS, Adelaide, Australia) for electrophoresis of the samples on an ABI 377 (*Applied Biosystems*) DNA sequencing machine. The sequencing of candidate genes was conducted on three Australian crossbreed F1 half-sib sires (Limousin x Jersey). DNA sequencing files of 3 sires obtained from IMVS were analysed by *CHROMAS 1.11 (Griffith University*) software and SNPs were detected with the *SEQUENCHER 4.0* software (*Gene Code Corporation*) by aligning the sequence data of the 3 sires to determine if any sequence variants were present. If sequence variants (usually single nucleotide polymorphisms or SNPs) were discovered, they were verified, first by sequencing the PCR product in the opposite direction, and then, by sequencing the PCR product from the grandparents of the sires to confirm Mendelian inheritance. Not all candidate genes were completely sequenced

because of GC-rich regions within the genes. Therefore, potentially functional SNPs may yet be discovered. Selected SNPs were genotyped in the mapping progeny. The SNP haplotype data generated were also used for association studies with the net feed efficiency data from the progeny.

2.1.7.8 Primer extension

SNP genotyping was performed by a primer extension method with an *AcycloPrime™-FP* SNP detection kit (Perkin Elmer). This kit is designed to determine the base at a SNP location in an amplified DNA sample by a modification of the Template-directed Dye-terminator Incorporation with Fluorescence Polarization detection (TDI-FP) method (Chen *et al*, 1999 and Hsu *et al*, 2001).

The TDI-FP process uses a thermostable polymerase to extend an oligonucleotide primer by one base that ends immediately upstream of the SNP position, using one of two fluorescent dye-labelled nucleotide terminators. The identity of the base added is determined by the increased fluorescence polarization of its linked dye. The process uses *AcycloTerminators™* and *AcycloPol™*, a novel mutant thermostable polymerase from the Archeon family (Figure 2.3).

In this single base primer extension technique, an oligonucleotide probe is designed to anneal immediately one base before to a SNP of interest in PCR-amplified product. In the presence of DNA polymerase and fluorescently labelled dideoxyribonucleoside triphosphates (ddNTPs), the probe is extended by a single base. The specific ddNTP incorporated is dictated by the polymorphic site in the target DNA sequence and results in termination of the extension reaction. Fluorescence polarization is a technique that measures the vertical and horizontal components of the fluorescence emission produced after excitation by plane polarized light by the fluorescent molecules. Fluorescence signals emitted from reaction is used to identify the ddNTP incorporated and assign genotype (Freeman 2002). Polarization values (in millipolarisation, mP units) are inversely related to the speed of molecular rotation of the fluorescent target. Since molecular rotation is inversely related to the molecular volume, incorporation of a fluorescent AcycloTerminator into a primer oligonucleotide increases its polarization (Figure 2.3). This assay was conducted as per manufacturer's technical manual (Perkin Elmer) (Appendix II).

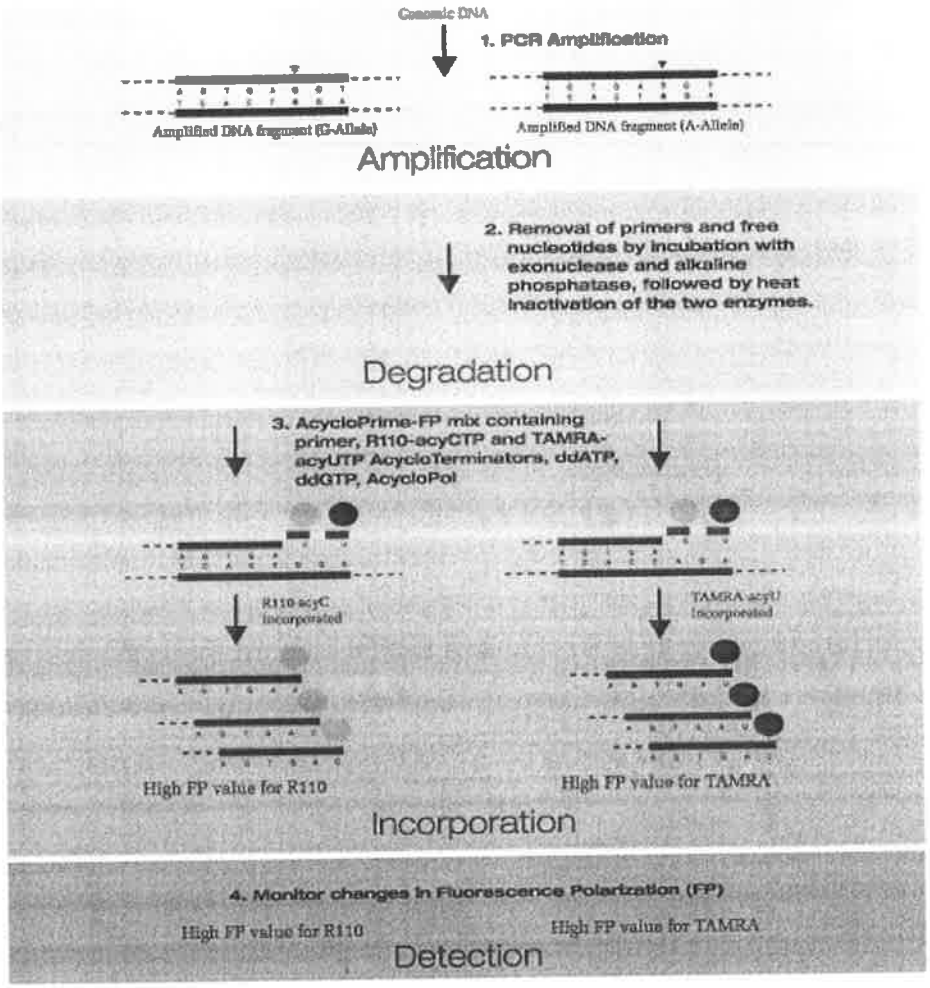

Figure 2.3 Overview of AcycloPrime-FP process (adopted from Perkin Elmer's Acycloprime-FP SNP detection handbook)

2.1.7.9 Statistical analysis for fine QTL mapping and SNP association

SNP markers were chosen such that 3 haplotypes per gene were present and at least 3 - 4 genes were informative in the sire of interest for each QTL. Thus, in general two SNPs per gene were chosen for both linkage analysis on BTA 1, 8, 11 and 20 and association testing (Table 2.2).

The low number of suitable candidate genes on BTA11 resulted in fewer informative genes for this chromosome. The chosen SNP markers were genotyped in the Davies backcross mapping progeny by primer extension. The SNP markers were placed on linkage maps using CRIMAP and SNP positions were also verified where possible from other databases (NCBI Map Viewer, Ensembl and USDA cattle genome map). QTL linkage analysis was performed using the USDA linkage map and "QTL Express" as described in section 2.1.5 (Fenton 2004).

Table 2.2 Number of genes containing SNPs included in the linkage analysis

BTA	Genes	Informative Genes[1]			Segregating sire(s) for NFE QTL
		361	368	398	
1	7	4	4	5	398
8	4	3	3	4	368, 398
11	4	3	2	0	361
20	7	3	5	4	361, 398

[1]Genes heterozygous for sires 361, 368, and 398

In addition to the linkage analysis, association (linkage disequilibrium) analyses were performed in a number of different ways. Initially, all SNPs were coded as factors with 3 levels (e.g. aa, ab, bb) and included in a mixed model across all animals with NFI records. One of the important parameters to estimate was the variance accounted for each SNP. This was a function of both the average effect of gene substitution (α) and the allele frequency (p) as follows:

$$\text{Variance} = 2p(1-p)\alpha^2$$
$$= 2p(1-p)(a+d(1-2p))^2$$

where a = additive effect and d = dominance (Falconer, 1981; Mather and Jinks (1971, 1977)).

The advantage of using the mixed model for testing SNPs is that the variance is estimated. The variance accounted for by a SNP is a function of both the size of effect and the allele frequency. If a SNP is to be commercially valuable, then the size of effect should be significant and the allele frequency ideally would be intermediate. Thus, the benefit of using a mixed model is that both of these are tested. If the SNP accounts for little variance, it converges to zero and is automatically not included in the final model. However, these variance estimates are poorly estimated with only 3 classes and for a number of the SNPs, there are very unequal numbers across the genotypes. The obvious alternative is to include the SNPs as fixed effects, but these results in a model that is highly parameterized with possibly overestimated size of effects.

It is expected that the primary use of SNP genotype information in the future will be to estimate breeding values. Thus, the genotypes can be coded as covariates with values –1, 0 or 1 representing aa, ab and bb, respectively. Fitting the SNPs in this form either saves a degree of freedom for each SNP (if fixed) or minimizes bias (if random). In addition to examining the single SNPs in the two methods outlined, when there were 2 SNPs per gene, haplotypes were formed and tested to see if they were more informative than the single SNPs.

The SNPs were fitted as random main effects and haplotypes and coded as factors with 3 classes or additive (covariate) effects. The model also included the fixed effect of breed of dam (Jersey or Limousin). In addition to the SNPs, an animal model to account for polygenic effects was included. However, for both genotype and additive effects, the largest two SNPs were sufficient to prevent the polygenic variance from being estimated. This was not unexpected because the population had a small number of very large half-sib families and therefore, was far from ideal for estimation of polygenic effects.

2.2 Mitochondrial proteomics and enzyme experiments

2.2.1 Selection lines

Experimental animals in the mitochondrial proteomics and enzyme studies came from the Angus Elite Progeny Testing Program. Industry Angus stud bulls were crossed with Angus cows from the net feed intake selection lines at Trangie, NSW (Department of Primary Industry, NSW). Data collected on the calves included growth performance, structural soundness and ultrasound measurements of fat depth, eye muscle area and marbling. The steer progeny were finished on grain and slaughtered, with additional measurements taken on net feed intake and carcass traits.

Samples were collected in 2 consecutive years in 2005 and 2006. 132 steers from 12 sires in year 2005 and 136 steers from 12 sires in year 2006 were used for sample collection. The steers were born at the Trangie Agricultural Research Station, New South Wales, in the months of July-August in 2003 and 2004. They were weaned in March 2004 and 2005, respectively. Animals born in 2003 were backgrounded at Glen Innes (NSW) or Rutherglen (Victoria), before transfer to Tullimba in November 2004 for feedlot finishing and NFI testing. They were slaughtered at AMH Beef City, Queensland in April 2005. Animals born in 2004 were backgrounded at Grafton, and then at Glen Innes, NSW. At Glen Innes, they were spilt into two groups and maintained in a feedlot in those two groups throughout the feed intake testing at Tullimba, before transfer to Warwick, Queensland in May 2006 for slaughter. The steers were adapted to the feeders for 14 days before starting the test for 70 days. During the test period, the steers were weighed every 14 days. The test was designed to allow animals to feed *ad lib* and record electronically how much the animal ate each time it entered the feeders. NFI was calculated for all the steers. At slaughter, data on carcass weight, eye muscle area, rib-fat, marbling, weight of bone (radius-ulna), chuck weight, meat pH and meat colour were recorded. Average body weight of the animals was 600 kg. Adjusted NFI distribution (that is adjusted for cohort) of the Angus steers of 2005 kill ranged from –2.69 to 3.63 kg/day and the 2006 kill ranged from -2.55 to 4.47 kg/day range (Figure 2.4).

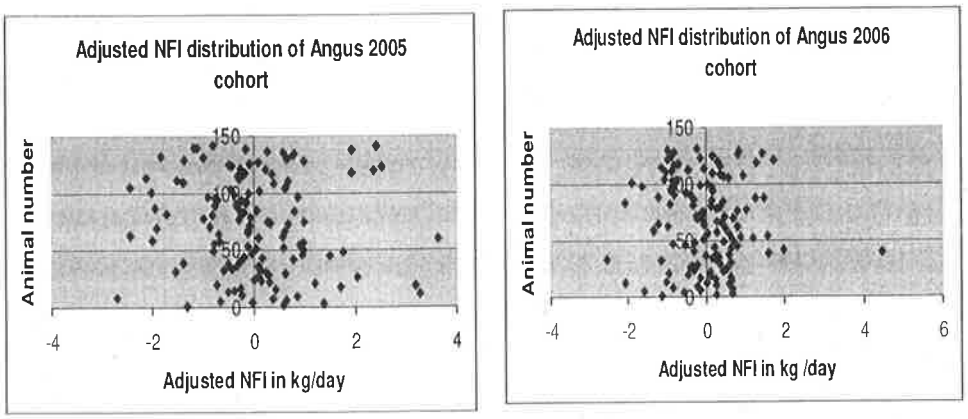

Figure 2.4 Adjusted NFI distributions in Angus animal cohort 2005 and 2006

2.2.2 Sample collection

For the mitochondrial proteomics and enzyme experiments, liver and muscle samples were collected. For the liver samples, 4 g was procured from the caudal left lobe of liver. Samples were collected approx 30 min after the animal was killed. For the muscle samples, 4-5 g of neck muscle (brachiocephalicus) were collected from the animal 5-10 min after the animal was killed. All samples were collected in 50 ml flat bottom containers (*Sarstedt*) and snap frozen in liquid nitrogen. Samples were air freighted to Roseworthy Campus on dry ice and stored at -80°C until analysed.

2.2.3 Isolation of mitochondria from liver and muscle samples

2.2.3.1 Mitochondrial preparations from frozen liver samples

The procedure for the isolation of mitochondria was adapted from Salt *et al* (1998), Cawthon *et al* (1998), Trounce *et al* (1996), Madapallimattam *et al* (2002) and Bhattacharya *et al* (1991). The entire procedure was performed at 4°C to avoid enzyme degradation. Samples were transferred from -80°C to 4°C briefly for cutting 4 gm from the sample for mitochondria purification and the remainder was transferred immediately back to -80°C for future use. The 4 gm of sample was finely chopped into small pieces and transferred to 5 ml ice-cold lysis buffer solution (Appendix III 1.2). The finely chopped tissue was incubated in ice-cold buffer for 15 min. and then homogenised with an *Ultra-Turrex* S25N-8G homogeniser (*IKA Labortechnik*) at 12,000rpm for 30 seconds. The samples were homogenised twice with 30 seconds on ice between each homogenisation burst and the homogeniser probes were chilled on ice (wrapped in aluminum foil) prior to use. Homogeniser probes were washed well between each sample and the probe was disassembled and any connective tissue that had accumulated behind the homogeniser head was removed to minimise cross-contamination of samples. The resulting homogenate was centrifuged with Beckman J2-HS refrigerated centrifuge with JA-20 rotor at 2500*g* for 10 min at 4°C. After filtering of the supernatant through two layers of nylon cloth, the supernatant was centrifuged at 14,000*g* for 30 min at 4°C to obtain the brown colored mitochondrial pellet. The cytosolic

fraction (supernatant) was used for AMP activated protein kinase (AMPK) enzyme assays. The mitochondrial pellet was re-suspended and washed twice in isolation buffer (Appendix III 1.3) to remove any non-mitochondrial impurities. The resulting pellet was resuspended in 0.3-0.5 ml isolation buffer and frozen at –80°C for subsequent biochemical analyses.

2.2.3.2 Mitochondrial preparations from frozen muscle samples

Several methods have been reported for the isolation of mitochondria from skeletal muscles from different species. Due to the tough myofiber content of skeletal muscle, collagen and other cytoskeletal components, muscle requires relatively high shearing force to release the mitochondria. However, high shear force causes heat production during homogenisation, which degrades the heat-labile proteins. Therefore, the bacterial proteinase enzyme nagarse (Sigma) was used to digest skeletal muscle cells. The procedure for the isolation of muscle mitochondria was adapted from Bhattacharya *et al* (1991). The entire procedure was performed at 0-4°C.

Muscle (4-5 g) was minced with a scalpel and transferred to a Petri dish containing 1-2 ml of medium I (Appendix III 1.4) for further dissection and fine chopping and teasing to remove visible connective tissue and fat. After transfer to 50 ml Falcon tubes, the sample was centrifuged at 2500*g* using a *Beckman J2-HS* refrigerated centrifuge with JA-20 rotor to remove debris by discarding the supernatant. Prior to homogenization, the pelleted minced tissue was incubated in 6 ml of medium II (Appendix III 1.5) containing nagarse proteinase medium for 5 min at room temperature. Then 20 ml of medium II without nagarse enzyme was added to dilute the concentration of nagarse and to stop the action of the enzyme. Nagarse was removed by centrifugation at 2500*g* for 10 min and discarding the supernatant. 5 ml of medium II without nagarse enzyme was added to the pellet and the sample homogenized with an *Ultra-Turrex* homogeniser *(IKA Labortechnik)* at 12,000rpm for 60-90 min. The resulting homogenate was centrifuged at 2500*g* for 10 min at 4°C. After filtering of the supernatant through two layers of nylon cloth, the supernatant was centrifuged at 14,000*g* for 30 min at 4°C to obtain the brown colored mitochondrial pellet. This pellet was then re-suspended and washed twice in medium III (Appendix III 1.6) to remove any non-mitochondrial impurities. The resulting pellet was resuspend in 0.3-0.5 ml isolation buffer (Appendix III 1.7) and frozen in –80°C for subsequent biochemical analyses.

2.2.4 Experimental animals

2.3.4.1 Mitochondrial enzyme studies

The top 20 animals from low and high NFE animals of the 2005 cohort were chosen to measure the enzymatic activity of complex I and top 10 low and high NFE animals were used to measure the enzymatic activity of complexes II and IV. The average difference in adjusted NFI between two groups

ranged from 1.45 to -1.47 kg/day (Table 2.3, Figure 2.5). There was no difference found in average daily gain (ADG) and traits such as metabolic mid weight (MMWT), eye muscle area (EMA) and left side hot carcass weight (HSCW) (Table 2.3).

Table 2.3 Growth and net feed intake differences in low *vs.* high net NFE animals (Angus 2005 cohort).

Variables	Low NFE (n=22)	High NFE (n=18)	p-value
Adjusted NFI (kg feed/day)	1.45 ± 0.20	-1.47 ± 0.17	<0.0001
MMWT (kg)	104.06 ± 1.22	102.13 ± 1.20	NS
ADG (kg)	1.43 ± 0.03	1.41 ± 0.03	NS
DFI (kg)	17.41 ± 0.26	13.33 ± 0.33	<0.0001
NFI (kg feed/day)	1.82 ± 0.19	-1.62 ± 0.26	<0.0001
Eye Muscle Area (cm^2)	80.23 ± 1.20	73.33 ± 1.125	0.06
EBV IMF	0.55 ± 0.12	0.63 ± 0.11	NS
EBV NFI	0.16 ± 0.04	-0.32 ± 0.06	<0.0001
Left side HCSW	174.63 ± 2.58	178 ± 3.07	NS

Values are least square means ± SE. NS, non-significant, P > 0.05. NFI: adjusted net feed intake; MMWT: metabolic body weight; ADG: average daily gain; DFI: daily feed intake; EBV: estimated breeding value; HSCW: hot carcass weight

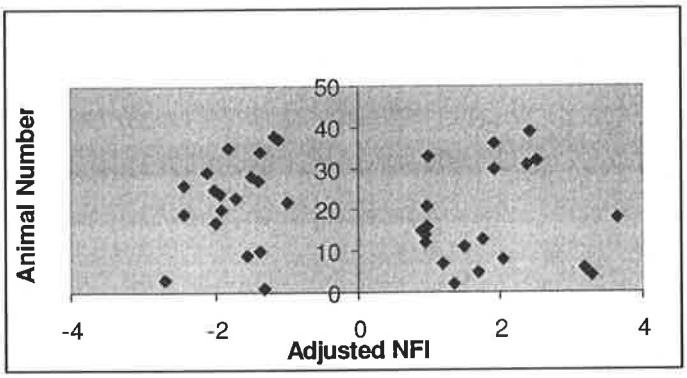

Figure 2.5 Adjusted NFI distribution of the Angus 2005 animals selected for measuring the mitochondrial enzyme complex activities.

2.2.4.2 Proteomics studies

Animals with extreme phenotypes in the Angus cohort 2005 (n = 14) and cohort 2006 (n=10) were selected for the proteomics experiments. There was no difference between the high and low NFE animals for average daily gain (ADG) and carcass composition traits such as metabolic mid weight (MMWT), eye muscle area (EMA) and left side hot carcass weight (HSCW). However, the adjusted NFI

varied from -2.2 to 2.59 kg feed per day in the 2005 cohort and -2.04 to 2.26 kg feed per day in the 2006 cohort (Table 2.4 and Table 2.5).

Table 2.4 Growth and net feed intake differences in selected low *vs.* high net NFE animals (Angus 2005 cohort) selected for proteomics studies

Variables	Low NFE (n=7)	High NFE (n=7)	P-value
Adjusted NFI (kg feed/day)	2.59 ± 0.21	-2.2 ± 0.11	<0.01
MMWT (kg)	100.12 ± 1.30	100.56 ± 1.59	NS
ADG (kg)	1.37 ± 0.44	1.33 ± 0.43	NS
DFI (kg)	17.19 ± 1.57	12.17 ± 1.32	<0.01
NFI (kg feed/day)	2.60 ± 0.23	-2.43 ± 0.33	<0.01
Eye Muscle Area (cm^2)	78.14 ± 1.33	72.14 ± 1.26	<0.05
EBV IMF	0.4 ± 0.1	0.6 ± 0.2	NS
EBV NFI	0.25 ± 0.1	-0.56 ± 0,06	<0.01
Left side HCSW	175.71 ± 3.05	172.57 ± 3.78	NS

(Abbreviations are mentioned in Table 2.3)

Table 2.5 Growth and net feed intake differences in selected low *vs.* high net NFE animals (Angus 2006 cohort) selected for proteomics studies

Variables	Low NFE (n=5)	High NFE (n=5)	p-value
Adjusted NFI (kg feed/day)	2.26 ± 0.55	-2.04 ± 0.15	<0.0001
ADG (kg)	1.7 ± 0.08	1.54 ± 0.17	NS
DFI (kg)	17.5 ± 0.73	11.71 ± 0.74	<0.01
NFI (kg feed/day)	1.88 ± 0.55	-2.42 ± 0.15	<0.0001
EBV IMF	0.44 ± 0.13	0.48 ± 0.16	NS
EBV NFI	0.292 ± 0.07	-0.54 ± 0.14	<0.01
Eye Muscle Area (cm^2)	76.4 ± 2.27	74.6 ± 3.13	NS

(Abbreviations are mentioned in Table 2.4)

2.2.5 Protein concentration measurements

For the enzyme assays, protein concentration was measured by using the *RC DC* protein assay kit (*Bio-Rad*). The RC *DC* protein assay is a colorimetric assay. This assay is based on the Lowry assay (Lowry *et al*, 1951), but has been modified to be reducing agent compatible as well as detergent compatible. Standard protein curves were prepared with bovine serum albumin in the 0.2-1.5 mg/ml range. All samples and standards were measured in a 300 µl flat bottom 96 well plate *(Nalgen Nunc In)* with 96 well plate reader *Titertek Multiscan* at 750 nm. The EZQ protein quantitation assay kit (Molecular Probes) was also used to measure the concentration of protein against an ovalbumin standard curve for the 2-D differential gel electrophoresis (2-D DIGE) experiments to improve the sensitivity of assay.

2.2.6 Assessment of mitochondrial preparations

2.2.6.1 Citrate synthase assay

The quality of the mitochondrial preparations was determined by first measuring the citrate synthase activity. Citrate synthase is the most commonly used matrix marker enzyme (Trounce *et al*, 1996; Robinson and Srere, 1985). Mitochondria are sufficiently pure if citrate synthase activity in the mitochondrial fraction is 3-4 fold higher than in the homogenate. Citrate synthase activity was assessed by reduction of 5, 5'- dithiobis-2-nitrobenzoic acid (DTNB) as a measured in a spectrophotometer at 412 nm (extinction coefficient 13.6 Mm^{-1} cm^{-1}) at 30ºC, coupled with the reduction of acetyl-CoA by the citrate synthase enzyme in the presence of the oxaloacetate substrate (Ian *et al*, 1996 Madapallimattam *et al*, 2002). The chemical coupling of reduced coenzyme A with DTNB reagent releases a mercaptide ion.

The reduction of DTNB was followed at 412 nm in a 1ml quartz cuvette at 30ºC. The reaction mixture of 0.1 M Tris-HCl, pH 8, 0.3 mM acetyl coA, 0.1mM DTNB and 10 µl (30 µg) cell mitochondrial protein was incubated at 30ºC for 10 min. The reaction was initiated by the addition of 0.5 mM oxaloacetate and the absorbance change was monitored for 1 min.

2.2.6.2 Electron microscopy

Mitochondrial density from extracted liver and muscle samples was also checked by transmission electron microscopy (TEM). A mitochondrial pellate from 50µl of the extracted mitochondrial samples was embedded in parafine blocks and cut into small blocks (approximately 1 x 1 x 2 mm in size) and fixed overnight in 4% paraformaldehyde/1.25% glutaraldehyde in PBS and 4% sucrose, pH7.2. The blocks were rinsed in washing buffer (PBS + 4% sucrose) for 5 mins. and post-fixed in 2% aqueous osmium tetroxide (OsO4) for 30mins. After post-fixing, samples were dehydrated in graded concentrations of ethanol as follows:

70% ethanol - 2 x 10 minutes

90% ethanol – 2 x 10 minutes

95% ethanol – 1 x 10 minutes

100% ethanol – 2 x 10 minutes

After a 10 minute rinse in propylene oxide, specimens were infiltrated with a 1:1 mixture of propylene oxide and epoxy resin (Procure Araldite Embedding Resin) for 30 minutes and then with two changes of 100% resin for 30 minutes each. Samples were embedded in fresh resin and polymerized at 70°C for 24 hours.

70nm thick sections were cut on a Reichert Ultracut E ultramicrotome, using a diamond knife. The sections were picked up on 200 mesh copper/palladium grids, and stained with uranyl acetate and lead citrate. They were imaged in a Philips CM100 Transmission Electron Microscope.

2.2.7 Assays of oxidative phosphorylation enzyme complexes

The oxidative phosphorylation complex enzyme assays were performed on mitochondria prepared from frozen tissue stored at -80°C without compromising enzyme activity (Fredriksson *et al* 2005; Brooks and Krahenbuhl, 2000; Rasmussen U and Rasmussen H, 2000). All reagents were purchased from Sigma.

2.2.7.1 Complex I activity (NADH ubiquinone:oxidoreductase)

The method for assessing the activity of complex I (NADH ubiquinone:oxidoreductase) was adapted from Ian *et al* (1996) Madapallimattam *et al* (2002) and Iqbal *et al* (2003). 100 µg mitochondrial protein was added to 1 ml solution containing 50 mM Tris-HCL and 1.3 mM 2,6 dichloroindophenol (DCIP). The reaction was measured by the addition of freshly prepared 15 mM NADH. Complex I activity was measured by following the decrease in the absorbance due to the oxidation of NADH at 600 nm in a 1ml quartz cuvette against the control (without NADH) for 10 min using a spectrophotometer (Shimadzu UV-160A). Activity was determined by using the NADH extinction coefficient of ε = 21 mM^{-1} cm^{-1}. Sensitivity of this assay was checked by the addition of the complex I inhibitor rotenone (2 µg / ml 100% ethanol).

2.2.7.2 Complex II activity (succinate:ubiquinone oxidoreductase)

The method for assessing the activity of complex II succinate:ubiquinone oxidoreductase was adapted from Ian *et al* (1996). 30 µg mitochondrial protein was incubated in a 1 ml mixture of 50 mM potassium phosphate, pH 7.4 and 20 mM succinate at 30°C for 10 min. Then another mixture of antimycin A (2 µg/ml 100% ethanol), rotenone (2 µg/ml 100% ethanol), KCN (2 mM), and 50 µM 2,6 dichloroindophenol

(DCIP) was added. The reaction was initiated by adding 50 µM of decylubiquinone (DB) prepared in 100% ethanol and the reduction of DCIP was measured at 600 nm absorbance with a spectrophotometer (Shimadzu UV-160A) in a 1 ml cuvette at 30^0C against a control without DCIP. Activity was determined by using an extinction coefficient of ε = 21 $mM^{-1}cm^{-1}$. The sensitivity of this assay was checked by using the complex II inhibitor melonate (0.5 M).

2.2.7.3 Complex IV activity: (ferrocytochrome c:oxidoreductase)

The method for assessing the activity of complex IV ferrocytochrome c:oxidoreductase was adapted from Ian *et al* (1996). 10 µg mitochondrial protein was added to 1 ml solution containing 50 mM KH_2PO_4, 15 µM reduced cytochrome c (Appendix III 1.8), 0.005% dodecylmaltoside. The oxidation of ferrocytochrome c was followed at 550 nm absorbance with a spectrophotometer (Shimadzu UV-160A) in a 1ml cuvette at 30^0C for 10 min against a control without protein. The sensitivity of this assay was checked by using the complex IV inhibitor potassium cyanide (2 mM KCN). The enzyme activity was determined by using an extinction coefficient of ε = 19.21 $mM^{-1}\,cm^{-1}$.

2.2.7.4 Statistical analyses of enzyme assays

Regression analyses were conducted to determine the relationship between net feed intake and the complex enzyme activities. Data were evaluated by single factor ANOVA and results were considered significant at the 5% level.

2.2.8 Two-dimensional differential gel electrophoresis (2-D DIGE)

The principle of 2-dimensional gel electrophoresis for protein separation involves 2 components; isoelectric point (*pI*) and molecular weight (MW). Isoelectric point (*pI*) of protein is based on the pH at which a protein carries no net charge and will not migrate in an electric field. Resolution of proteins based on isoelectric point is referred as the first dimensional separation. Separated proteins on an immobilized pH gradient (IPG) strip in the first dimension are further resolved by their mass or molecular weight by electrophoresis of the IPG strip on a sodium dodecyl sulphate–polyacrylamide gel (SDS-PAGE). This process is referred as the second dimensional separation.

2.2.8.1 Mitochondrial sample preparation

Aliquots of the mitochondrial preparations containing 50 µg of protein were pooled from the high and low efficiency animals. The samples were prepared for 2-D electrophoresis by protein precipitation using a 2-D Clean Up Kit (*GE HEALTHCARE*). The final pellet was resuspended in 100 µl of IEF buffer (7 M urea, 2 M thiourea, 2% 3-[(3-cholamidopropyl) dimethylammonio]-1-propanesulfonate, CHAPS) and 10 mM dithiothreiotol (DTT). The samples were left at ambient temperature for 1 hour and centrifuged at 8000g for 5 min. The protein supernatants were then collected and the pH of the samples was adjusted

to 8.5 with 0.2 M sodium hydroxide (NaOH). An EZQ assay was performed to determine the protein concentrations of the samples after purification.

2.2.8.2 Preparation of CyDye fluors

Dry CyDye reagents were purchased and reconstituted in high quality anhydrous dimethylformamide (DMF) so that final concentration of CyDye stock solution was 1nmol/µl as described by the manufacturer (GE HEALTHCARE). On reconstitution in DMF, the CyDye gives a deep colour; Cy2 = yellow, (3-(4-carboxymethyl) phenylmethyl)-3'-ethyloxacarbocyanine halide N-hydroxysuccinimidyl ester, Cy3 = red (1-(5-carboxypentyl)-1'-propylindocarbocyanine halide N-hydroxysuccinimidyl ester and Cy5 = blue (1-(5-carboxypentyl)-1'-methylindodicarbocyanine halide N-hydroxysuccinimidyl ester.

2.2.8.3 Labelling with CyDye

The CyDye working reagents were prepared after reconstitution as described by the manufacturer (*GE HEALTHCARE*). 1µl (400 pmol) aliquot of CyDye was added per 50 µg of protein. The samples were then incubated on ice in darkness for 30 minutes. The labelling reaction was stopped by the addition of 1µl of 10 mM lysine per 50 µg of protein. Dye swapping was performed among 2 pooled samples from high and low NFE animals to account for any technical variations such as differential labelling efficiencies, variation in 1st and / or 2nd dimensional electrophoresis, etc.

2.2.8.4 Sample preparations for iso - electric focusing

Once samples were labelled, the appropriate samples were combined with 55.5 µl of the unlabelled samples. Prior to iso-electric focusing, sufficient volumes of 0.5 M dithiothretiol (DTT) and 3-11 NL carrier ampholytes were added such that the final samples contained 65 mM DTT and 0.5% ampholytes, plus trace amounts of bromophenol blue (BPB) as a tracking dye.

2.2.8.5 Preparation of immobilised pH gradient (IPG) strip for iso-electric focusing (1st dimensional)

A broad range 24 cm NL immobilised pH 3-11 gradient IPG strip (*GE HEALTHCARE*) was selected to identify the global protein expression in mitochondria. The IPG strips were rehydrated (gel facing down) in an iso-electric focusing re-swelling tray overnight in 450 µl rehydration buffer containing 7 M urea, 2 M thiourea, 2-4% CHAPS, 2% 3-11 NL carrier ampholytes and 1.2% DeStreak reagent (*GE HEALTHCARE*).

2.2.8.6 Sample loading for iso-electric focusing (1st dimensional)

After the strips had rehydrated, they were moved to the iso-electric focusing tray gel facing up. Excess liquid from the strip was blotted with moist filter paper. Tap water wetted (not soaked) wicks were

positioned within the indentations of the channels at both end (cathode and anode) of the strip. Wicks are highly recommended at the end of IPG strips because they collect salts and other contaminants in the sample. The strips were covered with mineral oil before focusing to prevent evaporation and carbon dioxide absorption during focusing. IPG strip channels were filled with oil. 400 µg sample was applied to the IPG strip by cup-loading. Iso-electric focusing was performed using the following 6-step program with the current limited to 50 µA per strip. Iso-electric focusing was conducted using the *Ettan*™ IPGphor™ isoelectric focusing system (Amersham Biosciences). The strips had 52,700 total volt-hours over 20:29 hours.

Step	Voltage	Type	Duration (hours)
1	300	Step and hold	2
2	500	Step and hold	2
3	1000	Step and hold	2
4	1000-8000	Gradient	5
5	8000	Step and hold	3
6	500	Step and hold	10

2.2.8.7 IPG equilibration for second dimension

To solubilise the focused proteins and to allow effective sodium dodecyl sulphate (SDS) binding in preparation for the second dimension, it was necessary to equilibrate focused IPG strips in SDS containing buffers. After placing the strip gels face up in channel, the channel was filled with the 10 ml DTT-SDS equilibration buffer (Appendix III 1.9). After 20 min., the DTT buffer has reduced the sulfhydryl groups. The buffer was then decanted and the channels were refilled with equilibration buffer containing 250 mg /ml of iodoacetamide in place of DTT and incubated again for 10min. The iodoacetamide buffer alkylates the sulfhydryl groups.

2.2.8.8 Sodium dodecyl sulphate-polyacrylamide gel electrophoresis (SDS-PAGE)

Sodium dodecyl sulphate-polyacrylamide 12.5% gels (Appendix III 1.10) (SDS-PAGE) were prepared in-house on 25 x 20 cm low-fluorescence glass plates (*GE HEALTHCARE*). The backing plates were treated with a solution of 0.1% bind-silane prepared in 80% ethanol and 2% glacial acetic acid (*GE HEALTHCARE*) prior to casting, which helps in adhering the gel to the plate for subsequent staining, distaining and spot picking. The plates were prepared with a 1 mm spacer.

The equilibrated IPG strips were positioned directly on top of the SDS-PAGE. To secure the strip in place, 0.5% low melting point agarose (sealing solution, Appendix III 1.11) prepared in electrophoresis buffer (Appendix I 1.) was overlaid on the strip with 10 µl of bromophenol blue dye in order to track the ion front during the run. SDS-PAGE standards were used by dipping the wick into a molecular weight standard ranging from 200-6 kDa (*Invitrogen Mark 12*). The gels were electrophoresed in buffer

(Appendix III 1.12) at 5 W/gel for 45 minutes, followed by 17 W/gel for 2 hours and then 34 W/gel until the dye front emerged (4-5 hrs). SDS-PAGE was conducted in a *Ettan* DALT twelve large format vertical system (Amersham Biosciences).

2.2.8.9 DIGE image acquisition

After SDS-PAGE, the gels were scanned using a *Ettan* DIGE imager (*GE HEALTHCARE*) at 100 µm resolution with the exposure set at 0.8 seconds for Cy2, 0.2 seconds for Cy3 and 0.35 seconds for Cy5 scanning. The exposure setting was standardized based on 8 gel runs and the image quality examined before running experimental samples. The excitation/emission wavelengths for Cy2, Cy3 and Cy5 were 480/530, 540/590 and 620/680 nm, respectively. ImageQuant (*Molecular Dynamics*) software was used to adjust the brightness of the Cy3 and Cy5 channels and produce a yellow colour for the majority of spots. The red and green channels were electronically swapped using ImageQuant such that the high efficiency group was green and the low-efficiency group was red. Accordingly, those spots that were up-regulated in the high efficiency cattle relative to low efficiency cattle appeared more green than the average yellow spot, whilst those spots up-regulated in the low efficiency cattle relative to the high efficiency cattle appeared more red.

2.2.8.10 DIGE image analysis

Image analysis was undertaken using *DeCyder* 2D software (*version 6.5, GE HEALTHCARE*). *DeCyder* is composed of two modules, the data image analysis (DIA) and the biological variation analysis (BVA). The DIA software module provides consistent and accurate co-detection and differential quantification of protein spots from a set of images of Cy5, Cy3 and internal standard Cy2 (mixture of samples from two groups) from the same gel using novel algorithms (Figure 2.6). Background subtraction, quantitation, normalization and first level matching within a gel are automated for high-throughput analysis with low experimental variation. The DIA module measures spot protein abundance for both Cy5 and Cy3 images. The differential quantification is expressed as a spot ratio. It is a comparison of the spot volumes of the Cy5 and Cy3 images with the corresponding spot volumes of the Cy2 of the internal pooled standard. It links every sample to an internal pooled standard, which makes direct comparison of protein expression levels between multiple gels easier and more accurate (Alban *et al* 2003).

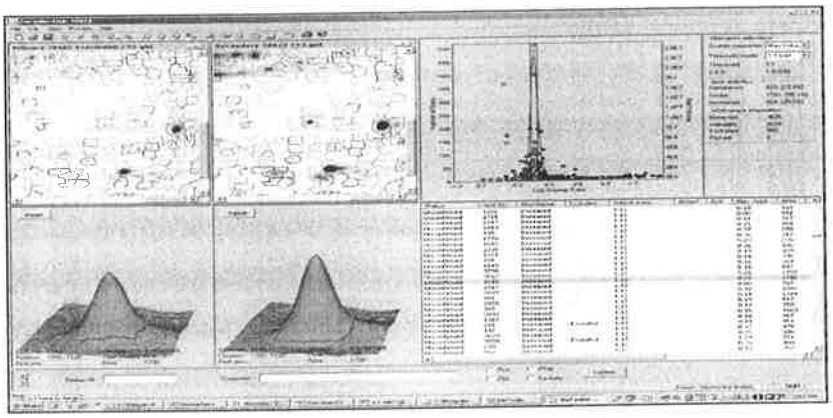

Figure 2.6 DIA user interface shows different quadrants: gel view, histogram view, 3-D view and Spot Table view. Each of these views is linked so that selecting a spot in one view will display related information of the same spot on other quadrants.

The batch-processing mode was used to which automates the process of spot detection, matching multiple gels, interpretation and exportation to the biological variation analysis (BVA) module without user interaction. Images are then matched between gels using the biological variation analysis (BVA) software module that looks for consistent differences between samples across all the gels and applies statistics to associate a level of confidence for each of those differences (Figure 2.7). The BVA module is used to establish the significance of changes in expression of specific proteins from different experimental groups. The student t-test was used to select differentially expressed proteins for picking, digestion, and subsequent analysis by mass spectrometry. Selection of protein spots was based on multiple criteria such as the statistical significance of change ($p<0.05$), the magnitude of the change, and the spot volume (Alban *et al* 2003). The statistical analysis functionality was not valid unless the experimental design includes an internal standard on every gel.

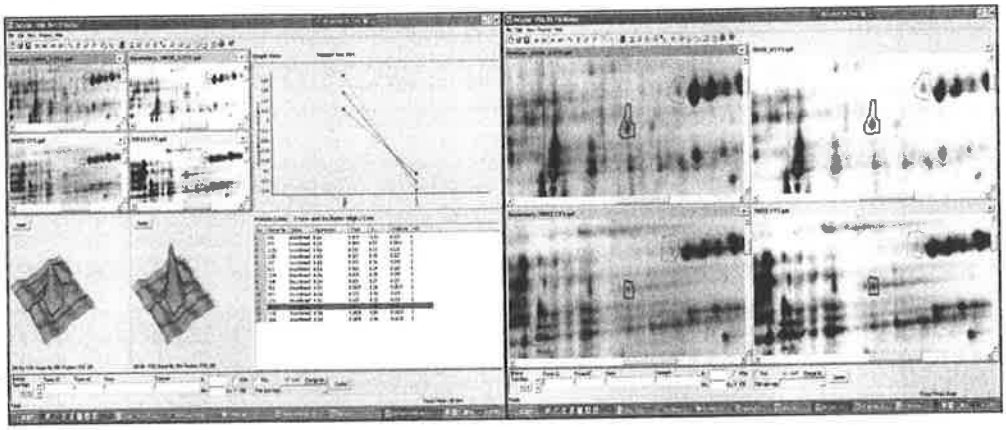

Figure 2.7 BVA module is used to detect and statistically quantitate sample differences between multiple gels.

The principle of the normalisation is based on the assumption that the protein spots do not change from one image to another. The spot volume ratio is based on a histogram representation of the $\log^{10}$, which

resembles a normal distribution. After fitting a model normal distribution to the main peak of the histogram, it identifies the actual volume ratio that should be mapped to a log volume ratio of zero. Histogram data below 10% of the main peak height are considered as outlier data and are removed in the fitting procedure. Using the centre of the model distribution, all individual volume ratios are mapped to align the log volume ratio histogram around zero (Alban *et al* 2003).

2.2.8.10.1 Spot detection

For the batch processor, the number of spots was estimated at 4000 and the exclusion filter applied to those spots had a slope of >1.1, an area of <600, a volume of <10,000 and a peak height of <80 and >65000. Slope refers to the relative abundance of protein and here "slope" is a parameter used to exclude artefacts. Dust particles give peaks of high slope that can be excluded when matching gels. Exclusion areas were also defined within the regions of the gel that showed high levels of streaking. Following the application of the filter, the threshold within the histogram window was manually set to the 1.5 - 2 SD. This standard deviation represents the fold-ratio that encompasses 95% of the spots and can be used as a guide to determine the level of experimental variation. The spots that were found to be differentially expressed between the two experimental samples, based on that threshold, were manually checked. If a spot was found to be an irregularity in the gel surface, they were excluded from further analysis. The exclusion of one or more spots modified the standard deviation for the dataset. Hence, the threshold also changed, thereby resulting in new spots being reported as differentially expressed. These spots were then manually checked for validity. This threshold adjustment/exclusion process was repeated until all of the differentially expressed spots for a particular standard deviation were validated. Spot editing was done manually using the *DeCyder* 2D software.

2.2.8.10.2 Background subtraction

The spot background intensity levels were calculated using the *DeCyder* 2D Software and based on the 10th percentile pixel value at the spot border. The background compensated spot volumes were then used to calculate the log volume ratio for each spot in the gel. This was done by dividing the volume in the secondary gel view by the volume in the primary gel view. The process was performed automatically.

2.2.8.10.3 Spot Matching

Spot matching was performed manually by choosing a gel as the reference or master gel. The gel for which the pooled internal standard (Cy2) demonstrated the highest number of spots was selected as the master gel. During the matching process, it was noted that certain spots were identified within one gel as a single spot, whilst in other gels; the corresponding spot was divided into two. These spots were merged to compensate for the inconsistency. Spot normalization was carried out for all matched spots.

2.2.8.10.4 Normalization of spot intensities

The spot margins and the total pixel intensity were determined to quantify the absolute spot intensity. While calculating the abundance ratios for the spot pairs in co-detected sample images (Cy3 and Cy5), the spot volumes need to be normalized to compensate for the experimental variation due to different laser intensities, differences in fluorescence and filter transmittance, differences in sample entry into the IPG strip or protein loss during iso-electric focusing. The normalization procedure used in the BVA module is based on the pooled internal standard image, which was included with each gel in the experiment. A standardized volume ratio for each standard image was set to the value of 1.0. The *expression volume ratio* of a sample spot is related to its corresponding standard spot (internal standard) within that particular gel, thus making it possible to compare ratios between matched protein spots in the different gels. In simple terms, *expression volume ratio* is the calculation of average spot volume ratio between two experimental groups for a matched protein spot. The ratio values were expressed as fold changes, i.e. a 1.5 fold increase was expressed as "1.5" and a decrease was expressed as "-1.5". No change in volume ratio was expressed as 1.00. This process was performed automatically by the *DeCyder* 2D software. Normalized spot volume was used in current study. Spot intensities (spot volume) were then normalized as percentage of the total spot volume for each CyDye using spots that were present in all gels and compared between gels.

2.2.8.11 Protein identification

The protein in a given spot was excised and digested with the proteolytic enzyme trypsin. The peptides produced by digestion were co-precipitated with an ultraviolet light-absorbing matrix such as α-cyano-4-hydroxycinnamic acid (HCCA). The peptides were then irradiated with a focussed short pulse of ultraviolet radiation of an appropriate wavelength under vacuum. This technique is called matrix-assisted laser desorption / ionisation (MALDI). Some of the peptides are ionized (referred as a protonated analyte ion) and can be accelerated by electric field potentials into a mass analyzer of choice. Peptide mass was determined by a time-of-flight (TOF) measurement of the elapsed time from acceleration of the peptide ion to the mass detector. TOF is dependent on the ratio of peptide mass (m) and its charge (z). Therefore, this technique is referred as MALDI-TOF. It generates spectra of peptide masses (m/z) with the sensitivity to detect molecules at a few parts per million (ppm). This process of peptide mass mapping can be use to match experimentally generated tryptic-digested peptides with those present in the database and a minimum match of three molecular weights is generally used to reduce false positives.

After having determined the m/z values and the intensities of all peaks in the spectrum, a mass spectrometer can obtain the primary structure (sequence) information about these peptides. This is called tandem mass spectrometry (MS) because it couples two stages of MS. In tandem MS, a

particular peptide ion is isolated, energy is imparted by collisions with an inert gas (such as nitrogen molecules, or argon or helium atoms) and this energy causes the peptide to break apart. A mass spectrum of the resulting fragment, the tandem MS (also called MS/MS or MS^2) spectrum, is then generated. In this second part of MS, the species that is fragmented is called "precursor /parent ion" and the ions in the tandem MS spectrum is called "product or daughter ion". MS^2 spectrum is the result of one particular precursor ion fragmenting at different amide bonds. The resulting ions are called b-ions if the charge is retained by the amino-terminal part of the peptide and y-ions if the charge is retained by the carboxy-terminal part. This whole process is called as MALDI-TOF tandem MS/MS. Protein identification based on tandem MS spectra is sometimes confusing due to the intervening peaks. Experts can determine and interpret tandem MS spectra, but computer algorithms are still unreliable for determining amino-acid sequences and protein identification. In both cases, the success of *de novo* sequencing depends upon the quality of the data in terms of mass accuracy and the resolution of the instrument, as well as the information content of tandem MS spectrum. A peptide fragmentation spectrum, therefore, might not contain sufficient information to unambiguously derive the complete amino acid sequence, but it may still have sufficient information to match it uniquely to a peptide sequence in the database on the basis of observed and expected fragment ions. There are several different algorithms used to search sequence databases with tandem MS spectra data, including PeptideSearch, Sequest, Mascot, Sonar ms/ms and ProteinProspector. The Mascot search engine involves calculating the theoretically predicted fragments for all the peptides in the database and is called probability based matching. The predicted fragments are matched to the experimental fragments in a top-down fashion starting with the most intense b- and y- ions. The probability that number of fragment matches is random is calculated, and the negative logarithm of this number (multiply by 10) is the identification score. The molecular weight search (MOWSE) and probability scores calculated by MASCOT were used as the criteria for protein identification (Steen and Mann, 2004).

2.2.8.11.1 Gel staining and storage

After gel scanning, imaging and analysis, the gels were stained with 0.1% Coomassie Brilliant Blue R-250 (w/v) in 40% methanol (v/v), 10% acetic acid (v/v) for 20 minutes to 1 hour and destained in 100 ml of 40% methanol and 10% acetic acid with gentle agitation. Gels were stored in destaining solution until protein spot excision and protein identification.

2.2.8.11.2 Sample preparation and sample loading

The spots of interest were excised from the gel using a *Ettan* spot picking robot (*GE HEALTHCARE*). The gel pieces were destained with NH_4HCO_3 prepared in 30% acetonitrile and digested with 100 ng of trypsin per sample. The resulting peptides were extracted from the gel with 50% acetonitrile containing 0.3% trifluoroacetic acid (TFA) followed by 100% acetonitrile. The volumes of the final samples were

reduced from approximately 100 µl to 5 µl by vacuum centrifugation. If the volume was less than 5 µl, then samples were reconstituted with 0.3% TFA. 1 µl of each sample was mixed with a 1 µl of matrix (3 mg/ml of α-cyano-4-hydroxycinnamic acid (HCCA) in ethanol-acetone, 2:1 by volume) and spotted on a 600 µm AnchorChip (*Bruker Daltonik GmbH*) in a matrix of α-cyano-4-hydroxycinnamic acid (HCCA) without drying, according to the manufacturer's thin layer method. 2 µl washing buffer (10 mM ammonium phosphate, monobasic in 0.1% TFA) was added to the residual liquid and the whole droplet was removed as completely as possible. The addition of 0.1% TFA before removing the analyte droplet helps to dilute the contaminants. Then 1 µl recrystallization mixture was applied to the spots to redissolve the thin layer with the attached analyte molecules. A recrystallization mixture was prepared in HCCA (0.1g/l in ethanol: acetone: 0.1% TFA, 6:3:1). The recrystallization mixture redissolves the thin layer with the attached analyte molecules, and the addition of HCCA forms larger crystals which allow more laser shots per spot.

2.2.8.11.3 Data acquisition - mass spectrometry (MS)

Matrix-assisted laser desorption / ionisation-time of flight (MALDI TOF) mass spectra were acquired using a Bruker ultraflex II MALDI TOF/TOF mass spectrometer (Bruker Daltonik GmbH) operating in a positive ion reflector mode under the control of the flexControl software (*Version 2.4, Bruker Daltonik GmbH*). The ion acceleration voltage was 20 Kv. External calibration was performed using peptide standards ranging from 1046.542 to 2465.189 u (Da) (*Bruker Daltonik GmbH*) that were analysed under the same conditions. Spectra were obtained randomly over the surface of the matrix spot at a laser intensity determined by the operator.

2.2.8.11.4 Tandem mass spectrometry (MS/MS)

Between 3 and 6 of the most highly abundant sample precursor ions (i.e. non-trypsin and non-keratin) were selected for MS/MS analysis. MALDI-TOF/TOF was performed in the LIFT mode using the same spot on the target.

2.2.8.11.5 Mass spectrometry data analysis

MS and MS/MS spectra were subjected to smoothing (Gauss, width = 0.02 m/z for MS and 0.05 m/z for MS/MS), background subtraction (Convex Hull) and peak detection (SNAP algorithm) using flexAnalysis (Version 2.4, Bruker Daltonik GmbH). The spectra and mass map lists were exported to BioTools (*Version 3.0, Bruker Daltonik GmbH*). The mass spectrometry and corresponding MS/MS spectra were combined and submitted to the on-line MASCOT database-searching engine (Matrix Science: http://www.matrixscience.com).

The specifications were as follows:

Taxonomy: Other mammalian / mammalian

Database: NCBI

Enzyme: Trypsin

Global modifications: Carbamidomethyl (C)

Variable modifications: Oxidation (M)

Mass values: Monoisotopic

Peptide mass tolerance MS: 100 ppm

MS/MS tolerance: 0.5 Da

Missed cleavages: 1

For each sample, the data were initially searched against the "other mammalian" database. This database includes the protein sequences from all mammals, including the known bovine sequences, with the exception of the orders *Primates* and *Rodentia*. If this failed to provide a positive identification, then the data were searched against the complete mammalian database including *Homo sapiens*. The molecular weight search (MOWSE) and probability scores calculated by MASCOT were used as the criteria for protein identification. The MS spectrum analysis report included the MS spectra and the details of the degree of sequence coverage. The sequence coverage indicates the regions covered by the MS data (i.e., the peptide mass fingerprint). On occasion, MASCOT analysis identified several proteins with significant MOWSE scores. This can be attributed to multiple database entries for the same protein or to protein homologs from different species, which may contain only a small number of amino acid changes. When this occurred, the most appropriate protein with the highest MOWSE score was imported into BioTools for further analysis. Isoelectric point and molecular weight predictions of the identified proteins were made using the Compute pI/MW calculator of the Expert Protein Analysis System (ExPASY) [http://au.expasy.org/tools/pi_tool.html].

2.3 Acknowledgements of technical assistance

This project was only being possible to complete successfully because of the assistance kindly provided by the following people.

Individuals	Contribution to project
Bozena Kruk, University of Adelaide	Assisted in mass genotyping with primer extension method and DNA sequencing
Scott Foster, University of Adelaide	Generated marker linkage map with CRI-MAP and assisted in fine mapping data analysis
Arthur Mangos, DNA Sequencing Center, Institute of Medical and Veterinary Science (IMVS)	Automated DNA sequencing
Wayne Pitchford, University of Adelaide	SNP association data analysis

Mike Goddard, Dannielle Hulett, Helen McPartlan, Ben Hayes and Lakshmi Krishnan, Department of Primary Industries, Victoria	Genotyping using SNPlex technology; provision of Angus QTL and SNP whole genome scan data
Chris Bagley and Megan Retallick, Proteomics Facility, Molecular Biosciences, University of Adelaide	Proteomics experiments were performed under the supervision of Chris Bagley

Chapter 3

Cattle net feed efficiency QTL mapping and candidate gene identification

3.1 Introduction

Very little information is available about the molecular genetic differences and the mechanisms influencing net feed intake of animals, particularly in cattle. For the development of effective breeding strategies and achieving desirable genetic goals, it is necessary to understand the genes responsible for net feed efficiency and their regulation in different environments.

For instance, based on the energy status of the body, the differential expression of genes may determine the partitioning of nutrients for catabolic purposes and for managing body reserves. With the help of molecular approaches such as quantitative trait loci (QTL) mapping and single nucleotide polymorphism (SNP) association studies, it is possible to identify chromosomal regions and important genes or genetic markers contributing to the partitioning of nutrients, and thus, affecting net feed efficiency traits. Determining the DNA allelic variants that improve feed efficiency is valuable because the favourable alleles can be used for early selection of efficient animals, and genetic gains can be made more rapidly and cheaply than by progeny testing. Therefore, identifying candidate genes and their potential underlying regulation of net feed efficiency is an important goal.

3.2 Background

Fenton (2004) conducted a genome wide scan of the 29 bovine autosomes in Jersey-Limousin backcross progeny from 6 cohorts for feed intake and efficiency traits. The scan was performed on the 3 half-sib families (sires 361, 368 and 398), each containing approximately 120 progeny. Interval mapping detected four suggestive QTL segregating for NFE on BTA 1, BTA 8, BTA 9 and BTA 20 across the families. A further six QTL (BTA 16, BTA 6, BTA 17, BTA 11, BTA 7 and BTA 5) with LOD scores between 1.5 and 1.9 were also detected (Table 3.1) (Fenton, 2004).

The QTL with the largest additive effect was on BTA 1 and accounted for 98% of the phenotypic standard deviation (1.52 kg/d) in the family of sire 398. In the same region, QTL were detected for daily feed intake, maintenance requirement, gross efficiency, mid-weight and average daily gain. In the progeny, the QTL resulted in animals that were 5% lighter, ate 16% less, had 14% lower maintenance requirement, and an 11% lower NFE. Consequently, these progeny were slightly lighter but significantly more efficient. Interestingly, the progeny of sire 398 had the lowest NFE, and in general, were significantly different from the progeny of the other 2 sires (361, 368) for the traits measured.

Table 3.1 Net feed efficiency QTL (across family analysis). QTL identified in the Davies Jersey x Limousin mapping herd cattle (Fenton, 2004)

Cattle chromo-some	NFE LOD score	NFE size*	NFE QTL position (cM)	DFI LOD score	Mid-wt LOD score	ADG LOD score
BTA 1	3.2	98	95	4.7	3.0	3.9
BTA 8	2.2	65	67	1.6	NA	NA
BTA 20	2.0	57	49	NA	NA	1.7
BTA 9	1.9	50	14	2.2	1.8	3.4
BTA 6	1.7	46	61	2.2	2.0	NA
BTA 16	1.6	50	27	2.1	2.2	NA
BTA 17	1.6	46	13	1.5	NA	1.5
BTA 11	1.5	51	74	NA	NA	2.5
BTA 7	1.5	46	39	NA	NA	2.9
BTA 5	1.5	45	31	2.3	2.3	NA

***Additive size of effect in percentage phenotypic standard deviations (1.55 kg/day in cattle) in family where the QTL had greatest effect, assuming no interaction between the QTL effect and sex or breed. NA: not available**

Four suggestive QTL for maintenance were found to overlap with the NFE suggestive QTL (BTA1, 8, 9, and 20). The sign and size of the additive effects of these maintenance QTL were of the same magnitude and segregating in the same sire families as the 4 NFE QTL. Five QTL (one significant and four suggestive) were found for daily feed intake. Two of these overlapped with the NFE QTL.

In addition, ten QTL were detected across six chromosomes for the eating behaviour traits (data not presented), including the number of eating sessions, eating rate, time spent on feeding, meal size and average length of each feeding session. Among these QTL, only one QTL was located near a NFE QTL on BTA 8. The remainder of the eating behaviour QTL were on BTA 13.

In summary, the family of sire 398 segregated many important QTL on BTA 1 including net feed intake, daily feed intake, maintenance requirements, gross efficiency, mid-weight and average daily gain, in addition to other NFE QTL on BTA8, BTA9 and BTA20. The family of sire 361 segregated not only NFE QTL on BTA 9 but also daily feed intake, maintenance requirements, gross efficiency, mid-weight and average daily gain. All eating behaviour trait QTL on BTA 13 were segregating in the sire family of 361. The sire 368 family did not have any NFE or maintenance QTL. Among the top six NFE QTL (BTA1, 6, 8, 9, 16, and 20), only the NFE QTL on BTA 9 was not independent of growth. Therefore, for identifying candidate genes affecting on net feed efficiency, the five NFE QTL regions on BTA1, BTA6, BTA8, BTA16 and BTA20 were targeted for further study (Table 3.1).

In additon, after the data were re-processed to remove outliers from any given day, an additional NFE QTL on BTA 11 was observed to be segregating in the sire family of 361. The re-processing of the data resulted in a re-ranking of the QTL in terms of size of effect and statistical support (Table 3.2).

Table 3.2 Re-ranking of QTL of NFE (across family analysis)

Previous analysis QTL ranking	F-value of QTL	Position of QTL	Recent analysis QTL ranking	F-value of re-ranked QTL	Position of re-ranked QTL
1	3.40	95	11	3.94	73
8	2.70	67	20	3.76	49
20	4.47	49	1	3.39	92
9	<2	14	8	2.69	68
16	<2	27	19	2.64	26
6	<2	61	3	2.64	84
17	<2	13	17	2.53	16
11	3.95	74	16	2.53	63

Therefore, candidate genes were also identified for the NFE QTL on BTA11.

3.3 Research strategy

The major objective of the research herein was to determine the genes and metabolic pathways controlling NFE in cattle. The experimental strategy was to:

1. identify potential candidate genes controlling NFE based on the NFE QTL from the Davies Limousin x Jersey backcross progeny (described above) using comparative mapping and the human genome databases,
2. sequence the 5' untranslated region (UTR), promoter, exons and 3' untranslated region of the candidate genes in the F1 mapping sires (361, 368 and 398),
3. identify single nucleotide polymorphism (SNPs) in the sequences of these candidate genes,
4. verify the SNPs and Mendelian inheritance by sequencing the grandsires and grand-dams,
5. reconstruct SNP haplotypes for the candidate genes,
6. genotype the mapping progeny for any potentially functional SNPs and a sufficient number of other polymorphic SNPs to construct haplotypes,
7. conduct linkage analysis and association studies with these SNP genotypes and net feed efficiency (NFE) phenotypic data from the mapping progeny to determine if the candidate genes are likely to be involved in cattle net feed efficiency, and
8. validate significant SNPs in a different cattle population.

3.4 Results

3.4.1 Candidate gene selection

The QTL regions identified in Fenton 2004 study were used to determine the homeologous regions in the human genome by comparative mapping. The human genome sequence databases were then used to identify potential candidate genes.

The cattle genome has been found to have more than 90% of synteny with the human genome even though these species diverged from each other millions of years ago (Larkin *et al* 2003; Liu *et al* 2004). Therefore, the cattle NFE QTL regions were mapped by comparative genome mapping with the help of available databases for comparative mapping (NCBI comparative mapping database http://www.animalgenome.org/cattle/maps/RHMap3/Itoh_Supplement5_28.html). This was necessary as the bovine Ensembl genome map (http://www.ensembl.org/Bos_taurus/index.html) was not available at the beginning of the project.

To do the comparative mapping, the microsatellites bracketing each NFE QTL were firstly aligned on the cattle linkage and radiation maps available on http://www.thearkdb.org, http://www.marc.usda.gov/, and http://www.animalgenome.org/cattle/maps/COMRAD/ (accessed in September 2003). Then the location of these bracketed regions on the equivalent homeologous region of the human genome map were identified using the human Ensembl (http://www.ensembl.org) and NCBI's MAPVIEWER (http://www.ncbi.nlm.nih.gov/mapview/map_search.cgi?taxid=9913&query=) genome databases. Locating these equivalent positions on the human genome sequence helped to prepare a list of potential candidate genes likely to be within the cattle NFE QTL regions. The exact location of 20-30% of identified genes from the human map could be confirmed using BOVMAP (http://locus.jouy.inra.fr).

The candidate genes were chosen for each NFE QTL based on their physiological function described in the Online Mendelian Inheritance in Man (OMIM) database. To develop a better understanding of the physiological role of specific genes, GENECARDS (http://bioinformatics.weizmann.ac.il/cards) and NCBI's PUBMED database (www.pubmed.gov) were also used. The bovine candidate gene sequence information was obtained by accessing the sequence databases of NCBI http://www.ncbi.nlm.nih.gov/entrez/query.fcgi?CMD=search&DB=nucleotide, EMBL-EBI (http://www.ebi.ac.uk/embl/index.html), Japan's http://www.ddbj.nigh.ac.jp/, and Genbank (http://bn1.angis.org.au). The location of the genes was confirmed by linkage analysis herein. After the release of the bovine Ensembl genome database (Btau 2.0), the exact physical locations of selected candidate genes could usually be confirmed by alignment of the human gene nucleotide sequence against the bovine Ensembl genome nucleotide sequence using the basic local alignment search tool BLASTN.

3.4.2 Cattle-human comparative mapping

The NFE QTL on BTA1 was flanked by microsatellite markers CSSM032 and BMS2263 (Fenton 2004). This bracket was found to be homeologous with the region 131 Mb – 166 Mb on human chromosome 3 (HSA 3) (Appendix 3.1). From the 46 candidate genes found in this QTL region, 19 genes were selected for sequencing based on their physiological importance (Appendix 3.5), and the gene information available at the commencement of this project. A total of 67 SNPs were found in these 19 genes (Table 3.3, Appendix 3.6) and 12 SNPs were used for the linkage mapping studies. The 12 SNPs selected for genotyping were located in 7 genes: growth hormone factor 1 (GHF-1) (also called pituitary-specific positive transcription factor 1 or Pit-1), uridine monophosphate synthetase (UMPS), somatostatin precursor (SST), alpha-HS-glycoprotein (AHSG), glucose transporter 2 (SLC2A2), interleukin 12 A (IL12A) and angiotensin receptor 1 (AGTR1).

The NFE QTL on BTA 8 was flanked by microsatellites BMS1341 and BMS836 (Fenton 2004). This bracket was homeologous with two regions on two different human chromosomes; the region 19 Mb – 26 Mb on human chromosome 8 (HSA 8) and the region 76 Mb – 120 Mb on human chromosome 9 (HSA 9) (Appendix 3.1). There were 53 candidate genes found and 9 genes were sequenced based on their physiological importance (Appendix 3.5), and the gene information available in the beginning of this project. A total of 31 SNPs found (Table 3.3), and 7 SNPs were used for the linkage mapping studies) (Appendix 3.6). These 7 SNPs were located in 4 candidate genes; cathepsin B (CTSB), nociceptin (PNOC), tyrosine kinase (endothelial) (TEK), and lipoprotein lipase (LPL) (Appendix 3.6).

The NFE QTL on BTA 20 was flanked by microsatellites TGLA126 and BM5004 (Fenton 2004). This bracket was homeologous with the 10 Mb – 63 Mb region on human chromosome 5 (HSA 5) (Appendix 3.1). There were 35 candidate genes found and 10 genes were sequenced based on their physiological importance (Appendix 3.5), and the information available at the beginning of this project. A total of 96 SNPs were found (Table 3.3), and 13 SNPs were used for the linkage mapping studies (Appendix 3.6). These 13 SNPs were located in 6 candidate genes: microtubule-associated protein -1B (MAP1B), follistatin precursor (FST), growth hormone receptor (GHR), 5'-AMP-activated protein kinase (PRKAA1), catalytic alpha-1 chain, prolactin receptor precursor (PRLR), and phosphatidylinositol 3-kinase P-85 - alpha subunit (PIK3R1) (Appendix 3.6).

The NFE QTL on BTA 6 and BTA 16 were flanked by microsatellites INRA133 - BM143 and CSSM28 - BM719, respectively (Fenton 2004). The homeologous regions on human chromosome were the 55-110 Mb and the 164-224 Mb regions on human chromosome 4 (HSA 4), respectively. There were 22 and 15 candidate genes identified for the QTL on BTA6 and BTA16, respectively. A total 5 and 10 genes were selected from BTA6 and BTA16 (Appendix 3.5), respectively, based on their physiological importance

and the gene information available at the beginning of this project. A total of 19 SNPs were found in the NFE QTL region of BTA 6 and 58 SNPs were found in the NFE QTL regions of BTA 16 (Table 3.3 and Appendix 3.6).

The NFE QTL on BTA 11 was flanked by microsatellites RM096 and RM363. This bracket was homeologous with the region 10 Mb – 47 Mb on human chromosome 2 (HSA 2) (Appendix 3.1). There were 34 candidate genes found and 8 genes were sequenced based on their physiological importance (Appendix 3.5), and the gene information available at the commencement of this project. Of the 37 SNPs found (Table 3.3), 9 SNPs were used for the linkage mapping studies (Appendix 3.6). These 9 SNPs were located in 4 candidate genes: follicle stimulating hormone receptor (FSHR), interleukin 1 beta (IL1 beta), pro-opiomelanocortin (POMC) and argininosuccinate synthase (ASS) (Appendix 3.6).

Table 3.3 Single nucleotide polymorphism discovery for association tests and QTL fine mapping

QTL regions	Total genes	Genes sequenced	Total SNPs	Potentially functional SNPs
BTA 1	46	19	67	8
BTA 8	53	9	31	3
BTA 11	34	8	37	5
BTA 20	35	10	96	11
BTA 6	22	5	19	0
BTA 16	15	10	58	0
Total	**205**	**61**	**308**	**27**

In summary, a total of 205 candidate genes were identified within six cattle NFE QTL. Of these 205 genes, the most likely 61 genes were selected for sequencing based on their physiological functions and metabolic roles (Appendix 3.5). In these 61 genes, 308 SNPs were discovered (Table 3.3, Appendix 3.6). A total of 106 SNPs were found in the promoters, 5' UTRs, exons and 3' UTRs. Of these 106 SNPs, 56 SNPs were exonic, and 27 SNPs involved amino acid substitutions. The remainder were silent. 202 SNPs were found in introns. 70% of these intronic SNPs were found in the vicinity of exons (less than 100 bp). The 308 SNPs were examined to determine if they create or obliterate micro-RNA sites, splice sites, or transcription factor binding sites using programs such as TRASFAC and or PATROCLES. None of the SNPs appear to affect such sites. However, these bioinformatic analyses should not be considered conclusive, and it is possible that a potentially functional SNP may have been overlooked.

3.4.3 QTL fine mapping

The top four NFE QTL after re-ranking (BTA1, 8, 11 and 20) were selected for further fine mapping. The SNPs on BTA6 and BTA16 have not yet been used in linkage analysis or association studies. The selected SNPs were genotyped in the Limousin x Jersey mapping progeny. Using the SNP genotypes, QTL fine mapping was performed by *QTL Express* for the NFE QTL regions on BTA 1, 8, 11 and 20. The linkage mapping results confirmed the previously detected NFE QTL regions (Fenton 2004) with marginal increases in the F-values (Table 3.4, 3.5). The exception was the F- value of NFE QTL on BTA8 and BTA11 for sire family of 368 and BTA 20, where there was a significant increase in the F-value in the sire families of 361 and 398. The QTL position on BTA 8 also shifted substantially from 73 cM to 95 cM for the family of sire 398.

Table 3.4 Linkage mapping results within families

BTA	Segregating sire families	F-value[1] (Without SNP)	F-value[2] (With SNP)	QTL location[1] (cM) (Without SNP)	QTL location[2] (cM) (With SNP)	Size of effect[1] (Without SNP) kg / day	Size of effect[2] (With SNP) kg / day
1	398	8.82	8.98	104	104	-1.09	-1.10
8	368	4.70	6.61	0	0	-0.50	-0.65
8	398	4.72	5.03	73	95	-0.80	-0.81
11	361	11.63	11.83	69	68	-1.17	-1.18
11	368	1.02	4.04	51	49	0.25	0.70
20	398	6.67	8.04	53	49	-1.00	-1.04
20	361	3.28	5.53	59	46	0.59	0.76

[1]Old = linkage analysis using microsatellite markers only
[2]New = linkage analysis using microsatellite + SNP markers
(+ or -) = Sign indicates effect of Limousin allele relative to Jersey allele

The linkage analysis also identified other NFE QTL on BTA 8 and BTA11 (at 0 cM and 48 cM, respectively), segregating in the family of sire 368 (Figure 3.1, Table 3.4, 3.5). These newly detected QTL regions had a significant increase in the size of effect without major shift in QTL position. Presumably, these QTL segregating in the sire 368 family were previously undetected because of the lack of informative markers in these chromosomal regions in the earlier linkage analysis. Similarly, it was apparent after including the SNP markers in the analyses that the QTL on BTA 20 was also segregating in the sire 361 family. The fine mapping with the SNP markers refined the QTL regions in terms of the F-ratio and the size of the effect (Appendix 3.2) as follows:

1) The NFE QTL on BTA 1 is flanked by microsatellite markers CSSM032 and BMS2263. The peak was at microsatellite marker BM1824 in the family of sire 398 with the largest size of

effect, -1.09 kg feed / day. The nearest gene to BM1824 found in fine mapping study was the angiotensin receptor 1 (AGTR1) with an F-ratio of 7.21 and a size of effect of 0.887 kg feed / day. In terms of the size effect, a significant size effect across families and within sire 398 family was observed between interleukin 1 beta (IL12A) and microsatellite marker BMS2263.

2) In the sire 398 family, the peak of the NFE QTL on BTA 8 was at the microsatellite marker BM711 with an F-value of 5.03. The size of effect at marker BM711 was 0.804 kg/day. In the sire 368 family, the QTL was proximal to nociceptin (PNOC) with an F-value 6.61. The size of effect at PNOC was 0.446 kg/day.

3) The QTL on BTA 11 was flanked by microsatellite markers RM096 and HEL13, with the peak at BM1048 (F-ratio 11.78) in the sire 361 family. The nearest genes with high F-values were pro-opiomelanocortin (POMC), interleukin1 beta (IL1B), and argininosuccinate synthase (ASS). In the case of the sire 368 family, the QTL peak was at interleukin 1beta (IL1B) with a modest F-value of 3.15.

   For the NFE QTL on BTA 11, almost all markers had significant effects in the sire 361 family with the greatest size of effect associated with marker BMS1048 (1.232 kg/day) and POMC (1.219 kg/day). The minimum size of effect was associated with BM2325 and follicle stimulating hormone receptor (FSHR) (0.35 kg/day). In the sire 368 family, the maximum size effect was -0.495 kg/day at IL1B.

4) The QTL on BTA 20 was flanked by microsatellite markers TGLA126 and BMS521. The peak was at microsatellite marker BMS703 with an F- ratio of 6.67 in the family of sire 398. The nearest genes with high F-values were growth hormone receptor (GHR) and prolactin receptor (PRLR). In case of the families of sires 361 and 368, the QTL peaks were at BMS703 and BMS521 with F-ratios of 4.64 and 5.56, respectively. The nearest genes to these peaks were GHR, 5'-AMP-activated protein kinase catalytic alpha-1 chain (PRKAA1), and PRLR.

   In the sire 361 family, the greatest size of effect was associated with PRLR (-0.773 kg/day), followed by GHR and PRKAA1. For the sire 368 family, the greatest size of effect was also PRKAA1 (0.542 kg/day), GHR (0.53 kg/day) and PRLR (0.442 kg/day). In the sire 398 family, the largest size of effect was associated with BMS703 (1.021 kg/day), followed by BM4107 (0.950 kg/day) and PRLR (0.944 kg/day).

Table 3.5 NFE QTL mapping results from Davies Limousin x Jersey progeny

BTA1

Trait -NFE			All sires	361	368	398
Without SNPs	Position (cM)		104	53	60	104
	Effect	361	-0.03			
		368	+0.01	0.40	0.30	-1.09
		398	-1			
	F		3.4	1.15	1.28	8.82
	F-Crit		4.35	6.74	6.59	6.72
With SNPs	Position (cM)		104	60	60	104
	Effect	361	0.01			
		368	-0.03	0.39	0.25	-1.10
		398	1			
	F		3.43	1.70	1.16	8.98
	F-Crit		4.47	7.23	7.63	7.58

BTA8

Trait - NFE			All sires	361	368	398
Without SNPs	Position (cM)		73	93	0	73
	Effect	361	-0.2			
		368	-0.06	-0.24	-0.50	-0.80
		398	-0.85			
	F		2.7	0.63	4.70	4.72
	F-Crit		4.11	6.38	6.01	6.48
With SNPs	Position (cM)		95	115	0	95
	Effect	361	-0.2			
		368	-0.05	-0.25	-0.65	-0.81
		398	0.86			
	F		2.79	0.64	6.61	5.03
	F-Crit		4.3	7.12	6.87	6.84

BTA11

Trait - NFE			All sires	361	368	398
Without SNPs	Position (cM)		69	70	51	4
	Effect	361	1.16			
		368	-0.01	-1.17	0.25	0.52
		398	0.36			
	F		3.95	11.63	1.02	1.51
	F-Crit		4.37	6.83	6.24	6.98
With SNPs	Position (cM)		68	70	49	4
	Effect	361	1.15			
		368	0.13	-1.18	0.70	0.52
		398	0.37			
	F		4.1	11.83	4.04	1.51
	F-Crit		4.21	7.29	7.76	6.74

BTA20

Trait - NFE			All sires	361	368	398
Without SNPs	Position (cM)		53	59	72	52
	Effect	361	-0.45			
		368	-0.43	-0.59	-0.55	1.00
		398	-1.02			
	F		4.47	3.28	5.56	6.67
	F-Crit		3.93	6.02	6.46	6.27
With SNPs	Position (cM)		49	46	72	49
	Effect	361	-0.6			
		368	-0.48	-0.76	-0.55	1.04
		398	0.99			
	F		5.55	5.53	5.56	8.04
	F-Crit		4.11	6.33	6.8	7.06

(+ or -) = indicates effect of Limousin allele on net feed efficiency relative to Jersey allele. (Table provided by Scott Foster, Biometrics SA, Waite Campus, University of Adelaide).

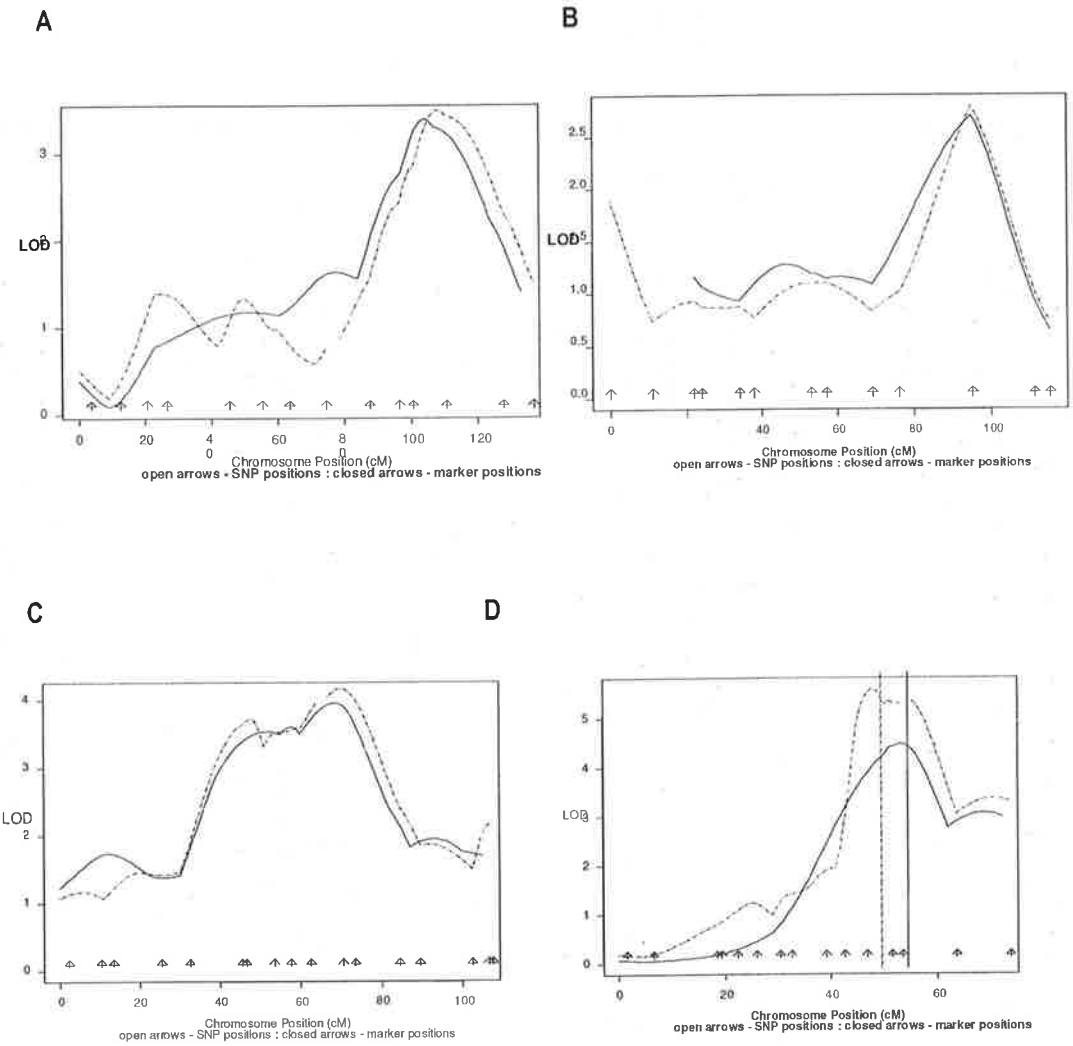

Figure 3.1 QTL graphs of NFE QTL in Davies mapping herd (Limousin x Jersey)

(A = QTL graph for BTA 1, B = QTL graphs for BTA 8, C = QTL graph for BTA 11, D= QTL graphs for BTA 20; dotted vertical line shows location of new QTL from old QTL analysis (solid vertical line). Closed arrows: Microsatellite marker, Open arrows: SNP marker, Solid line: Microsatellite only, Dotted line: with SNPs (Figure provided by Scott Foster, Biometrics SA, Waite Campus)

3.4.4 Initial SNP association study

A total of 41 SNPs selected for the linkage analysis were also used for a SNP association study. For 12 of the genes, there were non-zero variance if fit as additive effects. Most of the genes that were associated with variation in net feed efficiency had similar variance estimates when fitted as a genotype or additive effect (Table 3.6). The exception was IL12A. It is assumed that this exception arose because there were only 6 individuals with one of the homozygous genotypes and the lack of balance was less severe when fitting as an additive effect.

If the actual allelic effect was estimated and based on a simple t-test, three SNPs in 3 genes [(uridine monophosphate synthetase (UMPS), microtubule-associated protein-1B (MAP1B) and 5'-AMP-activated protein kinase, catalytic alpha-1 chain (PRKAA1)] also had a significant effect on net feed efficiency (Table 3.6). Breeding value estimates were calculated from a multiple regression model containing the fixed additive effects of the three significant genes (UMPS, MAP1B and PRKAA1). These were compared with breeding value estimates from the pedigree (animal) model. Only 18% of the variation in the estimated breeding value (EBV) was accounted for by the breeding value estimated from the SNPs, but more variation was accounted for by the inclusion of additional genes in the model [(e.g. interleukin 12 A (IL12A), cathepsin B (CSTB) and follistatin (FST)]. However, it should be noted that this is not an independent test since the breeding values and gene effects were estimated from the same dataset. Further analyses should be conducted on additional data sets from other populations.

An additional test of significance of the genes was to include the genes as covariates when undertaking linkage analysis. When these SNPs (UMPS, MAP1B, and PRKAA1) were fitted on chromosomes 1 or 20, they accounted for the QTL peak on their respective chromosomes, indicating they could be the genes harbouring the DNA variants affecting NFE or at least they are closely linked to the variants affecting NFE.

Table 3.6 Variances and effects of SNPs when fitted as genotype or additive effects on NFE[a]

BTA	Gene name	SNP#	Genotype	Additive	Size of additive effect[b]	Nearest ParAllele SNP
			kg feed/day	kg feed/day	kg feed/day	
1	Pituitary-specific positive transcription factor 1(Pit-1)	POU1F1#1	0.01	0	0	PA4062
1	Uridine monophosphate synthetase	UMPS#1		0.05	0.19±0.12	
		UMPS#2	0.01	0.13	0.32±0.15*	
1	Glucose transporter 2	SLC2A2#1				PA620
		SLC2A2#2	0			
		SLC2A haplotype		0.08	0.24±0.14	
1	Interleukin 12 A	IL12A#1	0.75	0.1	0.28±0.15	
1	Intestinal sucrase-isomaltase*c	SI#1	0.02	-	-	
1	Alpha-HS-glycoprotein	AHSG#1			0.39±0.17	PA620
8	Cathepsin B	CTSB#1	0			
		CTSB#2				
		CTSB haplotype		0.12	0.24±0.25	
8	Tyrosine kinase, endothelial	TEK#1	0.01	0.02	0.07±0.11	
		TEK#2		0.01	0.08±0.09	
8	Fructose-1,6-bisphosphatase isozyme 2* c	FBP2#1	0.004	-	-	PA6763, PA7648
8	Elongation protein 3 homolog* c	ELP3#3	0.01	-	-	
11	Follicle stimulating hormone receptor	FSHR#2	0.01	0.03	0.12±0.12	

		FSHR#1			0.24•	
11	Pro-opiomelanocortin☐	POMC#1				
		POMC#2				
		POMC haplotype	0.004	0.01	0.06±0.08	
11	Argininosuccinate synthase	ASS#1	0.03	0.04	0.15±0.12	
11	ATPase, H+ transporting, lysosomal 31kDa; V1 subunit E isoform 2*c☐	ATP6V1E2#1	0.0005	-	-	
11	Trifunctional enzyme alpha subunit, (TP-alpha) *c☐	HADHA#1	0.02	-	-	
11	Ribonucleoside-diphosphate reductase M2 chain	RRM1#1 c	0.003	-	-	
20	Microtubule-associated protein -1B	MAP1B#1	0.08	0.11	0.31±0.13*	PA6205
20	Growth hormone receptor☐	GHR#1	0.03	0.03	0.12±0.13	PA6205
		GHR#2		0.02	0.10±0.10	
20	Follistatin precursor	FST#2	0.05	0.11	0.27±0.18	PA6205
20	5'-AMP-activated protein kinase, catalytic alpha-1 chain☐	AMPK/ PRKAA1#1	0.07	0.1	0.29±0.14*	PA6205

[a]Only genes non-zero variances presented.
[b]All effects reported as positive but could be selected in either direction. The effect is for a single copy of the allele, so the difference between homozygotes is double this value.
P<0.05.: Converge to boundary.
***Based on a simple t-test of significance of difference from zero**
☑: potential candidate genes
c: model fitted as genotype, not additive effect
•: values are in percent variance
#: SNP number
(Table provided by Dr Wayne Pitchford, Discipline of Agricultural and Animal Science, University of Adelaide).

3.4.5 Second SNP association study

During the second half of the project (2005-2007), the Ensembl bovine genome sequence (Btau 2.0) was published, and more sequencing was conducted from those candidate genes whose sequence was not available in first half of the project (2003-2004). Based on the previous SNP data and the genes with significant NFE associations in initial SNP analysis, another 43 SNPs were selected for genotyping (Appendix 3.6) by SNPlex in collaboration with Department of Primary Industries, Victoria. Of these 43 SNPs, 9 SNPs could not be optimised. The analysis of the remaining 32 SNPs indicated 7 SNPs were associated with NFE (Appendix 3.4). These 7 SNPs included 2 SNPs in the intestinal sucrase-isomaltase (SI) gene and 1 SNP each in fructose-1,6-bisphosphatase isozyme 2 (FBP2), elongation protein 3 homolog (ELP3), ATPase H+ transporting lysosomal 31kDa V1 subunit E isoform 2 (ATP6V1E2), trifunctional enzyme alpha subunit, (TP-alpha) (78 kDa gastrin-binding protein) (HADHA), and ribonucleoside-diphosphate reductase M2 chain (RRM2).

While conducting the SNP association analysis, both the previous and new SNPs were included and checked for significant associations (genetic variance) with net feed efficiency and other traits (eye muscle area, intra-muscular fat and hot carcass weight). The genetic variances represent both additive and dominance effects. The model included fixed effects of cohort (6 combinations of sex and year of

birth) and breed of dam (Jersey or Limousin) (Appendix 3.4). Allele frequencies were checked for all the SNPs used in the analysis.

In terms of the proportion of variation in NFE, SNPs in 5 genes independently accounted for more than 2% of the variation, namely AMPK#1 (2.92%), PI3KR1#2 (2.80%), FST2 (2.50%) and HADHA#1 (2.46%). SNPs in another 14 genes independently accounted for less than 2% variation. Interestingly, with regards to the other traits, a SNP in tyrosine kinase endothelial (TEK1) explained 25% phenotypic variation in the intramuscular fat. The remainder of the SNPs did not explain much variation in the carcass traits (Appendix 3.4).

3.4.6 ParAllele SNP association analysis

A whole genome ParAllele 10K SNP linkage association experiment on the Trangie Angus selection line population was conducted at DPI, Victoria. Out of 9323 SNPs, they found 100 significant SNPs ($p<0.001$) associated with NFE (Hayes, 2006). This suggests there are many genes with small effects on NFE. However, many of the SNPs were located very close to each other, and therefore, multiple significant SNPs may be associated with a single mutation affecting NFE. Investigation of the SNP locations on the bovine genome revealed that there were 20 clusters of SNPs on 12 different chromosomes. Four of these regions overlapped with the NFE QTL found in the Davies Jersey x Limousin mapping (Figure 3.2). Moreover, 16 out of the 100 significant ParAllele SNPs were significant in the Davies Jersey mapping Limousin x Jersey population. Of these, 4 ParAllele SNPs were within 3 of the NFE QTL (BTA 1, 11, and 20). The locations of the remaining 12 SNPs were predicted by homologous mapping with bovine-human chromosomes. Sixty three potential candidate genes were found within 5Mb of these 12 significant SNPs within the 4 NFE QTL (BTA 1, 8, 11, and 20) (Appendix 3.5 and Appendix 3.6). Among the 63 genes, glucose transporter 2 (SLC2A2), microtubule-associated protein-1B (MAP1B) and interleukin 12 A (IL12A), sucrase-isomaltase intestinal (SI), cathepsin B (CTSB), elongation protein 3 homolog (ELP3), fructose-1,6-bisphosphatase isozyme 2 (FBP2), follistatin precursor (FST), and phosphatidylinositol 3-kinase P-85-alpha subunit (PIK3R1) had significant association with NFE in the Jersey x Limousin progeny in the first and second association studies (Table 3.6). This adds confidence to the SNP association results from the Angus whole genome scan.

The 100 significant ParAllele SNPs were genotyped in the Limousin x Jersey progeny. The allele frequencies were checked and found to be intermediate. The analysis determined that when fitted as genotype (2 homozygotes and heterozygote), ParAllele SNP PA7172 accounted for 7.00% of the genetic variation in NFE in the Limousin x Jersey population. Other significant SNPs included ParAllele SNP PA4593 (3.82%) and ParAllele SNP PA8867 (2.15%). Another 13 ParAllele SNPs explained less than 2.00% of the variation (Appendix 3.4).

QTL BTA1 = HSA21

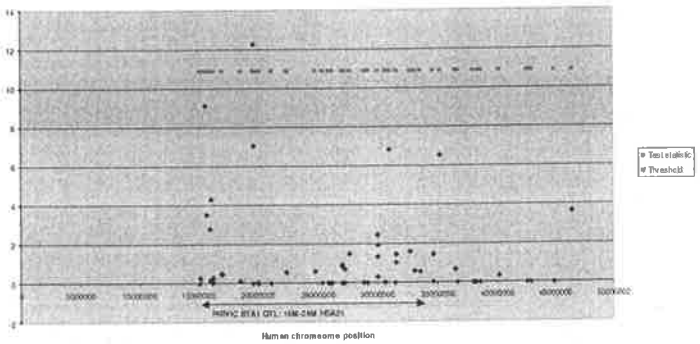

QTL BTA1 = HSA3

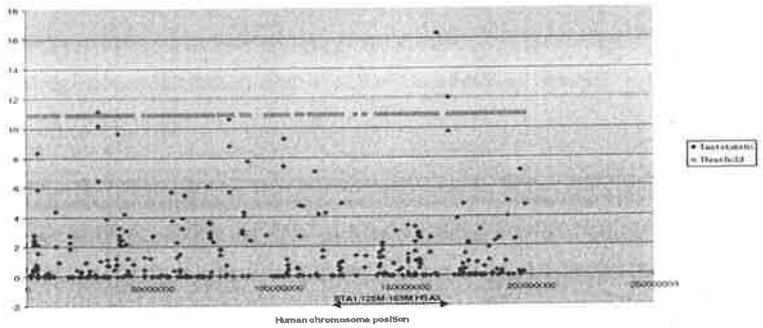

QTL BTA8 = HSA8

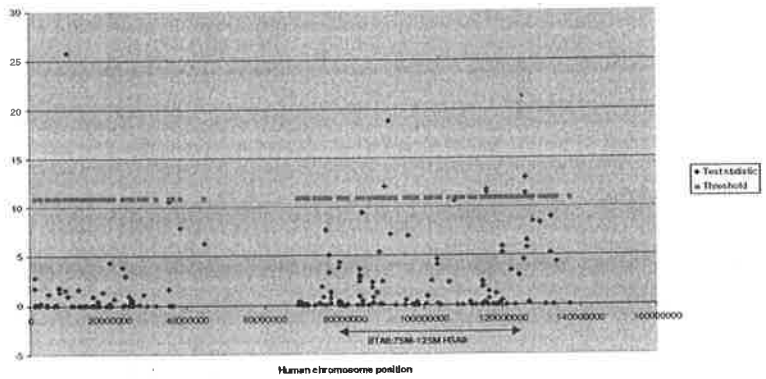

Figure 3.2 Location of ParAllele significant SNPs found in Angus Trangie herd and NFE QTL regions of Davies mapping herd (Limousin x Jersey backcross progeny). The x-axis of each graph is the physical position across the human chromosome, and the y-axis is the test statistic of significant SNPs (blue triangles). Pink line is a threshold. Blue spots above pink line were considered as significant (p<0.001). Two-way arrow line under X-axis is representing position of NFE QTL in Davies mapping herd. Figure provided by Dr Ben Hayes (DPI, Victoria) and Dr Cynthia Bottema, Discipline of Agricultural and Animal Science, University of Adelaide).

QTL BTA8 = HSA9

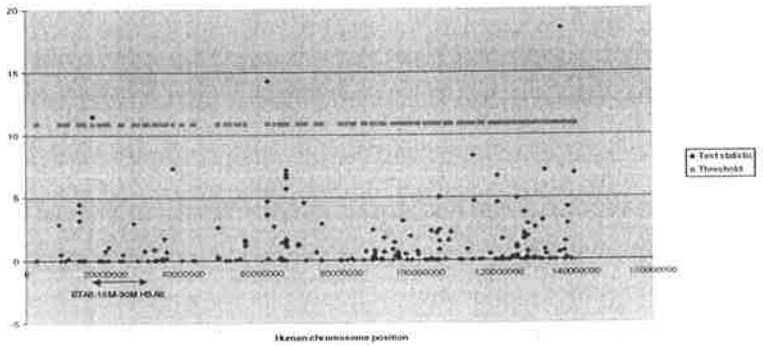

QTL BTA11 = HSA2

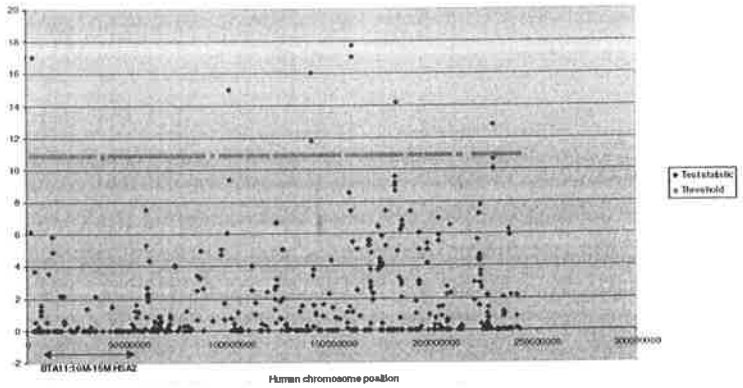

QTL BTA20 = HSA5

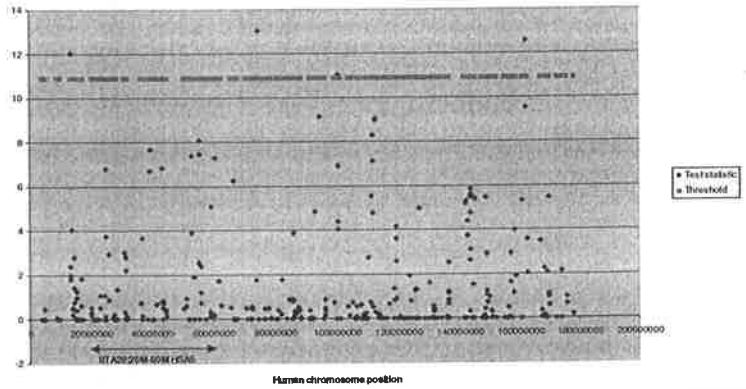

Figure 3.2 Continued ~ Location of ParAllele significant SNPs found in Angus Trangie herd and NFE QTL regions of Davies mapping herd (Limousin x Jersey backcross progeny). The x-axis of each graph is the physical position across the human chromosome, and the y-axis is the test statistic of significant SNPs (blue triangles). Pink line is a threshold. Blue spots above pink line were considered as significant (p<0.001). Two-way arrow line under X-axis is representing position of NFE QTL in Davies mapping herd. Figure provided by Dr Ben Hayes (DPI, Victoria) and Dr Cynthia Bottema, Discipline of Agricultural and Animal Science, University of Adelaide).

3.5 Discussion

Based on the NFE QTL mapping, Goddard et al (2006) conducted a second linkage mapping experiment on Trangie Angus cattle for NFE on BTA 1, 8, 11, and 20 autosomes using microsatellite markers (Goddard, M and Hayes, B, personal communication). They reported significant QTL on BTA 1, 8 and 20. There were also additional marginally significant QTL on BTA 1, 11 and 20. The significant QTL on BTA 8 and 20 were in a similar position to the QTL found in the Limousin x Jersey Davies herd as were the marginally significant QTL on BTA 1 and 11 (Figure 3.3).

Of these four QTL, two QTL also aligned with mouse NFE QTL (Fenton, 2004). The NFE QTL on cattle BTA 1 and BTA 20 overlapped with mouse homeologous NFE QTL regions on mouse chromosomes 16 and 13, respectively (Fenton, 2004). However, the mouse is not necessarily an ideal model for identifying candidate genes in cattle QTL because the mouse genome is very fragmented when aligned to non-rodent species. Thus, a given mouse genomic region will align to regions scattered across on several different cattle chromosomes (Liu *et al*, 2004). Therefore, it is very difficult to predict the position of genes based on mouse data. Nevertheless, the results in mouse as well as the Trangie Angus cattle provide support for the NFE QTL on BTA 1, 8, 11 and 20 (Figure 3.3).

The human chromosomes with conserved synteny to the NFE QTL regions were used to select candidate genes as the bovine genome sequence was not available at the time. In selecting these candidate genes from the homeolgous human regions, candidate genes within ±25cM of the QTL peak were chosen. This was because the NFE QTL had large confidence intervals. A total of 205 candidate genes were initially chosen. Based on the physiological roles of the genes and their metabolic pathways in the context of feed intake regulation and energy metabolism, 61 potential candidate genes were chosen for sequencing and SNP discovery. From the 205 initial SNPs discovered, 41 informative SNPs were selected for genotyping (Appendix 3.6). The selection was based on their physical chromosomal location and informativeness. SNPs were chosen to give at least 3 haplotypes per gene. Another 3 SNPs were selected for genotyping when the sequence data became available from the bovine genome project (Btau 2.1).

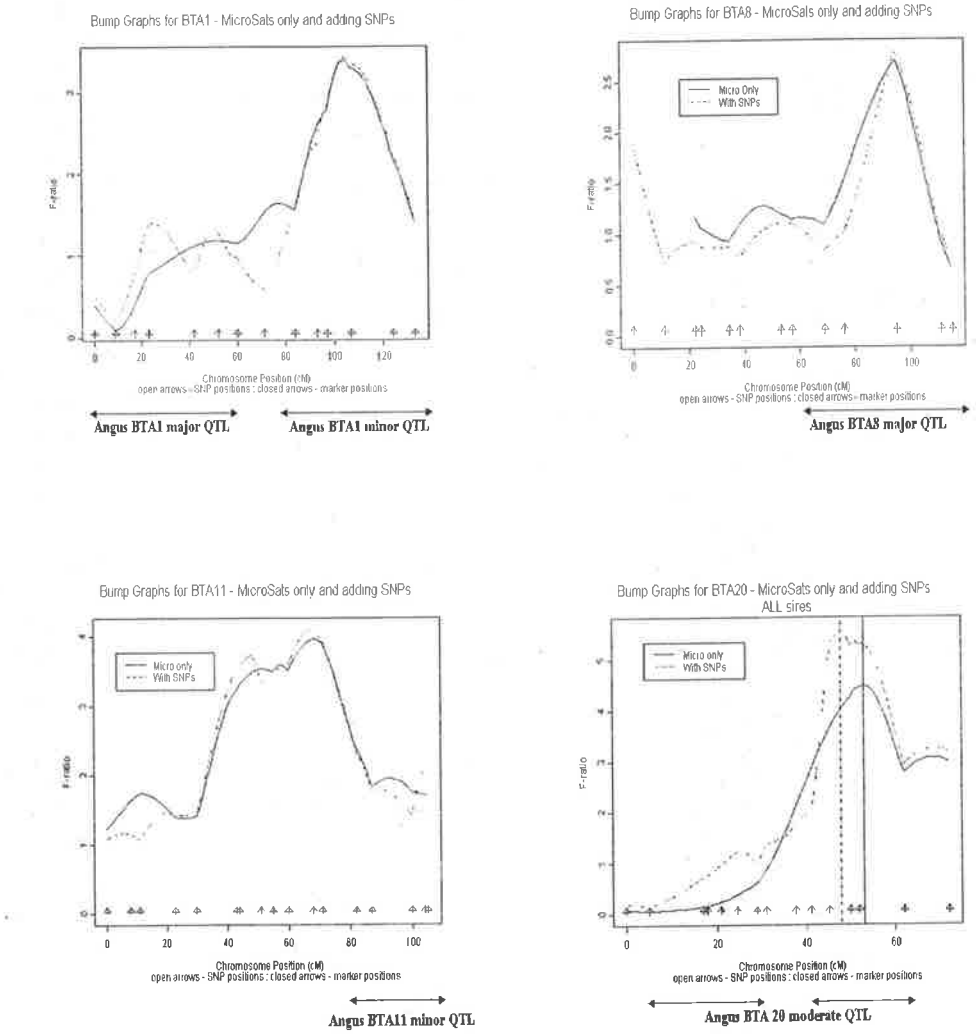

Figure 3.3 NFE QTL results in the Davies mapping herd and overlapping NFE QTL of Angus Trangie animals. Two-way arrow is the location of NFE QTL of Angus Trangie animals. (Figure provided by Prof C. Bottema, Discipline of Agriculture and Animal Science, Adelaide University)

3.5.1 QTL fine mapping

The addition of SNP markers in the QTL linkage mapping analysis increased the F- values for BTA 8 and BTA 20. For BTA 8 and BTA 20, most of the SNP markers were within the QTL region. Thus, the statistical support noticeably increased and the map location was refined (Table 3.4, 3.5). In addition, because there were more informative SNP markers on BTA8, a new QTL was discovered at the centromeric end of the chromosome (Figure 3.1). The increase in F-values was marginal for BTA 1 and BTA 11 with the inclusion of the SNP data. This is presumably a reflection of the fact that only a limited number of SNP markers were available within the QTL on BTA 11. In the case of BTA 1, although there were a larger number of markers, they may not be in linkage disequilibrium with actual genes controlling NFE. Genotyping additional markers for candidate genes within the NFE QTL on BTA1, BTA 8, BTA 11

and BTA 20 may improve the resolution of the identified QTL. Ideally though, more progeny would be available as additional informative meiosis would be a more powerful means of improving resolution.

3.5.2 SNP association studies in Jersey x Limousin

Based on the SNP association analyses, a total of 27 SNPs in 20 genes had non-zero variances (Table 3.6). Of these 20 significant genes, 12 genes are strong candidate genes based on their physiological role. The remaining 8 genes may be in linkage disequilibrium with the actual causative variant, since the metabolic roles of these genes are unlikely to affect feed intake. Most of the SNPs in the association studies were not likely to be functional as they are in either introns or are silent variants in exons. The exceptions are the SNPs in the growth hormone receptor (GHR), intestinal sucrase-isomaltase (SI), and uridine monophosphate synthetase (UMPS) genes, which alter amino acids.

However, several research studies have shown that SNPs do not have to be exonic to be important (Juszczuk-Kubiak *et al* 2007). Indeed, many significant associations of intronic SNPs with body composition in different species have been reported (Vykoukalová *et al* 2006, Thomas *et al* 2007). Nevertheless, it is most likely that the non-exonic SNPs are in linkage disequilibrium with the functional DNA variants of nearby genes. Several other strong potential candidate genes have been identified near the abovementioned 20genes. These include neurotransmitters, mitochondrial oxidative phosphorylation enzymes, and glucose and adipose tissue regulators (Appendix 3.5). These 20 genes were only sequenced for the promoter, 5' UTR, last exon, 3' UTR and 3' flanking region. SNPs in these regions might control mRNA stability, gene expression, or alternative splicing (Clop, 2006). However, these regions were purposefully sequenced with the intention to find more SNPs because they are more likely to harbour DNA variants than the protein coding exons. Therefore, more intensive sequencing of the remaining exons within these 19 genes is necessary in order to identify all potentially functional SNPs.

The candidate SNPs will be further examined by linkage disequilibrium analysis using the Trangie Angus selection lines. If the linkage disequilibrium of the SNPs extends to different cattle populations, these SNPs can be used for the selection of net feed efficiency even if they are not functional. Such SNPs should be tested in all available cattle. There are 180 more candidate genes identified within the QTL regions that have not been sequenced. To develop more SNP markers within NFE QTL regions on BTA 8 and BTA 11, a separate *in silico* SNP database has been generated from the Baylor bovine SNP database (http://www.animalgenome.org/bioinfo/resources/util/q_bovsnp.html) to dissect these regions more intensively.

3.5.3 Association study of ParAllele SNPs in the Limousin x Jersey population

As mentioned above, 16 ParAllele SNPs were associated with NFE in the Limousin x Jersey population out of significant 100 ParAllele SNPs found in the Angus population (Appendix 3.4). Due to poor annotation of the bovine genome sequence, the exact location of 12 of these 16 SNPs has not been assigned on bovine chromosomes. However, these 12 ParAllele SNPs were mapped by homeologous comparative mapping with human genome to identify candidate genes within a 5Mb region. The low number of significant ParAllele Angus SNPs (16 out of 100) was not unexpected in the association study of Limousin x Jersey progeny. The linkage disequilibrium of these SNPs across breed is less than 5Mb (Prof. Mike Goddard, personal communication). Therefore, the associations observed in Angus will not necessarily be observed in Limousin or Jersey.

3.5.4 Functional significance of candidate genes identified in NFE QTL

3.5.4.1 BTA 1

For the NFE QTL on BTA1, an association was found between NFE and five genes, including uridine monophosphate synthetase (UMPS), growth hormone factor 1 / pituitary-specific positive transcription factor 1 (POUF1), interleukin 12 A (IL12A), sucrase-isomaltase (intestinal), alpha-HS-glycoprotein and glucose transporter 2 (SLC2A2). Uridine monophosphate synthetase (UMPS) and alpha-HS-glycoprotein are found within 5Mb region to the significant Angus ParAllele SNPs PA620. Whereas, growth hormone factor 1 is found within 5Mb region to the significant Angus ParAllele SNP PA4062 (Table 3.7).

One functional SNP (alanine to proline) was found in the intestinal sucrase-isomaltase gene. In addition, this gene was associated with intramuscular fat. Sucrase-isomaltase is an enterocyte-specific small intestine brush-border membrane disaccharidase. It is required for the breakdown of starches (dextrin) and hydrolysis of dietary sucrose into glucose and fructose. Because absorption cannot take place until monosaccharides are produced, animals can suffer from malabsorption and negative energy balance if sucrase isomaltase activity is impaired (Blemont *et al* 2002). This can contribute to inducing metabolic stress and increasing feed intake to satisfy nutrient requirements.

As far as the other neighbouring candidate genes are concerned, glycogenin-1 is involved in glycogen synthesis (Shearer *et al* 2005). Glycogenin is a self-glycosylating protein involved in the initiation reactions of glycogen synthesis. During initiation, the covalent attachment of a glucose residue to glycogenin is followed by elongation to form an oligosaccharide chain. Glycogenin-1 covalently linked to glycogen acts as a primer for the action of glycogen synthase. Glycogenin-1 expression can determine glycogen accumulation in the cell (Mu *et al* 2007). Glycogen synthase kinase 3 beta is found within NFE QTL on BTA1.

NADH-ubiquinone oxido-reductase SGDH 75 kDa is another neighbouring gene and is a subunit of Complex I, part of oxidative phosphorylation electron transport chain. Oxidative phosphorylation is the mitochondrial energy producing pathway that involves the oxidation of fuel substrates for the generation of high-energy phosphates (ATP) used by the cell for energy-consuming pathways (Krauss *et al* 2005).

Glucose transporter 2 (SLC2A2) regulates glucose entry into the cell for either glycolysis for energy production or glycogen formation for energy storage. SNPs in SLC2A2 showed a significant additive effect on NFE (Table 3.6).

Growth hormone secretagogue receptor type 1 (ghrelin receptor) (POUF1) is involved in food intake regulation and is controlled by the peripheral energy sensor, ghrelin (Gayton *et al* 2005). SNPs found in the POUF1 gene were all located in introns and were significantly associated with NFE. POUF1 is within 5Mb of the significant ParAllele SNP PA1212 found in the Angus population (Table 3.7).

Another candidate gene close to POUF1 is the serotonin neurotransmitter 5-hydroxytryptamine 1F receptor (HTR1FR), which is also involved in food intake regulation (Curzon *et al* 1997). Two silent exonic SNPs were identified in the HTR1F gene and are currently being genotyped (Appendix 3.6).
The uridine monophosphate synthetase (UMPS) is responsible for mRNA turnover and uridine nucleotide synthesis (Lam *et al* 2001). Sequencing the sires found 4 SNPs: one potentially functional (cysteine to arginine), one silent in exon 3 and 2 in the 3' UTR region. The two SNPs (SNP1 AND SNP2) in exons had strong associations with feed intake (Table 3.6). UMPS is close to other genes that play important roles in energy metabolism and feed intake regulation. These include peroxisomal bifunctional enzyme (EHHADH), somatostatin precursor (SST), adiponectin (ADIPOQ) and 5-hydroxytryptamine receptor 3 subunit c (HTR3C) (Appendix 3.5).

Peroxisomal bifunctional enzyme (enoyl-CoA hydratase) is involved in the mitochondrial beta-oxidation of long chain fatty acids, which is an energy producing pathway (Watkins *et al* 1989). 5-hydroxytryptamine receptor 3 subunit C (HTR3C) is a neurotransmitter that is involved in feed intake regulation (Raybould *et al* 2003). Two silent exonic SNPs were identified in HTR3C (Appendix 3.6). Somatostatin controls insulin secretion and glucose regulation (Redmond *et al* 1994). DNA sequencing found one potentially functional SNP in a splicing junction between exon 1 and exon 2 (glutamine-lysine), which may result in alternative splicing. This SNP showed association with net feed efficiency in the across sire family analysis (Appendix 3.3). Alpha-HS-glycoprotein (AHSG) is close to the somatostatin gene. Sequencing of AHSG uncovered a potentially functional SNP (valine-isoleucine) in exon 7, which showing significant effect on NFE by association study. Mathews *et al* (2002) provided strong evidence that AHSG (fetuin) plays a critical role in the clearance and uptake of glucose from the

blood and in modulating insulin sensitivity. Although the exact mechanism of AHSG in regulating insulin sensitivity is not understood, it may be mediated by the auto-phosphorylation status of insulin receptor and subsequent downstream signalling of mitogen-activated protein kinase (MAPK) and Akt.

Adiponectin is located on BTA 1 close to alpha-HS-glycoprotein (AHSG). Adiponectin is an adipocyte-derived hormone has a role in regulating energy homeostasis and insulin sensitivity. Adiponectin appears to act by phosphorylating and activating AMP-activated protein kinase (AMPK). AMPK then phosphorylates and activates acetyl CoA carboxylase (ACC) (Wu, 2003). Activation of ACC leads to oxidation of nutrients for energy production and prevents fat deposition. Adiponectin is also involved in fatty acid oxidation in muscle and weight reduction (Freubis *et al* 2000). Peroxisomal bifunctional enzyme (EHHADH), somatostatin precursor (SST), adiponectin (ADIPOQ), alpha-HS-glycoprotein (AHSG) and 5-hydroxytryptamine receptor 3 subunit c (HTR3C) are found with 5Mb region to the significant Angus ParAllele SNP PA4062 (Table 3.7).

Other genes that might be important in the BTA 1 NFE QTL region are NADH-ubiquinone oxidoreductase SGDH subunit (NDUFB5), NADH-ubiquinone oxidoreductase B15 subunit (NDUFB4), Complex IV copper chaperon and vacuolar ATP synthase catalytic subunit alpha (ATP6V1A), all of which are involved in mitochondrial oxidative phosphorylation.

Of the remaining genes, D (3) dopamine receptor regulates CART (cocaine- and amphetamine-regulated transcript), which is involved in feed intake regulation (Genevieve *et al* 2004). Insulin-like growth factor II (IGF-II) mRNA-binding protein 2 (IGFBP2) controls IGF-II expression, which in turn is involved in growth (Baker *et al* 1993). Liver 6-phosphofructokinase (PFKB) is controlled by fructose 2, 6-biphosphate, involved in glycolysis (Murray *et al* 1989). PFKB is found close to 5Mb region to the 3 significant Angus ParAllele SNPs PA1212, PA3166 and PA3271. (Table 3.7). The other genes identified have a role in glucose turnover (phosphoinositide-3-kinase regulatory subunit 4 (p150) (PIK3R4), ADP-glucose receptor (P2Y12) and UDP-glucose receptor (P2Y14). Acetyl-CoA transporter (SLC33A1), mitochondrial acyl-CoA dehydrogenase family member 9 (ACAD9), sortin nexin 4 (SNX4) and lipase member H (LIPH) are all involved in lipid oxidation (Murray *et al* 1996). D (3) dopamine receptor and sortin nexin 4 (SNX4) are found close to 5Mb region to the significant Angus ParAllele SNP PA620 (Table 3.7).

Based on the function of the genes, the NFE QTL on BTA 1 strongly suggests the involvement of oxidative phosphorylation, lipid oxidation and/or glucose metabolic pathways in net feed efficiency (Table 3.7).

Table 3.7 Candidate genes in BTA1 NFE QTL

Candidate genes	Nearest ParAllele SNP*
Oxidative phosphorylation	
Complex I-SGDH 1 beta subcomplex, 5, 16kDa	
ComplexI-B15 subunit	
Complex IV copper chaperone	
Complex V catalytic subunit alpha	
Lipid oxidation	
Peroxisomal bifunctional enzyme (enoyl-CoA hydratase)	PA620
Acetyl-CoA transporter	
Mitochondrial acyl-CoA dehydrogenase family member 9	
Adiponectin precursor	PA620
Lipase, member H	
Sortin nexin 4	PA620
Glucose metabolism	
Glucose transporter 2	
Alpha-HS-glycoprotein	PA620
Sucrase-isomaltase (intestinal)	
Glycogenin	
Glycogen synthase kinase-3 beta	
IGF-II mRNA-binding protein II	
Liver 6-phosphofructokinase	
Phosphoinositide-3-kinase, regulatory subunit 4, p150	PA3271, PA3166, PA1212
ADP-Glucose receptor (P2Y12)	
UDP-Glucose receptor (P2Y14)	
Growth	
Growth hormone factor (POUF1)	PA4062
Somatostatin precursor	PA620
Ghrelin receptor	
Neurotransmitter	
5-hydroxytryptamine 1F receptor	PA4062
5-hydroxytryptamine receptor 3 subunit c	PA620
D-3 dopamine receptor	PA620

Significant Angus ParAllele SNPs within 5 Mb region of the candidate gene

3.5.4.2 BTA 20

Important genes found in the NFE QTL on BTA 20 associated with NFE were growth hormone receptor (GHR), 5'-AMP-activated protein kinase, catalytic alpha-1 chain (PRKAA1), microtubule-associated protein-1B (MAP1B) and follistatin (FST) (Table 3.6). The all four genes are found within 5Mb of the Angus ParAllele SNP PA6205 (Table 3.8).

Although the SNP found in MAP1B is significantly associated with NFE, the SNP is a silent variant. A recent study has found that the MAP1B light chain regulates the 5-hydroxytryptamine$_{3A}$ – receptor (Davies *et al* 2006). 5-hydroxytryptamine (5-HT), referred to as serotonin, is responsible for nutrient induced satiety and acts through receptors on the terminals of vagal afferent nerve fibres, resulting in a delay of gastric emptying. Thus, serotonin can regulate food intake (Raybould *et al* 2003).

While sequencing of the GHR gene on BTA 20, a total of 19 SNPs were found. Among them, 7 were in exons, 2 were in the 3' UTR, 1 was in the promoter and 9 were intronic. It is interesting that all 7 SNPs in exons were found in the last exon 10 of GHR. Of the 7 SNPs, three caused amino acids substitutions and are potentially functional SNPs. One of these SNP (alanine to threonine) was used for linkage analysis and had a significant size of effect (Appendix 3.6). The other 2 SNPs are currently being genotyped. The amino acids encoded by exon 10 of GHR regulate the intra-cytoplasmic domain of GHR. This intra-cytoplasmic domain is involved with various glucose intra-cellular signalling pathways (e.g., insulin receptor substrates 1 and 2, insulin-like growth factor 1), the MAP kinase pathway, and the myogenesis pathway (Moutoussamy *et al* 1998).

A neighbouring candidate gene of GHR is PRKAA1, which is also referred as AMP-activated kinase (AMPK). This enzyme is the down-stream component of a protein kinase cascade that acts as an intracellular energy sensor to maintain the energy balance within cell. Extra-cellular energy sensors like leptin, insulin and adiponectin activate AMPK to alter metabolic pathways in the muscle and liver. Levels of AMPK in the hypothalamus are regulated by a neurohormonal mechanism. Activation of AMPK increases the level of feed intake (Andersson *et al* 2004). There were 8 SNPs were found in this gene. Of these 8 SNPs, 2 were in the 5' UTR, 1 was in the promoter, 2 were in exons, and 3 were in the 3' UTR. The exonic SNPs were silent.

The other genes of interest close to GHR are mitogen-activated protein kinase kinase kinase 1 (MAP3K1), prolactin receptor precursor (PRLR), phosphatidylinositol 3-kinase P-85-alpha subunit (PIK3R1), and follistatin precursor (FST) (Appendix 3.6). Among these genes, MAP3K1, PRLR and PIK3R1 are important proteins in intracellular signal transduction pathway of GHR, glucose transport and insulin response. Partial sequencing of MAP3K1, PRLR and PIK3R1 genes found SNPs in the 3' UTR and silent SNPs in exons. MAP3K1 is found within 5Mb of the Angus ParAllele significant SNP PA6205 (Table 3.8). PRLR and PIK3R1 are found within 10Mb region of the Angus ParAllele significant SNP PA6205.

The follistatin gene (FST) is a well characterized reproductive endocrine hormone that inhibits follicle-stimulating hormone (FSH) secretion. In addition, it is also known to antagonise the function of several

members of the TGF-beta family of secreted signalling factors, including myostatin, the most powerful inhibitor of muscle growth (myogenesis) characterised to date (Amthor *et al* 2004). In the context of feed intake and weight gain, this gene is important because it controls muscle mass development and seems to be involved in total protein turnover and energy requirements. DNA sequencing results revealed 9 SNPs in FST, 8 in introns and one in an exon. The SNP in exon 5 substitute an alanine for proline, and has significant association with NFE (Appendix 3.6). Since functional mutations of this SNP show a reasonable size of effect, it will be interesting to study the indirect effect of follistatin SNP selection on reproduction. Interestingly, the follicle stimulating hormone - receptor gene (FSHR) on BTA 11 had 2 potentially functional SNPs in exons that also showed significant effects on feed intake (Appendix 3.6). Selection of DNA variants in the follistatin and follicle stimulating hormone-receptor genes for net feed intake selection could have negative effects in terms of reproduction traits.

Among other identified candidate genes, cocaine- and amphetamine-regulated transcript protein precursor (CART) protein is a putative component of the feeding-inhibitory circuitry and energy metabolism. CART is regulated by leptin. It has received much attention recently as an anorexigenic agent (Broberger, 2000). CART-containing neurons constitute a major population of the POMC-expressing neurons in the arcuate nucleus of the hypothalamus. CART expression is also observed in the sensory vagus nerve. Vagal sensory nerve endings are located in the gastrointestinal tract from the stomach to the ascending colon and send projections to the nucleus tractus solitarii (NTS) in the brainstem, which controls food intake regulation (Broberger, 2000). DNA sequencing found only one intronic SNP in the CART gene. CART is found within 5Mb of the Angus ParAllele SNP PA412 (Table 3.8).

Other important genes found within the NFE QTL on BTA 20 that have not yet been sequenced include: hydroxymethylglutaryl-CoA synthase, 5-hydroxytryptamine 1a receptor, insulin gene enhancer protein ISL-1, NADH-ubiquinone oxidoreductase 18 KDa subunit (complex I-18 kDa) and pro-melanin concentrating hormone-like protein 1 and 2. Hydroxymethylglutaryl-CoA synthase is involved in lipid metabolism. 5-hydroxytryptamine 1a receptor is a neurotransmitter involved in serotonin uptake and behaviour control (Raybould *et al* 2003). NADH-ubiquinone oxidoreductase 18 KDa subunit (complex I-18 kDa) is involved in the oxidative phosphorylation pathway. Pro-MCH-like protein 1 and 2 are the POMC derived neuropeptides (Krude *et al* 1998). Insulin gene enhancer protein ISL-1 is involved in insulin gene expression and glucose regulation (Peng *et al* 2005). The NADH-ubiquinone oxidoreductase 18 KDa subunit (complex I-18 kDa) is found within 5Mb of the Angus ParAllele SNP PA6205 (Table 3.8).

Therefore, based on the functions of the candidate genes found within NFE QTL on BTA 20, they can be placed under 4 metabolic categories: growth regulation, glucose metabolic pathways, neurotransmitters, and oxidative phosphorylation (Table 3.8).

Table 3.8 Candidate genes in BTA20 NFE QTL

Candidate genes	Nearest ParAllele SNP*
Growth	
Growth hormone receptor	PA6205
Follistatin	PA6205
Glucose metabolism	
Prolactin receptor	
Phosphatidylinositol 3-kinase P-85 -alpha subunit	
Insulin gene enhancer protein	
Mitogen-activated protein kinase kinase kinase 1	PA6205
Phosphatidylinositol-3 phosphate 3-phosphatase adaptor subunit	
Neurotransmitters	
5-hydroxytryptamine 1a receptor	
Pro-melanin-concentrating hormone-like 2	
Pro-melanin-concentrating hormone-like protein 1	
Cocaine- and amphetamine-regulated transcript protein precursor	PA412
Oxidative phosphorylation	
NAD(P) transhydrogenase	PA6205
NADH-ubiquinone oxidoreductase (Complex I) 18 KDa subunit	PA6205
3-hydroxy-3-methylglutaryl-coenzyme A reductase	
AMPK pathway	
5'-AMP-activated protein kinase	PA6205
Unknown	
Microtubule-associated protein -1B	PA6205

Significant Angus ParAllele SNPs within 5 Mb region of the candidate gene

3.5.4.3 BTA 11

For the NFE QTL on BTA 11, six genes were found to be associated with NFE: follicle stimulating hormone receptor (FSHR), proopiomelanocortin (POMC), argininosuccinate synthase (ASS), ATPase, H+ transporting, lysosomal 31kDa; V1 subunit E isoform 2 (ATP6V1E2), trifunctional enzyme alpha subunit (HADHA) and ribonucleoside-diphosphate reductase M2 chain (RRM2) (Table 3.6).

The POMC gene encodes a polypeptide hormone precursor that undergoes extensive, tissue-specific, post-translational processing via cleavage by subtilisin-like enzymes known as pro-hormone convertases. The POMC gene region is approximately 7.3 kb in length. There are eight potential cleavage sites within the polypeptide precursor. Depending upon the tissue type and the available

convertases, processing may yield as many as ten biologically active peptides involved in diverse cellular functions (Konig *et al* 2006). The encoded protein is synthesized mainly in corticotroph cells of the anterior pituitary where four cleavage sites are used to produce 4 hormones: 1) adrenocorticotrophin (ACTH), essential for normal steroidogenesis and the maintenance of normal adrenal weight, 2) lipotropin beta (ß-LPH) and their components, 3) gamma-LPH, and 4) beta-endorphin. LPH and beta-endorphin are the major end products, and independently possess biological activity (Watanbe *et al* 1982).

In other tissues, including the hypothalamus, placenta, and epithelium, all cleavage sites of POMC may be used, giving rise to peptides with roles in pain and energy homeostasis, melanocyte stimulation, and immune modulation. These include several distinct melanotropins, lipotropins, and endorphins that are contained within the adrenocorticotrophin and beta-lipotropin peptides. Mutations in POMC gene have been associated with early onset obesity, adrenal insufficiency, and red hair pigmentation (Krude *et al* 1998) Alternative splice transcript variants encoding the same protein have been found for this gene (Lee *et al* 2006).

DNA sequencing of POMC found 10 SNPs. Of these 10 SNPs, 1 was in an exon (silent), 6 in introns, and 3 in the 5' UTR (Appendix 3.6). The 6 intronic SNPs were found within 40 bases of exons and could potentially affect alternative splicing of the end products of the gene (Appendix 3.6). It would be interesting to determine if these SNPs have any effect on alternative splicing of POMC in brain tissues. Effects on splicing may alter the glucose sensing signal transduction pathway in glucosensing POMC neurons and other neurons (e.g. NPY/AgRP) in the arcuate nucleus (ARC) region of the hypothalamus, and hence, feed intake regulation. Ibrahim *et al* (2003) reported a small reduction of the extracellular concentration of glucose significantly inhibits POMC neuron firing. POMC neurons express Kir6.2 and SUR1 transcripts, which are glucose responsive. It is also known that POMC neurons express glucokinase, which is a necessary enzyme for glucose-sensing cells (Dunn-Meynell *et al* 2002).

In addition to activation by glucose, POMC neurons are also leptin responsive (Elias *et al* 1999). CART-containing neurons constitute a major subpopulation of POMC-expressing population in the ARC region of the hypothalamus. Upon leptin and glucose stimulation, both POMC and CART neurons are activated simultaneously (Elias *et al* 1998a). Cocaine and amphetamine regulated transcript (CART) is another gene found in the NFE QTL on BTA 20 (discussed above).

Based on the candidate gene list prepared from the comparative mapping, other potential genes close to the proopiomelanocortin (POMC) gene are the mitochondrial trifunctional enzyme alpha subunit (TP-alpha) (78kDa gastrin-binding protein) (HADHA), insulin receptor substrate 1 (IRS1), lipin1 (LPIN1),

urocortin (UCN), interleukin 1 receptor antagonist (IL1RN), suppressor of cytokine signalling 5 (SOCS5), NADH-ubiquinone oxidoreductase 19 kDa subunit (CI-19 kDa) (NDUFA8), MAPK / ERK kinase kinase kinase 3 (MAP4K3), ATPase, H+ transporting, lysosomal 42kDa and V1 subunit C isoform 2 (ATP6V1E2).

HADHA is a member of the enoyl CoA hydratase / 3-hydroxyacyl-CoA dehydrogenase family, which is involved in long chain fatty acid oxidation. It is also interesting that HADHA is a target for the cholecystokinin (CCK) receptor antagonist (Baldwin 1994). CCK is responsible for reduced gastric emptying and reduced food intake (Baldwin 1994). HADHA is found 1 cM downstream from the POMC gene and is co-located with the gene for the beta subunit of HADHA (ACAA1).

CI-19 kDa is a subunit of complex I involved in the electron–transfer mitochondrial oxidative phosphorylation pathway for energy production. The sequencing study discovered one potentially functional SNP (tyrosine-serine) in this gene (Appendix 3.6). ATPase, H+ transporting, lysosomal 42kDa and V1 subunit C isoform 2 are other 2 subunits from complex V involved in oxidative phosphorylation and flank the POMC gene.

Another gene in this region is lipin 1, which is 10cM downstream of POMC. Lipin 1 activates mitochondrial fatty acid oxidative metabolism by inducing peroxisome proliferator-activated receptor γ (PPARγ) coactivator 1α (PGC-1α), a transcriptional coactivator controlling several key hepatic metabolic pathways. Lipin 1 activates mitochondrial fatty acid oxidation, while suppressing lipogenesis and lowering circulating lipid levels (Fink *et al* 2006), by inducing expression of the nuclear receptor PPARα, a known PGC-1α target, and via direct physical interactions with PPARα and PGC-1α. Thus, lipin 1 is a selective physiological amplifier of the PGC-1α/PPARα-mediated control of hepatic lipid and energy metabolism that could contribute to net feed efficiency.

There are 2 important genes in the interval of 1-2cM upstream of POMC, insulin receptor substrate 1 (IRS1) and urocortin. IRS 1 plays a role in glucose metabolism. Urocortin and interleukin 1 receptor antagonist are involved in reducing feed intake by reducing gastric emptying (Asakawa *et al* 1999; Robinson *et al* 2000). Lastly, SOCS5 and MAPK are involved in the signal transduction pathway of GHR (Moutoussamy *et al* 1998).

Of the remaining important candidate genes, H^+ transporting, lysosomal 31kDa, V1 subunit E isoform 2, is a Complex V ATP synthase subunit, involved in mitochondrial ATP production. This gene is close to the follicle stimulating hormone receptor (FSHR) gene associated with NFE (Table 3.5).

The role of the other proteins in relation to NFE is not completely obvious given their metabolic functions. These genes (ribonucleoside-diphosphate reductase M2 chain (RRM1), argininosuccinate synthase (ASS) and interleukin 1beta (IL1B)) were used purely as markers for the BTA11 NFE QTL since no obvious candidate genes were in the vicinity. Nevertheless, they were associated with NFE. Either they have some unknown function related to NFE or are in linkage disequilibrium with the true causative gene variant. RRM1 provides the precursors necessary for DNA synthesis. It catalyzes the biosynthesis of deoxyribonucleotides from the corresponding ribonucleotides. Argininosuccinate synthase is a urea cycle enzyme that catalyzes the penultimate step in arginine biosynthesis: the ATP-dependent ligation of citrulline to aspartate to form arginosuccinate, AMP and pyrophosphate (Vilet 1990). This gene could have an important role in nitrogen balance. Interleukin-1 beta is known to be involved in regulating insulin mRNA and increases the level of heat shock protein hsp70 without impairing the glucose metabolism (Eizirik *et al* 1990). Therefore, interleukin-1 beta could be importance in glucose turnover.

It is possible to conclude that genes within NFE QTL on BTA 11 are likely to be involved in long chain fatty acid oxidation, glucose metabolism, the growth hormone receptor pathway, oxidative phosphorylation and gastric emptying (Table 3.9). None of the significant Angus ParAllele SNP were identified close to any candidate genes.

Table 3.9 Candidate genes in BTA 11 NFE QTL

Candidate genes	Nearest ParAllele SNP
Long chain fatty acid oxidation	
Lipin1	
Trifunctional enzyme alpha subunit	
Glucose metabolism	
Insulin receptor substrate 1 (IRS1)	
MAPK / ERK kinase kinase kinase 3	
Mitochondrial trifunctional enzyme alpha subunit	
Interleukin 1beta (IL1B)	
Growth hormone receptor pathway	
Suppressor of cytokine signalling 5	
Mitogen activated protein kinase	
Oxidative phosphorylation	
NADH-ubiquinone oxidoreductase 19 kDa subunit (CI-19 kD)	
ATPase, H+ transporting, lysosomal 42kDa, V1 subunit C isoform 2	
H+ transporting, lysosomal 31kDa, V1 subunit E isoform 2	
Gastric emptying	
Urocortin	
Interleukin 1 receptor antagonist	

Neurotransmitter	
Proopiomelanocortin	
Other	
Follicle stimulating hormone receptor	
Ribonucleoside-diphosphate reductase M2 chain (RRM1)	
Argininosuccinate synthase	

3.5.4.4 BTA 8

For the NFE QTL on BTA8, nociceptin (PNOC), cathepsin B (CSTB), tyrosine kinase, endothelial (TEK), fructose-1,6-bisphosphatase isozyme 2 (FBP2), and elongation protein 3 (ELP3) homolog were found to be associated with NFE (Table 3.6). Based on homeologous mapping, FBP2 genes is found close to significant ParAllele SNP PA6763 and PA7648.

Nociceptin (PNOC) is located close to cathepsin B and tyrosine kinase. Nociceptin is the opioid neuropeptide involved in increased food intake. It is expressed in the hypothalamus (Calo *et al* 2000). DNA sequencing identified 3 SNPs in exons, but they are silent. In terms of the size of effect, this gene accounted for significant variation in NFE (-0.643 kg /day) in the sire 368 family (Appendix 3.3). Cathepsin B is one of the most abundant lysosomal proteinases in animal tissues. *In vivo*, it degrades proteins mainly inside lysosomes and is involved in the processing of several pro-enzymes and in antigen presentation (Russo *et al* 2002). Fructose-1,6-bisphosphatase isozyme 2 is a strong positive allosteric effector of the glycolytic enzyme phosphofructokinase, and thus, is important for regulation of glycolysis. Fructose-1,6-bisphosphatase isozyme 2 is also an inhibitor of the gluconeogenic enzyme fructose-1,6-biphosphatase (Murray *et al* 1996). Based on the functions of tyrosine kinase, endothelial (TEK) and elongation protein 3 (ELP3) homolog, it is not clear how these proteins are related to feed intake. The tyrosine kinase is expressed predominantly in endothelial cells and is required for blood vessel formation and maintenance (Morris *et al* 2005). However, one of the metabolic partners of TEK is adapter protein ShcA, which is controls the tyrosine phosphorylation of regulatory p85 subunit of phosphatidylinositol 3-kinase (PI3K) (Audero *et al* 2004). Elongation protein 3 is a histone acetyltransferase subunit of the elongator complex, which is a component of the RNA polymerase II holoenzyme whose activity is directed specifically towards histones H3 and H4 (Ait-Si-Ali *et al* 1998).

Due to poor gene mapping information for BTA 8, finding candidate genes close to the markers associated with NFE was difficult. However, based on homeologous comparative mapping with human genome, identified genes were categorise based on their metabolic roles. Some of these genes were found within 5Mb of the significant ParAllele SNPs identified in the ParAllele genome scan on the Trangie Angus cattle (Table 3.10).

Of the candidate genes, 14 genes are involved in glucose metabolism. They are aldolase B fructose biophosphate (ALDOB), fructose-1,6-bisphosphatase isozyme 2 (FBP2), UDP-glucose-hexose-1-phosphate uridylyltransferase (GALT), beta-1,3-galactosyl-O-glycosyl-glycoprotein (GCNT1), insulin-like growth factor binding protein-like 1 (IGFBP1), insulin-like peptide 4 (INSL4), insulin-like peptide 6 (INSL6), gluconokinase-like protein, insulin-like growth factor-dependent IGF binding protein 4 protease, glucose transporter type 6 (SLC2A6), glucose transporter type 8 (SLC2A8), and phosphoglucomutase.

Eight candidate genes are involved in the growth hormone signal transduction pathway: tyrosine kinase endothelial (TEK), docking protein 2 (DOK2), tyrosine-protein kinase (JAK2), muscle skeletal receptor tyrosine protein kinase precursor (MUSK), SH2 domain containing 3C isoform 2 (SH2D3C), Src homology 2 domain containing adaptor protein B (SHB), SHC transforming protein 3 (SHC3), and mitogen-activated protein kinase phosphatase 2 (DUSP4).

Four candidate genes are involved in oxidative phosphorylation: complex vacuolar proton pump B isoform 2 (Complex V) (ATP6V1B2), vacuolar proton pump G subunit 1 (Complex V) (ATP6V1G1), ubiquinone biosynthesis protein COQ4 homolog (Complex IV) (COQ4), and NADH-ubiquinone oxidoreductase B17 subunit (Complex I) (NDUFB6).

Three candidate genes are involved in lipid metabolism. They were fatty acid transporter (SLC24A4), very low-density lipoprotein receptor precursor (VLDLR) and lipoprotein lipase precursor (LPL). Lipoprotein lipase precursor gene in located in the middle of the NFE QTL on BTA 8. Adipose tissue lipoprotein lipase (LPL) is a likely candidate for hormonal peripheral modulation of food intake because this enzyme regulates the uptake of serum triglycerides by adipose tissue (Garfinkel *et al* 1967 and Robison *et al* 1972) and thereby, may affect both energy flux and caloric storage of the organism. DNA sequencing found 6 SNPs in exon 10, the last exon of LPL. Among the 6 SNPs, one is a potentially functional SNP (threonine-cysteine).

Three candidate genes are neurotransmitters: orexigenic neuropeptide (QRFP), nociceptin precursor (PNOC) and gamma-aminobutyric acid type B receptor, subunit 2 precursor (Gb2). Nociceptin precursor was found in association with NFE in the Jersey x Limousin cattle population herein.

Based on the categories, the genes underlying the NFE QTL on BTA 8 are involved in glucose metabolism, the GHR signal transduction pathway, oxidative phosphorylation and lipid metabolism (Table 3.10).

Table 3.10 Candidate genes in BTA 8 NFE QTL

Candidate genes	Nearest ParAllele SNP*
Glucose metabolism	
Aldolase B fructose biophosphate	
Fructose-1,6-bisphosphatase isozyme 2	PA6763, PA7648
UDP-glucose-hexose-1-phosphate uridylyltransferase	
Beta-1,3-galactosyl-O-glycosyl-glycoprotein	
Insulin-like growth factor binding protein-like 1	
Insulin-like peptide 4	PA1301
Insulin-like peptide 6	PA1301
Gluconokinase-like protein	PA6763, PA7648
Insulin-like growth factor-dependent IGF binding protein 4 protease	
Glucose transporter type 6	
Glucose transporter type 8	
Phosphoglucomutase	
Growth hormone signal transduction pathway	
Docking protein 2	
Tyrosine kinase endothelial	
Tyrosine-protein kinase	PA1301
Muscle skeletal receptor tyrosine protein kinase precursor	
SH2 domain containing 3C isoform 2	PA4603
Src homology 2 domain containing adaptor protein B	
SHC transforming protein 3	PA6763, PA7648
Mitogen-activated protein kinase phosphatase 2	PA5991, PA4603
Oxidative phosphorylation	
Complex vacuolar proton pump B isoform 2 (Complex V)	
Vacuolar proton pump G subunit 1 (Complex V)	
Ubiquinone biosynthesis protein COQ4 homolog (Complex IV)	
NADH-ubiquinone oxidoreductase B17 subunit (Complex I)	
NADH-19kDa	PA4603
Lipid metabolism	
Fatty acid transporter	
Very low-density lipoprotein receptor precursor	PA1301
Lipoprotein lipase precursor	
Neurotransmitters	
Orexigenic neuropeptide	
Nociceptin precursor	
Gamma-aminobutyric acid type B receptor, subunit 2 precursor	PA6763, PA7648

Genes found within 5Mb of the significant ParAllele SNPs based on homeologous comparative mapping

3.6 Summary

From the metabolic roles and physiological functions of the candidate genes underlying four NFE QTL, 7 broad categories of potential pathways controlling NFE were identified (Table 3.11). Three of these major metabolic pathways were deemed as being the most likely to be involved in NFE, viz. oxidative phosphorylation, glucose metabolism and the growth hormone receptor pathway (Figure 3.4). These 3 pathways had genes located in all 4 NFE QTL.

Table 3.11 Major metabolic pathways identified in NFE QTL

Pathways	BTA
Energy metabolism	
Oxidative phosphorylation	BTA1, BTA8, BTA11, BTA20
Malonyl coenzyme A / long chain fatty acid CoA pathway	BTA20
Energy homeostasis	
Glucose metabolism	BAT1, BTA8, BTA11, BTA20
Growth hormone receptor pathway	BTA8, BTA11, BTA20
Insulin / Insulin receptor substrate (IRS) pathway	BTA8
Lipid metabolism	BTA1, BTA11
Neurotransmitters	BTA8 , BTA11, BTA20

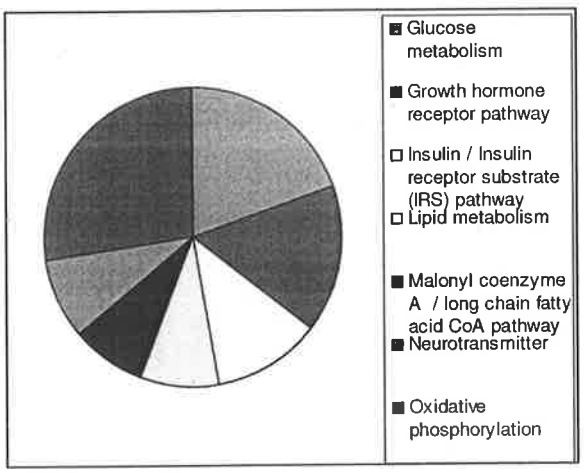

Figure 3.4 Distribution of candidate gene metabolic pathways within NFE QTL.

3.7 Technical issues: involved in QTL mapping and discovery of genes from candidate genes underlying NFE QTL

QTL mapping

Net feed efficiency trait is a complex trait. Linkage mapping of genes affecting complex traits is hampered by the fact that genotypes cannot be inferred with confidence from phenotype because other genes and environmental effects influence the phenotype. Therefore, QTL analysis of such complex traits like NFE, where heritability is less than 50% show multiple QTL with small individual effect either due to large background noice due to unavoidable environmental factors and / or errors in feed intake data mesuremnts of individual animals. Heritability associated with individual QTL controlling complex traits is also a fraction of heritability of complex trait. Therefore, multiple QTL with small contribution makes difficult to pinpoint the genes responsible for NFE. Unless QTL effect is large and low environmental variation by replication, it is difficult to reduce confidence interval to less than 10cM. Therefore, QTL true position in current study could be ±30 cM which is quite a large region of the chromosome for fine mapping. Big confidence interval is another major problem associated with NFE QTL mapping. Identifying candidate genes within 60cM genomic region is a huge task. Due inavailability of bovine genome sequence in the beginning of this project, human genome sequence was used based on comparative mapping for candidate gene selection. But this approach has also limitations because in bovine genome, not all the genes are in same sequence format of human genome. Some of the genes were found completely in different location. In few cases NFE QTL region is split into 2 different locations on human genome. Therefore based on this background, it is very difficult to judge right sequence of genes and selecting 2 SNPs per 10cM region which could complicate QTL analysis. To reduce the statistical error, the most important factor is number of genotypes tested, but in cattle species, there are practical limitations to increase number of experimental animals due associated expenditure to maintain per animal.

Discovery of genes

As mentioned earlier, in the beginning of this project, due to lack of availability of bovine genome sequence, list of candidate gene and SNP identification were conducted based on human genome. Today although bovine genome sequence is available but the annotation of bovine genome sequence is not complete which becomes a major restriction in the progress of discovering the gene. Another major problem is NFE which is a quatitative trait controlled by many genes and affected by metabolic pathways which are showing redundancy. Therefore, pinpointing exact mechanism controlling NFE is highly confounded. It is much more complicated due to overlapping other QTL were detecected on BTA 1 for daily feed intake, maintenance requirement, gross efficiency, mid-weight and average daily gain and daily feed intake on BTA 8. Seperating the NFE trait from above traits is very difficult. Therefore,

narrowing down the list of candidate genes controlling only NFE remains one of the most challenging factor.

3.8 Future studies:

To validate the results herein and develop markers for selecting for net feed efficiency, the following steps should be undertaken:

1. To validate the 27 SNPs that had significant association with NFE in the Limousin x Jersey progeny, the 27 SNPs are being genotyped in the Angus Trangie NFE selection line in collaboration to Department of Primary Industries (DPI), Victoria. Analysis of the genotyping data should verify those SNPs most likely to be valuable as markers for NFE selection programs.

2. The ParAllele SNPs that were significantly associated with NFE in the Trangie cattle should be tested in additional Angus and other cattle breeds including Davies Limousin x Jersey mapping herd for cross-validation.

3. Although number of useful SNPs identified in the Limousin x Jersey population close to significant ParAllele SNPs of Angus population is low, high number of candidate genes identified close to ParAllele SNPs, which are not yet sequence. Therefore, these identified candidate genes close to the significant ParAllele SNPs in Angus poluation should be sequenced for SNP discovery or screened for *in silico* SNPs using the available SNP haplotype databases. Identified SNPs should be tested for association with NFE in the Trangie Angus and Davies Limousin x Jersey cattle.

4. SNPs that have been validated should be commercialized with the caveat that the results of marker selection for NFE are reported so that accuracy of EBVs and potential negative associations (eg changes in body composition, lower conception rates etc.) can be monitored.

Since the genes involved in energy metabolism were consistently found to be associated significantly with NFE, 2 experimental approaches were undertaken to pinpoint the specific metabolic pathways and the genes involved in NFE. These 2 approaches involved 1) oxidative phosphorylation enzyme assays and 2) mitochondrial protein profiling by 2-dimensional differential in gel electrophoresis (2-D DIGE).

Chapter 4

Assessment of mitochondrial oxidative phosphorylation enzyme activities in high and low net feed efficiency beef cattle

4.1 Introduction

The ability to adjust food intake in response to energy requirements is essential for survival. An imbalance between total energy intake and energy utilisation leads to disorders and makes animals less efficient. Energy balance and metabolic homeostasis are controlled by complex regulatory systems, which include energy sensors, mitochondrial energy production, nutrient sensing mechanisms, fat storage and neuroendocrine networks. Among these different mechanisms, mitochondrial energy production is central to maintaining energy homeostasis and providing cellular energy. Production of energy in the form of ATP takes place through the respiratory chain in the oxidative phosphorylation (OX-PHOS) pathway of mitochondria (Rabilloud *et al* 2002). The respiratory chain is located in the inner mitochondrial membrane and comprises 5 multi-subunit enzyme complexes: Complex I (NADH ubiquinone:oxidoreductase) made up of 46 subunits, Complex II (succinate:ubiquinone oxidoreductase) made up of 5 subunits, Complex III (ubiquinol: ferricytochrome c oxidoreductase) made up of 11 subunits, Complex IV (ferrocytochrome c:oxidoreductase) made up of 13 subunits, and Complex V (ATP synthase) made up of 16 subunits (Ian *et al* 1996, Iqbal *et al* 2004). Of these 91 complex subunits, only 13 subunits are encoded by the mitochondrial genome and synthesized within mitochondria. The remainder are encoded by the nuclear genome, synthesized in the cytoplasm, and transported to the mitochondria (Rabilloud *et al* 2002). Coordinated expression of the genes in the mitochondrial and nuclear genomes maintains the required ratio of subunits in the complexes for efficient energy production.

These complexes transport electrons from NADH and $FADH_2$ produced by the oxidation of glucose and fatty acids in the cytoplasm and mitochondria (Figure 4.1). The transfer of electrons through the respiratory chain complexes I, III and IV allows protons to be pumped out of the mitochondrial matrix, creating a proton gradient across the inner mitochondrial membrane. This is referred to as the "chemiosmotic potential" or "proton motive force" (Murray *et al* 1990).

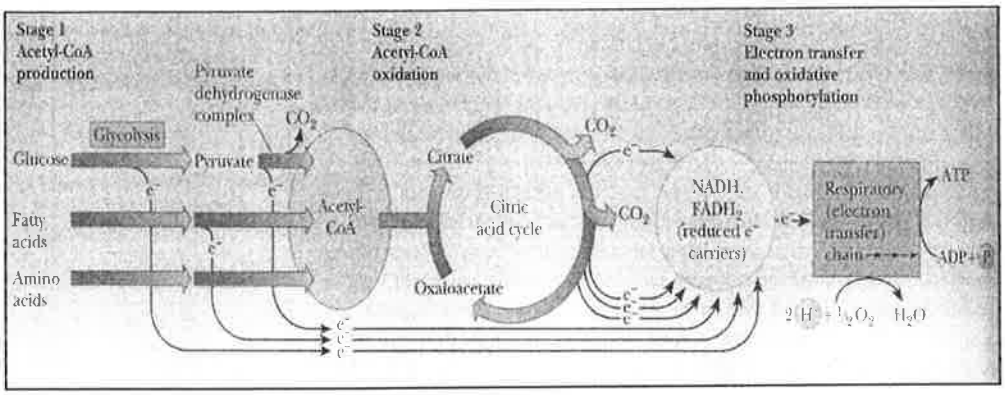

Figure 4.1 Central relationship of the citric acid cycle and oxidative phosphorylation (from Principles of Biochemistry, Lehninger, 2nd ed., Worth Publishing, Co., 1982)

The energy generated due to the proton motive force is used to produce ATP as the protons return down the thermodynamic gradient into the mitochondria. Returning the protons to the mitochondria is facilitated through the integral membrane protein, ATP synthase (that is, Complex V) (Murray 1990). ATP synthase binds ADP and inorganic phosphate at its catalytic site inside the mitochondria, and requires a proton gradient for activity in the forward direction. ATP synthase is composed of 3 fragments: F_0, which is located inside the membrane; F_1, which protrudes from the inside of the inner membrane into the matrix, and the oligomycin sensitivity-conferring protein (OSCP), which connects F_0 to F_1. The movement of the electrons through the respiratory chain electron transport, the proton gradient and ATP synthesis are all coordinated processes to produce energy (Murray *et al* 1990). The structural and functional integrity of these complexes determines the energy status of mitochondria and provides ATP for metabolic activities (Bottje *et al* 2002).

The regulation of this oxidative pathway depends on the energy needs of the body. The abundance of ATP, NADH and the metabolic intermediates regulates key steps in oxidative phosphorylation. Glycolysis and the Krebs cycle generate reduced electron carriers (e.g. NADH and $FADH_2$) through dehydrogenase enzymes (Lehninger *et al* 1993). One of the most important dehydrogenases connected to oxidative phosphorylation is succinate dehydrogenase, also referred to as Complex II. This enzyme oxidizes succinate to fumarate by producing $FADH_2$ from FAD. $FADH_2$ is re-oxidised to coenzyme Q and yields QH_2 (reduced), which is involved in the electron transfer of the respiratory chain (Murray 1990). On the other hand, NADH is oxidized aerobically by Complex I. Complex I activity is the rate-limiting step of oxidative phosphorylation (Genova *et al* 2003), and Complex I enzyme activity depends upon the ATP/ADP ratio (Figure 4.2).

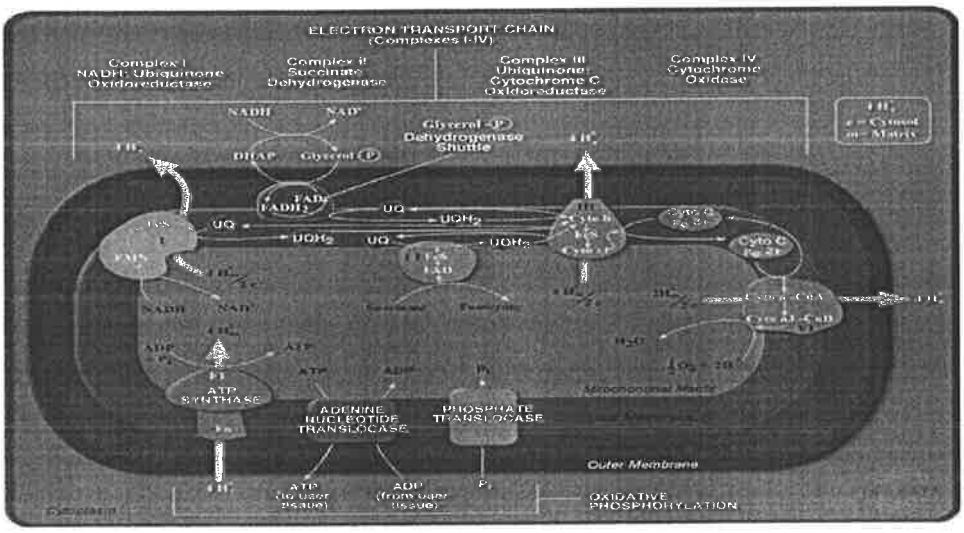

Figure 4.2 Oxidative phosphorylation pathway in mitochondria (from BioCarta Inc)

Any genetic mutations, post-translational and post-transcriptional protein modifications, up- or down-regulation of gene expression, changes in the ratios or the stability of the complex subunits can affect the efficiency of the respiratory chain function due to incomplete electron transfer. Inefficient electron transfer will increase free radical concentrations, and thereby, further affect the activity of the oxidative phosphorylation enzyme complexes.

Since the QTL experiment (chapter 3) suggested that oxidative phosphorylation may be involved in net feed efficiency, the enzyme activities of the respiratory chain complexes I, II, and IV were measured. Complex I is the rate-limiting enzyme whose activity depends on the energy needs of the body. Complex II (succinate dehydrogenase) is the enzyme involved in mitochondrial tricarboxylic acid cycle (TCA), which not only feeds electrons to the respiratory chain, but also acts as an indicator of TCA activity. Complex IV is the final step in the electron transfer chain, which terminates at Complex V. These respiratory chain complexes were selected to assay in order to determine the status of mitochondrial oxidative phosphorylation activity in high and low NFE animals.

The mitochondrial experiments were conducted with the hypothesis that there would be variation in enzyme activity in relation to NFE, especially in the rate-limiting Complex I. Specifically, efficient electron transfer and less production of free radicals would lead to energy homeostasis in high NFE animals. Therefore, less enzyme activity would be required to satisfy the energy demands in the high NFE animals compared to the low NFE animals.

The visceral organs consume approximately 73% of maintenance energy (Ruppert *et al* 2002). In many ways, the liver is ideally situated to sense peripheral metabolic events given its essential role in regulating the levels of nearly all essential body fuels (Seeley and York 2005). The liver consumes 40-50% of total maintenance energy, and therefore, has the single largest impact on the maintenance energy requirements of animals (Ruppert *et al* 2002). It was postulated that if oxidative phosphorylation enzyme activity differs between high and low NFE animals, then there would be a larger in the liver compared to other tissues. The mitochondrial enzyme studies were, therefore, performed herein in the liver and muscle to assess the oxidative phosphorylation differences between high and low NFE animals.

4.2 Results

Initially, the mitochondrial enzymatic studies were conducted on liver and brachiocephalicus muscle samples from the 10 most extreme high and low NFE animals of the Angus 2005 cohort with an average of ±1.45 kg/day difference in adjusted NFI. The data showed no significant differences in growth or carcass composition between these high and low NFE animals (Table 2.3).

4.2.1 Mitochondrial quality analysis

Mitochondria were isolated by differential centrifugation (see section 2.2.3). Mitochondrial protein yield and quality were assessed by three approaches, namely 1) by measuring protein concentration using the RC DC protein assay (see section 2.2.5), 2) by measuring activity of a mitochondrial marker enzyme, citrate synthase (see section 2.2.6) to ensure there was no cytoplasmic contamination, and 3) by conducting electron microscopy to evaluate the mitochondrial density (see section 2.2.6).

4.2.1.1 Protein concentration measurements

The mitochondrial protein concentration was found to be lower in the muscle samples (n= 20) than liver samples (n =40) (Figure 4.3). This was expected because it was very difficult to break the muscle fibers and release mitochondria from the muscle tissue (Bhattacharya *et al* 1991, Bizeau *et al* 1998). Mitochondrial protein yield in high and low NFE groups were not significantly different (P>0.05) in both liver and muscle samples.

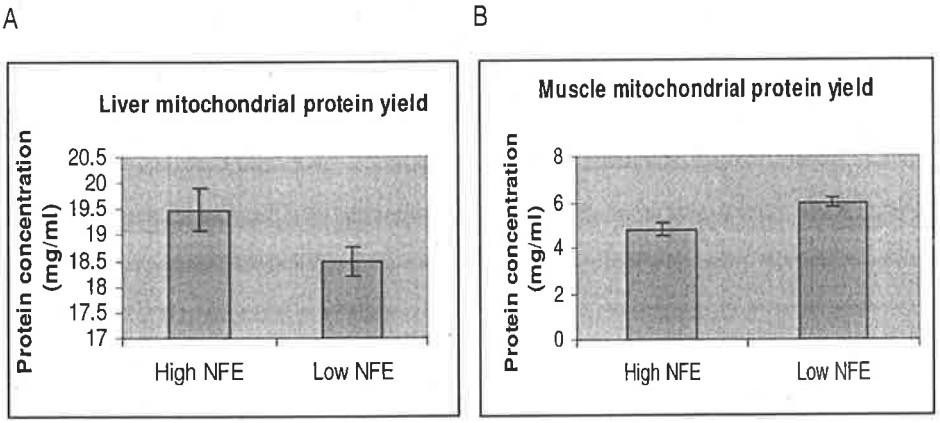

Figure 4.3: Mitochondrial protein yield in A) liver (P = 0.63) and B) muscle (P = 0.29).

4.2.1.2 Citrate synthase enzyme activity assay

Citrate synthase, an enzyme in the TCA cycle, is commonly used as a marker for mitochondria (Trounce *et al* 1996; Robinson and Srere, 1985). Citrate synthase activity was assayed in the samples extracted from the liver and muscle of the 10 most extreme high and low NFE animals to verify the quality of the mitochondria (Figure 4.4 A, B). The level of enzyme activity differed between the liver and muscle, but these levels were similar to those reported elsewhere (Vezinna and Williams 2005). Variation in the levels of citrate synthase enzyme activity between the tissues was not unexpected because the level depends on tissue type (Vezinna and Williams 2005). Differences in citrate synthase activity in the high and low NFE animals were barely non-significant (P =0.07 and P = 0.11 for liver and muscle, respectively).

A

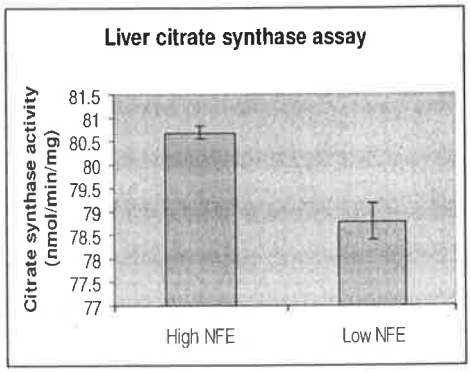

B

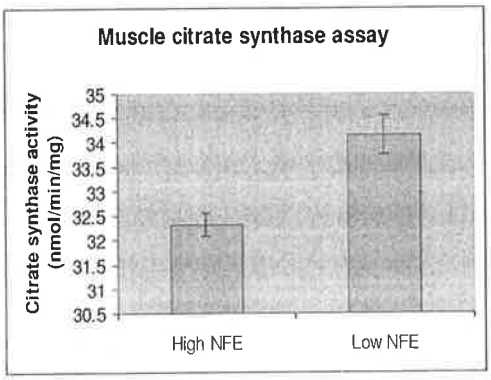

Figure 4.4 Citrate synthase assay in A) liver (P = 0.07) and B) muscle (P = 0.11).

4.2.1.3 Electron microscopy

The same samples measured for citrate synthase were used for electron microscopy (EM) studies. The electron micrographs revealed the expected broken mitochondria membranes in the samples (Figure 4.5, 4.6). It should not be surprising that mitochondrial membranes were disrupted if the samples underwent a freeze / thaw cycle. As recommended by Christensen (1971), the samples were collected, snap frozen in liquid nitrogen and stored at -80^{0}C. During the isolation of the mitochondria, the samples underwent a freeze thaw cycle and sonication as described for mitochondrial enzyme kinetic studies (Harmon *et al* 1982; Bhattacharya *et al* 1991).

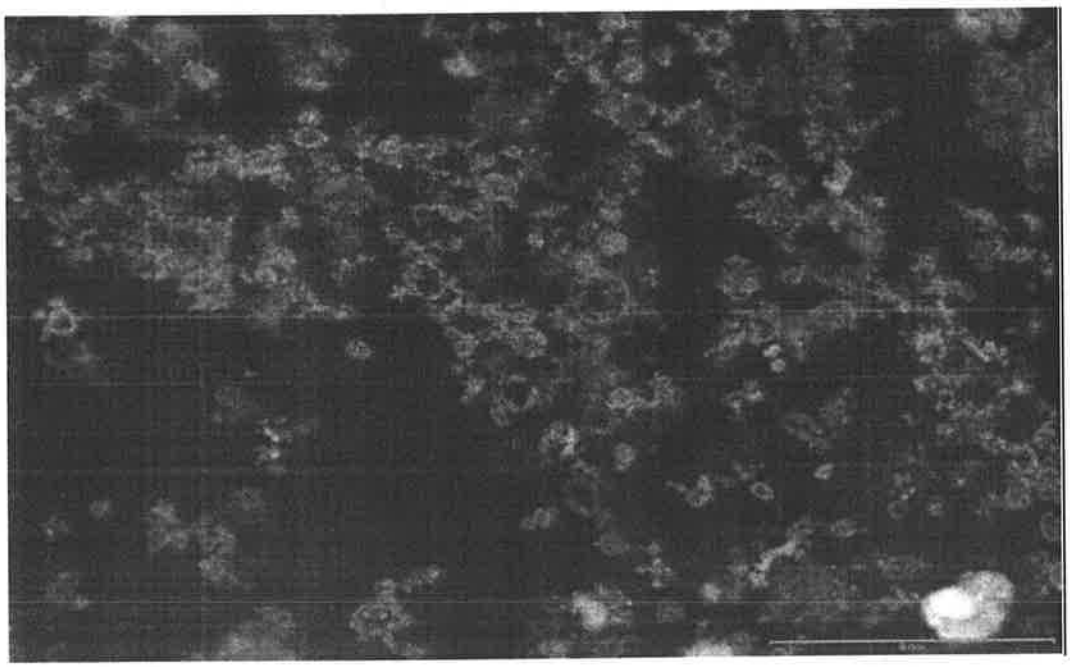

Figure 4.5 Transmission electron microscopy of liver mitochondria under 10,000x.

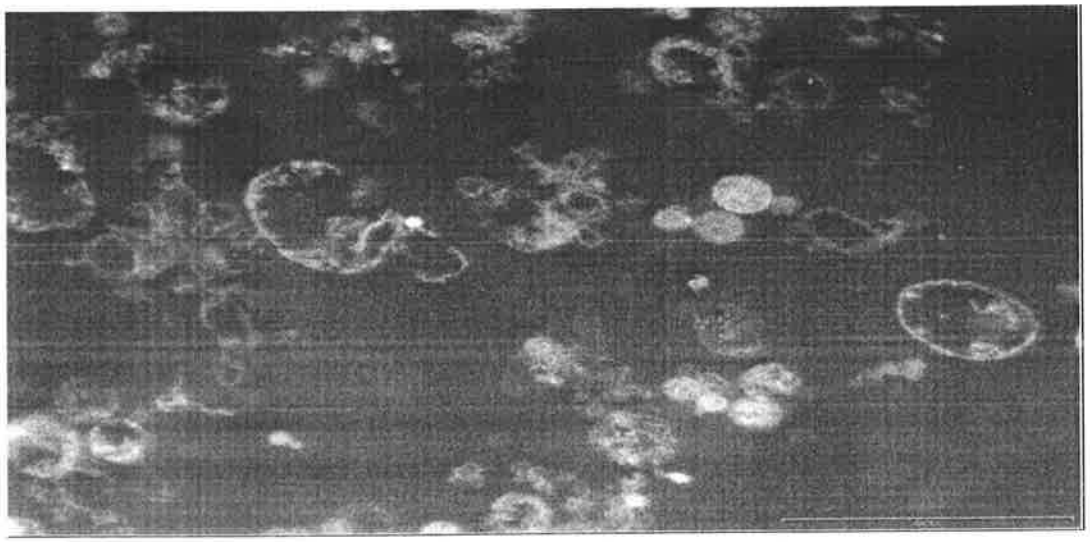

Figure 4.6 Transmission electron microscopy of muscle mitochondria under 10,000x.

4.2.2 Oxidative phosphorylation complex enzyme activity in high and low NFE animals

Having assessed the mitochondrial preparations, the enzyme activities of complexes I, II and IV in the samples were measured by spectrophotometer and analysed by single factor analysis of variance. In the liver samples, the high NFE cattle had 19% lower Complex I activity than the low NFE cattle ($P < 0.0006$) (Table 4.1, Figure 4.7). The Complex II activities in the liver were found to be 10% higher in the high NFE animals. However, this difference was not significant ($P = 0.52$) (Table 4.1, Figure 4.7). For the Complex IV, the activity in high NFE animals was 30% higher in liver than in the low NFE cattle. However, there was much more experimental variation in the measurement of Complex IV activity than Complex I, and this difference was also not significant ($P = 0.24$) (Table 4.1, Figure 4.7).

Since a significant difference was found in the Complex I activity in liver, the experiment was repeated three times using liver samples from the top 20 high and low NFE animals from the Angus 2005 cohort. The results were confirmed as the high NFE animals consistently had a lower activity ($P = 0.0006$) (Table 4.1, Figure 4.7). However, when the Complex I activity was measured in the mitochondria from the high and low NFE muscle samples ($P = 0.90$), there was no difference in the enzyme activity (Table 4.1, Figure 4.7).

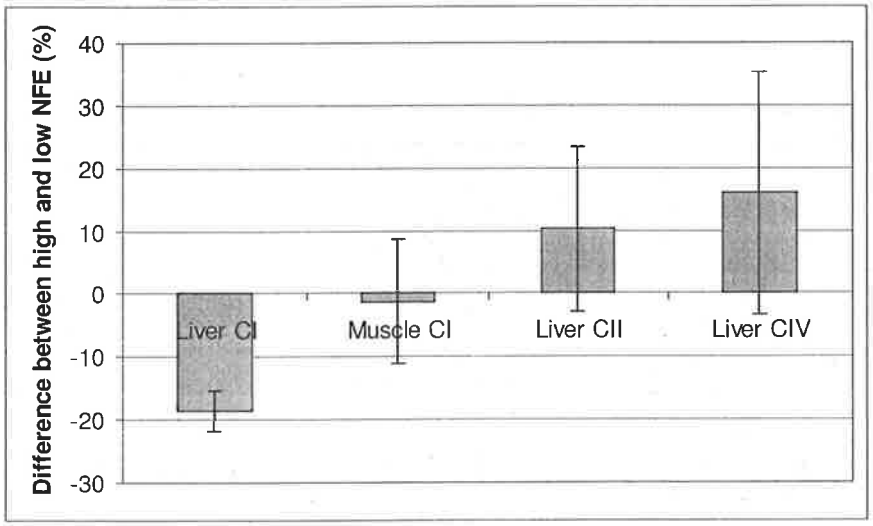

Figure 4.7 Enzyme activities of high NFE animals relative to low NFE animals (Angus 2005 cohort). CI: Complex I, CII: Complex II, CIV: Complex IV

Table 4.1 Mitochondrial complex activities in high *vs.* low NFE animals (Angus 2005 cohort). Values are means ± SE

Tissue	OXPHOS Complex	High NFE (nmol/mg/min)	Low NFE (nmol/mg/min)	P-value
Liver	Complex I (n=40)	21.16 ± 0.83	25.09 ± 0.99	0.0006
	Complex II (n=20)	7.07 ± 0.84	6.41 ± 0.56	0.52
	Complex IV (n=20)	258.1 ± 42 .83	222.6 ± 32.62	0.24
Muscle	Complex I (n=16)	39.27 ± 3.89	39.8 ± 2.69	0.90

4.2.3 Regression analysis of complex enzyme activities in high and low NFE animals

Regression of the liver mitochondrial Complex I enzyme data on NFI showed a positive correlation with net feed intake (r = 0.53) (Table 4.2). Complex I activity in the muscle mitochondria was not correlated (r = 0.014) with net feed intake (Figure 4.8). Liver Complex I enzyme activity was weakly negatively correlated with intra-muscular fat (IMF) (r = -0.22) and moderately positively correlated with daily feed intake (DFI) (r = 0.39), but not average daily gain (ADG) (r = -0.09) (Table 4.2). Complex I activity in the muscle mitochondria was weakly positively correlated with IMF, ADG and DFI with correlations of 0.24, 0.15, and 0.21, respectively (Table 4.2).

A

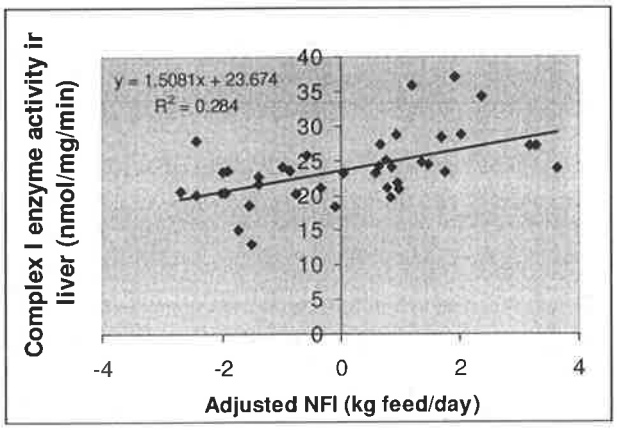

B

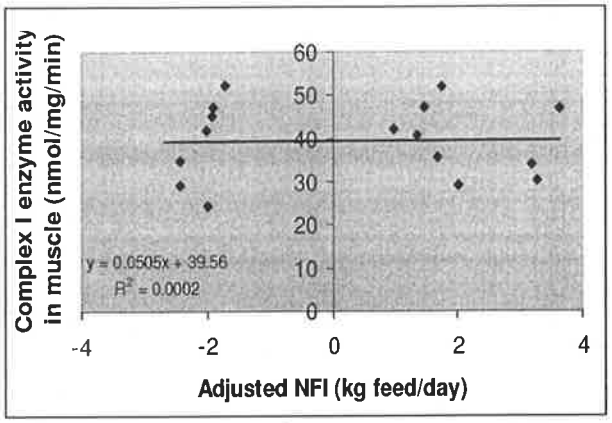

Figure 4.8 Adjusted NFI *vs.* enzyme activity of Complex I in A) liver and B) muscle tissues (Angus cohort 2005)

The liver Complex II enzyme activity had a weak negative correlation (r = -0.20) with NFI (Figure 4.9). The Complex II enzyme activity was moderately correlated with average daily gain (ADG) (r = 0.34), weakly correlated with intra-muscular fat (IMF) (r = 0.17), and weakly but negatively correlated with daily feed intake (DFI) (r = -0.13) (Table 4.2).

Regression analysis of liver mitochondrial Complex IV enzyme activity with NFI also showed a moderate negative correlation (r = -0.28) (Figure 4.10). The Complex IV enzyme activity was only weakly correlated with intra-muscular fat (IMF) (r = 0.15), whereas it was negatively correlated with daily feed intake (DFI) (r = -0.44) (Table 4.2). No correlation between Complex IV enzyme activity and average daily gain (ADG) (r = 0.06) was observed.

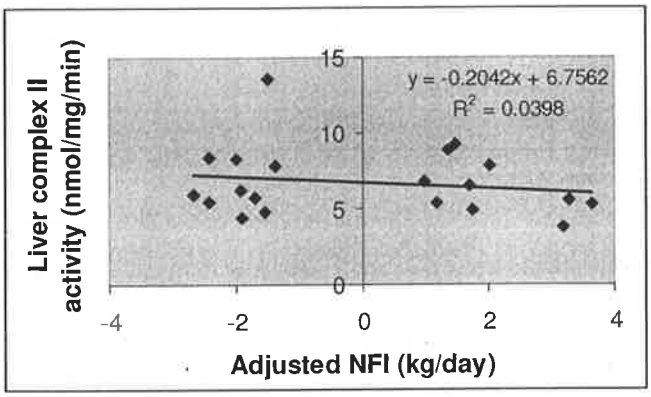

Figure 4.9 Adjusted NFI vs. enzyme activities of Complex II in liver tissues of high and low NFI animals (Angus cohort 2005).

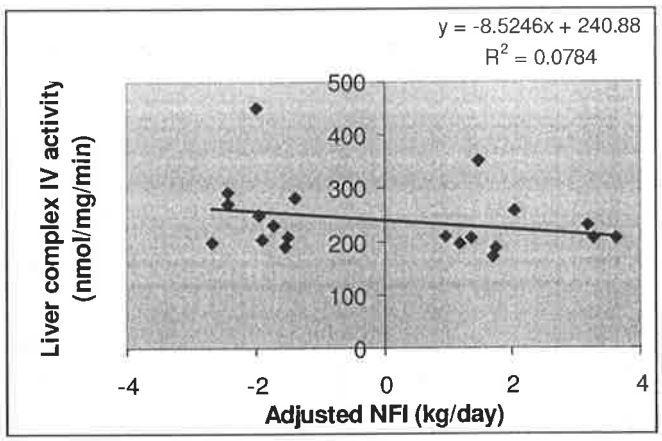

Figure 4.10 Adjusted NFI vs. enzyme activities of Complex IV in liver tissues of high and low NFI animals (Angus cohort 2005).

Table 4.2 Correlations of Complex activities with traits

Traits	Liver Complex I	Muscle Complex I	Liver Complex II	Liver Complex IV
ADG	-0.09	0.15	0.34	0.06
DFI	0.39***	0.21	-0.13	-0.44**
IMF	-0.22	0.24	0.17	0.15
NFI	0.53****	0.01	-0.20	-0.38*

ADG: Average daily gain; DFI: Daily feed intake; IMF: intra-muscular fat; NFI: Net feed intake
(*: ≤0.05, **: ≤0.025, *:≤0.01, ****: ≤0.005)**

4.3 Discussion

Several studies have reported relationships between mitochondrial metabolic activity and longevity, breed differences, stress, diet, and body composition in mammals (mouse, poultry), reptiles (lizards, turtles) and fish (Mukherjee *et al* 1970; Dziewiecki and Kolataj, 1976; Renner *et al* 1979; Wolanis *et al* 1980; Dzapo and Wassmuth, 1983; De Schrijver and Privett, 1984; Brown *et al* 1986; Toyomizu *et al* 1992 a,b,c; Hand and Hardewig, 1996; Hocquette *et al* 1998; Iqbal *et al* 2004; Pomp *et al* 2006). There are also studies showing correlations between mitochondrial oxidative phosphorylation activity, heat loss and feed efficiency in cattle (Kolath *et al* 2006), poultry (Bottje *et al* 2005) and rats (Hocquette *et al* 1998, Lutz and Stahly, 2003; Nielsen and McDonald, 2006). However, very few studies have been conducted to examine the variation in mitochondrial enzyme activity and the effect on net feed efficiency in cattle. Therefore, respiratory chain enzyme assays were performed to develop a greater understanding of the relationship between mitochondrial oxidative phosphorylation and net feed efficiency in beef cattle.

The mitochondrial Complex I enzyme activity in the liver was 19% lower in the high versus the low NFE animals. The increased enzyme activity of Complex I in the low NFE animals could be due to a compensatory mechanism to maintain adequate oxidative phosphorylation. The hypothesis would be that mitochondrial function in the low efficiency animals is somehow impaired (e.g. an alteration in the structure of one of the enzyme complex subunits, an imbalance in subunit ratio, etc) and therefore, Complex I activity is elevated so that the same level of ATP can be produced. Such compensatory mechanisms of mitochondria have been described previously. Li *et al* (2007) reported compensatory increase in Complex III activity by suppressing expression of the nuclearly encoded subunit 4 of Complex IV.

Instead of impaired oxidative phosphorylation, another possibility is that there is inadequate reduction of oxygen and / or proton leakage in the low NEF animals. Either of these 2 scenarios would result in an increase in oxidative stress due to the production of free radicals (referred to as reactive oxygen species or ROS) in the low NFE animals. Any increase in proton leakage increases the uncoupling reactions. These uncoupling reactions generate heat without energy production, and therefore, increase the energy demand. In order to compensate for the increased energy demand, the oxidation of nutrients and protein turnover also increases. Therefore, in low NFE animals, increased Complex I enzyme activity could be part of a compensatory mechanism to counteract oxidative stress. In other words, it could hypothesize that in high NFE animals, oxidative phosphorylation is tightly controlled and proton leakage is low. Therefore, the development of oxidative stress and ROS production is prevented. Consequently, Complex I enzyme levels would be lower in more efficient animals.

There is an increasing evidence that Complex I itself is a major source of reactive oxygen species, such as superoxide (O_2^-) in the mitochondria, and therefore, Complex I is a significant contributor to cellular oxidative stress (Kussmaul and Hirst, 2003; Turrens 2003; Brad *et al* 2004,). Increases in ROS concentrations also accentuate oxidative stress because ROS are responsible for 1) mitochondrial mutations, 2) oxidative damage to mitochondrial proteins and lipids, and 3) decreased capacity to degrade proteins (Wei, 1998).

With regards to ROS production, Complex II participates in the electron transport chain via the succinate to ubiquinone pool in the TCA cycle, which bypasses the respiratory chain Complex I. Complex II does not participate in proton translocation, and it only feeds electrons into the electron transport chain. Therefore, Complex II is not involved with generating ROS. Although Complex III is considered as another source of superoxide (O_2^-) production, Complex III produces much less O_2^- than Complex I (Kussmaul and Hirst, 2003). Complex IV reduces oxygen to water using an electron from cytochrome C and also produces little or no superoxide (Lambert & Brand, 2004). The role of Complex V is to control proton movement and maintain the membrane potential.

Thus, it is most likely that alterations in Complex I itself would affect ROS production, accentuating oxidative stress and decreasing the energy status of the cell. This oxidative stress would be expected to be reflected by high feed intake, less average daily weight gain and more heat production ("heat of wasting") due to uncoupled oxidative phosphorylation in the less efficient animals. This hypothesis is in agreement with the Complex I results in liver samples herein as there were positive correlations between daily feed intake (DFI, r = 0.39) and net feed intake (NFI, r = 0.53) (Table 4.1). Low heat production in high NFE animals has been observed by other research groups. For instance, high NFE mouse lines had lower heat production (13-39%), marginally lower post-weaning weight (0-12%), little difference in mature weight (0-3%) and were fatter (6-50% depending on age at measurement) (Pitchford, 2004). In the current study, the Complex I enzyme activity was negatively correlated with intra-muscular fat (IMF, r = -0.22).

Interestingly, the muscle Complex I activity was not significantly different between the high and low NFE animals. There could be a number of explanations. Two of the more likely explanations would be: 1) the enzyme activity of Complex I in the muscle was already up-regulated or 2) the type of muscle sampled was not indicative. Notably, the enzyme activity in the muscle was substantially higher (~ 50%). Moreover, variation in mitochondrial activity in different muscle types has been reported by many research groups (Thakar, 1977; Chanseaume *et al* 2006). It has been shown that the level of mitochondrial oxidative phosphorylation depends on the type of muscle (white or red), metabolic pattern (glycolytic or oxidative), location of the muscle and the activity involved. Red muscles are known to have

a high mitochondrial content, high vascularity, plus high aerobic and oxidative metabolism. Whereas, white muscles have higher glycolytic enzyme activities, are more anaerobic, and are more suitable for short rapid contractile activity. In the current study, the muscle samples were collected from the neck (brachiocephalicus). Based on the location and activity, the brachiocephalicus is classified as red muscle. Since muscles like the brachiocephalicus are adapted for sustained activity, the mitochondrial function could be elevated with less variation in enzyme activity (Thakar, 1977; Kwong and Sohal 1998).

Significant differences were not found between high and low NFE cattle in Complex II and IV enzyme activities. These are not rate-limiting enzymes, and would not necessarily be expected to differ between the high and low NFE animals. Interestingly, the trend of decreased Complex II and IV activities in the low NFE animals are similar to those reported for poultry. Complex I activity in low NFE chickens was also decreased though (Bottje *et al* 2005; Ojano-Dirain *et al* 2005a).

The correlation between the mitochondrial complex activities and the phenotypic traits had opposite trends for Complex I versus Complex II and IV activities (Table 4.1). In case of NFI and DFI, Complex I activity was positively strongly correlated, while Complex II and IV activities were negatively correlated. Only Complex II had a correlation with average daily gain. Since NFE is independent of weight, one might expect correlations between the Complex enzyme activities and NFI, but not ADG, if the Complex enzyme activities are related to NFE.

With regards to the citrate synthase results, it is of interest that there may be difference in the activity of this enzyme between high and low NFE animals. The difference observed was just not significantly (P= 0.07) in the liver mitochondria. Citrate synthase controls the first committed step of the TCA cycle (Murray *et al* 1996). Increased activity of this enzyme should indicate enhanced activity of the TCA cycle in general. If the TCA cycle is highly active, there will be higher levels of reduced equivalents (namely NADH and $FADH_2$) for oxidative phosphorylation. Therefore, up- or down- regulation of citrate synthase could significantly affect the energy balance of efficient animals. For the studies herein, citrate synthase was only used as a marker to assess the mitochondrial preparation, and hence, only 10 animals were assayed. Citrate synthase should be part of a more extended study of mitochondrial enzymes with more samples assayed to verify the results herein.

4.4 Future studies

Since there were significant differences in the liver Complex I enzyme activity between high and low efficiency cattle, a more detailed investigation of mitochondrial function in the high and low NFE animals using polarographic measurements of oxygen consumption should be conducted to determine the respiratory control ratio and ADP:O ratio (Iqbal *et al* 2003). The respiratory control ratio ratio represents

the degree of coupling or efficiency of electron transport chain activity, and therefore, would provide a clearer picture of any oxidative phosphorylation differences due to proton leakage. The levels of adenine nucleotide translocators could be assayed to determine the ATP/ADP ratio, and thus, the energy status of body (Malgat *et al* 2000). Measurement of free radicals (e.g. hydrogen peroxide) and carbonyl levels would help to determine the status of oxidative stress and protein degradation, respectively (Chaudhari *et al* 2006). These studies are warranted to develop a better understanding of the consequences of oxidative stress and protein degradation on oxidative phosphorylation ATP production in high and low NFE animals.

The size of mitochondrial genome is 16,400-bp sequence. The maternally inherited mitochondrial genome is highly susceptible to mutation (Thomas *et al* 2004). Mutations in mitochondrial DNA can be responsible for metabolic diseases (Wallace, 1999). As far as genetic variation in terms of SNPs are concerned, on an average, 9.8 and 8.9 mutations were reported in the mitochondrial genome of high and low-RFI Angus steers respectively (Kolath *et al* 2006). In the same experiment, Kolath *et al* (2006) found a lack of mutations across animals in either the high or low RFI group indicating that polymorphisms of mitochondrial DNA were not related to the RFI status in a contemporary group of Angus steers.

Since the majority of genetic progress in the industry comes through selection of superior males. Thus, the key in most selection breeding programs would be to target nuclear genes that affect mitochondrial function rather than the mitochondrial genes *per se*.

Chapter 5

Mitochondrial protein expression profiling by two-dimensional differential gel electrophoresis (DIGE)

5.1 Introduction

Two-dimensional (2-D) polyacrylamide gel electrophoresis (PAGE) is a well established proteomics tool for generating quantitative protein expression profiles. This tool develops a global view of the proteome state by resolving proteins based on their charge and mass, whereby thousands of spots can be visualised (Gorg *et al* 2000). Every protein and its isoform have a unique position on a polyacrylamide gel (Ducret, 2000). Based on the spot position, pattern and intensity, samples from different groups can be compared for differential expression or changes in the protein profile. Such experiments can lead to the identification of protein biomarkers or can be used to study the behaviour or regulation of cellular metabolic pathways in particular physiological or pathological states (Frisco, 2000).

A major limitation of conventional 2D methods is that they rely upon comparisons between images from 2 or more different gels. Frequently, because of differences in gel quality, sample preparation, loading, and electrophoresis conditions, the two gel images can not be directly superimposed and warping is required to overlay the images (Tonge, 2001). The high degree of gel-to-gel variation in the spot patterns makes distinguishing true biological variation from experimental variation problematic. Even equivalent protein samples can have different positions with variable intensities, complicating image comparisons. Therefore, many repetitions of an experiment with the same biological samples are required to generate an electronic image replication database for comparisons. Such replication is costly in terms of both time and money.

To avoid these problems with conventional 2-D imaging, the 2-D differential gel electrophoresis (DIGE) technique was developed (Unlu, 1997). In the 2-D DIGE method, protein samples are labelled with spectrally resolvable fluorescently cyanine dyes, such as Cy3 and Cy5. The samples are run simultaneously on the same gel. The gel is scanned using specific filters for the respective cyanine dyes. This approach avoids running separate gels for each sample. The technique, therefore, increases the confidence of matching, detecting, and quantifying differentially expressed proteins. Another advantage of this technique is that the protein spots can be compared against an internal standard run on the same gel. The internal standard is labelled with another cyanine dye (e.g. Cy2) for the comparison. The internal standard is usually a pool of all the samples. Thus, the internal pooled sample represents an average all the proteins to be compared. The internal pooled standard is also used to normalise the spot volume ratios within and between multiple gels. This normalisation step, using an internal pooled standard, reduces the experimental variation greatly (Alban, 2003). Having discovered which proteins are differentially expressed by DIGE, the proteins themselves are identified by the tandem mass spectrometry MS/MS, which uses matrix assisted laser desorption/ionisation-time of flight/time of flight analyses (MALDI-TOF/TOF).

The purpose of the proteomic study herein was to aid in the selection of genes within the NFE QTL regions. Based on the initial candidate gene selection from the QTL regions, more than 50% of the genes contribute to energy pathways, including the citric acid cycle, oxidation of fatty acids and oxidative phosphorylation (OXPHOS). The proteomic experiments were based on the hypothesis that any functional alteration in the subunits of the OXPHOS complexes or other mitochondrial proteins would affect oxidative phosphorylation or other pathways related to energy metabolism and glucose turnover. This would ultimately affect the total energy intake and energy homeostasis of the animal, resulting in either high and low feed efficiency. Therefore, the primary focus was to study the differential expression pattern of the mitochondrial proteins between high and low net feed efficiency animals.

5.2 Results

5.2.1 Differential mitochondrial protein expression in high *vs.* low net feed efficiency animals

Mitochondrial protein expression was compared between high and low net feed efficiency (NFE) animals in liver and muscle samples from two Angus cohorts (2005 and 2006). The 2-DIGE technique was used with a pooled Cy2 labeled internal standard containing protein extracts from both the high and low NFE animals. The high and low NFE protein samples were labeled with 2 fluorescent dyes, Cy5 or Cy3. Dye swapping was conducted to control labeling efficiency errors. The control sample (also referred as a pooled internal standard) was labeled with Cy2 and represented an equal amount (µg protein) of the two test samples. Fluorescent images of Cy2, Cy3 and Cy5 protein spots were analyzed using the data image analysis (DIA) and biological variation analysis (BVA) module of the DeCyder software. The analyses revealed changes in the abundance of individual proteins as determined by statistical variance of average spot volume ratio between the high and low NFE animals at the 95% confidence level (Student t-test; $p<0.05$). Due to intrinsic technical variation caused by factors such as dye fluorescence intensity and changes in the iso-electric focusing conditions, only those proteins showing consistent differential expression were considered for further analysis, namely protein identification by MALDI-TOF-TOF mass spectrometry analysis.

5.2.1.1 2-D DIGE experiments on liver samples from Angus cattle (cohort 2005)

The first experiment was conducted on the extreme six high and six low NFE animals from the Angus 2005 cohort. These animals had an average 2.4 kg/day net feed intake difference. A total of six gels with 2 randomly selected liver mitochondrial protein samples from 1 high and 1 low NFE individuals were run (Table 5.1). These six 2-D gels were analyzed by *Ettan DIGE imager (GE HEALTHCARE)* laser scanning and 18 images were obtained (3 images per gel; Cy2, Cy3 and Cy5). The total number of spots resolved by DIGE ranged between 500-800 (Figure 5.1). Due to a large number of spots detected on Gel 4 (Table 5.2), it was selected as a master or reference gel for comparison to the other gels.

Table 5.1 Experimental design for labeling the CyDye fluors low NFE (105, 101, 59, 69, 63, and 8); High NFE (12, 19, 48, 3, 26, and 60)

Gel	Cy2	Cy3	Cy5
1	Pooled internal standard (105, 12)	Sample 105	Sample 12
2	Pooled internal standard (19, 101)	Sample 19	Sample 101
3	Pooled internal standard (59, 48)	Sample 59	Sample 48
4	Pooled internal standard (3, 69)	Sample 3	Sample 69
5	Pooled internal standard (63, 26)	Sample 63	Sample 26
6	Pooled internal standard (60, 8)	Sample 60	Sample 8

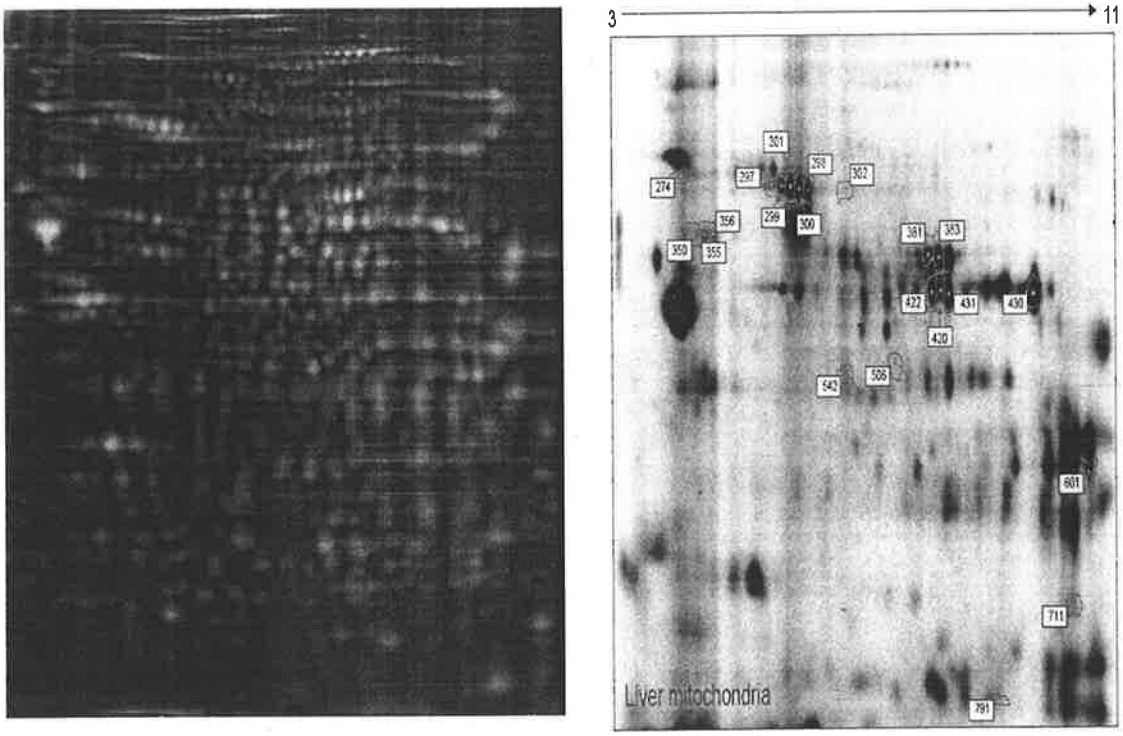

Figure 5.1 Example of a fluorescently labelled 2 DIGE image and Coomassie Brillant Blue R-250 image of liver mitochondrial proteins from the Angus experimental 2005 cohort.

Table 5.2 Total number of spots found on 6 individual gels from liver protein samples and number of matched Cy2, Cy3 and Cy5 fluorescent spots within individual gel (cohort 2005)

Animal number	Gel no.	Image no.	No. of total spots[a]	Number of spots matched[b]
105, 12	1	1, 2, 3	490	261
19, 101	2	4, 5, 6	433	304
59, 48	3	7, 8, 9	549	370
3, 69	4	10, 11, 12	853	853
63, 26	5	13, 14, 15	773	310
60, 8	6	16, 17, 18	813	530

a: Total number of spots identified, b: number of spots matched with master gel

After electrophoresis, the image analysis was performed by compiling all the images with *DeCyder* software. Spot detection and quantification was performed automatically by comparing gel images of Cy2 (internal pooled standard)/Cy3 ($sample_{An}$) and Cy2 (internal pooled standard/Cy5 ($sample_{Bn}$) using the Difference in Image Analysis (DIA, GE HEALTHCARE) module. The spot volume was used as a measure of protein abundance. Standardized abundance for each spot was expressed as a volume ratio between the internal pooled standard and the co-detected sample within the gel. In this manner, volume ratios of each spot from the co-detected images (Cy3 and Cy5) were calculated based on the internal pooled standard (Cy2) within a gel and between gels. The spot map, developed by using the Biological Variation Analysis module (BVA), was matched for the 2 groups and a t-test was used to determine if there was a significant difference in the volume ratios between high and low NFE samples. Spots that had P-values ≤ 0.05 were filtered and considered to be differentially expressed proteins. The spots that were found to be differentially expressed between the experimental samples were also checked manually in the 3-dimensional format of the DIA module (Figure 5.3). By comparing within gel standard/sample volume ratio measurements from different gels, the gel-to-gel experimental variation of spot volume and migration could be compensated. After the spot map analysis, 18 spots were found to be reduced (ratios from -1.16 to -1.74) and 7 spots were found elevated in the high NFE animals (ratios from +1.20 to +1.60) (Figure 5.2).

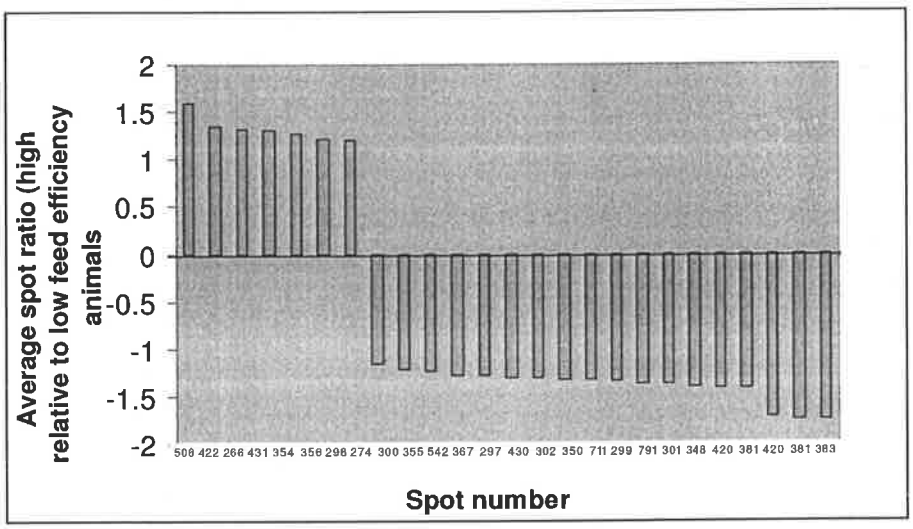

Figure 5.2: Proteins found to be differentially expressed between the low and high NFE groups (P< 0.05). An average ratio of > 0 indicates that the protein was up-regulated in high NFE relative to low NFE animals. An average ratio of < 0 indicates that the protein was down-regulated in high NFE relative to low NFE animals.

Spot No. and protein name	Low NFE	High NFE
348 Catalase		
422 Glutamate dehydrogenase		
298 Annexin VI		
350 Heat shock protein 60 kDa	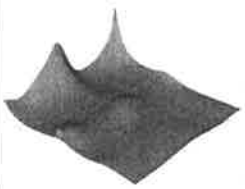	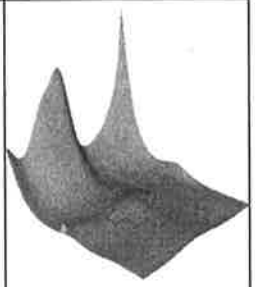
302 succinate dehydrogenase		

Figure 5.3 Representation of 3-dimensional expression profile images from differentially expressed spots. Samples were liver mitochondria from the Angus 2005 cohort. The purple outline encompasses the peak. Figure was generated using Decyder software.

5.2.1.2 Mass spectrometry results of liver samples from Angus cattle (cohort 2005)

The 11 differentially expressed proteins were identified by MALDI-TOF/TOF using peptide mass fingerprinting and confirmed by MS/MS sequencing of 3 selected peptide ions, which were fragments of each protein. The peptide mass fingerprinting and the mass spectrometry sequencing spectra were interpreted with MASCOT software. Protein identity was confirmed by setting the probability score of MASCOT higher than 64 (Appendix 5.1).

The protein with the largest MOWSE (**Mo**lecular **W**eight **SE**arch database) score did not always correspond to a known bovine protein. This can be attributed to the large number of entries in the NCBInr database for homologous proteins from different species, which may be identical or may contain a small number changes. Consequently, it is possible to obtain larger MOWSE scores for proteins that do not originate from the target species. When this occurred, the bovine protein with the largest MOWSE score was imported into BioTools 2.0 software (Bruker Daltonics, Germany) for further identification of protein. Identities were obtained for 19 of the 24 spots corresponding to eleven different proteins and their isoforms. The five protein spots that could not be identified had extremely faint spots on the 2-DE gel (Figure 5.1.). Hence, the amount of material was insufficient for the mass spectometry analysis.

Amongst the 11 identified proteins, the levels of nine proteins were lower in high NFE animals. These were NADH dehydrogenase (ubiquinone) 1- alpha subcomplex, 5 (19 kDa), catalase, albumin, heat shock protein 70 kDa, heat shock protein 60 kDa, Complex V subunit (F1 ATPase) ATPase V1 subunit G2, TNF receptor - associated factor 2 isoform 2, succinate dehydrogenase and aldolase B. Two proteins were elevated in the high NFE animals, lipocortin VI (also referred as annexin VI) and glutamate dehydrogenase (Appendix 5.1).

Two isoforms were found for the heat shock protein 70 kDa (spots 297, 299), lipocortin VI (spots 298, 300), complex V subunit (F1 ATPase) (spots 420, 430) and glutamate dehydrogenase (spots 422, 431). There were 3 isoforms for catalase (spots 348, 381 and 383) and heat shock protein 60 kDa (spots 350, 355 and 356) also found.

In the case of the two isoforms of lipocortin VI (spots 298 and 300), the isoform in spot 300 was lower in the high NFE animals (average fold ratio -1.21), whereas the expression of the other isoforms in spot 298 was elevated (average fold ratio 1.20) in the high NFE animals. However, for spot 300, only a tentative assignment could be made due to the low MOWSE score. The assignment was based on the similarities observed in the mass spectra and their close proximities to lipocortin VI. Given the

discrepancy in the expression levels in the high NFE animals, the assignment of lipocortin to spot 300 may be incorrect.

Spots 420 and 430 matched bovine mitochondrial F1-ATPase chain C, complexed with the peptide antibiotic efrapeptin (gi|1942370). This entry is equivalent to "ATP synthase, H+ transporting, mitochondrial F1 complex, alpha subunit, isoform 1, cardiac muscle" from *Bos taurus* (Swiss prot entry ATPA1_bovin). F1-ATPase is a Complex V subunit. Both spots had lower levels (average fold ratio -1.41 and -1.35 for spots 420 and 430, respectively) in the high NFE animals. It appears that these two proteins are isoforms. However, spot 420 was also found to contain peptides that matched glutamate dehydrogenase 1.

The identification of glutamate dehydrogenase isoforms in spots 422 and 431 was based on good MOWSE scores. Both isoforms showed 1.33 fold elevated expression in the high NFE animals compared to the low NFE animals. All three isoforms for catalase, found in spots 348, 381 and 383 were lower in the high NFE animals.

Although 3 isoforms (spots 350, 355 and 356) were found for the heat shock protein 60 kDa, spot 356 was a tentative assignment because of a low MOWSE score. The assignment was based on the similarities observed in the mass spectra and the close proximity to heat shock protein 60 kDa. The two isoform in spots 350 and 355 had lower levels (average fold ratio -1.32 and -1.23, respectively) in high NFE animals, while the isoform in spot 356 was increased (average fold ratio was 1.21). However, as pointed out, the identification of spot 356 was tentative.

The relative positions of the spots on the gel correlated with the predicted molecular weights of the identified proteins. The predicted isoelectric points of the spots, however, did not always correspond to observed isoelectric point. For instance, the observed isoelectric point differed for albumin, catalase, chain C bovine mitochondrial F1- ATPase complex with the peptide antibiotic efrapeptin, heat shock protein 60 kDa (similar to LOC511913) and LOC515263 (similar to aldolase B). These proteins had a difference of more than one pH unit removed from the predicted value. This may be due to the presence of unknown post-translational modifications or, in the case of LOC511913 and LOC515263, incorrect annotations in the database. The protein sequences of LOC511913 and LOC515263 were compared to NCBI mammalian protein database using the basic local alignment search tool BLAST:http://www.ncbi.nlm.nih.gov/BLAST). It was found that LOC511913 was 99% similar to the 60 kDa heat shock protein from *Bos taurus* (gi|76644268), and LOC515263 was 99% similar to aldolase B from *Ovis aries* (gi|560487).

5.2.1.3 2-D DIGE experiments on muscle samples from Angus cattle (cohort 2005)

A second set of DIGE experiments was conducted on mitochondria from the neck muscle samples of the same 12 extreme NFE animals used previously for the liver mitochondrial DIGE experiments. Experimental conditions were identical to the liver DIGE experiments except a 24 cm IPG strip was used and the isoelectric focusing conditions were extended for better protein resolution. The most extreme six NFE animals were selected from both the low and high NFE groups and their muscle mitochondrial protein samples were mixed in equal amounts and labeled with Cy-dye (Cy3 or Cy5). The two pooled samples were then run together with an internal pooled standard labeled with Cy 2. The experiment was repeated, but the dyes for each group were swapped (Table 5.3). Gel No 73151 was chosen as the master gel because of the high number of total spots. A total of 6 images were obtained (Figure 5.4 A and B) and analyzed in the BVA module as described above. Thirteen spots were found to be significantly different ($p<0.05$) between the protein profiles of the muscle mitochondria prepared from the high and low NFE cattle (Figures 5.5 and 5.6). Preparative amounts of un-labeled protein were loaded on both gels (03283 and 73151) to allow the 13 candidate spots to be excised for identification by mass spectrometry without running additional gels.

Table 5.3 Total number of spots found on 2 gels from pooled muscle protein samples and matched spots in Cy2, Cy3 and Cy5 fluorescent images within individual gel

Gel no.	Label	Group	No. of total spots[a]	Number of spots matched[b]
3283	Cy2	Standard (8,19, 12, 48, 3, 26 60, 63,105, 101, 59, 69)	1995	747
	Cy3	Low NFE (60, 12, 19, 26, 48, 3)	1995	747
	Cy5	High NFE (8, 63, 105, 101, 59, 69)	1995	747
73151 (Master gel)	Cy2	Standard (8,19, 12, 48, 3, 26 60,105, 101, 59, 69)	2144	2144
	Cy3	High NFE (8, 63, 105, 101, 59, 69)	2144	2144
	Cy5	Low NFE (60, 12, 19, 26, 48, 3)	2144	2144

a: Total number of spots identified, b: number of spots matched with master gel

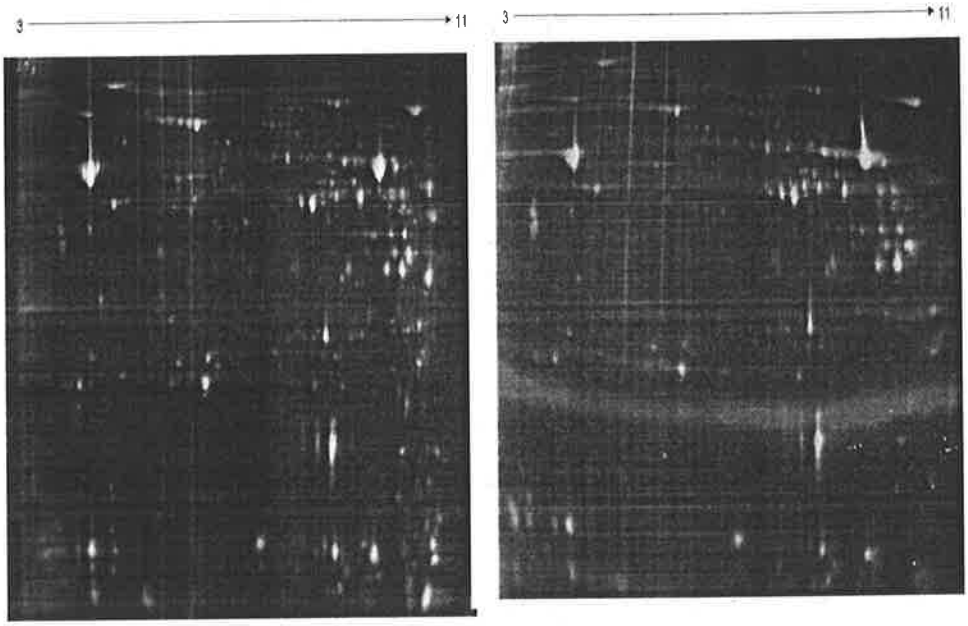

Figure 5.4A Fluorescently labelled 2 DIGE image of muscle mitochondrial proteins from the Angus experimental 2005 cohort.

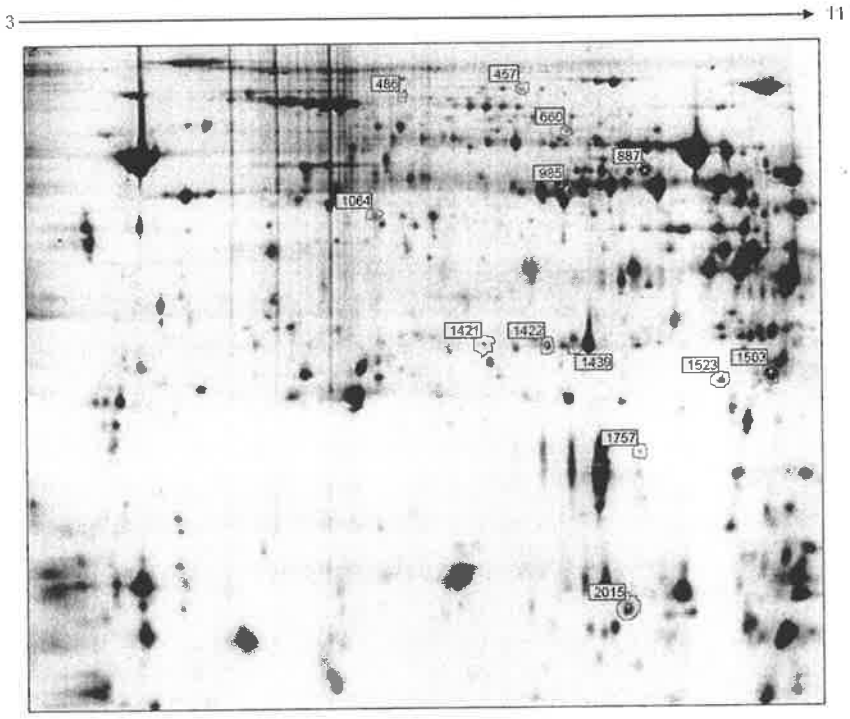

Figure 5.4B Coomassie Brillant Blue R-250 image of muscle mitochondrial proteins from the Angus experimental 2005 cohort.

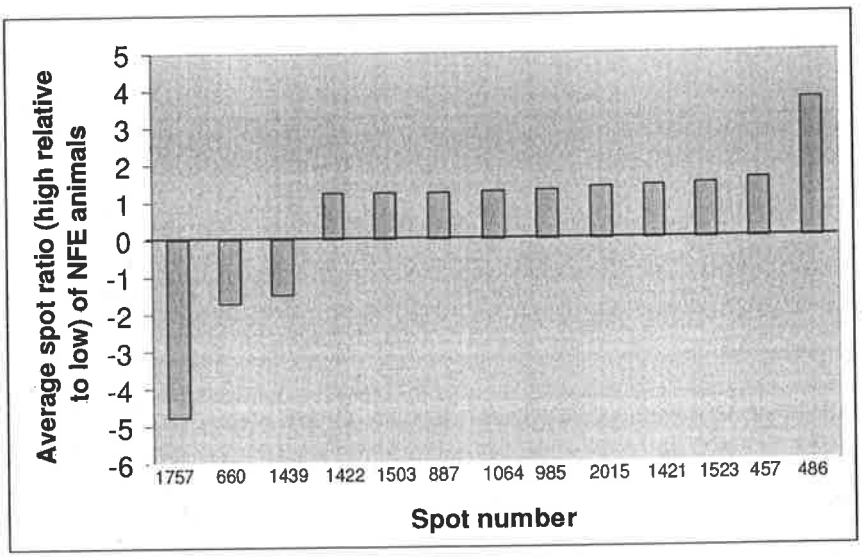

Figure 5.5: Proteins found to be differentially expressed between the high and low NFE Angus 2005 cohort (P<0.05). An average ratio of > 0 indicates that the elevated expression of protein in the high NFE group relative to low NFE group. An average ratio of < 0 indicates that the low protein levels in the high NFE group compare to the low NFE group.

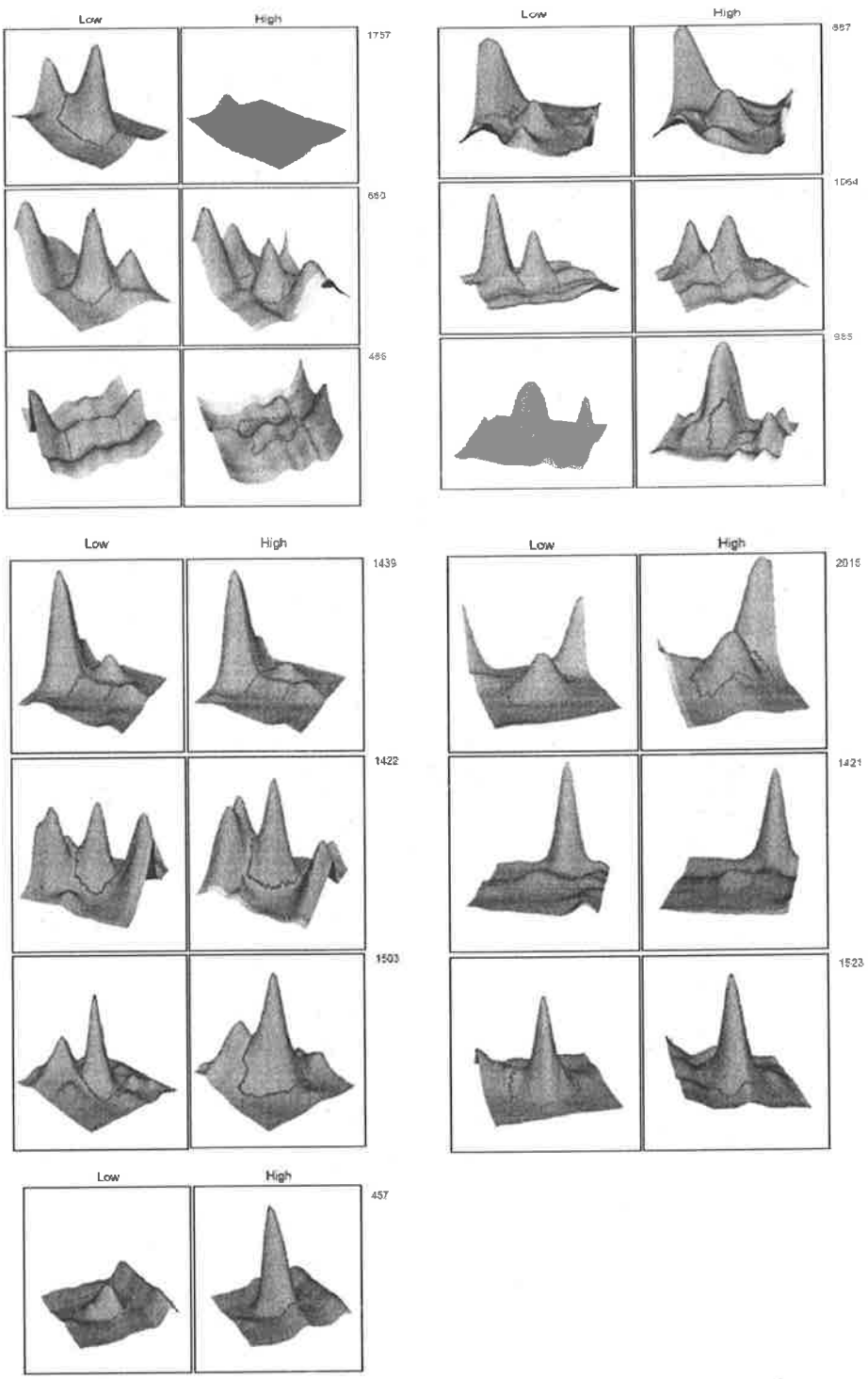

Figure 5.6 3-dimensional expression profile images of the differentially expressed spots from the muscle mitochondria of the Angus 2005 cohort. Figure generated by *DeCyder* software (*GE HEALTHCARE*).

5.2.1.4 Mass spectrometry results of muscle samples from Angus cattle (cohort 2005)

Protein identities were obtained for 8 of the 13 spots of interest (Appendix 5.2). They were catalase, enolase 3, chain B crystal structure of bovine mitochondrial Bc1 complex / complex III, NADH dehydrogenase (ubiquinone) 1- alpha subcomplex-10 (42 kDa), triosephosphate isomerase, NADH dehydrogenase (ubiquinone) 1- alpha subcomplex-10 (22 kDa), adenylate kinase 1, and NADH dehydrogenase (ubiquinone) 1- alpha subcomplex-5 (13 kDa). Identity between H (+)-transporting ATP synthase, and bovine mitochondrial cytochrome Bc1 complex (E chain / complex III) was not confirmed. Appendix 5.2).

Of these 8 proteins, only catalase had lower levels in high NFE animals. The remainders of the proteins were elevated in the high NFE animals. Three of the proteins elevated in high NFE animals (spots 1064, 1503 and 2015) were identified as the 42 kDa, 22 kDa and 13 kDa subunits of NADH ubiquinone:oxidoreductase (complex-I) enzyme, respectively, involved in mitochondrial oxidative phosphorylation. Spot 1064 matched both NDUFA10 and the NADH dehydrogenase (ubiquinone) 1-alpha subcomplex. The sequences of these two proteins differ by only two amino acid residues, and thus, represent protein isoforms.

H(+)-transporting ATP synthase and bovine mitochondrial cytochrome Bc1 Complex E were both identified in spot 1439. These are subunits of ATP synthase (Complex V) and ubiquinol: ferricytochrome c oxidoreductase (Complex III) enzymes involved in mitochondrial oxidative phosphorylation. Of the 7 masses assigned to H(+)-transporting ATP synthase and 5 masses to bovine mitochondrial cytochrome Bc1 complex E chain, only the 816.538 ion overlapped between the two. MS/MS analysis of this parent ion failed to identify the peptide as either EGDIVKR from H(+)-transporting ATP synthase or GKPLFVR from bovine mitochondrial cytochrome Bc1 complex E chain. The predicted pI and MW values of the H(+)-transporting ATP synthase are quite different from the bovine mitochondrial cytochrome Bc1 complex E chain. The protein identities of spots 985 and 1439 were found to be the B chain and E chain of the bovine mitochondrial cytochrome Bc1 of complex III. Both proteins had increased levels in the high NFE animals compared to low NFE animals (average fold ratio 1.38 and 1.22, respectively).

With the exception of the H(+) transporting ATP synthase, the predicted pI and MW values of the other matched proteins correlated reasonably well with their observed positions on the gel. The other proteins elevated in the high NFE animals were identified as enolase 3 (887), triosephosphate isomerase (1422), and adenylate kinase 1 (1523).

Spots 1757, 457, 486 and 1421 could not be identified due to a lack of material. These spots produced poor quality spectra, and consequently, could not be identified even when matched to the complete mammalian database that included human and rodent sequences.

5.2.1.5 2-D DIGE experiment on liver samples of Angus cattle (cohort 2006)

A third set of DIGE experiments was conducted as a biological replicate using a different Angus cohort (cohort 2006). The liver mitochondrial sample preparation and all other experimental conditions were identical to the previous 2-D DIGE experiments on muscle tissue. The most extreme five animals in the low and high NFE groups were selected, and had a 2.0 kg/day difference in net feed intake. Mitochondrial protein samples were mixed in equal amounts for each group and labeled with CyDye (Cy3 or Cy5). The two pooled samples were then run with the internal Cy2 labeled pooled standard. The experiment was repeated with the dyes (Cy3 and Cy5) swapped for the two groups (Table 5.4).

Table 5.4 Total number of spots found on 2 gels from pooled samples of high and low NFE cattle from the Angus 2006 cohort.

Gel	Label	Group	No. of total spots[a]	Number of spots matched[b]
70922 (Master)	Cy2	Standard (33, 83, 12, 101, 98, 54, 39, 121, 42, 40)	3173	3173
	Cy3	High NFE (33, 83, 12, 101, 98)	3173	3173
	Cy5	Low NFE (54, 39, 121, 42, 40)	3173	3173
70928	Cy2	Standard (33, 83, 12, 101, 98, 54, 39, 121, 42, 40)	2985	725
	Cy3	High NFE (33, 83, 12, 101, 98)	2985	725
	Cy5	Low NFE (54, 39, 121, 42, 40)	2985	725

a: Total number of spots identified, b: number of spots matched with master gel

Gel no 70922 was chosen as a master gel because of the higher number of total spots. A total of 6 images were obtained (Figure 5.7) and analysed using the BVA module. Fewer spots matched with gel 70928 because of vertical streaking. Nevertheless, 83 spots were identified as being significantly different ($p<0.05$) between the protein profiles of the high-efficiency and low-efficiency animal liver mitochondria. Manual inspection revealed that a number of these spots corresponded to dust and/or regions of streaking on the gel, which were exacerbated by the poor resolution of gel 70928. Following the exclusion of these spots, the list of significant spots was narrowed to 43 (Figure 5.8 and Figure 5.9).

Preparative amounts of un-labeled protein had been included on gels 70922 and 70928 so that the differentially expressed proteins could be excised for mass spectrometric analysis without running

additional gels. To reduce the number of spots for protein identification, the results of this experiment were compared to the results of previous experiments. Specifically, the spots found to be of the same relative intensity and positions (25 spots) as those identified in previous two experiments were not picked for MS/MS sequencing. Furthermore, the spot intensity levels were evaluated when selecting the candidates for protein identification to ensure there was as sufficient material for sequencing. On this basis, 14 additional spots were selected from the list of 43 differentially displayed spots for protein identification.

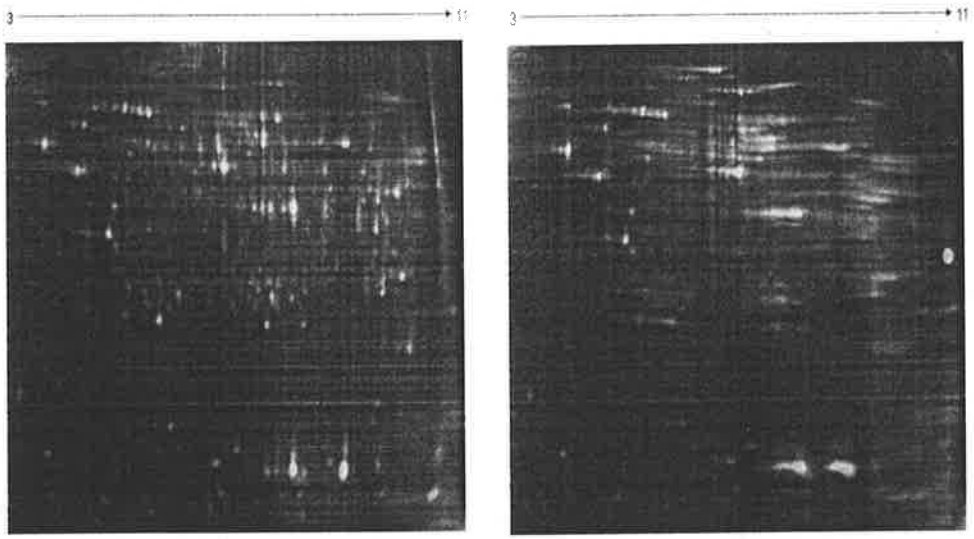

Figure 5.7 Fluorescently labelled 2 DIGE image (left to right, 70928 and 70922) and Coomassie Brillant Blue R-250 image of pooled liver mitochondrial protein samples from the high and low NFE Angus experimental 2006 cohort.

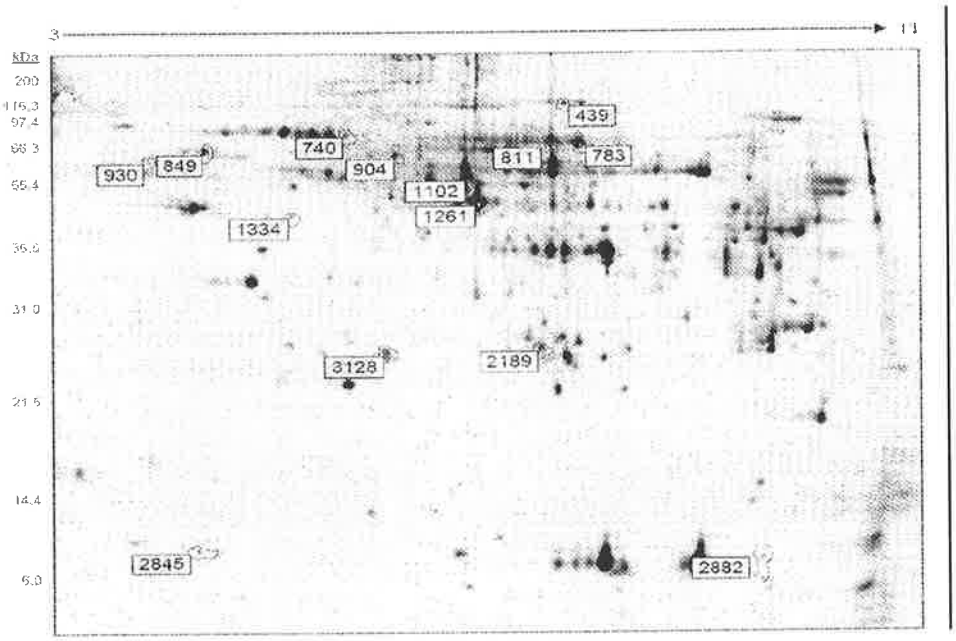

Figure 5.7 Fluorescently labelled 2 DIGE image (left to right, 70928 and 70922) and Coomassie Brillant Blue R-250 image of pooled liver mitochondrial protein samples from the high and low NFE Angus experimental 2006 cohort (continuation).

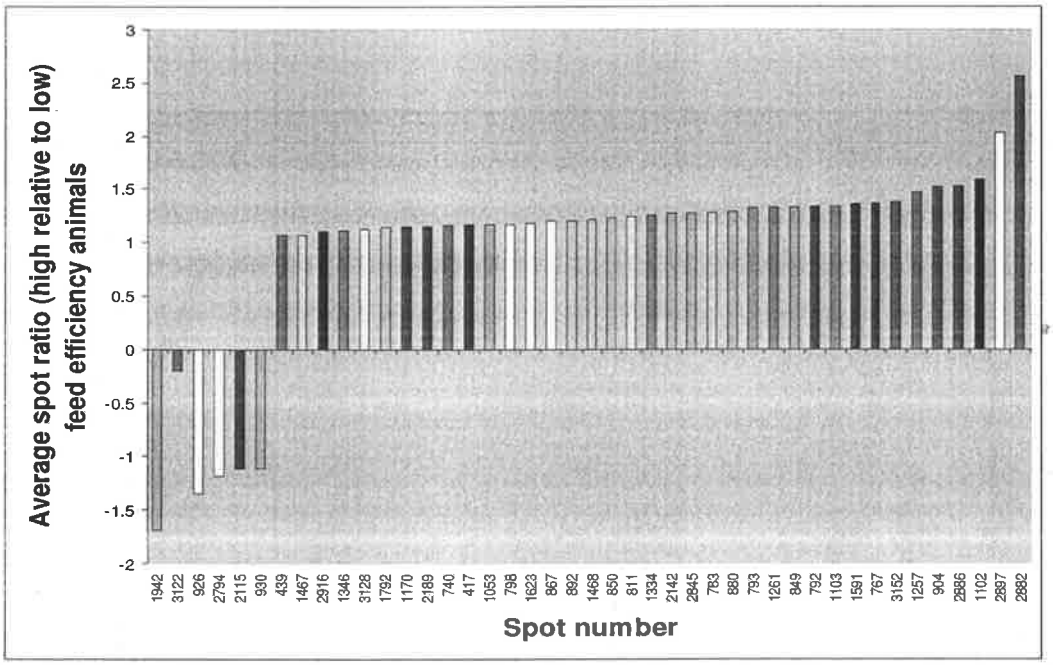

Figure 5.8: Proteins found to be differentially expressed between the high and low NFE groups with a P-value of <0.05 from the Angus 2006 cohort. An average ratio of > 0 indicates that the elevated expression in high NFE animals relative to low NFE animals.

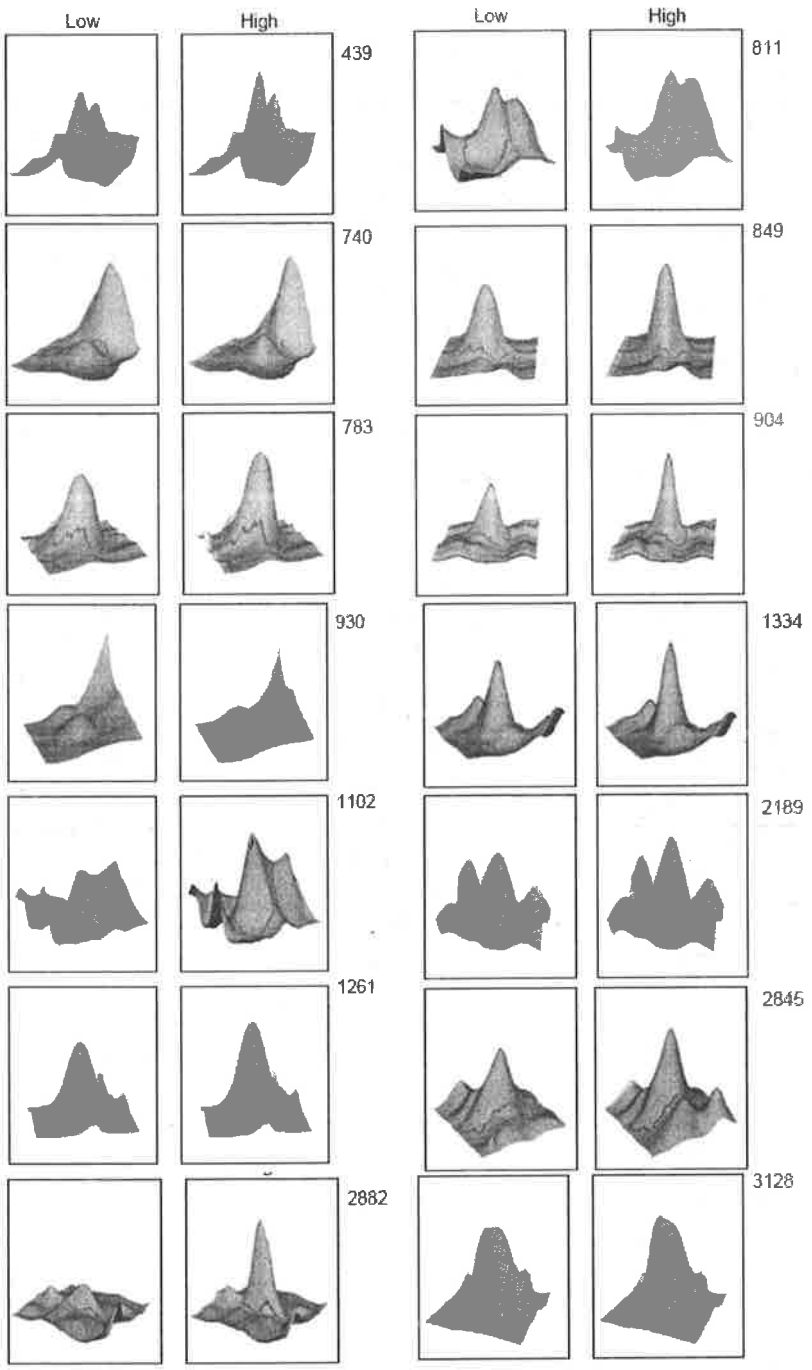

Figure 5.9 3-dimensional expression profile images of 14 differentially expressed spots from muscle mitochondria from experimental animals 2006 from *DeCyder* software (*GE HEALTHCARE*).

5.2.1.6 Mass spectrometry results of liver samples from Angus cattle (cohort 2006)

Identities were obtained for 10 of the 14 spots, which corresponded to 10 different proteins (Appendix 5.3). The two proteins (spots 2845 and 2882) that could not be identified had less material on the 2-DIGE gel. Hence, the amount of material was insufficient, presumably for MS analysis.

Of the 10 differentially expressed proteins, 9 of the identified proteins were elevated in the high NFE animals. They were C-1-tetrahydrofolate synthase, lipocortin (annexin VI), mitochondrial phosphoenolpyruvate carboxykinase 2 isoform 1 precursor isoform, 60 kDa heat shock protein, protein disulfide-isomerase, Tu translation elongation factor, succinyl-CoA synthetase, glutathione S transferase Mu 1 and heat shock 27 kDa protein. Identity between angiomotin like 2 & integrin beta-2 and kidney-specific protein (KS) & aspartate aminotransferase 1 were not confirmed (Appendix 5.3). Vimentin was the only one protein found to be decreased in the high NFE animals.

Positive MOWSE scores were obtained for four different isoforms of C-1-tetrahydrofolate synthase C (C1-THF synthase) in spot 439. Peptides corresponding to isoforms 1 to 4 were detected within the spectra. The peptide sequence could not clearly distinguish between isoforms 1 to 4. Therefore, based on the data available in this experiment, it is not possible to determine whether spot 439 comprised of only one C1-THF synthase isoform or a mixture of all four isoforms. Interestingly, spot 439 occurs within the centre of a "train" of spots (Figure 5.7). Therefore, the neighbouring spots would also represent alternate isoforms of C1-THF synthase. The predicted isoelectric point of isoforms 3, 2, 1 and 4 are 6.63, 6.91, 6.91 and 5.08, respectively, which corresponds to the pattern observed on the gel. To further investigate this possibility, the neighboring spots (spot numbers 417 and 447) should be excised from the gel, digested with trypsin and analysed by MALDI-TOF or liquid chromatography coupled to ion trap mass spectrometry detection with electron ionization interface (that is the LC-ESI- ion trap MS method). By searching specifically for those peptides that differentiate the four isoforms, it should be possible to determine which C1-THF synthase isoform is present and in which spot.

Three proteins were identified within spot 811: 1) mitochondrial phosphoenolpyruvate carboxykinase 2 isoform 1 precursor isoform 1 (MPCK2_1_1), 2) kidney-specific protein, partial (KSP), and 3) aspartate aminotransferase 1 (AA1). There were five masses that matched to both MPCK2_1_1 and AA1, and two overlapping masses between KSP and AA1. MS/MS analysis of the 1356.796 peak, which matched both KSP and AA1, identified a clear sequence tag that was consistent with the KSP sequence (results not shown). However, the identified KSP protein is based on only partial bovine protein sequence. Therefore, KSP may not be the true protein. Based on the number of matches with masses, MPCK2_1_1 and AA1 are equally likely be the true proteins.

Spot 849 corresponded to a protein with a positive MOWSE score entitled "Unknown (protein for IMAGE:7943409)". However, this protein was found to have the same set of peptides as heat shock protein 60 kDa (HSP60), identified in the earlier experiment in the liver samples of the 2005 Angus cohort (Appendix 5.1). Therefore, spot 849 could be the heat shock protein 60 kDa.

Two proteins were also identified within spot 1102: angiomotin-like 2 from *Bos taurus* and integrin beta-2 from *Bos indicus*. The MASCOT scores obtained for angiomotin-like 2 and integrin beta-2 were only slightly above the cut-off value. To improve the quality of the matches, MS/MS spectra were produced for the most intense ions from each protein. However, these spectra were of poor quality, and hence, could not provide any supporting evidence for the protein assignments (data not shown). The predicted pI and molecular weights values for both angiomotin-like 2 and integrin beta-2 did not correlate to the observed position of spot 1102 on the gel. The reason for these discrepancies is not known. Peptides corresponding to the N- and C-terminal regions of angiomotin-like 2 were identified within the spectra. Thus, the observed reduction in molecular weight is unlikely to be attributed to a cleaved form of this protein. The observed molecular weight of spot 1102 is more than 4 times the predicted mass of integrin beta-2. BLAST analysis of peptide ion sequencing revealed that it was identical to integrin beta-2 from *Bos taurus* (accession number gi|41386721). Although the available data cannot confirm the protein identity of spot 1102, it can resolved by repeating the protein digest experiment to obtain good quality MS/MS spectra.

Positive MASCOT scores were obtained from two proteins in spot 1261: Tu translation elongation factor, mitochondrial and thioredoxin family Trp26. Based on the number of peptides that matched Tu translation elongation factor, including four confirmatory MS/MS spectra (data not shown), this protein appears to the most abundant species in the spot. As such, Tu translation elongation factor is probably the differentially expressed protein in this spot on the 2-dimensional gels. The match to thioredoxin family Trp26 was against a *Canis familiaris* protein. BLAST analysis of the protein sequence showed that a bovine homologue is present in the database (accession number gi|76611449). The bovine protein, however, is missing the first 100 amino acids of the dog sequence. When the MS results were compared with the bovine sequence using BioTools, it was found that only five masses matched in contrast to seven masses within the equivalent region of dog sequence (i.e. amino acids 101-311). The two unmatched peptides contain amino acid changes from Leu-268 to Phe-168 and Arg-299 to Lys-199 (dog to bovine). Therefore, the matches to the dog sequences are likely to be false positive. Two of the five masses that matched to peptides from bovine thioredoxin family Trp26 also matched the Tu translation elongation factor (1901.027 and 2159.220). MS/MS analysis of the 2159.220 parent ion showed that the sequence was consistent with Tu translation elongation factor (results not shown). Therefore, the match to bovine thioredoxin family Trp26 appears to be a false positive result.

For spot 1334, the protein with the highest MOWSE score was *Sus scrofa* chain B, crystal structure of pig GTP-specific succinyl-CoA synthetase in complex with GTP. Interestingly, a large number of peptides matched the porcine sequence better than the bovine sequence. The protein entitled hypothetical protein LOC537713 was very similar to the porcine succinyl-CoA synthetase. The two masses that matched the porcine, but not the bovine sequences (peaks 1135.516 and 1284.561), had calibration error rates greater than 50 ppm from the expected values based on the peptide sequences. The 2310.054 peak that matched to bovine, but not the porcine protein, had an error of 15.1 ppm, which correlated with the peptide mass data. This suggests the matches to porcine sequences were false positive. The 1261.645 peak matched both a bovine and a porcine peptide, but also appeared to be false with an error rate of greater than 50 ppm in both sequences.

For spot 740, the protein with the highest MOWSE score was bovine annexin VI (calcium bound). This result corroborated to the previous results from liver samples (Angus cohort 2005) in which it was found to be elevated in high NFE animals. Unambiguous single protein identities (excluding multiple database entries for similar or identical proteins) were also obtained for protein spots 783 (phosphoenolpyruvate carboxykinase 2 isoform 1 precursor isoform), 930 (vimentin), 2189 (glutathione S transferase Mu 1) and 3128 (heat shock 27 kDa protein).

5.3 Discussion

The number of human scientific studies is growing rapidly in the field of proteomics, but thus far, there are no research reports available either on 2-D PAGE or DIGE of mitochondrial protein profiling in cattle. This is the first report of using a 2-D DIGE mitochondrial proteomic analysis to search of phenotypic markers related to net feed efficiency in cattle.

5.3.1 Technical issues

There are many techniques used in humans for rapid discovery of biomarkers on a mass scale, including 2-D PAGE, multidimensional protein identification technology (Mud-Pit), isotope coded affinity tag (ICAT), surface-enhanced laser desorption/ionization-time of flight (SELDI-TOF), matrix-assisted laser desorption/ionization-time of flight (MALDI-TOF), protein microarrays and 2-D DIGE (Somiari *et al* 2005). Huang *et al* (2006) compared several protein resolving techniques with 2-D DIGE. The 2-D PAGE technology has several limitations in terms of resolving proteins and the repeatability of the results. Although the isotope coded affinity tag technique gives reproducible results and is high-throughput, the number of proteins identified is much lower than 2-D DIGE. Mud-Pit has much higher and rapid resolving power for identification of proteins and peptides in a complex mixture without the need of labeling protein samples with fluorescent dyes. However, 2-D DIGE is superior for data handling and interpretation compared to the Mud-Pit technology. The protein microarray technology is still under

development. The 2-DIGE has the advantage of detecting and quantifying patterns of protein expression accurately and consistently with little technical error. It can also be coupled with either SELDI-TOF or MALDI-TOF for protein identification. 2-D DIGE detects a broader range of proteins compared to either silver and Coomassie Brilliant Blue staining. Moreover, the DIGE images have significantly higher sensitivity in comparison to the Coomassie Brilliant Blue gel staining. Less than 1 ng protein can be identified by the DIGE technique versus the 40 ng protein required for the Coomassie Brilliant Blue R-250 images (Huang *et al* 2006).

Since 2-D DIGE is a fluorescent protein labeling technique, proteins can be separated on one 2-D polyacrylamide gel for three samples at once. In the present study, an internal standard was used in all gels. The internal standard was a pool of all samples from the two NFE groups. Therefore, each protein present in the analyzed samples was represented within the internal pooled standard. This facilitates spot matching in the gels. Although 2-D DIGE can run three different samples on one gel, it is still laborious and costly. Therefore, in the current study, a sample pooling strategy was used to overcome this disadvantage in the later experiments.

The number of spots detected varied between the liver tissue samples from the 2005 cohort with the muscles samples from the 2005 cohort and the liver samples from the 2006 cohort. This is a function of several factors. For example, the first DIGE gels from the 2005 cohort liver samples were performed using 13 cm IPG strips rather than the 24 cm strips. The 24 cm strips were used for the later experiments to increase the spot resolution. The iso-electric focusing conditions were also partially modified to extend the early phase of focusing to increase spot resolution. In addition, the actual spot number detected depends upon the intensity of the fluorescent signal as well as the resolution of the gels. Despite efforts to perform experiments in a consistent manner, the intensity can vary from experiment to experiment due to technical issues, such as sample preparation and handling. There was some adjustment of the settings for image acquisition for each set of gels to correct for the various intensities of the three fluorescent colors. Technical variation due to fluorescence intensity was partially resolved by swapping the fluorescence dyes. Lastly, the experiments using muscle from 2005 cohort and liver from the 2006 cohort were pooled samples versus the individual liver samples used for the 2005 cohorts. In practice, the validation of spots, which is often performed manually, will reduce the total number of spots to a more useful and reliable subset for identification and comparison between the groups.

For the third experiment on liver tissues from the 2006 cohort, gel 70922 had horizontal streaking (Figure 5.8). The most probable reason for horizontal streaking was incomplete iso-electric focusing such that the proteins were not focused into discrete spots (Berkelman *et al* 2005). A potential

explanation for incomplete focusing is that two IPG strips were focussed at the same time. Conventional IEF cells are set for a total current limit for the whole tray. If one particular sample is more conductive, it will draw most of the current and reduce the focusing rate of the other strips in the tray. However, since validation of differentially expressed spots were analysed manually, there was no difficulty in matching the spots in spite of the streaking.

The presence of protein isoforms and fragments on the 2-D DIGE gels made the protein identification difficult. However, the isoforms and fragments can be quantified and compared based on altered molecular weights and isoelectric points for the same protein. For example, spot 439 (C-1-tetrahydrofolate synthase) was within the center of "train" of spots (Figure 5.7). Therefore, the neighbouring spots may represent the alternative isoforms of C-1-tetrahydrofolate synthase. If identified, then the total number of the isoforms can be determined.

In rare cases, protein isoforms can be found in the same spot and become very difficult to quantify. As an example in the muscle samples, based on the detection of masses 832.348 and 1675.804 in the spectra, the peptide mass fingerprint data indicated that both isoforms of NDUFA10 and NADH dehydrogenase (ubiquinone) 1-alpha subcomplex were present within spot 1064 (Appendix 5.2). These masses corresponded to the peptides FYDYPK from NDUFA10 and FYDDPKSNDGNSYR from NADH dehydrogenase (ubiquinone) 1-alpha subcomplex, respectively. The sequence of the protein fragments differed by just two amino acid residues, and therefore, are likely to be isoforms. The mass 1105.676 was also assigned to different peptides from the NDUFA10 and NADH dehydrogenase (ubiquinone) 1-alpha subcomplex, despite the fact that the VVEDIEYLK peptide (assigned to NDUFA10) is identical in both sequences. This can be explained by the fact that the LQAWLYASR peptide from NADH dehydrogenase (ubiquinone) 1-alpha subcomplex differs completely from the NDUFA10 isoforms, but has a virtually identical theoretical mass to VVEDIEYLK. Thus, MS/MS analysis failed to determine whether the 1105.676 parent ion corresponded to VVEDIEYLK or LQAWLYASR.

For spot 1439 from the muscle samples (cohort 2005), the two assigned proteins, H(+)-transporting ATP synthase and bovine mitochondrial cytochrome Bc1 complex E chain, have different predicted isoelectric point and molecular weight values. So it is unclear as to why these two proteins may have co-migrated on a 2D-electrophoresis gel (Appendix 5.2). It is most likely that only one or neither protein is the correct assignment.

In the liver samples from the 2006 cohort (Appendix 5.3), a total of 43 spots were identified as differentially expressed. However, only 14 spots were selected for mass spectrometry identification because all of the differentially expressed proteins identified in the liver tissue of the cohort 2005 were

also found. There were a greater number of spots observed in the 2006 cohort samples because the isoelectric focusing conditions were extended and a larger 24 cm IPG strip was used.

In the liver tissue for cohort 2006 (Appendix 5.3), three proteins were identified within spot 811: 1) mitochondrial phosphoenolpyruvate carboxykinase 2 isoform 1 precursor isoform 1 (MPCK2_1_1), 2) kidney-specific protein, partial (KSP), and 3) aspartate aminotransferase 1 (AA1). A plausible explanation would be that calibration errors associated with the masses matched to AA1 were greater than those observed for MPCK2_1_1 and KSP (not shown), and therefore, AA1 may be mis-assigned. Furthermore, 11 of the 17 masses that matched to the AA1 peptides contained no trypsin cleavage sites compared to 5 out of 22 for MPCK2_1_1. KSP also had a reasonably high proportion of no trypsin cleavage sites at (60%). Missed trypsin cleavage sites occur when the protein is not digested to completion by trypsin protease. Too many missed trypsin cleavage sites decreases the specificity of trypsin digested protein database. MS/MS analysis, however, identified both KSP and AA1 with clear sequence tags that were consistent with the KSP and AA1 sequences (results not shown). Therefore, the presence of AA1 in spot 811 cannot be ruled out, and future confirmatory studies are required to identify the protein. According to the NCBI database, the KSP sequence is incomplete at both ends. Although the sequence of the entire bovine protein has not been submitted, a 616 amino-acid *Canis familiaris* equivalent kidney specific protein (accession number gi:73958947) was identified by BLAST analysis (http://www.ncbi.nlm.nih.gov/BLAST/Blast.cgi). The overlapping regions of dog and bovine KSP show 80% identity at the amino acid level. The predicted isoelectric point and molecular weight values of dog KSP are 8.72 and 69,076, respectively. Whilst the pI is far more basic than expected, the molecular weight corresponds to the observed position on the 2-dimensional gel.

The prediction of the isoelectric point and molecular weight of a matched protein was performed by using the ExPASy compute pI/ MW tool. There were discrepancies found between the observed and expected values for two reasons (Appendix 5.1, 5.2 and 5.3). First, the measured pI is not very precise as the pH of any position on the IPG strip is approximated by reference to a standard pH gradient supplied by the company (GE Healthcare) rather than through direct measurement. Second, the conceptual protein sequence from the NCBI database, derived from cDNA sequence, does not consider post-translational modifications. For mitochondrial proteins, there are likely to be signal sequences that are removed as well as modifications to the side-chains of amino acid residues. To obtain the best estimate of the predicted isoelectric point and molecular weight of a protein, one would need to investigate whether the protein is undergoing specific processing.

Annexin VI (also referred as lipocortin VI) was a protein identified in liver samples with elevated levels in the high NFE animals from both the 2005 and 2006 cohorts. However, the physiological function in

context to NFE of annexin VI is not clear. Annexin VI is from the Ca[2+]-dependent phospholipid-binding protein family that participates in the signal transduction of the intracellular Ca[2+] (Naciff *et al* 1996). Other proteins found to have the same patterns of expression in both cohorts included: albumin, ATPase V1 subunit G2, succinate dehydrogenase, NADH dehydrogenase (ubiquinone) 1- alpha subcomplex-5 (19 kDa), bovine mitochondrial F1- ATPase chain C, glutamate dehydrogenase 1, and aldolase B. These proteins are involved in stress regulation, oxidative phosphorylation and glucose turnover (discussed in chapter 6).

The only protein that was differentially expressed in both the muscle and liver tissues was catalase. Irrespective of the tissue differences, catalase was consistently lower in the high NFE animals in comparison to the low NFE animals. The lack of other proteins in common could be due to tissue specific variation in metabolic patterns (Thakar 1977; Chanseaume *et al* 2006). For example, some proteins (such as enolase) identified in the muscle samples are muscle specific proteins. Other mitochondrial proteins have generally elevated expression in the liver versus other tissues like muscle (e.g. aldolase B and carnitine palmitoyltransferase 1 isoform CPT1A) (Price *et al* 2003). In these cases, the expression may be too low to the detected in one of the tissues examined herein.

There was no complete loss of expression identified for any proteins between the high and low NFE animals. This proteomics study was performed over a wide pH range of 3-11. Therefore, in future, the separation of proteins over narrower ranges would be useful to discover less abundant proteins. This study also demonstrated the high reproducibility and consistency of the spots between experiments, which shows the reliability of 2-D DIGE techniques.

5.3.2 Functional significance of differentially expressed proteins

The proteins identified as having lower levels in the mitochondria of high NFE animals included catalase, heat shock protein subunits (60 and 70 kDa), albumin, aldolase B, 1 subunit of Complex I, 1 subunit of complex II and 2 subunits of complex V. Proteins found to be elevated in the high NFE animals included 4 complex I subunits, 1 subunits of complex III, 1 subunit of complex V, glutathione S transferase Mu 1, a heat shock protein subunit 27 kDa, mitochondrial phosphoenolpyruvate carboxykinase 2 isoform 1 precursor isoform, carnitine palmitoyltransferase isoenzyme, enolase 3, triosephosphate isomerase, adenylate kinase 1, glutamate dehydrogenase1, Tu translation elongation factor and mitochondrial succinyl-CoA synthetase. Based on the metabolic roles of these differentially expressed proteins, six classes were identified in order to develop hypotheses concerning their potential involvement in feed intake regulation and feed efficiency. These six classes are: 1) oxidative phosphorylation, 2) stress related proteins, 3) energy production and glucose turnover, 4) protein

turnover and nitrogen balance, 5) mitochondrial DNA and protein biosynthesis, and 6) cytoskeleton (Appendix 5.4).

Among the six classes, the oxidative phosphorylation pathway was represented the most heavily in the list of candidate genes from the QTL regions. This may not be surprising given the large number of proteins involved in oxidative phosphorylation. Oxidative phosphorylation is the mitochondrial process that links the oxidation of fuel substrates to the generation of high-energy phosphate (ATP) used by the cell for energy-consuming pathways (Krauss *et al* 2005).

The proteomics results found a total of 5 subunits from complex I, complex II (1 subunit), complex III (1 subunits) and complex V (2 subunits) were differentially expressed. Amongst 5 subunits of complex I, NADH dehydrogenase (ubiquinone) 1- alpha subcomplex, 5, 19 kDa (complexI-19kDA) subunit was found within the NFE QTL on BTA 11 (Appendix 5.4).

Four subunits of Complex I and one subunit of Complex III were found to be elevated in the high NFE animals in comparison to the low NFE animals. However, lower expression of one subunit of Complex I and II and two subunits of Complex V were observed in the high NFE animals. These differences in the levels of the subunits either might be due to DNA variants, oxidative stress or post-translational modifications (Lei and Wei, 2001).

Another metabolic group found to be differentially expressed in the current study was the stress related proteins. These stress related proteins included antioxidant enzymes (e.g. catalase and glutathione-s-transferase), heat shock proteins (e.g. 70 kDa, 60 kDa and 27 kDa), and albumin.

The level of catalase was found to be lower in the liver and muscle tissues of the high NFE 2005 cohort animals. Since catalase is a strong antioxidant enzyme, this clearly suggests that mitochondrial energy production in the high NFE animals is very effective and oxidative stress is limited. Under high oxidative stress, the level of catalase is increased (Suttorp N, 1986). The ultimate consequence of oxidative stress would be compromised ATP generation and a cellular energy crisis due to inefficient electron transfer (Stewart and Heales, 2003). Therefore, the low NFE animals are likely to be under oxidative stress as catalase is elevated.

The other stress related proteins with lower expression in the liver of the high NFE animals were the heat-shock proteins and albumin. In response to high oxidative stress, both heat shock proteins (except 27 kDa) and albumin levels increase, and this is consistent with the results herein (Jolly *et al* 2000; Zylicz *et al* 2001; Bito, 2005). Heat shock proteins are upregulated under conditions such as heat shock,

inhibition of energy metabolism, exposure to heavy metals, inflammation and oxidative stress (Jolly *et al* 2000; Zylicz *et al* 2001). Albumin acts as a multifaceted antioxidant. The total antioxidant activity of albumin is a composite of many individual antioxidant activities. Albumin binds to fatty acids cystein, glutathione, bilirubin, and pyridoxal-5'-phosphate, thereby preventing their oxidation. Albumin also binds copper and prevents copper from participating in oxidation reactions (Bito, 2005).

Interestingly, glutathione-s-transferase was found to be elevated in the high NFE animals Glutathione-s-transferases conjugate glutathione to free-radicals or xenobiotics, and thereby, help to decrease free radical concentrations in cells (Bekris *et al* 2005). Again this suggests that the high NFE animals would under low oxidative stress as the presence of glutathione-s-transferases would prevent oxidative stress in the high NFE animals.

Cells under high oxidative stress undergo apoptosis, due to the accumulation of mitochondrial DNA mutations and decreased capacity to degrade oxidatively damaged proteins and other macromolecules. Free radicals also repress mitochondrial transcription, which leads to mitochondrial dysfunction by inhibiting the synthesis of the respiratory chain proteins (Kristal *et al* 1994, 1997). These phenomena could be related to the lower levels of three enzymes, mitochondrial translation elongation factor Tu, succinyl-CoA synthetase, and C(1)-tetrahydrofolate (THF) synthase in the low NFE animals. These enzymes are responsible for the maintenance of mitochondrial deoxyribonucleoside triphosphate (dNTP) pools, the replication of mtDNA and protein biosynthesis (Chiron *et al* 2005, Orly *et al* 2005). The eukaryotic trifunctional enzyme C(1)-tetrahydrofolate (THF) synthase interconverts folic acid derivatives between various oxidation states and is critical for normal cellular function, growth, differentiation, and purine biosynthesis (Shannon and Rabinowitz, 1986; Howard *et al* 2003).

The ontological analysis of the differentially expressed proteins found that eight of the proteins are in energy production and glucose turnover pathways. It was hypothesised that proteins involved in generating energy and maintaining glucose homeostasis may be elevated in the high NFE animals. Indeed, six such key enzymes were found to be increased in the high NFE animals. They were succinyl-CoA synthetase, mitochondrial phosphoenolpyruvate carboxykinase 2 isoform 1, carnitine palmitoyltransferase isoenzyme, enolase 3, triosephosphate isomerase and adenylate kinase 1 (Appendix 5.4). The two proteins that were lower in the high NFE animals were aldolase B and tumor necrosis factor (TNF) receptor.

Succinyl-CoA synthetase is involved in mitochondrial DNA replication, but is also the only enzyme that generates high-energy phosphate at the substrate level during the TCA cycle (Lowenstein, 1969). Succinyl-CoA synthetase is responsible for the continuation of the TCA cycle by converting succinyl

CoA to succinate and producing guanosine tri-phosphate (GTP). Altered expression of succinyl-CoA synthetase would affect the overall production of reducing agents, like NADH and $FADH_2$, which are involved in the electron transfer during oxidative phosphorylation. The gene for succinyl-CoA synthetase protein is located on BTA 11 within the NFE QTL.

Mitochondrial phosphoenolpyruvate carboxykinase 2 isoform 1 precursor (MPCK2_1_1) is part of the anapleurotic biochemical pathways that replenish TCA cycle intermediates (Croniger, 2002). This enzyme is actively involved in gluconeogenesis by converting oxaloacetate to phosphoenolpyruvate.

Carnitine palmitoyltransferase isoenzyme (CPT) is involved in the adenine mono-phosphate activated protein kinase (AMPK) and long chain fatty acid-CoA (LCFA-CoA) fuel sensing pathway. CPT is responsible for the transfer of LCFA-CoA molecules from the cytosol to the mitochondria and for the oxidation of LCFA-CoA molecules during high-energy demand. Thus, any alteration in the expression of this enzyme affects the energy balance of cell (Obici and Rossetti, 2003). CPT is negatively controlled by the level of malonyl-CoA, and levels of malonyl-CoA are regulated based on the energy status of animal. Malonyl-CoA is a key intermediate in the AMPK pathway and is involved in the *de novo* synthesis of long chain fatty acids (Obici and Rossetti, 2003). During energy surplus, malonyl-CoA levels increase and inhibit CPT. Thus, long-chain fatty acids are converted into triglycerides and diacylglycerol (Obici and Rossetti, 2003). Disturbance in the levels of CPT and malonyl CoA, therefore, could affect total feed intake and the deposition of fat.

Adenylate kinase 1 is a member of the adenylate kinase family of phosphotransfer enzymes and is involved in the maintenance of cellular energy, enabling skeletal muscle to perform at the lowest metabolic cost. Low expression of adenylate kinase 1 causes a high ATP turnover rate and larger amounts of ATP are consumed per muscle contraction, thereby increasing the maintenance energy requirements (Janssen, 2000). Genetic ablation of adenylate kinase 1 disturbs the muscle energetic economy and decreases tolerance to metabolic stress, despite adaptations by the alternative high energy phosphoryl transfer pathways (Janssen *et al* 2003). The gene for this protein is located on BTA 11 within the NFE QTL (Appendix 5.4).

One of the most important mitochondrial enzymes is enolase 3. This is a homodimeric enzyme that catalyses the reversible dehydration of 2-phospho-D-glycerate to phosphoenolpyruvate as part of the glycolytic and gluconeogenesis pathways. It is also involved in the importation of cytoplasmic tRNA into the mitochondria (Entelis, 2006). Therefore, enolase 3 is indirectly involved in regulating mitochondrial protein synthesis. Down-regulation of enolase 3 will not only hamper glucose turnover, but mitochondrial protein synthesis as well.

Triosephosphate isomerase is a glycolytic enzyme that catalyzes the reversible interconversion of glyceraldehyde 3-phosphate and dihydroxyacetone phosphate. Therefore, this enzyme plays important role in glycolysis and is essential for efficient energy production (Lolis, *et al* 1990). Low levels of triosephosphate isomerase eventually affect ATP production due to decreased production of NADH and pyruvate. NADH provides reducing power for energy metabolic pathways, like oxidative phosphorylation, while pyruvate is used in the citric acid cycle.

Two proteins were lower in the high NFE animals, aldolase B and tumour necrosis factor receptor. The gene for aldolase B is in the NFE QTL on BTA8. Aldolase B is an isoenzyme of fructose 1,6-bisphosphate aldolase (aldolase A), which cleaves fructose 1-phosphate to form glyceraldehyde and dihydroxyacetone phosphate (DHAP). These 2 products are utilised in glycolysis pathway. Aldolase B, thus, controls fructose metabolism and glycolysis (Cox *et al* 1988, Lolis *et al* 1990). Since this enzyme has role in glycolysis and ultimately energy production, an elevated level of aldolase B might be expected in the high NFE animals compared to the low NFE animals. However, if glycolysis is elevated in the high NFE animals as predicted, then fructose will not be converted by aldolase B to glyceraldehyde and dihydroxyacetone phosphate. Instead, fructose will be diverted to glycogen production in the hexosamine biosynthesis pathway (Marshall *et al* 1991) (as discussed in Chapter 1) and aldolase B levels would be minimal.

Tumour necrosis factor receptor (TNFR) is involved in glucose clearance and insulin resistance (Robinson *et al* 2000). The ligand for the TNFR, tumour necrosis factor, antagonises insulin action and reduces the nutrient availability to the cells. Increased levels of TNFα are thought to contribute significantly to the insulin resistance associated obesity and sustained over-eating (Bullo-Bonet *et al* 1999; Vernon *et al* 2001 and Frubeck *et al* 2001). Therefore, a lower level of TNFR was observed in the high NFE animals as expected since there should be decreased feed intake in comparison to low NFE animals.

Another metabolic class of differentially expressed proteins were those involved in protein turnover and nitrogen balance *viz*: glutamate dehydrogenase 1 and aspartate aminotransferase. As might be expected, glutamate dehydrogenase 1 was found to be elevated in the high NFE animals. The glutamate dehydrogenase 1 forward reaction is the first committed step on the common pathway for nitrogen excretion, leading eventually to urea (Miller *et al* 1990). It converts glutamate to α-ketoglutarate (KG). The cofactor for the glutamate to α-ketoglutarate reaction, which produces ammonium, is NAD^+. The cofactor for the reverse reaction from α-ketoglutarate to glutamate is $NADP^+$. The reverse reaction uses ammonium to incorporate nitrogen into glutamate. Thus, in the reverse reaction, glutamate dehydrogenase 1 provides an oxidizable carbon source used for the production of

energy as well as a reduced electron carrier, NADH. NADH is then utilised in the oxidative phosphorylation respiratory chain for ATP production. This is a key anapleurotic process, linking amino acid metabolism with TCA cycle activity. This dehydrogenase acts as a marker for the TCA and oxidative phosphorylation activities. As a consequence, glutamate dehydrogenase plays a central role in mammalian nitrogen flow, serving as both a nitrogen donor and nitrogen acceptor.

Glutamate dehydrogenase 1 is regulated by the cell energy balance. When the cellular energy charge is low, glutamate is converted to ammonia and oxidizable TCA cycle intermediates (Hillar, 1974). About 75% of ingested protein nitrogen involves glutamate metabolism through the glutamate dehydrogenase reaction. Glutamate is also a principal amino donor for other amino acids in transamination reactions. The multiple roles of glutamate in nitrogen balance provide a gateway between free ammonia and the amino groups of most amino acids. Therefore, glutamate dehydrogenase plays an important role between catabolic and biosynthetic pathways, involving both protein turnover and nitrogen balance. Therefore, any alteration in the function of this enzyme might affect the production of energy, amino acid metabolism, total protein turnover, nitrogen balance, and eventually feed intake regulation.

Aspartate aminotransferase (AA1/AST) was detected in the same spot 811 (Appendix 5.3) on the 2-DIGE gels with two other enzymes, mitochondrial phosphoenolpyruvate carboxykinase 2 isoform 1 precursor isoform 1 (MPCK2_1_1) and kidney-specific protein, partial (KSP). Based on the MALDI-TOF-MS/MS analysis, the protein is either MPCK2_1_1 and/or AA1. MPCK2_1_1 was clearly identified in another spot 783 (Appendix 5.3) as being differentially expressed (discussed above). Ironically, given the functions of these proteins, AA1 is more likely to be differentially expressed in the high NFE animals. AA1 is one of the most active enzymes in the cell. It exists as mitochondrial and cytosolic variants, and the iso-enzyme pattern is tissue-specific (Christen *et al* 1985). The metabolic importance of this enzyme is that it brings about a free exchange of amino groups between glutamate (which is the most common amino acid) and aspartate (which is a second major amino acid). Glutamate and aspartate are each required for separate, but essential steps, in the urea cycle, which is responsible for ammonia detoxication and nitrogen excretion. The free movement of nitrogen between the glutamate and aspartate pools is an important balancing process that is vital for normal cellular metabolism. This reaction is close to equilibrium in both the cytoplasm and the mitochondrial compartments (Palaiologos *et al* 1989). It forms an integral part of the malate - aspartate shuttle, which is effectively responsible for the transport of NADH across the inner mitochondrial membrane (Barron *et al* 1998).

The lower levels of glutamate dehydrogenase 1 and potentially aspartate aminotransferase (AA1/AST) in the low NFE animals could have an effect on the total protein turnover and nitrogen balance. As an aside, these enzymes are very important in terms of the balance of glutamate and glutamine synthesis.

Increased glutamate levels leads to glutamine formation. This depletes the glutamate stores that are needed in neural tissues since glutamate is both a neurotransmitter and a precursor for the synthesis of aminobutyrate (GABA), another neurotransmitter (Fonnum, 1984). Therefore, a reduction in the brain glutamate concentrations can affect energy production as well as neurotransmission (Palaiologos *et al* 1989). Any change in levels of these two enzymes might contribute to behavioural changes, in addition to the energy and protein turnover status of animal.

The sixth class of differentially expressed proteins were proteins involved in cytoskeleton development. However, their relation with net feed efficiency is not clear. These included annexin VI and vimentin. The identity of angiomotin-like 2 and integrin beta-2 was not confirmed by high MOWSE scores.

Vimentin is a member of the intermediate filament family of proteins. Intermediate filaments are an important structural feature of eukaryotic cells. Intermediate filaments, microtubules and actin microfilaments make up the cytoskeleton. Besides this role in the cytoskeleton, vimentin has been found to control the transport of low density lipoprotein (LDL)-derived cholesterol from the lysosome to the site of esterification (Sarria *et al* 1992). By blocking the vimentin transport of LDL-derived cholesterol inside the cell, cells store a much lower percentage of the lipoprotein than normal cells. Lower levels of vimentin were found in high NFE animals.

Annexin VI, also referred as a lipocortin VI, is a 68 kDa protein whose actin binding is positively regulated by calcium. Other actin binding proteins are typically negatively regulated by calcium. Annexin VI may bind G- as well as actin filaments and lipids. Annexin VI has been localized to stress fibres, membrane ruffles, microspikes and focal contacts. Three isoforms were found in liver samples. The two of them were elevated and one of them at reduced level in high NFE animals in comparison to low NFE animals. Kaetzel *et al* (1994) reported differentially expressed annexin VI isforms in different tissues, which may explain the variation in levels of 3 isoforms found herein.

Integrin beta-2 is also referred as leukocyte cell adhesion molecule CD18. The leukocyte cell adhesion molecule belongs to a class of cell membrane glycoproteins known as integrins. Mutations in the beta-2 subunit of the leukocyte cell adhesion molecule have been found to cause the autosomal recessive disorder of neutrophil function known as leukocyte adhesion deficiency. Integrin beta-2 contributes in inflammation and cellular immunity (Hynes 1992). Elevated levels were found in the high NFE animals.

Angiomotin is a newly discovered molecule that regulates the migration and tubule formation of endothelial cells. It, therefore, has been implicated in the control of angiogenesis under physiological and pathological conditions (Jiang *et al* 2006). This protein was elevated in the high NFE animals.

These proteins were previously reported to be in the mitochondrial matrix by several researchers (please see Appendix 5.4 for references). It could be postulated that these proteins may be involved in mitochondrial biosynthesis. Hence, as argued earlier, they would elevate in animals not under oxidative stress (that is, elevated in the high NFE animals).

5.4 Conclusions

In this study, the 27 identified differentially expressed proteins could be grouped into six different metabolic classes potentially associated with net feed efficiency (appendix 5.4). These proteins are specifically involved in energy metabolic pathways, namely oxidative phosphorylation, stress regulation and glucose turnover.

Most of the proteins found in the energy producing metabolic pathways were found to be elevated in expression in the high NFE animals compared to the low NFE animals. Elevated expression of proteins involved in glucose turnover and energy production in the high NFE animals suggest efficient utilization of nutrients for energy production. The proteomics results indirectly suggest that energy production by oxidative phosphorylation is more efficient in the high NFE animals and is disturbed in the low NFE animals, which increases the mitochondrial oxidative stress. This is supported by the elevated levels of oxidative stress related proteins in the low NFE animals (e.g. the antioxidant enzyme catalase and heat shock proteins). It may be possible, therefore, to select animals based on their levels of antioxidant proteins or free radicals in order to increase the overall net feed efficiency of animals. Future research should focus on nutritional manipulation or additives to control oxidative stress if possible.

The results suggest that energy production and homeostasis mechanisms are less efficient in the low NFE animals due to high oxidative stress. Therefore, these animals consume more feed to satisfy their maintenance metabolic energy, which increases their average net feed intake. It would be interesting to determine if mitochondrial dysfunction affects cytoplasmic metabolic pathways as this would be expected. In addition, specific protein levels (e.g. albumin, glutathione transferase Mu 1, heat shock proteins, etc) in the serum should be compared between high and low NFE animals, as this may help to develop a blood based biomarker test for selecting high NFE animals.

Glutamate dehydrogenase 1, which is involved in neurotransmitter production, appetite regulation and feed intake, should be studied in more detail. If this enzyme differs between high and low NFE animals, there should be a relationship between elevated levels of this protein and the cerebrospinal fluid neurotransmitter profile in high NFE animals. Neurotransmitter profiling study can be undertaken by analyzing cerebrospinal fluid using liquid chromatography-mass spectrometry.

The proteomics study herein support the hypothesis that energy production in high NFE animals should be more efficient than in low NFE animals. The results firmly suggest that the differentially expressed proteins herein and those candidate genes related to energy metabolism, oxidative stress and mitochondrial function within the NFE QTL should be targeted for SNP discovery and association studies.

Chapter 6

General discussion

In beef cattle, the requirement of metabolizable energy for maintenance relative to performance appears as differences in feed intake, and is mirrored in the altered partitioning of nutrients. Despite substantial fluctuations in feed intake, animals maintain a remarkably stable body weight because overall calorie intake and expenditure are exquisitely matched and stabilised through the process of energy homeostasis (Cummings and Overduin, 2007). Understanding these physiological processes is important for identifying candidate genes for net feed efficiency within QTL. The knowledge of the physiological pathways involved in net feed efficiency will help to also predict the correleated responses in other associated traits to selection for net feed efficiency. Alternatively, these associated traits may be less expensive to measure than feed intake and could be used for selection of net feed efficiency itself. Therefore, for the study herein, a genetic approach and a biochemical approach were taken to examine the differences between high and low net feed efficient cattle.

6.1 NFE QTL from Limousin x Jersey mapping herd

The linkage mapping confirmed four NFE QTL (BTA 1, 8, 11, and 20) identified earlier (Fenton 2004) (Table 6.1). The results obtained in the fine mapping experiment conducted on the Limousin x Jersey Davies progeny were corroborated by a microsatellite mapping experiment on the Trangie NFI selection Angus line population, which confirmed the 2 NFE QTL on BTA 8 and BTA 11. There were also 2 minor QTL on BTA 1 and BTA 20 in the Trangie NFE selection Angus line population.

The NFE QTL on BTA 1, 8, 11 and 20 were used to identify candidate genes for SNP discovery. The mitochondrial proteomics results supported candidate genes within the NFE QTL on BTA 8 and BTA 11, and the oxidative phosphorylation enzyme assays supported candidate genes within the NFE QTL on BTA 11 and BTA 20.

The SNP association study on 71 SNPs discovered in the Limousin x Jersey population determined that 27 SNPs in 20 different candidate genes within the NFE QTL were associated with NFE (Table 3.6). There were also 100 ParAllele SNPs identified as being associated with NFE in a whole genome 10K SNP scan of the Trangie NFI Angus selection families. Among the 100 ParAllele SNPs, 16 SNPs were associated with NFE in the Limousin x Jersey population.

Of these four identified NFE QTL regions, the NFE QTL on BTA 20 is the most promising. This QTL was confirmed in both the Limousin x Jersey and Angus populations, and there was also supporting evidence from the mitochondrial enzyme studies, a mouse NFE mapping experiment and the SNP association studies (Table 6.1). However, the other studies provide additional support for the remaining NFE QTL as well.

Table 6.1 NFE QTL in different studies

BTA	JL QTL	Mouse QTL	Angus QTL	Angus ParAllele SNPs	JL candidate SNPs	Mitochondrial enzyme assays	Mitochondrial Proteomics	Angus ParAllele SNPs confirmed in JL
1	✓	✓✓	☑	xxx	*****	-	-	+
8	✓	-	✓✓	XXXXXXX	****	-	c	+
11	✓	-	✓✓	X	******	c	c	+
20	✓	✓✓	☑	X	****	c	-	+

(JL: Jersey x Limousin); ✓: QTL identified; ✓✓: major QTL confirmed with JL population; ☑: minor QTL confirmed with JL population; X: number of significant SNPs within JXL NFE QTL; *: number of candidate genes with non-zero variances; +: number of significant ParAllele SNPs in NFE QTL with non-zero variances; -: no confirmation); c: candidate genes within QTL

These 4 QTL regions harbour a large number of potential candidate genes. In the case of the NFE QTL on BTA 20, the 5 cM region flanking the GHR gene at 18 cM has a cluster of genes potentially contributing to growth and glucose metabolism. This is also true for the NFE QTL on BTA 11 where the POMC gene is located at 53 cM. The candidate genes within a 4 cM region flanking POMC are involved in fat metabolism pathways. Therefore, intensive sequencing of these small regions is warranted to develop a haplotype map and determine the linkage disequilibrium with NFE QTL. However, since there are likely to be many potential genes involved in determining net fed efficiency scattered over the genome, a large genome SNP scan with >50K SNPs should be also undertaken in a larger cattle population to develop further haplotype associations with net feed efficiency. Nevertheless, many highly significant associations were observed herein between NFE and various candidate genes. These associations should be verified in different cattle populations as soon as possible to determine if they may be useful as markers in selection programs.

Candidate pathways

Based on the 4 NFE QTL, 9 metabolic candidate pathways were recongnised as potentially regulating net feed intake. They could be classified in two categories: 1) growth and feed intake regulation, and 2) energy metabolism. These included:

Growth and feed intake regulation

1. Growth hormone receptor (GHR) pathway: involved in growth
2. Insulin / IRS pathway: involved in glucose metabolism

3. Leptin-insulin pathway: involved in neurohumoral regulation of glucose and fat levels
4. Mammalian target of rapamycin (mTOR) pathway: involved in appetite control

Energy metabolism

1. Oxidative phosphorylation (OX-PHOS): involved in ATP generation
2. Malonyl coenzyme A (CoA) / long chain fatty acid (LCFA) CoA pathway: involved in fatty acid metabolism
3. Hexosamine biosynthesis pathway (HBP): involved in glucose turnover
4. Ubiquitin-proteosome pathway: involved in protein turnover and nitrogen balance regulation

6.2 Mitochondrial oxidative phosphorylation

Among the aforementioned pathways, mitochondrial oxidative phosphorylation was identified as one of the pathways most likely to affect feed intake. Indeed, the proteomics study indicated that there are elevated levels of stress related proteins (such as albumin, catalase, heat shock proteins 70kDa and 60kDa) and lower levels of oxidative phosphorylation Complex I and III subunits in low NFE animals compared to high NFE animals. This suggests a picture of decline in respiratory function and an increase in oxidative stress in the form of mitochondrial reactive oxygen species (ROS) in the less efficient animals.

6.2.1 Consequences of oxidative stress

Oxidative stress is a state that develops due to an imbalance between the intracellular ROS and antioxidant enzymes. To cope with ROS, cells express several antioxidant ROS detoxification enzymes including catalase (CAT), glutathione peroxidase (GPx), copper/zinc superoxide dismutase (Cu/ZnSOD) and manganese superoxide dismutase (MnSOD) (Esposito *et al* 1999). Increased levels of the antioxidant enzyme catalase in the liver and muscle tissues support the hypothesis of disturbed mitochondrial oxidative phosphorylation in low NFE animals, whereas in the high NFE animals, oxidative phosphorylation is presumably better controlled.

Any increase in free radicals or reactive oxygen species (ROS) leads to oxidative damage of mitochondrial DNA (mtDNA), as well as mitochondrial proteins and lipids (Kristal *et al* 1994, 1997; Lee and Wei, 2001). Oxidative damage to mtDNA, micro- and macro-molecules increases the imbalance between the nuclear and mitochondrial subunits inside the mitochondria. Thus, oxidative phosphorylation activity is disturbed, and this will ultimately affect energy (ATP) production.

In addition, oxidative damage to proteins involved in maintaining the levels of mitochondrial transcripts and protein biosynthesis affect mitochondrial respiration. In the proteomics study, it was observed that

there were higher levels of the mitochondrial Tu translation elongation factor and succinyl-CoA synthetase in the high NFE animals in comparison to low NFE animals (Appendix 4.4). Mitochondrial Tu translation elongation factor and succinyl-CoA synthetase proteins are involved in mtDNA replication and energy production in the TCA cycle (Chiron *et al* 2005, Orly *et al* 2005; Appendix 4.4), and the elevated levels of these proteins in the high NFE animals indicates ongoing mtDNA synthesis and energy production.

As a consequence of the ROS effects on mitochondrial ATP production, oxidative stress can affect any ATP-utilising reaction (such as protein synthesis which accounts for 20% of whole body use of ATP in mammals) because these reactions are very sensitive to the ATP/ADP ratio in the cell (Waterlow 1984). Adenylate kinase 1 is a phosphotransferase enzyme involved in maintaining the ATP/ADP ratio by producing ATP from ADP. This enzyme was found to be elevated in the high NFE animals, suggesting better cellular energy homeostasis in high NFE animals. Oxidative damage can also increase uncoupled reactions due to proton leakage. Increased uncoupled reactions leads to increased heat production without energy generation as described earlier (Chapter 4).

Lastly, oxidative damage can cause early induction of mitochondrial apoptosis and protein degradation. The decreasing ability to replace damaged mitochondria is another energetic burden on the cells, and could contribute to less efficient nutrient management of animals. Increased mitochondrial biogenesis can be either an adaptive or compensatory process to replace damaged mitochondria and improve cellular energy supply. The cumulative oxidative damage of mtDNA leads to defects in mitochondrial function and initiates adaptive mitochondrial biogenesis and turnover in the cell (Kowald 1999) (Figure 6.1). Alternatively, mitochondrial biogenesis can be due to the accumulation of damaged mitochondrial proteins and cross-linking of proteins by ROS to macromolecules (Kowald 1999).

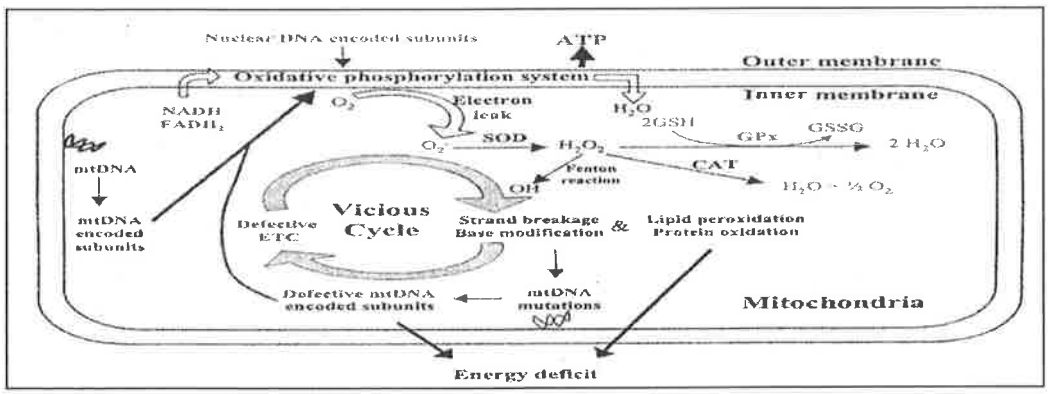

Figure 6.1 Oxidative stress responses and its effect on intra-mitochondrial machinery. Intracellular oxidative stress is elicited by electron leakage from oxidative phosphorylation of mitochondria or by reactive oxygen species (ROS) and free radicals. These alterations decrease mitochondrial oxidative phosphorylation, and cause damage to DNA, proteins and lipids. In response to free radicals, anti-oxidant enzyme levels (e.g. superoxide dismutase (SOD), catalase (CAT)) are elevated. (Figure adapted from Lee and Wei, 2001.)

In particular, oxidative damage of mitochondrial proteins and DNA leads to activation of the ubiquitin-proteosomal pathway, which is involved in protein degradation and turnover. Two proteins related to protein turnover (aspartate aminotransferase 1 and glutamate dehydrogenase 1) were found to be differentially expressed in the proteomics experiment (Appendix 4.4). These proteins are involved in amino acid degradation, protein turnover and nitrogen balance regulation (Cuervo and Dice 2000a). Aspartate aminotransferase 1 and glutamate dehydrogenase 1 levels were found to be elevated in high NFE animals in comparison to low NFE animals. Elevated levels were not necessarily expected in the high NFE animals given that their mitochondria should be less damaged than in low NFE animals. However, these enzymes are also involved in nitrogen balance. As high NFE animals have elevated mitochondrial function, nitrogen turnover should be increased.

6.2.2 Reductive stress

The proteomics study also indicated up-regulation of Complex II (succinate dehydrogenase) in the low NFE animals. This up-regulation could potentially result in the accumulation of reduced metabolites, such as FADH (Yan *et al* 1997). This condition is referred as "reductive stress", and causes an increased production of ROS through auto-oxidation of the reduced metabolites (Stadtman 1988, 1990). Therefore, reductive stress can also initiate a cascade with the potential to cause oxidative burden inside the cell.

6.2.3 Role of complex I in net feed efficiency

The comparative mapping and proteomics results found that within the 4 NFE QTL, there were 18 subunits from the mitochondrial oxidative phosphorylation complexes out of a total of 91 subunits genes. There were 9 Complex I subunits, 1 Complex II subunit, 3 Complex III subunits, and 5 Complex V subunits (Appendix 6.1). Thus, among the 70 cytoplasmic synthesized subunits of complexes involved in oxidative phosphorylation, 17 subunits were identified as potential candidates from the QTL and proteomic studies.

The Complex I subunit-19kDa, identified in both the QTL and proteomics experiments, has a potentially functional amino acid substitution (Y- S) in exon 3. This SNP is currently being genotyped for association studies. The complex I subunit NDUFA10 (42 kDa) had 2 isoforms differentially expressed in the proteomics experiment (chapter 4), which could be due to polymorphisms or post-translational changes. The QTL and proteomics experiments identified a total 5 alpha subunits and 4 beta subunits of complex I as candidate genes (Appendix 6.1). Of these, 4 subunits of complex I had higher levels in the high NFE animals than the low NFE animals (Appendix 4.4). However, the Complex I enzyme activity was found to be decreased in the high NFE animals in comparison to the low NFE animals. One possible explanation would be that in the low NFE animals, the Complex I specific enzyme activity is

higher in compensation for the lower number of Complex I subunits. In corroboration, Marsh *et al* (2000) observed high sodium pump enzyme activity despite low protein levels of the α-subunit of the Na^+, K^+-ATPase sodium pump in sea urchin studies.

There is an alternative explanation. Since Complex I is the rate-limiting enzyme in oxidative phosphorylation and a major source of reactive oxygen species in the mitochondria (Brad *et al* 2004, Turrens 2003 and Kussmaul and Hirst, 2003), any structural alteration in Complex I could lead to a disturbance in electron transfer, proton leakage and/or inefficient energy production. This, in turn, could lead to cellular oxidative stress. One mechanism by which oxidative stress can alter ATP production is to directly affect the enzyme activities of the oxidative phosphorylation complexes such as Complex I. Therefore, oxidative stress could explain the increased activity of Complex I in the low NFE animals as a part of a compensatory effect to the energy crisis.

Whatever the explanation is the results pinpoints the value of conducting enzyme assays in addition to measuring protein levels. The data herein suggest that the integrity of the Complex I multi-subunit structure in high NFE animals is well-maintained, which helps to provide efficient oxidative phosphorylation during ATP generation. The hypothesis would be that in low NFE animals, Complex I would be less efficient and ATP production is compromised. The evidence obtained here suggests Complex I is actively involved in determining net feed efficiency in animals due to its effects on energy production.

6.2.4 Future mitochondrial studies

To provide more support for the hypothesis that Complex I affects NFE, it would be interesting to examine the effects of DNA variants in the individual Complex I subunits on the structure of Complex I, the level of the beta oxidation of fatty acids and oxidative stress. The effect of mutations in the subunits on the structural integrity of Complex I can be studied by examining mitochondrial electron transfer. This is done by polarographic measurements of the oxygen consumption in mitochondria using a Clark-type oxygen electrode (Estabrook, 1967; Cawthon *et al* 1999). Such studies measure the oxygen consumption (expressed in nmol/min per mg protein) to determine the respiratory control ratio and ADP:O ratio. These two parameters indicate the degree of coupling or efficiency of the electron transport chain activity.

Any DNA variants of Complex I subunits can be identified by the genomic sequencing as well. DNA sequence variants might explain variation in enzyme activity and energy metabolism differences in animals. The structure of Complex I can be studied by single particle electron microscopy and X-ray crystallography (Dudkina *et al* 2006).

The affects of Complex I on fatty acid oxidation can be assayed using standard biochemical methods (Moon and Rhead 1987). To assess the oxidative stress due to ROS, carbonyl levels can be measured (Chaudhari *et al* 2006). The results suggest herein that levels of ROS might be used as a phenotypic marker for selection of high NFE animals. An integrated nutri-metabolomics approach could attempt to manage any oxidative stress with the help of dietary supplements.

In addition, the proton kinetics of mitochondria can be studied in order to follow the percentage of the proton leakage and its association with NFE. Proton leakage across the mitochondrial inner membrane dissipates the mitochondrial membrane potential. Brand *et al* (1994) used simultaneous measurements of membrane potential and O_2 consumption to determine the proton leakage kinetics. Proton leakage kinetics helps to distinguish between the 2 main contributors to respiration: substrate oxidation and proton conductance. Increased proton leakage is represented by a higher respiration rate but a lower mitochondrial membrane potential, whereas increased substrate oxidation gives a higher respiration rate and higher membrane potential (Brand *et al* 1994). The membrane potential can be measured by using fluorescent probes like rhodamine 123 (R123), tetramethylrhodamine methyl ester (TMRM), or tetramethylrhodamine ethyl ester (TMRE) (Scaduto and Grotyohann 1999).

In addition to these oxidative phosphorylation Complex subunits, there were another 180 genes identified as potential candidate genes for NFE. Within 4 NFE QTL, since there are too many genes for sequencing for SNPs, either a whole genome scan with a dense SNP chip or an *in silico* SNP panel for these 4 specific NFE QTL genomic regions should be considered.

6.3 Nutrient sensing pathways

Among the other 180 candidate genes, a major group of genes are those involved in nutrient sensing. Intracellular oxidative stress and protein turnover leads to energy crises that increase the demand for energy for compensatory metabolic activities. Therefore, pathways involved in nutrient oxidation are activated to support this energy demand. The study herein identified two important fuel sensing pathways as potentially being involved in NFE, the malonyl coenzyme A (CoA) / long chain fatty acid (LCFA) CoA / adenine monophosphate-activated protein kinase (AMPK) pathway and the β-oxidation of fatty acids.

6.3.1 AMPK pathway

AMP-activated protein kinase is a down-stream component of the protein kinase cascade that acts as an intracellular energy sensor and maintains the energy balance within the cell (Andersson *et al* 2004). AMPK is activated by physiological or pathological stresses that deplete cellular ATP. Examples of such stresses include glucose deprivation, uncouplers of oxidative phosphorylation, oxidative stress, exercise, hypoxia, ischaemia and muscle contraction (Xue and Kahn 2006). Activation of AMPK inhibits

ATP-consuming anabolic pathways by suppressing enzymes such as fatty acid synthase and stearoyl CoA desaturase. AMPK activation triggers ATP-producing catabolic pathways by inducing metabolic enzymes related to the oxidation of fatty acids and cholesterol (Minokoshi *et al* 2002), glucose metabolism and protein synthesis (Kahn *et al* 2005). AMPK also regulates energy intake and body weight by coordinating the regulation between the hypothalamus, various peripheral glucose-sensing neurons and tissues to maintain energy homeostasis. SNP in AMPK (AMPK #1) was found to be in association with NFE (Table 3.5).

Decreased phosphorylation of acetyl-CoA carboxylase (ACC), the downstream target of AMPK, stimulates ACC activity, and thereby increases the level of malonyl-CoA levels. Malonyl-CoA is a potent allosteric inhibitor of carnitine palmitoyltransferase (CPT1) (Figure 6.2). The CPT1 enzyme controls entry of long-chain fatty acid (LCFA)-CoA into the mitochondria for further β-oxidation of the fatty acids for energy production. Entry of long-chain fatty acid (LCFA)-CoA into the mitochondria is the rate-limiting step for the oxidation of fatty acids. In the presence of high levels of nutrients (such as glucose), malonyl-CoA levels increase. This inhibits CPT1, thereby favouring fat deposition (Obessi and Rossetti 2003).

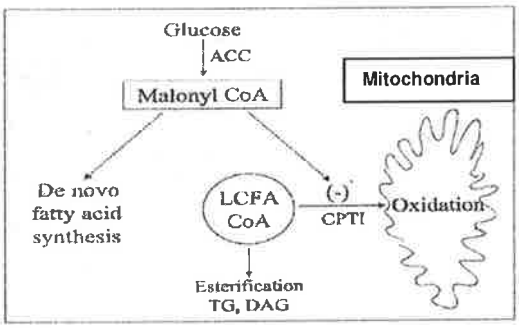

Figure 6.2 Fatty acid partitioning. Malonyl CoA is an inhibitor of CPT1, the enzyme that controls the transfer of long chain fatty acyl (LCFA) CoA molecules from the cytosol to mitochondria for beta fatty acid oxidation. When malonyl CoA levels are elevated, CPT1 is inhibited and esterification of LCFA to form triglycerides (TG) and diacylglycerol (DAG) is favoured (adapted from Rudermann *et al* 2003).

Long chain fatty acyl-CoA enters the mitochondria via the acetyl-CoA transporter and carnitine palmitoyltransferase 1. The long chain fatty acyl-CoA is oxidized to acetyl CoA in the mitochondria, generating NADH in the process. Acetyl CoA is further oxidized in the citric acid cycle (Figure 6.3). Since carnitine palmitoyltransferase 1 (CPT1) acts as a transporter of cytoplasmic long chain fatty acids into the mitochondria, beta oxidation of fatty acids is, in fact, an extension of the AMPK pathway (Figure 6.2). In relation to the β-oxidation of fatty acids, various enzymes in the pathway (peroxisomal bifunctional enzyme (enoyl-CoA hydratase), acetyl-CoA transporter, mitochondrial acyl-CoA dehydrogenase family member 9, and the mitochondrial trifunctional enzyme alpha subunit, (TP-alpha/ HADHA) (78 kDa gastrin-binding protein) were found within the NFE QTL (Appendix 3.6 and 3.7). In

particular, SNPs in HADHA were associated with NFE (Table 3.5). This gene is also found close ParAllele significant SNP PA3607 (Appendix 3.4).

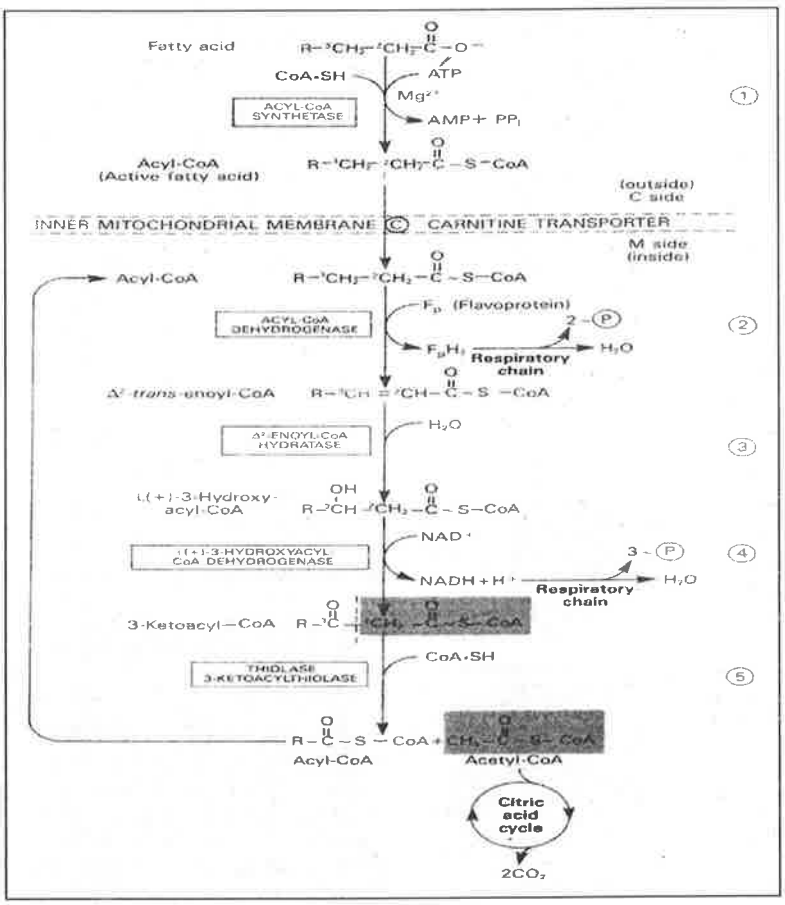

Figure 6.3 ß-Oxidation of fatty acids. Long-chain acyl CoA is cycled through reactions 2-5, acetyl-CoA being generated each cycle by thiolase (reaction 5). When the acyl radical is only 4 carbon atoms in length, 2 acetyl-CoA molecules are formed in reaction 5 (adapted from Harper's Biochemistry, 22nd ed.).

Alterations in the enzymatic activities of CPT1 or AMPK could have significant effects on the beta-oxidation of fatty acids and cellular energy production. The proteomics study strongly supported this hypothesis as carnitine palmitoyltrasferase 1 (CPT1) was one of the proteins found to be differentially expressed in NFE animals. Elevated levels of CPT1 were observed in high NFE animals (Appendix 5.4). This can contribute to early satiety signals by increasing ATP levels. Increased oxidative stress in the low NFE animals should increase energy demand. However, due to low levels of CPT1, the energy status would remain negative. In turn, this would increase nutrient oxidation and feed intake in the low NFE animals as a compensatory effect to satisfy the energy needs of the body. Low NFE animals would be expected to have lower CPT1 enzyme activity. The differentially expression of CPT1 could be due to genetic variation in the CPT1 gene and/or negative metabolic regulators. A contribution of the AMPK pathway in net feed efficiency was supported by the results from Lee (2005), who showed increased

enzyme activities of AMPK in high NFE Angus cattle compared to low NFE animals. These results were expected and are in corroboration with this hypothesis.

6.3.1.1 Cross-talk between AMPK and mTOR-PI3K nutrient sensing pathways

Recently, two new downstream targets of AMPK were identified; cyclic AMP response element binding protein (CREB) activity 2 (TORC2) and the mammalian Target of Rapamycin (mTOR) (Koo *et al* 2005). TORC2 is essential for the regulation of hepatic gluconeogenesis by mediating CREB-dependent transactivation of peroxisome proliferator-activated receptor-gamma coactivator-1 (PGC1α) and its gluconeogenic targets, phosphoenolpyruvate carboxykinase (PEPCK) and glucose-6-phosphatase (G6Pase) (Koo *et al* 2005). AMPK suppresses hepatic gluconeogenesis by blocking the expression of gluconeogenic genes (Yamaguchi *et al* 2002). In relation to this regulation of gluconeogenesis, PEPCK produces phosphoenolpyruvate, a glycolytic intermediate in glucose catabolism, which is utilised in the citric acid cycle for energy production (German 1993). PEPCK was found to be elevated in the high NFE animals in comparison to the low NFE animals in the proteomics study. Enzyme assays using samples from these same animals demonstrated (Lee 2006) elevated AMPK activity in the high NFE animals although Yamaguchi *et al* (2002) reported an inverse relationship between AMPK and PEPCK.

The mammalian Target of Rapamycin (mTOR) represents another potential NFE pathway identified from the QTL linkage mapping study. mTOR is a novel downstream target of AMPK (Reiter *et al* 2005). mTOR not only integrates the nutrient and hormonal signals for growth and development, but also integrates insulin signalling with cellular fuel status. mTOR contains a C-terminal region with strong homology to the catalytic domain of phosphatidylinositol 3-kinase (PI3K) and phosphatidylinositol 4-kinase (Schmelzle and Hall 2000). In response to amino acids and growth factors, mTOR controls the protein translation machinery by phosphorylating downstream targets, such as p70 ribosomal S6 kinase ($p70^{s6k}$), eukaryotic initiation factor 4E-binding protein 1 (4E-BP1) and eukaryotic initiation factor 4G (eIF4G). mTOR is controlled upstream by the insulin receptors, insulin receptor substrate (IRS), AMPK, and phosphatidylinositol 3-kinase (PI3K) (Figure 6.4). AMPK activation inhibits mTOR signalling, suppressing protein synthesis (Tokunnaga *et al* 2004). Recently, Cota *et al* (2006) showed that the mTOR signalling pathway in the hypothalamus contributes significantly to regulating food intake and body weight. mTOR is co-localised with AgRP/NPY and proopiomelanocortin neurons in the arcuate hypothalamus.

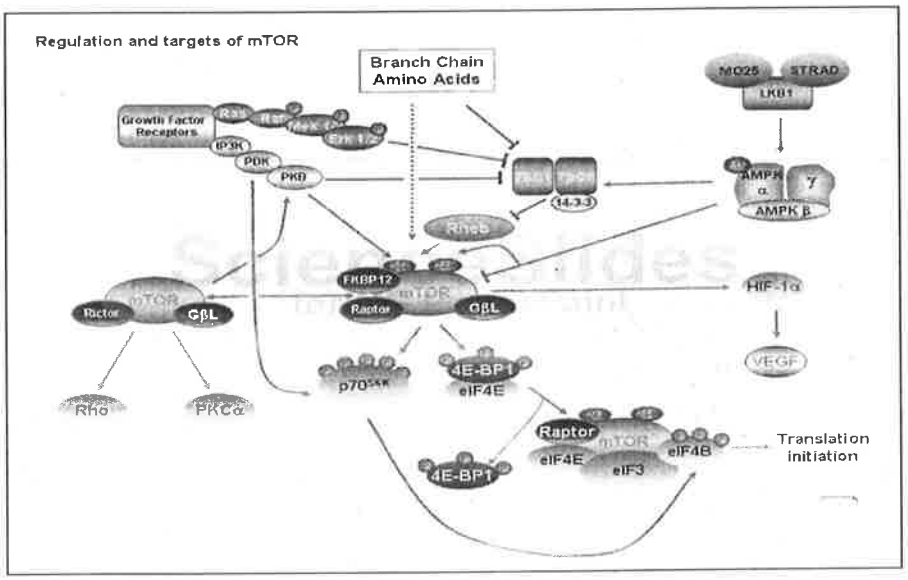

Figure 6.4 The mammalian Target of Rapamycin (mTOR) signalling pathways. mTOR is a downstream target of phosphatidylinositol 3-kinase (PI3K) and adenine monophosphate-activated kinase (AMPK, α, ß, γ). AMPK inhibits mTOR pathway. mTOR is activated in response to amino acids and growth factor receptors via PI3K, 3'-phosphoinositide-dependent kinase-1 (PDK-1), and protein kinase B (PKB). mTOR itself activates p70 ribosomal S6 kinase ($p70^{s6k}$), eukaryotic initiation factor 4E-binding protein 1 (4E-BP1) and eukaryotic initiation factor 4G (eIF4E), eukaryotic initiation factor 4B (eIF4B), eukaryotic initiation factor 3 (eif3) and regulatory associated protein of TOR (Raptor). An arrow represents stimulation and a cross bar represents inhibition. (Adapted from http://visiscience.com/sciencesslides.php).

6.3.1.2 Conclusion

Results supported the hypothesis of the involvement of AMPK and ß-oxidation of fatty acids in the regulation of NFE. Changes in AMPK activity act through the acetyl CoA carboxylase (ACC)-malonyl CoA- carnitine palmitoyltransferase (CPT1) pathway to regulate food intake and other metabolic processes. Downstream of AMPK, pathways like mTOR also mediate the effects of AMPK on energy expenditure, fatty acid oxidation, energy balance and glucose homeostasis (Figure 6.5). The genes for the AMPK and PI3K subunit 85 were found within the NFE QTL on BTA 20 and the gene for the PI3K subunit 150 was found within the NFE QTL on BTA 1. Identified SNPs identified in the AMPK pathway, like AMPK#1 and HADHA#1, show good association with NFE in the cattle tested thus far (Table 3.5). The experimental evidence from the integrated genomic, proteomic and biochemical approaches herein suggest the new hypothesis that high activity of AMPK and increased beta fatty acid oxidation could lead to improved net feed efficiency.

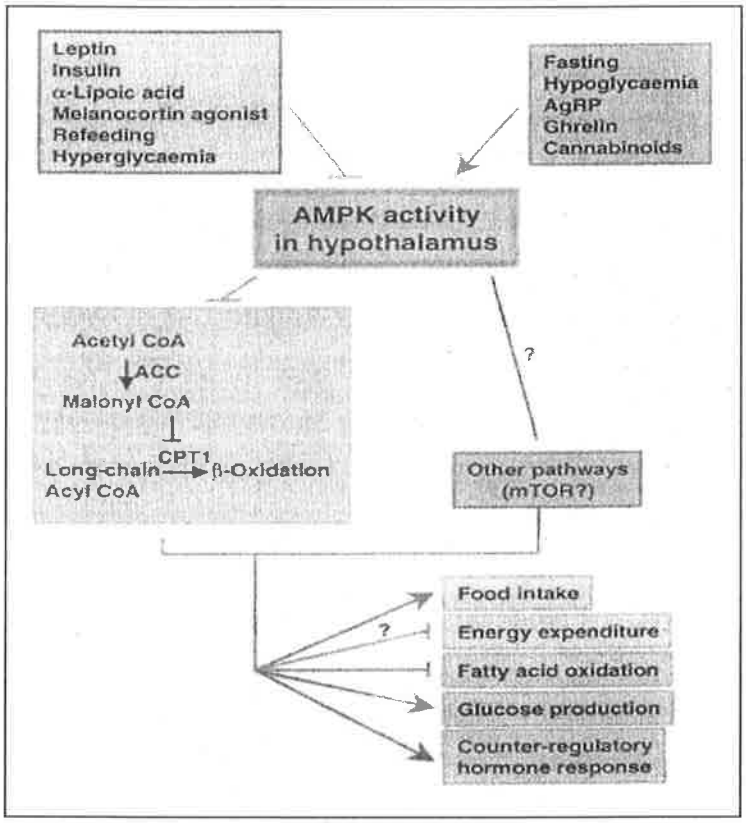

Figure 6.5 Relationship between AMPK, mTOR and their downstream effects. Multiple hormones, peptides, nutrients and altered metabolic states regulate AMPK activity in the hypothalamus. AMPK acts through the acetyl CoA carboxylase (ACC)-malonyl CoA-carnitine palmitoyltransferase (CPT1) pathway to regulate several metabolic processes including food intake and glucose production. Downstream of AMPK, mammalian Target of Rapamycin (mTOR) also mediates the effects of AMPK on energy balance and glucose homeostasis. An arrow represents stimulation and a cross bar represents inhibition (adapted from Xue and Kahn 2006).

6.3.1.3 Future studies

The data on the AMPK pathway and the beta-oxidation of fatty acids looks sufficiently promising to warrant further study of these pathways in relation to NFE. The substrates and enzymes involved in the AMPK, beta-oxidation of fatty acids (e.g. malonyl CoA and carnitine palmitoyltransferase1) and mTOR-PI3K pathways should be measured by enzyme assays (Moon and Rhead 1987; Andersson *et al* 2004, Patti and Kahn 2004) in high versus low NFE animals. It would be interesting to test the effect of inhibiting the AMPK pathway in knockout mice or by siRNA techniques. In addition, the AMPK pathway has the potential to be manipulated for muscle specific fat deposition (marbling). Therefore, the relationship between NFE and fat deposition should be examined more closely by taking relevant measurements on a large number of carcasses from cattle measured for NFI.

6.3.2 Cross-talk between nutrient sensing pathways and peripheral energy sensors

A related group of candidate genes are those involved in sensing energy peripherally. Growth hormone, leptin, insulin, prolactin and insulin-like growth factor affect protein, lipid and glucose metabolism by

interacting and inducing the necessary metabolic signals upon binding with their corresponding receptors. These receptors are activated whenever there is a need to produce more energy or to convert nutrients into suitable energy stores.

6.3.2.1 Growth hormone (GH) signal transduction pathway

Growth hormone (GH) exerts its effect by binding to the extracellular domain of the GHR where one molecule of GH binds to two receptors. The dimerised GHR then activates downstream signalling pathways by recruiting cytoplasmic tyrosine kinases, which phosphorylate the tyrosine residues in the intracellular domain of GHR. Among the many tyrosine kinases, JAK2 has a major role. The phosphotyrosine residues on both GHR and JAK2 provide docking sites for a variety of signalling proteins that contain phosphotyrosine-binding motifs, such as SRC homology 2 (SH2). SOCS proteins are thought to inhibit these signalling proteins by inhibiting the kinase activity of JAK2 (Herrington and Carter-Su, 2001).

The GHR-JAK2 assembly activates the epidermal growth factor receptor, and concomitantly, increases mitogen-activated protein (MAP) kinase activity. Shc is the main signalling molecule involved in MAP kinase activation. After tyrosine phosphorylation, Shc binds the SH2 domain of GHR bound protein-2 (Grb2). Through this interaction, Shc plays a role in the activation of the MAP kinase cascade by insulin (Dominici and Turyn 2002) (Figure 6.6). However, recent reports indicate that PI3K also mediates GH-regulated gene transcription, independently of MAP-kinase (Piwien-Pilipuk *et al* 2001).

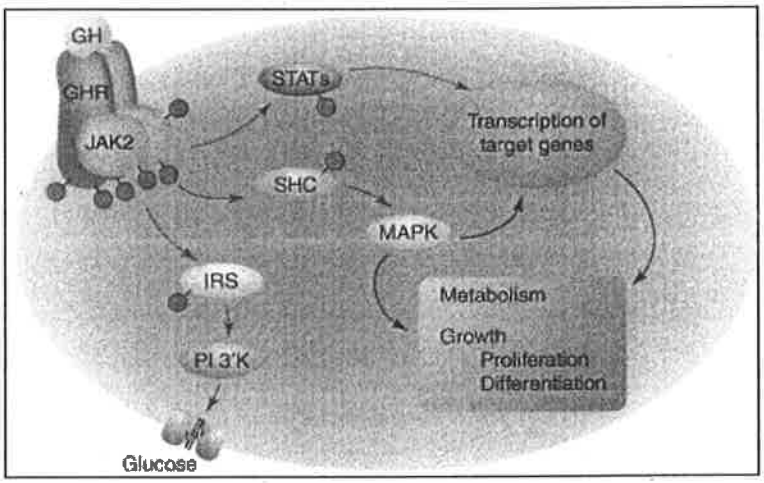

Figure 6.6 Growth hormone signalling pathways. Signalling pathways initiated by GH activation of JAK2 are shown. JAK2 phosphorylates SHC, leading to activation of MAPK (blue arrows). JAK2 also phosphorylates STAT transcription factors. MAPK and STATs are important for GH regulation of gene transcription (purple arrows). JAK2 phosphorylates IRS proteins, which are thought to lead to activation of PI3'-kinase (PI3K: red arrows). GH activation of PI 3'-kinase via IRS proteins may be important for GH stimulation of glucose transport. Abbreviations: GH, growth hormone; GHR, growth hormone receptor; IRS, insulin receptor substrates; JAK2, Janus kinase 2; MAPK, mitogen-activated protein kinase; P, phosphate; PI 3'K, phosphatidylinositol 3-kinase; STAT, signal transducers and activators of transcription (adapted from Herrington and Carter-Su, 2001).

In addition, GH activates insulin receptor substrate (IRS)-PI3K activity via tyrosine phosphorylation of IRS 1, 2 and 3 by JAK2, which provides a docking site for the SH2 domain of the 85-kDa regulatory subunits of phosphatidylinositol (PI) 3'-kinase (Smith *et al* 1999, Liang, 1999). This activates the catalytic subunit of PI3K, p110, which has lipid-metabolizing activity. The lipid products of PI3K activity, phosphatidylinositol-4,5-biphosphate (PIP2) and phosphatidylinositol-3,4,5-triphosphate (PIP3), recruit protein kinase B (PKB, also known as Akt) to the plasma membrane. This step is central to the regulated movement of the glucose transporter, GLUT4, from the intracellular vesicles to the cell surface for glucose uptake and glycogen synthesis (Staubs, 1998). Activated PKB/Akt interacts with mammalian Target Of Rapamycin (mTOR) and the forkhead transcriptional factor subfamily forkhead box O1 (FOXO1) (Figure 6.7). The phosphorylation of FOXO1 by Akt inhibits FOXO1 action. FOXO1 mediates the metabolic actions of insulin, including hepatic gluconeogenesis, skeletal muscle glucose disposal, adipocyte differentiation and pancreatic ß-cell growth.

Growth hormone and insulin share other common signalling pathways. Among its insulin-like actions, GH increases glucose and amino acid transport, lipogenesis and protein synthesis. GH is involved in lipolysis by activating cAMP-specific phosphodiesterase PDE4A5 in a PI3K-dependent mechanism (MacKenzie *et al* 1998). GH also regulates the transcription of a number of other important proteins, including the insulin-like growth factors.

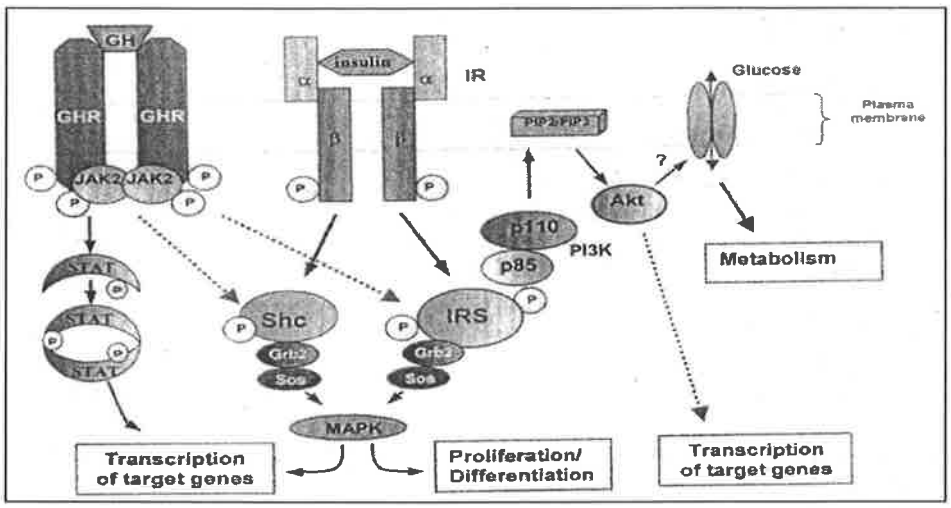

Figure 6.7 Convergence of growth hormone and insulin signalling. The insulin receptor (IR) phosphorylates insulin receptor substrate (IRS) proteins, which in turn bind to the SH2 domains in the p85α regulatory subunits of phosphatidylinositol 3-kinase (PI3K). Activation of PIP2 and PIP3 recruit protein kinase B (Akt) to the plasma membrane. PI3K mediates insulin responses including insulin-induced glucose uptake and glycogen synthesis through PI3K subunits p110. Engagement of Grb2/Sos by tyrosyl-phosphorylated IRS proteins and SHC activates the mitogen activated protein kinase (MAPK) cascade. Growth hormone (GH) induced dimerisation of growth hormone receptor (GHR) leads to activation of Janus kinase2 (JAK2) and phosphorylation of several cytosolic proteins, including signal transducers and activators of transcription (STAT), SHC and IRS proteins. This signalling crosstalk (represented by dotted line) is thought to be important for the insulin-like effects of GH (Figure adapted from Dominici and Turyn 2002).

There are many proteins apart from GHR itself within the NFE QTL that are part of the GHR signal transduction pathway. These include suppressor of cytokine signalling 5 (Socs5), docking protein 2, Janus kinase 2 (JAK2), SH2 domain containing 3C isoform 2 (SH2D3C), Src homology 2 domain containing adaptor protein B (SHB), SHC transforming protein 3 (SHC3), insulin receptor substrate 1 (IRS1), epidermal growth factor (EGF), and mitogen-activated protein kinase (MAPK) related proteins (Appendix 6.2). It will be interesting to sequence these genes to find DNA variants, if any, affecting on NFE. Bernier (1986) reported that the C57 hg/hg natural mouse mutants (Socs2 mutation) have increased body size and increased energy efficiency by 50%. SHC and Socs2 have found to be an inhibitory effect on the GHR signal transduction pathway in these mice studies. Therefore, any mutations in the GHR signal transduction inhibitors could affect energy efficiency and body growth. There were 19 SNPs found in the GHR gene. Among them, 7 SNPs (including 3 potentially functional SNPs) were in exon 10 that codes for the intracellular domain of GHR. As discussed above, this intracellular domain of GHR induces many downstream signal transduction pathways by JAK2 tyrosine phosphorylation. GHR SNP1 (Ala-Thr) and SNP2 (located in the 3' UTR) were associated with net feed efficiency herein (Table 3.5).

Based on the available evidence, the GHR pathway also merits further investigation. In particular, the effect of mutations in the intracellular domain of GHR on downstream nutrient sensing pathways (eg. AMPK, mTOR, PI3K and insulin receptor substrate) and the functional properties of GHR in context to feed efficiency should be studied more intensively.

6.3.2.2 Insulin and leptin receptor transduction pathways

Insulin acts via a cell surface insulin receptor (IR) that comprises an extracellular alpha-subunit involved in insulin binding and an intracellular beta-subunit that transduces the insulin signals inside the cell. The beta subunit has intrinsic tyrosine kinase activity, which assists insulin binding and activates intracellular signalling proteins by tyrosine phosphorylation (Cheatham and Kahn 1995) (Figure 6.8). The tyrosine phosphorylated proteins (including insulin receptor, insulin receptor substrate (IRS) -1 and -2 (IRS -2), Tub and Shc) bind several Src homology 2 (SH2) domain-containing proteins, that cause downstream signalling. IRS-1 and IRS-2 mutations increase food intake and fat stores, while a loss-of-function mutation of Tub causes obesity in "Tubby" mice. Therefore, it is hypothesized that defective insulin signalling in the brain results in obesity and increased food intake (Schwartz *et al* 2000). In this context, functional SNP found in alpha-HS-glycoprotein (AHSG) on NFE QTL1. AHSG inhibits insulin-induced insulin receptor (IR) autophosphorylation and tyrosine kinase activity. AHSG knock-out mice demonstrate increase downstream signalling of IRS and MAPK pathways.

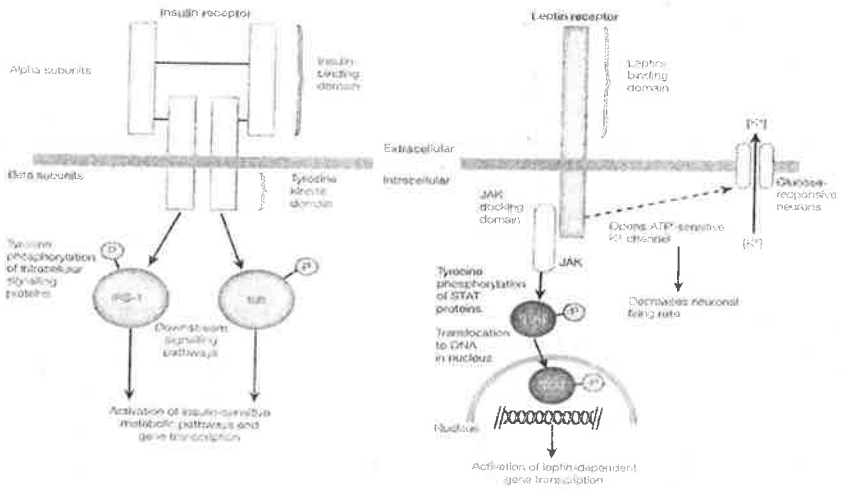

Figure 6.8 Leptin and insulin receptor signalling. Insulin receptors are activated by the binding of insulin to the alpha-subunit and the intracellular domain beta-subunit is phosphorylated due to intrinsic tyrosine kinase activity. Insulin receptor transduces the insulin signal to the cell by phosphorylating intracellular signalling molecules, like insulin receptor substrate 1 (IRS1) and tub. Leptin receptor is a member of cytokine receptor family which does not have intrinsic tyrosine kinase activity. Leptin receptors though have a docking site for Janus kinase (JAK), a member of the tyrosine kinases involved in intracellular signalling. JAK phsophorylates signal transduction and transcription factor (STAT) which stimulates transcription of target genes. Leptin thus induces the JAK-STAT pathway and affects the potassium channels of the glucose sensing neurons. Leptin binding keeps the potassium channels open and reduces neuronal firing, thereby decreasing food intake. (Figure adapted from Schwartz *et al* 2000.)

Benomar *et al* (2005) showed that leptin and insulin are major signals in the hypothalamus for regulating energy homoeostasis and body adiposity. Insulin receptors and leptin receptors (long isoform, ObRb) share a number of signalling cascades; such as JAK2/STAT-3 (Janus kinase 2/signal transduction and activator of transcription 3), MAPK and PI3K. Benomar *et al* (2005) and Xu *et al* (2005) also showed that insulin and leptin are able to activate PI3K through insulin receptor substrate 1 and 2 (IRS-1 and IRS-2), respectively, in the hypothalamic ARC neurons (Figure 6.8). Phosphatidylinositol (PI) 3'-kinase (PI3K) induces various insulin-stimulated biological responses, including glucose transport, glycogen synthesis, and protein synthesis (Dominici and Turyn 2002).

Leptin or insulin treatment increases basal PI3K activity and IRS-1 or IRS-2 association with p85, which most likely accounts for the cross down-regulation of leptin and insulin receptors (Benomer *et al* 2005). Kim *et al* (2006) found that the effects of leptin and insulin on feeding are inhibited when the hypothalamic forkhead transcriptional factor subfamily forkhead box O1 (FOXO1) is activated. FOXO1 is a downstream target of PI3K. In other words, PI3K activation decreases FOXO1 activity through the activation of insulin and leptin. FOXO1 is also involved in the transcriptional regulation of neuropeptides in the arcuate nucleus region (ARC) of the hypothalamus. FOXO1 increases the expression of orexigenic agouti-related protein (Agrp) / neuropeptide Y (NPY) expression and decreases the

expression anorexigenic pro-opiomelanocortin (POMC) and cocaine- and amphetamine regulated transcript (CART).

There were 8 insulin related genes found within the NFE QTL (Table 6.2). Since these genes were not examined for association with NFI herein, they should be sequenced for SNP detection.

Table 6.2: Glucose metabolism related genes within NFE QTL

Name of the gene	Abbreviation	Cattle chromosome
Insulin-like growth factor-II mRNA-binding protein 2	IGFBP2	BTA8
Insulin-like growth factor binding protein-like 1	IGFBP1	BTA8
Insulin-like growth factor 2 receptor	IGF2R	BTA8
Insulin gene enhancer protein ISL-1	ISLET-1	BTA8
Insulin-like peptide 4	INSL4	BTA8
Insulin-like peptide 6 precursor	INSL6	BTA8
Insulin-like growth factor-dependent IGF binding protein 4 protease	PAPPA	BTA8
Insulin receptor substrate 1	IRS-1	BTA11

6.3.2.3 Prolactin and insulin like growth factor-1 receptor transduction pathways

The prolactin receptor (PRLR) and insulin like growth factor-1 receptor (IGF1R), which like GHR belongs to the cytokine receptor superfamily, activate Janus kinase (JAK) 2 tyrosine kinase. Thus, these receptors are able to induce tyrosine phosphorylation of both IRS-1 and IRS-2 (Liang, 1999, Dudek *et al* 1997). The activation of the Ras/MAP kinase pathway by PRLR has also been reported (Erwin *et al* 1996). On the other hand, IGF1R activates MAP kinases, such as the extracellular signal-regulated kinases (ERK) 1 and 2, through the shc-grb2-IRS1 pathway (Dudek *et al* 1997) (Figures 6.9 and 6.10). The prolactin receptor was another gene found the cluster of GHR, AMPK and PI3K genes in the NFE QTL on BTA 20, but was not found to be associated with NFE.

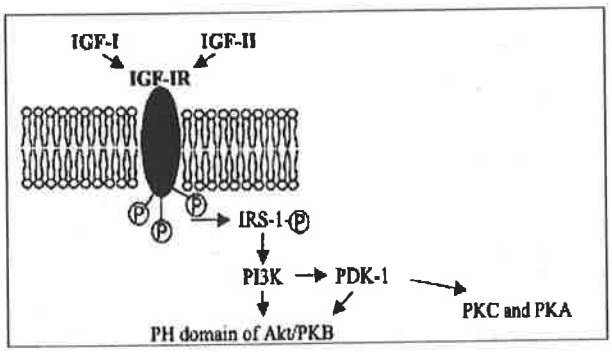

Figure 6.9 Insulin-like growth factor 1 receptor (IGF1R) and IRS1-PI3K signal transduction pathway. IGF1R activates Janus kinase 2 (JAK2) after binding with insulin-like growth factor I (IGF-I) and II (IGF-II) and / or phosphorylates insulin receptor substrate 1 (IRS-1), which in turn, activates phosphatidylinositol 3-kinase (PI3K). PI3K further stimulates protein kinase B (PKB/Akt) and 3'-phosphoinositide-dependent kinase-1 (PDK-1), protein kinase A PKA and protein kinase C (PKC) downstream signalling proteins. (Figure adapted from Vincent and Feldman 2002.)

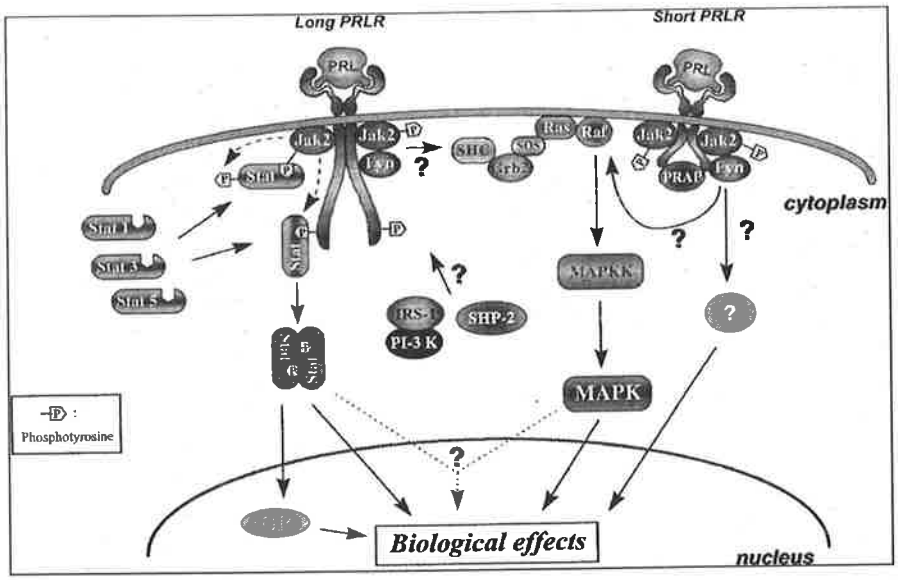

Figure 6.10 Prolactin receptor (PRLR) signal transduction pathway. PRLR activates signal transducers and activators of transcription 1, 3 and 5 (Stat1, Stat3, and Stat5). Interaction of Stat5 with the glucocorticoid receptor (GR) has been reported. Whether the short PRLR isoform activates the Stat pathway is currently unknown. PRAP (PRLR-associated protein) seems to interact preferentially with the short PRLR. The mitogen activated protein kinase (MAPK) pathway involves the Shc, Grb2, Sos, Ras, Raf cascade and is presumably activated by both PRLR isoforms. Connections between the JAK-Stat with MAPK, and interactions between prolactin receptors, Src kinases (*e.g.*, Fyn), SHP2, insulin receptor substrate 1 (IRS-1), phosphatidylinositol 3-kinase (PI-3 K), and other transducing molecules have been suggested. (Figure adapted from Bole-Feysot *et al* 1999.)

6.3.2.4 Conclusion

It had been believed that the growth hormone receptor, insulin receptor, leptin receptors, prolactin receptor and insulin like growth factor-1 receptor signal transduction pathways were independent. However, there is increasing body of evidence suggesting that not only growth hormone receptor, insulin receptor, and leptin receptor but the insulin-like growth factor receptor and prolactin receptor share several points of convergence and synergism with each other by recruiting JAK2, IRS and PI3K molecules for the downstream signalling of the mTOR pathway and other key energy homeostasis

neurocircuits. Among these 5 receptors, growth hormone receptor, leptin receptor and prolactin receptor are from the cytokine-receptor superfamily (Kaczmarski and Mufti 1991), whereas the insulin receptor and insulin-like growth factor receptor are from the tyrosine kinase receptor family (Benomar *et al* 2005). The physiological importance of the cross-talk between these different hormone pathways through the 3 predominant intermediate proteins (i.e. JAK2, IRS and PI3K) is not yet clear. The inter-relationship between these five signal transduction pathways allows metabolic redundancy. It is known that different cell types regulate the IRS-PI3K-mTOR pathway through different receptors when there is a need for nutrients in an energy crisis situation. However, there is very little information available on the recruitment of these receptors and their regulation in relation to feed intake.

6.3.2.5 Future studies

GHR, AMPK, and PI3K have multiple SNPs that could be studied in more detail by conducting cellular assays to observe any functional effects. These studies can be conducted by transfecting hepatic or fibroblast cells with vectors expressing normal and variant copies of these genes using the LHRE-luciferase reporter plasmid and exposing the cells to their respective ligand to measure the transcriptional activity of the reporter construct. These assays should be performed with increasing concentrations of the ligands in combination with different exposure times (Santos *et al* 2004).

6.4 Glucose metabolism

There were two pathways identified in the category of glucose metabolism potentially involved in NFE: the glycolytic pathway and the hexose biosynthesis pathway.

6.4.1 Glycolytic pathway

Glucose nutrients enter the cell through glucose transporters regulated by the intra- and extra-cellular energy status of the body via an intracellular PI3K mechanism (Figure 6.7). Complex sugars, like sucrose and starch, are simplified to glucose and fructose with the help of enzymes such as sucrase-isomaltase[1], for rapid absorption. Glucose is phosphorylated to glucose 6-phosphate by glucokinase in liver and hexokinase in muscle. Glucose 6-phosphate is converted to glucose 1-phosphate by phosphoglucomutase. Glucose 1-phosphate reacts with uridine triphosphate (UTP) to form the active nucleotide uridine diphosphate glucose (UDPGlc) as catalysed by UDPGlc pyrophosphorylase. Glycogen synthase creates a glycosidic bond between the C_1 of the activated glucose of UDPGlc and the C_4 of the terminal glucose residue of glycogen, liberating uridine diphosphate (UDP) and glycogen.

[1] Underlined genes were found within NFE QTL

In the glucose breakdown pathway, glucose 6-phosphate is converted into fructose 6-phosphate by phosphohexose isomerase. Fructose also can be converted to fructose 6-phosphate by hexokinase. Fructose 6-phosphate is converted into fructose1,6-bisphosphate by fructose-1,6-bisphosphatase. Fructose-1,6- bisphosphate is further metabolised into glyceraldehyde 3-phosphate by aldolase B. Glyceraldehyde 3-phosphate enters the glycolysis pathway by conversion into pyruvate via 2-phosphoglycerate. Glyceraldehyde 3-phosphate also is converted into dihydroxyacetone phosphate by phospho-triose isomerase. This is a glycolytic enzyme that catalyzes the reversible interconversion, and therefore, plays an important role in glycolysis and is essential for efficient energy production (Figure 6.11). Phospho-triose isomerase was elevated in high NFE animals in the proteomics experiment. This was expected because the phospho-triose isomerase helps to produce intermediates from the glycolytic pathway for the energy production (Appendix 4.4).

Skeletal muscle enolase 3 is involved in the glycolytic activity of muscle by catalysing the reversible dehydration of 2-phospho-D-glycerate to phosphoenolpyruvate as part of the glycolytic pathway. Skeletal muscle enolase 3 was found to be elevated in high NFE animals. This was expected as other glycolytic enzymes (eg PEPCK and phospho-triose isomerase) were also elevated in the high NFE animals.

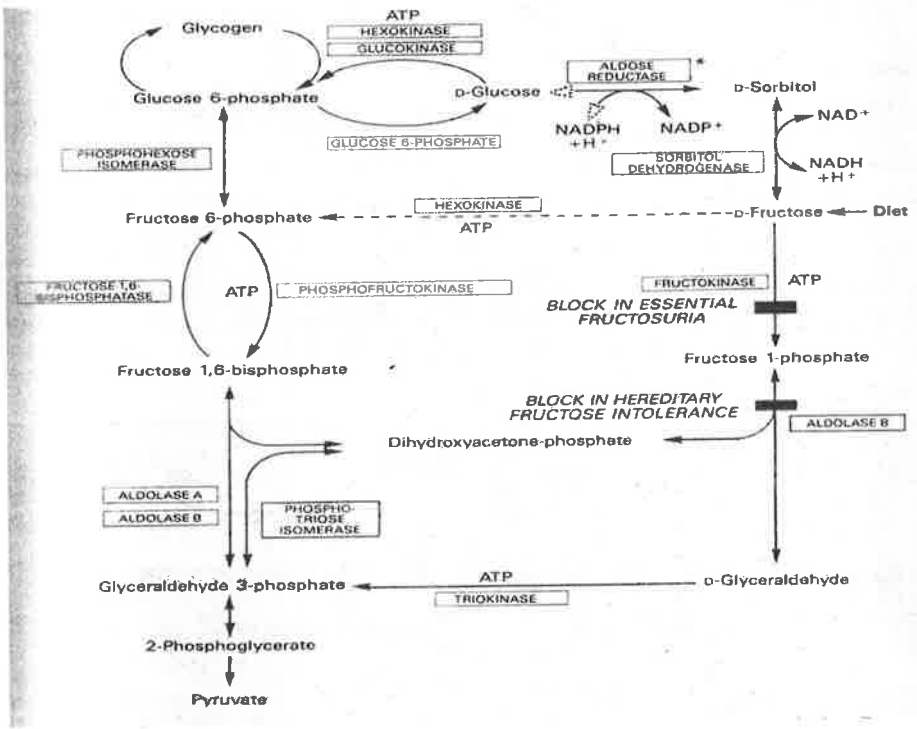

Figure 6.11: Glycolysis pathway. This pathway shows the reversible reactions where glycogen and glucose can be converted eventually to pyruvate. Pyruvate is further oxidized through the TCA cycle in the mitochondria for energy production (adenine tri-phosphate, ATP). (Figure adapted from Harper's Biochemistry, 22nd ed.).

6.4.2 Hexosamine biosynthesis pathway

Hexosamine biosynthesis is another pathway identified herein involved in glucose metabolism. In skeletal muscle and adipose tissue, glucose is converted to glucose-6-phosphate and eventually to fructose-6-phosphate. Glucose-6-phosphate and fructose-6-phosphate mainly undergo glycogenesis or glycolysis. However, a small portion is shunted through into the hexosamine pathway by the rate-limiting enzyme glutamine:fructose-6-phospahte amidotrasferase (GFAT), which converts fructose-6-phosphate to glucosamine-6-phosphate. The end product of this pathway is uridinediphosphoglucose-*N*-acetyl-glucosamine (UDP-GlcNAc), which serves as a substrate for most glycosylation pathways. The flux through this pathway affects the stability and activity of many proteins. Their gene expression is involved in cellular energy regulation (Ravussin 2002). Glycosylation of transcriptional factors affects insulin action and fuel oxidation. In particular, glucose-*N*-acetyl-glucosamine (O-GlcNAc) modification occurs in transcriptional factors involved in the regulation of oxidative phosphorylation genes, such as Sp1, peroxisome proliferator activator receptor γ coactivator-1 α (PGC-1α), and nuclear respiratory factor 1 (NRF1). Thus, glycosylation ultimately affects mitochondrial oxidative phosphorylation (Obici and Rossetti 2003) (Figure 6.12).

The hexosamine biosynthetic pathway is not only a major mediator of carbohydrate metabolism, but also represents a biochemical link between nutrient availability and the molecular response to energy expenditure (Obici *et al* 2002). Two enzymes in the hexosamine biosynthetic pathway were found to be within NFE QTL: UDP-glucose-hexose-1-phosphate uridylyltransferase and UDP-GalNAc:polypeptide N-acetylgalactosaminyltransferase 14. These two enzymes need to be sequenced to find if there is any SNP association with NFE.

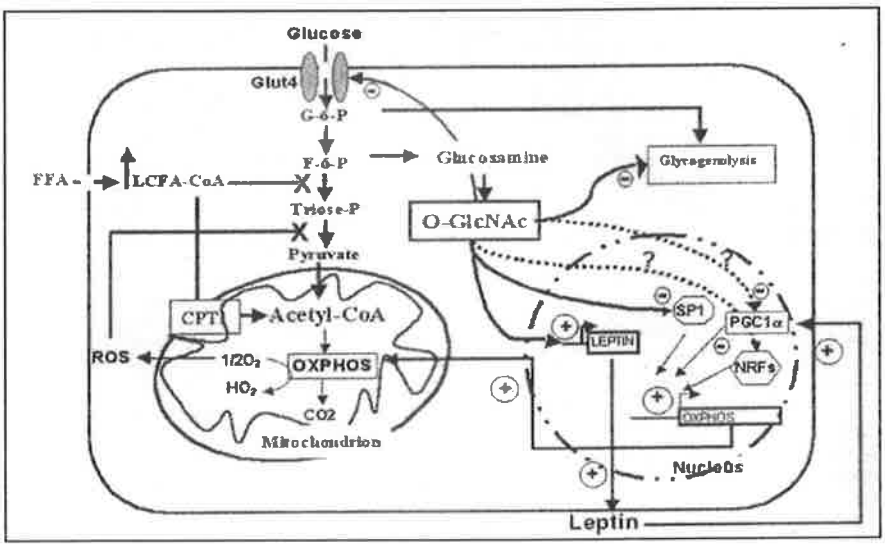

Figure 6.12: Biochemical link between glucose nutrient sensing in modulating insulin action, mitochondrial energy production and long chain fatty acyl-coenzyme A (LCFA-CoA) pathway. Nutrient-sensing pathways stimulate

secretion and biosynthesis of insulin and leptin respectively. Persistent glucose oxidation increases carbon fluxes through the hexosamine biosynthesis pathway (HBP) and increases intracellular levels of glucose-*N*-acetyl-glucosamine (O-GlcNac). O-GlcNac modifies the transcription factors involved in the regulation of oxidative phosphorylation (OXPHOS) genes, such as SP1 transcription factor, peroxisome proliferator activator receptor γ coactivator-1 α (PGC-1α), and nuclear respiratory factor 1 (NRF1), that may ultimately cause a decline in mitochondrial function and oxidative phosphorylation. Direct modification of Sp1 function by O-GlcNac has been reported (shown in solid arrows) and there is direct interaction of HBP with PGC-1α. However, an interaction with NRF1 is still speculative (broken arrows). HBP activates the expression of the leptin gene in adipose and other tissues. Leptin counteracts the suppressive effects of HBP on oxidative phosphorylation by increasing the gene expression of oxidative phosphorylation and uncoupling proteins. Increase in level of free fatty acid (FFA) and LCFA-CoA inhibits glucose oxidation. Glut 4: glucose receptor, G-6-P: glucose-6-phosphate, F-6-P: fructose-6-phospahte; ROS: reactive oxygen species. (Figure adapted from Obici and Rossetti 2003.)

6.4.3 Conclusion

The results from the work herein not only supports the involvement of the glucose turnover pathways in NFE but leads to a new hypothesis that states the glycolytic pathway is elevated in high net feed efficiency animals in comparison to low NFE animals. To confirm this hypothesis, the levels of various enzymes involved in glucose metabolism could be studied individually by Western blotting experiments and/or enzyme assays.

If there is an increase in glycolytic energy metabolism in the high NFE animals, then high NFE animals should have increased fat depots. This is because in adipocytes, fatty acids are synthesized from glucose rather than other lipogenic precursors like acetate (Smith and Crouse, 1984). However, the Angus experimental animals herein had no significant difference in intramuscular or P8 fat (Table 2.4). McDonagh *et al* (2001) also did not find any difference in marbling score or objectively measured intramuscular fat (IMF) for carcasses of feedlot steers divergently selected for NFE. There is one report supporting a genetic correlation between NFE and intramuscular fat (Robinson *et al* 1999). Moreover, in other NFE cattle studies, researchers have found a genetic correlation between subcutaneous fat with NFE (Arthur *et al* 2001a; Schenkel *et al* 2004). Basarab *et al* (2003) also provided phenotypic evidence for a negative association between NFE and carcass fatness in crossbred steers as the high NFE animals tended to be leaner and carcass fat depth was slightly lower. In contrast to results in cattle, experiments conducted on mouse selection lines for net feed efficiency consistently resulted in high NFE mice lines with 6-50% higher carcass fat in comparison to low NFE lines (Bishop and Hill (1985); Nielsen *et al* (1997a); Hastings *et al* (1997); Bunger *et al* (1998); Nielsen *et al* (1997a), (1997b); Archer and Pitchford (1996) and Hughes *et al* (1998), (2003)). Therefore, results to date on the correlations between intramuscular fat or subcutaneous fat with NFE are not conclusive.

Increased glycolytic muscle metabolism and increased fat deposition in the high NFE animals contradicts the hypothesis of an elevated AMPK pathway activity in the high NFE animals. Since AMPK is involved in the mitochondrial oxidation of long-chain fatty acids for energy production, it could be expected that there would be less fat in high NFE animals in comparison to low NFE animals. However, increases in the level of glycolysis and fat can be related to efficient nutrient partitioning between the

amounts of glucose for energy production versus fat deposition in high NFE animals. In the AMPK pathway, malonyl Co-A acts as a switch from fatty acids to glucose oxidation if there is a high level of glycolysis. Thus, there can be a high level of AMPK activity and a high level of glycolysis.

However, this raises question as to why there is a high level of glycolysis in high NFE animals. To increase glycolysis activity, a high concentration of glucose is needed. To activate the glycolytic pathway, the level of insulin would also have to be elevated sufficiently to enhance glucose transport into the cell. If animals are insulin resistant, it is possible to affect intra-cellular nutrient oxidation and partitioning. Therefore, based on this paradigm, high NFE animals could have an increased level of insulin and thus, elevated insulin sensitivity in comparison to low NFE animals as the low NFE animals would be more insulin resistant. The molecular mechanism for insulin resistance can be through the altered regulation of 1) specific membrane receptors for insulin, 2) intracellular signalling molecules (such as insulin receptor substrate 1, phosphoinositide 3-kinase or the mammalian Target of Rapamycin), or 3) glucose transporters (such as Glut2 and Glut4). Therefore, glucose tolerance tests should be conducted to see if there is any significant difference between high and low NFE animals.

6.4.4 Future studies

To confirm these new hypotheses, intensive screening of these fuel-sensing metabolic pathways could be undertaken by measuring their activity using non-invasive determination of intracellular pools of radiolabelled (^{13}C, ^{31}P) intermediate metabolites by advanced nuclear magnetic resonance (NMR). In this technique, kinetic measurements of substrate consumption and end product formation can be measured with a time resolution of less than 30 seconds (Neves *et al* 2000). This would help to develop an understanding of how cells adjust their energy demanding tasks to the amount of fuel available.

Moreover, based on the candidate genes identified herein and from the available literature, it would be possible to develop a microarray specifically designed to assess the gene expression of candidates from the various pathways, particularly, oxidative phosphorylation and the nutrient sensing pathways. When selecting the genes for microarray studies, pathways involved in fat deposition should be considered because these genes are metabolically connected to energy turnover. Such a microarray could be used to screen high and low NFE animals and provide a more detailed understanding of the specific metabolic pathways regulating net feed efficiency and fat traits.

6.5 Summary

The current study confirmed four NFE QTL on four different cattle chromosomes by linkage mapping and SNP association studies in a Limousin x Jersey cattle population. These four NFE QTL were also validated in Trangie Angus NFE selection line cattle by microsatellite linkage mapping and a 10K

ParAllele whole genome scan. Within the 4 NFE QTL, candidate genes were identified based on homeologous mapping with the human genome and nine potential metabolic pathways have been identified. These included oxidative phosphorylation, beta-oxidation of fatty acids, the AMPK cascade and the glucose sensing metabolic pathways involving JAK2-IRS1-PI3K-mTOR signalling molecules. Among these pathways, the involvment of oxidative phosphorylation was supported based on the mitochondrial proteomics results. The proteomics studies also suggest that high net feed efficient animals are under less metabolic and oxidative stress relative to the low net feed efficient animals. Low levels of the rate-limiting Complex I activity in oxidative phosphorylation and elevated levels of adenylate kinase 1 in the high NFE animals suggests better cellular homeostasis. In other words, the results indicate that the fuel-sensing mechanism reads 'full' in high NFE animals and stops excessive feed intake. The results also suggest that marker selection or other methods leading to less oxidative stress could increase net feed efficiency in cattle.

Liver and adipose tissues are two of the most important peripheral organs that sense the available cellular fuel (such as glucose and lipids). By releasing energy sensors (mainly leptin and insulin), the liver and adipose tissues communicate the peripheral energy status to brain, which regulates feed intake and energy expenditure. The literature and current results strongly supports the hypothesis that peripheral glucose and lipid nutrient sensing pathways (including AMPK, β-fatty acid oxidation, mTOR-PI3K, glycolysis, and hexosamine biosynthesis) play crucial roles in maintaining the balance between nutrient uptake and oxidation, which ultimately affects net feed intake. Several research studies also support the idea of cross-talk between the cytokine-receptor superfamily and the tyrosine kinase receptor family through their common downstream signalling proteins, such as IRS, PI3K, mTOR and AMPK. Therefore, an important question is: how is the impairment of mitochondrial oxidative phosphorylation or oxidative stress reflected in IRS, PI3K, mTOR and AMPK metabolic activities?

Glucose acts as a primary nutrient and plays a significant role in altering the overall activity of the metabolic sensing neurons involved in appetite behaviour, feed intake and energy homeostasis. The glucose sensing neurons (POMC, CART, NPY and AgRP) in the hypothalamus interact with the peripheral energy sensors, such as leptin and insulin. These neurons have a high concentration of glucose-specific metabolic enzymes, including glucokinase and hexokinase. These neurons respond to leptin or insulin based on their respective receptors to initiate glucose-excitatory or glucose-inhibitor pathways through IRS-PI3K-mTOR-AMPK mechanisms. Therefore, mutations identified in PI3K, AMPK, POMC and CART could also have a significant effect on fuel-sensing mechanisms determining net feed efficiency. The results herein suggest that this may well be the case as SNPs in these genes were associated with feed intake regulation and thus NFE.

6.6 Conclusion

The research herein focused on the most likely molecular mechanisms controlling net feed efficiency. Some components of these pathways were identified as likely to be involved in the regulation of feed intake. However, the precise cascade of molecular events within the identified pathways and their interactions has not been explored. Defining the molecular steps in oxidative phosphorylation, AMPK-beta fatty acid oxidation, the growth hormone receptor pathway, glucose and protein turnover, and ROS production that affect net feed efficiency will be an important contribution. More research is also required on the neuro-hormonal regulation of the partitioning of nutrient utilisation among tissues. In the current study, although only a few pathways have been discussed that are likely to be involved in net feed efficiency, redundancy of these pathways was apparent. The physiology and biochemistry of net feed efficiency as a trait is complex, making it difficult to target candidate genes and specific pathways. Also many splice variants of genes have alternative functions, increasing the difficulty of determining whether a specific gene is involved in feed efficiency. Therefore, the ontology of metabolic pathways and their interactions should be always considered in addressing net feed efficiency.

Herein, locations of candidate genes were predicted based on comparative mapping with the human genome due to unavailability of bovine genome sequence. Complete bovine genome annotation will help to validate the current results of fine mapping and to identify more candidate genes and SNPs that may have been missed in the sequence analysis. The use of dense genome-wide SNP chips will not only narrow down the QTL regions and shorten the list of candidate genes, but can be used to develop haplotypes for linkage disequilibrium mapping.

APPENDIX

Appendix I Gastrointestinal peptides regulating feed intake

Gastrointestinal peptides	Contribution in feed intake regulation
Cholecystokinin	Cholecystokinin widely distributed in the gastrointestinal tract, but is concentrated in the duodenum and jejunum (Gibbs et al, 1973). CCK slows gastric emptying and reduces food intake in both animals and humans by terminating the feeding episode. Cholecystokinin has been reported to be a secretagogue of both insulin (Karlsson and Ahrèn 1992) and pancreatic polypeptide (Liddle et al 1990) in nonruminants.Choi et al (2000) studied the effect of a cholecystokinin type A (CCKA) receptor antagonist on feed intake and plasma concentrations of metabolites, insulin, and pancreatic polypeptide in Holstein dairy cattle. Elevated plasma cholecystokinin concentrations depressed feed intake of dairy cattle. There was a negative relationship between concentrations of plasma CCK and insulin and a positive relationship between CCK and pancreatic polypeptide in lactating cows (Choi and Palmquist 1996). In sheep, exogenous CCK decreased plasma insulin levels when infused into cerebrospinal fluid (Della-Fera and Baile 1981). The direct effect of endogenous CCK on plasma insulin concentration is yet to be shown.
Glucagon-like Peptide 1	Glucagon-like peptide (GLP-1) is produced by the post-translational processing of pro-glucagon in the L-cells of the intestinal mucosa (Drucker, 2002). The majority of these L-cells are located in the distal ileum and colon. GLP-1 secretion is regulated by both nutritional signals and neural-hormonal signals, originating from the more proximal areas of the gut. GLP-1 inhibits gastric emptying in humans at concentrations within the physiological range that might be achieved after meal ingestion (Edwards et al 2001). GLP-1 also suppresses appetite and food consumption with peripheral administration in normal and diabetic humans. It is hypothesized that GLP-1 is involved in lowering fasting plasma glucose and delaying gastric emptying, thereby reducing food intake (Edwards et al 2001).
Ghrelin	Ghrelin is a 28 amino acid peptide that was originally identified as an endogenous ligand for the growth hormone secretagogue receptor (Horvath 2001). Ghrelin is produced predominately by the stomach, but also in lesser amounts by the gastrointestinal tract, kidney and hypothalamus. Ghrelin stimulates food intake by binding specific receptors in the hypothalamus and activating the well-characterized arcuate nucleus neurons, which produce neuropeptide Y (NPY) and agouti- related peptide (AGRP) to stimulate feeding (Wren et al 2001). In ruminants, ghrelin levels were found to be associated positively with growth hormone levels (Hashizume et al 2005). Ghrelin has been reported to act on other signalling pathways in the hypothalamus and much work is underway to fully understand the signalling pathways and role of ghrelin in the regulation of food intake (Wren et al 2001).

Gastrointestinal peptides	Contribution in feed intake regulation
Apolipoprotein A-IV	Apolipoprotein A-IV (Apo A-IV) protein is produced by the liver and intestine, and is incorporated into chylomicrons and lipoproteins (Tso et al 2001). Apo A-IV mRNA and protein have recently been found in the rat hypothalamus (Lui et al 2001). The synthesis of apo A-IV is stimulated by fat absorption. In mice experiments, Apo A-IV inhibits food intake by acting on the central nervous system, and its rapid synthesis following lipid absorption suggests a major role in the short-term regulation of food intake. Fasting reduces hypothalamic Apo A-IV and re-feeding with lipid increases its levels.
Enterostatin	Enterostatin is a pentapeptide derived by the tryptic digestion of pancreatic procolipase in the intestinal lumen ((Lui et al 1999). Procolipase synthesis and release is stimulated by a high fat diet. Procolipase is found in stomach, small intestine and pancreatic secretions. Enterostatin inhibits food intake, (in particular, fat intake) when given to rodents as an intraperitoneal injection or directly into the central nervous system. The inhibition of fat intake with peripheral enterostatin administration is dependent on intact vagal afferents (Rossner et al 1995).
Gastrin-Releasing Peptide (GRP)	Gastrin-releasing peptide is one member of a family of peptides, which include neuromedin B, neuromedin C and bombesin. Bombesin was originally isolated from frog skin and is functionally related to gastrin-releasing peptide and the neuromedins (Merali et al 1999). These peptides are produced by the gastric mucosa and bind to three distinct receptors, the gastrin-releasing peptide receptor, the neuromedin B receptor, and the bombesin-3 receptor. Gastrin-releasing peptide and bombesin given peripherally stimulate the release of gastrin, CCK, insulin and other gut peptides (Leibowitz et al 1998). Bombesin and gastrin-releasing peptide inhibit food intake in both rodents and humans through both vagal afferents and direct centrally mediated effects (Bray 2000).

Appendix II Primer extension protocol

Amplification of target DNA

DNA sequence of less than 150 bp amlicon containing the SNP of interest was amplified in a 25µl PCR reaction in a Palm Cycler (Corbett Research) with *AmpliTaq Gold* enzyme (*Perkin Elmer*) and 100 ng DNA, to increase the quantity (for sensitivity) and to reduce the complexity of the target (for specificity). The best results were obtained when the amount of product in each sample was consistent and a large amount of product was produced. If there was too little PCR product, insufficient signal was produced. If multiple bands were produced, the amount of specific target sequence available for primer extension was decreased and non-specific sites may be available to bind the SNP primer. The following PCR conditions were used:

Primers 2.5-25 µM
dNTPs 1.25 mM
Genomic DNA 100 ng
Amplicon Size 80-275 bp
Cycles 35

Three touch-down PCR cycling conditions were used to optimise the PCR conditions as follows: an initial denaturation and enzyme activation step at 95°C for 11 minutes, followed by 35 cycles consisting of 94°C for 1 minute (denaturation), 70°C - 62°C / 60°C - 50°C / 55°C - 45°C for 1 minute (annealing of primer), and 72°C for 1 minute (extension). After a final primer extension step at 72°C for 10 minutes, the reactions are cooled to 4°C until used.

Processing of PCR Product

Primers and dNTPs used in the PCR reaction were removed because they interfered with the *AcycloPrime-FP* reaction. This was accomplished by an enzymatic digestion using the PCR Clean-Up Reagent (10X) and the PCR Clean-Up Dilution Buffer in 96-well skirted black plates (MJ research). To avoid evaporation, aluminium foil was used for sealing. Each analysis uses a single microplate well, with each step performed sequentially by adding the next set of reagents. To avoid sample transfer

steps, the microplate must be compatible with both the thermocycler and the fluorescence polarization reader. The steps involved in PCR clean up reaction are as follows:

a. The PCR Clean-Up Reagent were diluted 10-fold with the PCR Clean-Up Dilution Buffer provided in the kit (Perkin Elmer) to prepare the PCR Clean-Up Reagent, 1X. The dilution step was performed just prior to use. The PCR Clean-Up Reagent is a Exo-SAP-IT™ mixture supplied by USB Corporation which contains a mixture of exonuclease I and shrimp alkaline phosphatase in buffer with glycerol.

b. 2 µL PCR Clean-Up Reagent (1X) was added to each 5 µL amplification reaction. The samples were incubated at 37°C for 60 minutes and then 80°C for 15 minutes to inactivate the enzymes in the PCR Clean-Up Reagent.

After processing PCR product, the following AcycloPrime-FP Protocol was used for primer extension reaction:

1. 13 µl of AcycloPrime-FP Mix was added to each well containing 7 µl of amplified and processed target DNA.

2. After an initial denaturation at 95°C for 2 minutes, 25 thermal cycles consisting of: 95°C for 15 seconds and 55°C for 30 seconds were performed.

   The fluorescence polarization was read in *CHAMELEON™ (Hidex)* instrument. Spectral filters were used for following wavelength

For the R100 dye:

Excitation wavelength = 485nM

Emission wavelength = 535nM

For the TAMRA dye:

Excitation wavelength = 545nM

Emission wavelength = 590nM

AcycloPrime-FP Mix

The appropriate amount of *AcycloPrime-FP* Mix was prepared as described in the following table (some excess allowed for losses in liquid transfer):

AcycloPrime-FP Mix

Reagent	µl / single reaction	µl / 96 wells
AcycloPol	0.05	6
10X Reaction buffer	2	240
Acyclo Terminator Mix	1	120
SNP Primer (10uM)	0.5	60
Water	9.45	1134
Total Volume	13	1560

- *AcycloPol* contains a mutant thermostable polymerase in buffer with salts, reducing agent and glycerol.

- Each *AcycloTerminator* Mix contains one R110-labeled *AcycloTerminator*, one TAMRA-labeled *AcycloTerminator* and two unlabeled terminators. A suitable *AcycloTerminator* Mix was chosen based on the SNP to be identified and the orientation of the SNP primer. This is more clear in the following example:

For example, the following sequence for two heterozygous chromosomes containing a G/A SNP (bold) on the forward strand (5'-3'). There is a C/T SNP the reverse strand (3'-5').

5'-ACGGCCTATTGGGTTCACTCGC**A**GACTATTTAACCTGACCATGGGCCT-3'
3'-TGCCGGATAACCCAAGTGAGCG**T**CTGATAAATTGGACTGGTACCCGGA-5'
5'-ACGGCCTATTGGGTTCACTCGC**G**GACTATTTAACCTGACCATGGGCCT-3'
3'-TGCCGGATAACCCAAGTGAGCG**C**CTGATAAATTGGACTGGTACCCGGA-5'

If the SNP primer (forward) has the sequence underlined on the upper strands, the next base added will be an A or a G, so the G/A kit is used. If the SNP primer (reverse) has the sequence underlined on the lower strands, the next base added will be either a C or a T, so the C/T kit is used. Therefore, two different kits are required

to perform the assay with both forward and reverse SNP primers.

- 10X Reaction Buffer contains Tris-HCl containing magesium sulphate ($MgSO_4$) and detergent.

- A SNP primer was a synthetic oligonucleotide complementary to the sequence adjacent to the SNP site. The next base added to the primer was, therefore, complementary to the base at the SNP location on the target DNA strand. Primers were checked to ensure a melting temperature (Tm) in the range of 60-80°C. It was helpful to select sequences that minimized secondary structure (*e.g.*, hairpin loops) and had less than a 50% G+C content. The length was short (usually 17-25 bases). The SNP primers were dissolved at 100 µM in TE Buffer (10 mM Tris-HCl, pH 7.6 containing 0.1 mM EDTA). Before use in the AcycloPrime-FP reaction, 100 µM SNP primers were diluted to 10 µM with water.

Allele assignment

Based on the set florescence polarisation (FP) threshold value for the known allele which acted as an control, the allele assignment were based on comparing the sample FP value against the control allele value. The data were also rechecked based on the inheritance pattern to remove any allele calling mistakes. The florescence polarisation value was calculated in the instrument MicroWin 2000 Hidex software by following formula:

$$mP = 1000 \times [Ivv - Ivh]/[Ivv + Ivh]$$

where mp is a millipolarization units for florescence polarisation, Ivv is the emission intensity measured when the excitation and emission polarizers were parallel and Ivh is the emission intensity measured when the emission and excitation polarizers were oriented perpendicular to each other. Allele scoring was based on incorporation of the R-110 and TAMARA fluorescent dyes. A graphic plot of the polarization of R110 versus the polarization of TAMRA gave four data clusters representing the two homozygotes, the heterozygotes and the negative controls based on their mP fluorescent values (Figure 2.1).

Note: Before reading the plates, the G-factor calibration for each fluorescence dye (R-110 and TAMARA) was conducted receiving a new batch. These values were used in the MicroWin 2000 Hidex software before reading sample plates to reduce errors in allele assignments. With the G-factor set to 1.0, the S and P intensities (polarising direction, Figure 2.2) were read for a 20 µl solution containing 1 µl of any Terminator Mix and 2 µl of 10X Reaction Buffer. It was useful to average the results for several wells to get an accurate measurement and to reduce background noise. The following equation was then used to calculate the G-factor that gives a value of 50 mP for the unincorporated terminators:

G = [(950*S) / (1050*P)].

After adding the new G factor into the software, mP values were read again and should be near 50 mP. This was done twice, once for R110 and once for TAMRA.

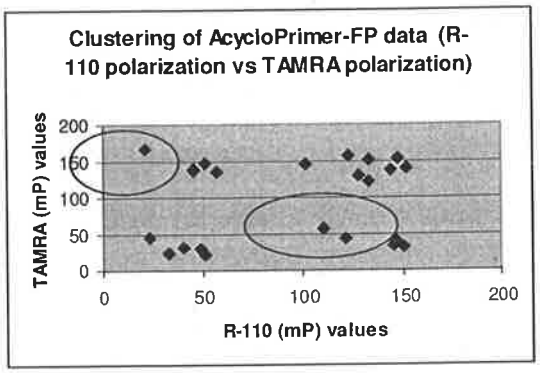

Figure 2.1 Genotyping based on R-110 *vs.* TAMRA polarization mP values

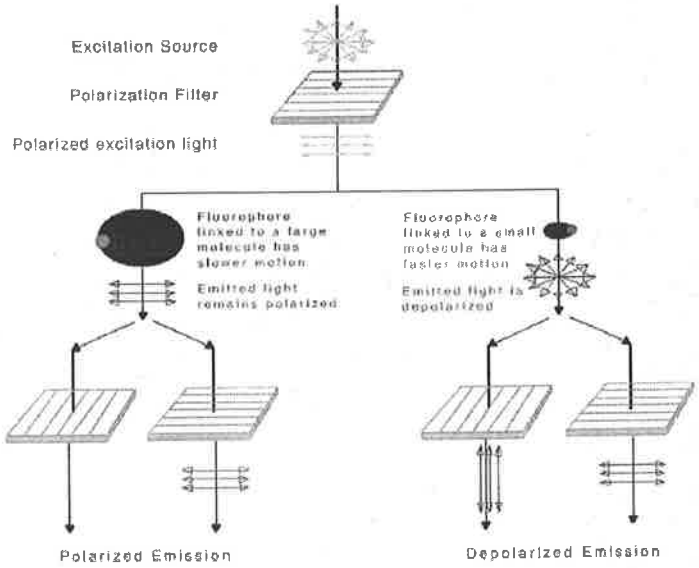

Figure 2.2 Fluorescence polarization showing polarizing directions (vertical and horizontal) (Figure adopted from Perkin Elmer's Acycloprime-FP SNP detection handbook)

The clustering of AcycloPrime-FP data values in mP were obtained by plotting the R110 polarization versus the TAMRA polarization. The homozygous TAMRA genotypes appear as the cluster in the upper left of the graph. Similarly, the homozygous R110 genotypes were represented by the cluster in the lower right. Heterozygotes appeared in the upper right cluster. Negative controls and failed PCR reactions were in the lower left cluster.

Appendix III Chemicals and solutions

1.1 TAE buffer (50X)

TRIZMA: 242 gm

EDTA (disodium salt): 18.62 gm

Glacial acetic acid: 57.1 ml

Milli Q water: upto 1 litre

Adjust pH to 8.0

1.2 Lysis buffer (for liver)

TRIS-HCl, 20 mM *(Sigma)* (pH 7.4)

1% Triton X-100 *(Sigma)*

NaCl, 50 mM

Sucrose, 250 mM *(Sigma)*

Sodium fluoride, 50 mM *(Sigma)*

Sodium pyrophosphate, 5 mM *(Sigma)*

Dithiothreitol (DTT), 2 mM *(Sigma)*

Leupeptin, 4 mg /L *(Sigma)*

Trypsin inhibitor, 50 mg/L *(Sigma)*

Benzamide, 2 µM *(Sigma)*

Phenyl methyl sulfonyl fluoride (PMSF), 0.5 mM/L *(Sigma)*

1.3 Isolation buffer (PH 7) (for liver)

d-mannitol, 220 mM *(Sigma)*

Sucrose, 70mM *(Sigma)*

HEPES, 2mM *(Sigma)*

1.4 MEDIUM I (for muscle)

TRIS-HCl, 20 mM (pH 7.4) *(Sigma)*

1% Triton X-100 *(Sigma)*

NaCl, 50 mM *(Sigma)*

Sucrose, 250 mM *(Sigma)*

Sodium fluoride, 50 mM *(Sigma)*

Sodium pyrophosphate, 5 mM *(Sigma)*

Dithiothreitol (DTT), 2 mM *(Sigma)*

Leupeptin, 4 mg /L *(Sigma)*

Trypsin inhibitor, 50 mg/L *(Sigma)*

Benzamide, 2 µM *(Sigma)*

Phenyl methyl sulfonyl fluoride (PMSF), 0.5 mM/L *(Sigma)*

1.5 MEDIUM II (for muscle)

KCl, 46 mM
EDTA, 10 mM *(Sigma)*
Tris HCl 100 mM *(Sigma)*
Sucrose, 100 mM (*Sigma)*
Nagarse, 20 mg% *(Sigma)*
pH 7.4

1.6 MEDIUM III (for muscle)

Sucrose, 220 mM *(Sigma)*
Mannitol, 70 mM *(Sigma)*
Tris HCl, 10 mM *(Sigma)*
EDTA, 1 mM *(Sigma)*
pH 7.4

1.7 ISOLATION BUFFER (for muscle)

d-mannitol, 230 mM *(Sigma)*

Sucrose, 70mM *(Sigma)*

TRIS-HCL, 20mM *(Sigma)*

Potassium phosphate monobasic (KH_2PO_4), 5mM *(Sigma)*

pH 7.4

1.8 Reduced cytochrome C, 15 µM

123.5 mg cytochrome *c* (Sigma) was dissolved in 1 ml of 50 mM of potassium phosphate, pH 7. Absorbance was checked on a spectrophotometer at 550 nm and 565 nm.Then sodium dithionite (7.5 mg/ml) was added to reduce the cytochorme c

and the mixture was incubated in the dark on ice for 5 min. The mixture was purified on a 10 K MWCO spin filter (Amicon Ultra-4, Millipore). Absorbance was checked again at 550 nm and 565 nm to ensure the 550 nm / 565 nm ratio was greater than 6. 100 µl aliquots were dispensed and tube was closed under a gentle stream of nitrogen gas to displace the oxygen from the tube. This helps to minimize oxidation of the cytochrome during storage. The reduced cytochrome c was stored at -70^0C.

1.9 DTT- SDS equilibration buffer

	Final conc.	Amount
Tris Chloride (1.5 M, pH 8.8)	50mM	6.7 ml
Urea (MW60.06)	6 M	72.07 g
Glycerol (87% [v/v], MW 92.09)	30% (v/v)	69 ml
SDS (MW 288.38)	2% (w/v)	4.0 g
Bromophenol blue (0.002%)	trace	a few grains
Dithiotreiotol (100 mg/ml)		200 mg
Distilled or deionized water		to 200 ml

Store at $-20\ ^0$C. This is a stock solution. Add DTT or iodoacetamide before using.

1.10 Sodium dodecyl sulphate-polyacrylamide (SDS-PAGE) 12.5%T gels (Homogeneous gel solutions 900 ml)

Final % T	Volume required for (ml) 12.5%
Acrylamide stock	375
1.5 M Tris Cl, pH 8.8	225
Water	281
10% sodium dodecyl sulphate (SDS)	9
10% ammonium persulfate (APS)	9
10% N,N,N',N'-tetramethylethanediamine TEMED)	1.24

1.11 Sealing solution

	Amount
Sodium dodecyl sulphate (SDS) electrophoresis buffer (see 1.12.1)	25 ml
Agarose	125 mg
Bromophenol blue	a few grains

Combine all ingredients in 250 ml Erlenmeyer flask. Swirl to disperse. On a low setting, heat in microwave oven until agarose is completely melted, about 1 min. Do not allow solution to boil over. Allow agarose to cool slightly before using. Do not adjust pH.

1.12 1 x SDS Electrophoresis buffer

	Final conc.	Amount
Tris (MW 121.14)	0.25mM	60.5 G
Glycine (MW 75.07)	192mM	288.0 g
Sodium dodecyl sulphate SDS (MW 288.38)	0.1% (w/v)	20.0g
Distilled or deionized water		to 20 L

Do not adjust pH of this solution and stored at room temperature
(Please not all samples were purchased from Sigma-Aldrich Chemicals Ltd.)

Appendix 3.1 Comparative map locations of QTL markers (from USDA (www.animalgenome.org/cattle/maps) and Ensembl (www.ensemble.oeg/index.html) as accessed from 12/05-12/06)

QTL	Marker	cM	Bovine Mb	rads	Rad marker	rads	Flanking genes	HSA	Ensembl position
BTA1									
Flanking marker 1	CSSM032	98	69268709 – 69268938	970	DIK2774	1003.8	IL12A	3q25.33	161,189,331
	(BM864)						SI	3q26.1	166,179,389
Peak marker	BM1824	125	87234102 - 87234283	1195	TC206864	1204.3	FOXL2	3q22.3	140,147,132
							COPB2	3q23	140,559,133
Flanking marker 2	BMS2263	150	98996130 - 98996281	1340	TC210974	1352.41	ITGB5	3q21.2	125,964,486
							PIK3R4	3q21.3	131,880,476
BTA8									
Flanking marker 1	BMS1341	55	23805508 - 23805629	293	TC192660	328.56	GCNT1	9q21.13	76,303,700
							BICD2	9q22.31	96,553,200
Peak marker	LPL	78	35866343- 35892358	515	LPL	379.11	LPL	8p21.3	19,841,058
	BM711	97	48094361 - 48094523		ADRA1A	446.97	ADRA1A	8p21.2	26,661,953
					TC218895	516.77	ALDOB	9q31.1	101,263,214
							ZNF189	9q31.3	101,240,718
Flanking marker 2	BMS836	125	60937432 - 60937529	567	TC191867	576.06	ATP6V1G1	9q33.2	114,429,580
							C5	9q32	120,794,170

7009

Appendix 3.1 Comparative map locations of QTL markers (from USDA (www.animalgenome.org/cattle/maps) and Ensembl (www.ensemble.oeg/index.html) as accessed from 12/05-12/06) (continuation)

QTL	Marker	cM	Bovine Mb	rads	Rad marker	rads	Flanking genes	HSA	Ensembl position
BTA11									
Flanking marker 1	RM096 (CA096)	40	23417726 – 23417833	315	MCFD2	320.45	MCFD2	2p21	47,040,688
							CALM2	2p21	47,298,956
Peak marker	BMS1048	82	57535964 – 57536092	718	DIK4390	718.86	PUM2	2p24.1	20,370,083
							POMC	2p23.3	25,295,439
Flanking marker 2	RM363 (BM3501)	97	66543862 – 66544050	NA (919)	TXNCD7	914.09	ODC1	2p25.1	10,531,106
							MYCN	2p24.3	16,031,284
BTA20									
Flanking marker 1	TGLA126 (ILSTS068)	32	12158768 – 12158920	288	TC191486	283.87	ITGA2	5q11.2	52,321,041
							HTR1A	5q12.3	63,292,034
Peak marker	BMS703	60	29876187 - 29876343	515	DIK5178	453.44	NPR3	5p13.2	32,747,422
							PRLR	5p13.3	35,084,621
Flanking marker 2	BM5004	72	35301025 - 35301167	686	TC187581	688.51	CDH6	5p13.3 5p15.2	31,229,553
							CCT5		10,303,401

Appendix 3.2 Marker-wise F-values. Values for sire 361, 368, 398 families and all three families (across) used in NFE QTL mapping

BTA	Marker	Position cM#	F-ratio (across)	F-ratio (361)	F-ratio (368)	F-ratio (398)
1	BMS2321	0	0.52	0.71	0.08	0.47
1	BMS711	7.3	0.2	0.03	0.08	0.35
1	POUF1 *	19.4	0.99	0.39	0.11	1.45
1	BMS4017	20.8	1.39	0.85	0.37	1.79
1	UMPS *	38.3	0.79	1.58	0	0.37
1	SST *	50	0.98	1.59	1.12	0.25
1	AHSG *	50.8	1.28	1.44	0.47	1.67
1	INRA49	53.5	0.98	1.59	1.12	0.25
1	SLC2A2 *	61	0.6	0.44	0.66	0.2
1	IL12A *	67.4	0.88	0.12	0.42	1.63
1	CSSM032	74.2	1.5	0	0.13	4.23
1	AGTR1 *	74.3	2.54	0.05	0.03	7.21
1	BMS1789	86.9	2.77	0.06	0.01	8.68
1	BM1824	94.6	3.35	0	0.18	11.68
1	BMS599	111.8	2.25	0.01	0.61	5.75
1	BMS2263	121.1	1.43	0.06	0.23	3.63
8	RM321	0	0.93	0.09	3.79	0.04
8	CTSB *	1	0.74	0.49	2.69	0.1
8	RM372	3.3	0.87	0.05	3.61	0.01
8	PNOC *	5	1.89	0.07	6.61	0.79
8	TEK *	10.3	0.76	0.09	2.35	0.11
8	BMS1591	12.3	0.87	0.08	3.61	0.39
8	BM4006	31.3	1.09	0.14	2.1	0.64
8	LPL *	35	1	0.01	1.31	1.12
8	TGLA13	35.6	1.1	0.14	1.91	0.76
8	BMS1341	35.6	1.1	0.14	1.91	0.76
8	BMS2072	43	0.82	0.11	0.92	0.84
8	BM711	67.8	2.79	0.31	0.09	5.03
8	CSSM147	94.7	1.02	0.39	0.09	2.24
8	BMS836	98.4	0.71	0.64	0.09	1.22
11	BM827	0	1.07	0.91	0.5	1.51
11	BMS2131	9.5	1.14	1.19	0.5	1.51
11	BMS2325	11.7	1.07	1.04	0.5	1.48
11	FSHR *	24	1.07	1.04	0.5	1.48
11	BM304	24.4	1.42	3.29	0.5	0.52
11	IL1B *	31	3.31	7.58	3.15	0.37
11	RM096	31.3	1.46	3.65	0.94	0.03
11	INRA111	43	3.49	9.13	1.78	0.44
11	BMS1716	47.7	3.58	9.25	1.82	0.48

Appendix 3.2 Marker-wise F-values. Values for sire 361, 368, 398 families and all three families (across) used in NFE QTL mapping (continuation)

BTA	Marker	Position cM#	F-ratio (across)	F-ratio (361)	F-ratio (368)	F-ratio (398)
11	POMC *	53	4.1	11.72	0.38	0.61
11	BMS1822	61.2	3.52	10.42	0.36	0.26
11	RM150	65.5	3.57	9.36	0.73	0.76
11	BMS1048	75.8	3.94	11.78	0.02	0.5
11	ASS *	81	2.07	6.07	0.01	0
11	BMS989	85.5	2.33	8.02	0	0.05
11	RM363	90.9	1.77	5.85	0.01	0
11	BMS2315	103.3	1.41	4.16	0.01	0.01
11	HEL13	114.5	2.06	6.07	0.01	0
20	RM106	0	0.09	0.35	0.27	0.3
20	BM1225	5.3	0.06	0.35	0.09	0.3
20	MAP1B *	6.3	0.24	3.04	0	0.3
20	FST *	13	0.73	3.1	0.23	0.84
20	ITGA2 *	14.4	1.35	4.29	1.21	1.78
20	TGLA304	17.3	0.15	2.35	0.37	0.14
20	GHR *	18	3.22	5.53	2.99	4.86
20	PIK3R1 *	19.9	0.35	3.08	0.18	0.45
20	PRKAA1*	19.9	2.38	4.99	2.57	3.45
20	PRLR*	27.9	3.89	5.56	3.59	5.98
20	TGLA126	28.5	0.61	2.8	0.06	0.67
20	BM4107	49.7	4.24	4.52	3.93	6.55
20	BMS1120	51.1	4.39	4.59	4	6.65
20	BMS703	52.2	4.43	4.64	3.67	6.67
20	BMS5004	61.6	2.78	3.75	3.42	2.72
20	BM521	72.3	2.98	3.75	5.56	1.78

*denotes SNP markers selected for fine mapping
cM positions accessed in bovine ArkDB; http://texas.thearkdb.org/browser?species=cow
(Table provided by Scott Foster, Biometrics SA, Waite Campus, University of Adelaide).

Appendix 3.3 Size of effect (kg feed / day) of markers on NFE

BTA	Marker	Across Family Analysis			Within Family Analysis		
		361	368	398	361	368	398
1	BMS2321	-0.2	0.047	-0.289	-0.204	0.038	-0.263
1	BMS711	-0.063	0.04	-0.219	-0.068	0.032	-0.216
1	POUF1*	0.134	0.007	-0.529	0.129	0.018	-0.494
1	BMS4017	0.222	-0.051	-0.548	0.213	-0.048	-0.509
1	UMPS*	0.422	0.133	-0.209	0.371	0.112	-0.249
1	AHSG*	0.357	0.31	-0.474	0.302	0.29	-0.572
1	INRA49	0.36	0.38	-0.05	0.315	0.367	-0.239
1	SST*	0.36	0.38	-0.05	0.315	0.367	-0.239
1	SLC2A2*	0.168	0.381	0.25	0.127	0.361	0.135
1	IL12A*	0.058	0.338	0.545	0.026	0.315	0.517
1	CSSM032	-0.09	0.251	0.658	-0.102	0.224	0.729
1	AGTR1*	-0.137	0.182	0.798	-0.158	0.135	0.887
1	BMS1789	-0.141	0.138	0.899	-0.163	0.089	0.985
1	BM1824	-0.033	-0.045	1.104	-0.09	-0.085	1.171
1	BMS599	-0.069	-0.187	0.848	-0.103	-0.212	0.873
1	BMS2263	0.077	0.093	0.617	0.03	0.097	0.679
8	PNOC*	-0.009	0.643	0.446	0.036	0.645	0.354
8	CTSB*	0.123	0.409	0.149	0.178	0.389	0.101
8	RM321	0.011	0.464	0.142	0.042	0.434	0.071
8	RM372	-0.007	0.472	0.12	0.019	0.442	0.026
8	BMS1591	0.023	0.382	0.32	0.033	0.357	0.233
8	TEK*	0.034	0.447	0.229	0.037	0.419	0.129
8	BM4006	0.05	0.385	0.44	0.082	0.363	0.335
8	TGLA13	0.048	0.359	0.438	0.086	0.341	0.345
8	BMS1341	0.048	0.359	0.438	0.086	0.341	0.345
8	BMS2072	0.032	0.241	0.428	0.07	0.236	0.352
8	LPL*	-0.034	0.301	0.464	0.003	0.29	0.413
8	BM711	-0.18	-0.039	0.841	-0.164	-0.05	0.804
8	CSSM047	0.2	-0.053	0.57	0.235	-0.069	0.572
8	BMS836	0.262	-0.057	0.4	0.281	-0.075	0.413
11	BM827	0.394	-0.22	0.522	0.383	-0.201	0.557
11	BMS2131	0.428	-0.188	0.445	0.426	-0.171	0.475
11	BMS2325	0.35	-0.177	0.438	0.351	-0.161	0.468
11	FSHR*	0.35	-0.177	0.438	0.351	-0.161	0.468
11	BM304	0.511	-0.139	0.229	0.501	-0.127	0.263
11	RM096	0.557	-0.17	0.03	0.543	-0.163	0.06
11	INRA111	0.847	-0.168	0.228	0.837	-0.175	0.241
11	BMS1716	0.833	-0.164	0.253	0.823	-0.172	0.252
11	IL1B*	0.835	-0.495	0.25	0.833	-0.487	0.233
11	BMS1822	0.959	-0.322	0.212	0.96	-0.294	0.187
11	RM150	0.966	0.052	0.358	0.965	0.079	0.321
11	POMC*	1.219	0.035	0.359	1.232	0.039	0.296

Appendix 3.3 Size of effect (kg feed / day) of markers on NFE (continuation)

BTA	Marker	Across Family Analysis			Within Family Analysis		
		361	368	398	361	368	398
11	BMS1048	1.232	-0.074	0.324	1.253	-0.064	0.257
11	BMS989	0.864	-0.122	0.03	0.899	-0.111	-0.078
11	RM363	0.728	-0.084	0.125	0.758	-0.075	-0.011
11	BMS2315	0.571	-0.068	0.184	0.578	-0.071	0.033
11	ASS*	0.715	-0.074	0.149	0.703	-0.077	0.023
11	HEL13	0.729	-0.075	0.136	0.717	-0.079	0.02
20	RM106	-0.255	0.054	-0.144	-0.295	0.051	-0.219
20	BM1225	-0.231	-0.013	-0.131	-0.267	-0.006	-0.198
20	TGLA304	-0.423	0.135	-0.03	-0.458	0.156	-0.046
20	MAP1B*	-0.438	0.011	-0.088	-0.47	0.054	-0.08
20	PI3KR1*	-0.484	-0.136	-0.148	-0.518	-0.084	-0.113
20	TGLA126	-0.469	0.478	-0.22	-0.493	0.458	-0.148
20	FST*	-0.529	0.398	-0.284	-0.552	0.366	-0.171
20	ITGA2*	-0.515	0.452	-0.082	-0.532	0.41	0.096
20	PRKAA1*	-0.694	0.542	0.437	-0.742	0.498	0.533
20	GHR*	-0.654	0.53	0.225	-0.706	0.492	0.303
20	PRLR*	-0.773	0.442	0.857	-0.857	0.411	0.944
20	BM4107	-0.623	0.464	0.919	-0.699	0.433	0.95
20	BMS703	-0.648	0.435	0.991	-0.731	0.406	1.021
20	BM5004	-0.571	0.303	0.604	-0.65	0.3	0.605
20	BMS521	-0.686	0.444	0.568	-0.778	0.434	0.516

*denotes SNP markers selected for fine mapping. Signs under effect were showing effect of Limousin allele on feed intake relative to Jersey allele. Therefore, size of effect sign are not relevant but magnitude should be consider. (Table provided by Scott Foster, Biometrics SA, Waite Campus, University of Adelaide).

Appendix 3.4 SNP association analysis with net feed intake (NFE) and other traits

(Note that model was fitted as genotype, not additive effect. Values are % phenotypic variance accounted for. 0 value = converge to boundary) EMA: eye muscle area, IMF: intra-muscular fat; HSCW: hot carcass weight

Gene Name	BTA	SNP name	NFE	EMA	IMF	HSCW
Angiotensin receptor 1	1	AGTR1#1	0	0	0	0
		AGTR1#2	0	0	0	0
Alpha-HS-glycoprotein	1	AHSG#1	0	0	0	0
		AHSG#2	0	0	0	0
5'-AMP-activated protein kinase, catalytic alpha-1 chain	20	PRKAA1	2.92	0.82	0	0
		PRKAA2	0	0	0	0
Argininosuccinate synthase	11	ASS1	0	0	0	0
		ASS2	0	0.66	0	0
ATPase, H+ transporting, lysosomal 31kDa, V1 subunit E isoform 2	11	ATP6V1E2#1	0.05	0	0	0
Cocaine- and amphetamine-regulated transcript protein precursor	20	CARTPT1	0.70	0	0	0
Cathepsin B	8	CSTB#1	0	0	0	0
		CSTB#2	0	0	0	0
Elongation protein 3 homolog	8	ELP3#2	0	0	0	0
		ELP3#3	1.59	0	0	0
Fructose-1,6-bisphosphatase isozyme 2	8	FBP2#1	0.48	0	0.22	0
Follistatin precursor	20	FST1	0	0	0.17	0
		FST2	2.57	0.69	0	0
Follicle stimulating hormone receptor	11	FSHR1	0.24	0	0	0
		FSHR2	0	0	1.03	0
Follistatin-related protein 1 precursor	1	FSTL1#2	0	0	0.17	0
Growth hormone receptor	20	GHR1	0.51	1.47	0	0.66
		GHR3	0	1.00	0	0
		GHR2	0.99	0	0	0
		GHR4	0	0	0	0
Glucose transporter 2	1	SLC2A2#1	0	0	0	0
		SLC2A2#2	0	0	0.55	0
Glucose transporter 2	1	SLC2A2#3	0	0	0.52	0
Glycogenin-1	1	GYG1#1	0	0.24	0.69	0
		GYG1#2	0	0	0	0
Trifunctional enzyme alpha subunit, mitochondrial precursor (TP-alpha) (78 kDa gastrin-binding protein)	11	HADHA#1	2.47	0	0	0.18
Integrin alpha 2	20	ITGA2#1	1.17	0	0	0

Appendix 3.4 SNP association analysis with net feed intake (NFE) and other traits (continuation)

Interleukin 1beta	11	IL1B#1	0	0	0	0
Interleukin 1beta	11	IL1B#3	0	0.21	0	0
Interleukin 1beta	11	IL1B#2	0	0	0.18	0.38
Interleukin 12 A	1	IL12#1	0	0	0	0
Lipoprotein lipase	8	LPL1	0	0	0	0
		LPL3	0	0	0	0
		LPL2	0	0	0.18	0.3
Microtubule-associated protein -1B	20	MAP1B1	0	0	0.26	2.2
Mitogen-activated protein kinase kinase kinase 1	20	MAP3K1#2	0	0	0	0
NADH-ubiquinone oxido-reductase SGDH subunit, mitochondrial precursor (complex I-SGDH) 1 beta subcomplex, 5, 16kDa	1	NDUFB5#1	0	0	0	0
		NDUFB5#2	0	0.49	1.22	0.51
Neurofilament M subunit	8	NEFM1	0	0	0	0
Nociceptin	8	PNOC1	0	0.16	0	0
Phosphatidylinositol 3-kinase P-85 - alpha subunit	20	PI3KR1#2	2.81	0.76	0	0
		PI3KR1#1	0	0	0	0
		PI3KR1#3	1.22	0	0.07	0
Protein Kinase C iota	1	PKCI#2	0	0.39	0	0
		PKCI#1	0	0	0.95	3.49
		PKCI#3	0	0	0	0
Prolactin receptor precursor	20	PRLR1	0	0	0	0
		PRLR2	0	0	0	0
Proopiomelanocortin	11	POMC1	1.41	0	0	0
		POMC2	1.87	0	0	1.57
Growth hormone factor 1 / Pituitary-specific positive transcription factor 1(Pit-1) (GHF-1).	1	POU1F1#1	0	0	0	0
		POU1F1#2	0	0	0	0
Ribonucleoside-diphosphate reductase M2 chain	11	RRM1#1	0.37	0	0	0
Sucrase-isomaltase, intestinal	1	SI1	0	0	1.38	0
		SI3	0	0	0.68	0
		SI4	0	0	0	0
Somatostatin precursor	1	SST1	0	0	0.01	1.88
Tyrosine kinase, endothelial	8	TEK1	0	0	25.8	0
		TEK3	0	0	0.27	0
		TEK2	0.15	0	0	0

Appendix 3.4 SNP association analysis with net feed intake (NFE) and other traits (continuation)

Uridine monophosphate synthetase	1	UMPS1	1.11	0.13	0	0
		UMPS3	0	0	0	0
		UMPS2	0	0	0	0
		UMPS4	0	0	0	0
ParAllele SNP	1	PA1212	1.2	16.69	0	0
ParAllele SNP	1	PA3166	0.9	0.27	0	0
ParAllele SNP	2	PA4499	1.9	11.76	8.02	0
ParAllele SNP	2	PA7828	0	0.53	3.32	0
ParAllele SNP	3	PA4325	0	0	0	0.09
ParAllele SNP	4	PA2405	0.45	0.53	0	0
ParAllele SNP	4	PA2697	0.07	0	0	0
ParAllele SNP	5	PA5269	0	0	0	0
ParAllele SNP	5	PA5485	0	0	3.28	0
ParAllele SNP	5	PA5954	0	0	0	0.59
ParAllele SNP	5	PA6548	0	0	0	3.23
ParAllele SNP	5	PA766	0	0.45	0	0
ParAllele SNP	6	PA1671	0	1.86	0	0
ParAllele SNP	6	PA311	0	0	0	0.24
ParAllele SNP	6	PA4593	3.82	0.07	1.1	0
ParAllele SNP	7	PA2666	0	0	2.36	0
ParAllele SNP	8	PA4603	0	0	0.14	0
ParAllele SNP	8	PA5747	0	0	0	3.72
ParAllele SNP	8	PA5991	0.11	0.91	0	0
ParAllele SNP	8	PA684	0	0	0.12	0
ParAllele SNP	9	PA1351	0	0	0	2.06
ParAllele SNP	9	PA1767	0	1.44	0	0
ParAllele SNP	9	PA6191	0	0.81	0.4	0
ParAllele SNP	9	PA7007	0	0.09	0	0
ParAllele SNP	9	PA8867	2.16	0.01	0	0
ParAllele SNP	11	PA1588	0	0	0	0.88
ParAllele SNP	11	PA3607	1.49	0.4	0	0.36
ParAllele SNP	11	PA5156	1.33	0	0	0
ParAllele SNP	11	PA8620	0	1.9	0	0
ParAllele SNP	12	PA3894	0	0	0.71	0
ParAllele SNP	12	PA4904	0	0	0.79	0
ParAllele SNP	12	PA6951	0	0	0.17	0
ParAllele SNP	14	PA7655	0	0.28	0	0
ParAllele SNP	14	PA8317	0	0.84	0.45	5.41
ParAllele SNP	15	PA5890	0	0	0.44	0
ParAllele SNP	17	PA1160	0	0	1.09	6.62
ParAllele SNP	17	PA4433	0	0.5	0	5.67
ParAllele SNP	17	PA7600	0	0.43	0	1.3
ParAllele SNP	18	PA4483	0	0.8	0.29	0
ParAllele SNP	18	PA7018	0	0.02	0	1.16

Appendix 3.4 SNP association analysis with net feed intake (NFE) and other traits (continuation)

ParAllele SNP	18	PA7090	0	0.05	0	0
ParAllele SNP	20	PA6205	0	0	0.38	0.93
ParAllele SNP	23	PA1683	0.42	0	1.48	0
ParAllele SNP	27	PA4831	0	0.64	0	0
ParAllele SNP	28	PA2641	0	0	0	0.28
ParAllele SNP	28	PA3987	0	0	1.9	0
ParAllele SNP	28	PA4611	1.44	0	0.08	0
ParAllele SNP	X	PA9171	0.7	0	0	0
ParAllele SNP	NA	PA2174	0	0	0.05	0
ParAllele SNP	NA	PA2250	0	0	3.79	0
ParAllele SNP	NA	PA2487	0	0	0	0.72
ParAllele SNP	NA	PA2661	0	0	0.38	0
ParAllele SNP	NA	PA4068	0	0	0.02	0.82
ParAllele SNP	NA	PA4646	0	0	0	0.8
ParAllele SNP	NA	PA466	0	1.46	0	0
ParAllele SNP	NA	PA5667	1.32	0	0	0
ParAllele SNP	NA	PA5718	0	1.11	0	0
ParAllele SNP	NA	PA6348	0	0.08	0.26	0
ParAllele SNP	NA	PA6581	1.7	1.45	0	0.11
ParAllele SNP	NA	PA7127	0	0	9.15	0
ParAllele SNP	NA	PA7172	7.07	1.12	1.38	0.6

Appendix 3.5 SNPs in candidate genes

NAME OF THE GENE	HGNC SYMBOL	BTA	SNP	LOCATION
Growth hormone factor 1 / Pituitary-specific positive transcription factor 1(Pit-1) (GHF-1)	POU1F1	1	5	Intron
5-Hydroxytryptamine 1F receptor	HTR1F	1	2	Exon
Follistatin-related protein 1 precursor	FSTL1	1	3	2 intron, 1 exon
Sortin nexin 4	SNX4	1	5	Intron
Uridine monophosphate synthetase	UMPS	1	4	2 intron, 2 3' region
Somatostatin precursor	SST	1	1	Splicing
Peroxisomal bifunctional enzyme	EHHADH	1	5	2 exon, 3 intron
Alpha-HS-glycoprotein	AHSG	1	4	1 functional, 1 silent, 2 intron
Eukaryotic translation initiation factor 4 gamma 1	EIF4G1	1	1	Intron
5-Hydroxytryptamine receptor 3 subunit c	HTR3C	1	2	Exon
Glucose transporter 2	SLC2A2	1	6	Intron
Protein Kinase C iota	PRKCI	1	8	Intron
NADH-ubiquinone oxido-reductase SGDH subunit, mitochondrial precursor* (complex I-SGDH) 75 kDa	NDUFB5	1	6	Intron
Interleukin 12 A	IL12	1	1	Silent exon
Sucrase-isomaltase, intestinal	SI	1	4	1 exon, 3 intron
Angiotensin receptor 1	AGTR1	1	2	Exon
Glycogenin-1	GYG1	1	5	Intron
Neprilysin (Neutral endopeptidase) (NEP) (Enkephalinase) (Neutral endopeptidase	MME	1	2	3' region
G Protein -coupled receptor kinase GRK7	GPCRK	1	1	3' region
Epidermal Growth factor	EGF	6	7	Intron
Bone Sialoprotein	SIAL	6	2	Intron
Microsomal triglyceride transfer protein	MTP	6	1	Intron
Osteopontin-k	SPP1	6	1	Exon
Alpha –s1-casein	CSN 1	6	8	7 exons and 1 intron
Cathepsin B	CTSB	8	5	3' UTR and 2 introns
Nociceptin	PNOC	8	3	3 exons
Tyrosine kinase, endothelial	TEK	8	4	Introns
Lipoprotein Lipase	LPL	8	6	1 functional and 5 exons
Neurofilament M subunit	NEFM	8	2	2 3' UTR

Elongation protein 3 homolog	ELP3	8	3	1 exon, 1 UTR and 1 intron
Fructose-1,6-bisphosphatase isozyme 2	FBP2	8	1	Exon
SHC transforming protein 3 (SH2 domain protein C3)	SHC3	8	2	1 exon and 1 intron
Clusterin	CLU	8	5	5 introns
ATPase, H+ transporting, lysosomal 31kDa, V1 subunit E isoform 2	ATP6V1E2	11	1	Intron
Follicle stimulating hormone receptor	FSHR	11	5	2 exons, 3 introns
Interleukin 1beta	IL1B	11	10	1 exon and 9 introns
Proopiomelanocortin	POMC	11	10	6 introns, 1 exon (silent) and 3 5' UTR
Trifunctional enzyme alpha subunit, mitochondrial precursor(TP-alpha) (78 kDa gastrin-binding protein)	HADHA	11	2	2 3' region
Ribonucleoside-diphosphate reductase M2 chain	RRM1	11	6	4 3' region and 2 intron
NADH-ubiquinone oxidoreductase 19 kDa subunit	NDUFA8	11	1	Exon 3 (Tyr-Ser)
Argininosuccinate synthase	ASS	11	2	Intron
Presenilin 2	PSN2	16	9	Intron
Myogenin	MYOG	16	3	Intron
Interleukin 10	IL10	16	2	Intron
Fibromodulin	FMOD	16	2	Exon
Glutamine synthetase	GLUP	16	2	3' region
6-Phosphofructo-2-kinase	PFKFB2	16	6	Intron
C4BP beta chain	C4BPB	16	4	Intron
P selectin	SELP	16	9	Intron
Complement factor H 1	CFH	16	15	Intron
ATPase, Ca++ transporting, plasma membrane 4	ATP2B4	16	6	1 3' UTRand 5 3' region
Microtubule-associated protein -1B	MAP1B	20	1	Exon (silent)
Mitogen-activated protein kinase kinase kinase 1	MAP3K1	20	2	3' region
Follistatin precursor	FST	20	9	1 exon (functional) and 8 introns
Integrin alpha 2	ITGA2	20	42	1 exon and 41 introns
Growth hormone receptor	GHR	20	19	7 exons , 2 3' regions, 1 promoter and 9 introns
5'-AMP-activated protein kinase, catalytic alpha-1 chain	PRKAA1	20	8	1 exon, 1 intron, 1 promoter, 2 5' UTR and 3 3' UTR
Prolactin receptor precursor	PRLR	20	3	1 3' region and 2 introns
Cocaine- and amphetamine-regulated transcript protein precursor	CART	20	1	Intron

Phosphatidylinositol 3-kinase P-85 -alpha subunit	PIK3R1	20	10	2 exon (silent), 1 3' region and 7 introns
Transportin	TNP01	20	1	Intron

Appendix 3.6 Candidate gene SNPs

Name of the Gene	Symbol	BTA	SNP Sequence context	SNP location	Position in Mb on chromosome	Sire	SNPs used for genotyping	Method of genotyping
Growth hormone factor 1 / Pituitary-specific positive transcription factor 1(Pit-1) (GHF-1).	POU1F1	1	5' AGATCTTCCCRACCCAGGGATT	Intron	19.4	NA		
Growth hormone factor 1 / Pituitary-specific positive transcription factor 1(Pit-1) (GHF-1).	POU1F1	1	5' TGCCAACTCCYCACCTCCCAG	Intron 5-6	19.4	361, 368	POU1F1#1	Primer extention
Growth hormone factor 1 / Pituitary-specific positive transcription factor 1(Pit-1) (GHF-1).	POU1F1	1	5' GCTAACAAATWTATCGTTAAA	Intron	19.4	NA		
Growth hormone factor 1 / Pituitary-specific positive transcription factor 1 (Pit-1) (GHF-1).	POU1F1	1	5' TCTCATTCTA(A/-)CATCTCTACT	Intron	19.4	NA		
Growth hormone factor 1 / Pituitary-specific positive transcription factor 1 (Pit-1) (GHF-1).	POU1F1	1	5' GTGTTTTCAGYGTCTTTAGGT	Intron	19.4	NA	POU1F1#2	SNPlex
Growth hormone factor 1 / Pituitary-specific positive transcription factor 1 (Pit-1) (GHF-1).	POU1F1	1	5' CCGGGAAAGASCCCATGGACT	Intron	19.4	NA		SNPlex didn't work
5-Hydroxytryptamine 1F receptor	HTR1E	1	5' TCTATTACAARATATATAA(G/A)GCAG	exon (silent)	20.8	361, 398	HTR1E#1	SNPlex
5-Hydroxytryptamine 1F receptor	HTR1E	1	5' ACAA(G/A)ATATATAARGCAGCAAAGA	exon (silent)	20.8	361, 398	HTR1E#2	SNPlex
Follistatin-related protein 1 precursor	FSTL1	1	5' CTGGCCTGAARACTAGATAAA	Intron	30	398		
Follistatin-related protein 1 precursor	FSTL1	1	5' CTGCTACGACYGCCAAATCAC	Exon	30	398	FSTL1#1	SNPlex didn't work

Name of the Gene	Symbol	BTA	SNP Sequence context	SNP location	Position in Mb on chromosome	Sire	SNPs used for genotyping	Method of genotyping
Follistatin-related protein 1 precursor	FSTL1	1	5' TGTCACCACC**R**GGCCCGTCCT	Intron	30	398	FSTL1#2	SNPlex
Sortin nexin 4	SNX4	1	5' TGACAAAGCT**Y**AGCTGAAATT	Intron	37.4	398		SNPlex didn't work
Sortin nexin 4	SNX4	1	5' GTGTGAAATC**Y**AAGAATTTCT	Intron	37.4	398	SNX1	SNPlex
Sortin nexin 4	SNX4	1	5' GAATTTTGAT**S**TGGTCAAA(C/A)ATTT	Intron	37.4	398	SNX2	SNPlex
Sortin nexin 4	SNX4	1	5' AT(G/C)TGGTCAAA**M**ATTTTATACT	Intron	37.4	398	SNX3	SNPlex
Sortin nexin 4	SNX4	1	5' GAAGACTCAA**Y**TTCTCAGTGG	Intron	37.4	398	SNX4	SNPlex
Uridine monophosphate synthetase	UMPS	1	5' TTTGGGAAAC**Y**GCTGAGGTTC	Exon 3 (silent)	38.3	398, 368	UMPS#1	Primer extention
Uridine monophosphate synthetase	UMPS	1	5' CACAGTGCTG**Y**GTATTCTTGA	Exon 3 (Cys-Arg)	38.3	398	UMPS#2	Primer extention
Uridine monophosphate synthetase	UMPS	1	5' GCAGATGGAA**M**ATTTTATTTT	Intron	38.3	398	UMPS#4	SNPlex
Uridine monophosphate synthetase	UMPS	1	5' TTTCCAGTTG**Y**ATAAATCTTA	Intron	38.3	368	UMPS#3	SNPlex
Somatostatin precursor	SST	1	5'CCCCATGCAG**R**AACTGGCCAA	Splicing junction Ex1-Ex2 (Glu-Lys)	50	361,368	SST#1	Primer extention
Peroxisomal bifunctional enzyme	EHHADH	1	5' ATGTCCATCT**Y**AATATGGTAC	Intron	50.2	398	EHHADH5	SNPlex
Peroxisomal bifunctional enzyme	EHHADH	1	5' TTGATATAGA**W**AACAGTTCCA	Intron	50.2	398	EHHADH4	SNPlex
Peroxisomal bifunctional enzyme	EHHADH	1	5' GCCCAACATG**K**ATGCCATTTT	Exon	50.2	398	EHHADH1	SNPlex

Name of the Gene	Symbol	BTA	SNP Sequence context	SNP location	Position in Mb on chromosome	Sire	SNPs used for genotyping	Method of genotyping
Peroxisomal bifunctional enzyme	EHHADH	1	5' TCGGCGATCARTCCGGGGACG	Intron	50.2	398	EHHADH3	SNPlex
Peroxisomal bifunctional enzyme	EHHADH	1	5' CTTCTGTGCARGTAATGTGTC	Exon	50.2	398	EHHADH2	SNPlex didn't work
Alpha-HS-glycoprotein	AHSG	1	5' ACACTTTCTCYGGGGTGGCCT	Exon7 (silent)	50.8	361,398	AHSG#1	Primer extention
Alpha-HS-glycoprotein	AHSG	1	5' GCAGCCTAGCRTTCCTGGAGG	Exon 7 (Val-Ile)	50.8	368	AHSG#2	Primer extention
Alpha-HS-glycoprotein	AHSG	1	5' GGAGGGTGGTGRGAGAAAAGGG	Intron Homozygous SNP	50.8	(G)398, (A)361, 368-		
Alpha-HS-glycoprotein	AHSG	1	5' ATCAGCTCTTRTAAGTATCAG	Intron	50.8	361,368, 398	AHSG-14-3	SNPlex
Eukaryotic translation initiation factor 4 gamma 1	EIF4G1	1	5' ACTTGGATTTSGTTCTTTTCA	Intron	51.12	398	EIF4G1#1	SNPlex
5-Hydroxytryptamine receptor 3 subunit c	HTR3C	1	5' TTCATCTCCTMCCTGCTGGAC	exon	51.2	398	HTR3C#1	SNPlex
5-Hydroxytryptamine receptor 3 subunit c	HTR3C	1	5' CTGCTGGACCYGGCCACCACC	exon	51.2	398	HTR3C#2	SNPlex
Glucose transporter 2	SLC2A2	1	5' GTACAGAGACWTAGGCTTTTT	Intron	61	361	SLC2A2#3	SNPlex
Glucose transporter 2	SLC2A2	1	5' TATTACTAATYCACGCCTCAC	Intron 5-6	61	361	SNP 1/SLC2A2#4	Primer extention
Glucose transporter 2	SLC2A2	1	5' TTGGCACTGARGGTGACCTGG	Intron	61	361	SLC2A2#5	SNPlex
Glucose transporter 2	SLC2A2	1	5' AGTTCTGGGTMATCGTCCAAG	Intron 5-6	61	398	SLC2A2#2	Primer extention
Glucose transporter 2	SLC2A2	1	5' GTGCTTAAAARTTTGGTTGAT	Intron	61	361		

Name of the Gene	Symbol	BTA	SNP Sequence context	SNP location	Position in Mb on chromosome	Sire	SNPs used for genotyping	Method of genotyping
Glucose transporter 2	SLC2A2	1	5' AACCATAAACRTTCACACAAG	Intron	61	361		
Protein Kinase C iota	PRKCI/ PKCI	1	5' CATTTATGAARTTCCACATTT	Intron	62	398	PKCI#1	SNPlex
Protein Kinase C iota	PRKCI/ PKCI	1	5' CATTATTTCCWTCATATGAAT	Intron	62	398	PKCI#2	SNPlex
Protein Kinase C iota	PRKCI/ PKCI	1	5' TGAGCTGTCAYCCATTATGTC	Intron	62	398		
Protein Kinase C iota	PRKCI/ PKCI	1	5' ACAGTACTTGYCATTTTCTCC	Intron	62	398		
Protein Kinase C iota	PRKCI/ PKCI	1	5' TTGCTGACACRTATTGYCTCT	Intron	62	398		
Protein Kinase C iota	PRKCI/ PKCI	1	5' ACACRTATTGYCTCTAATTCT	Intron	62	398		
Protein Kinase C iota	PRKCI/ PKCI	1	5' CAAGGTATAARTTGTATATAA	Intron	62	398		
Protein Kinase C iota	PRKCI/ PKCI	1	5' GAGTTTCAGGYGACATAAAAT	Intron	62	398	PKCI#3	SNPlex
NADH-ubiquinone oxido-reductase SGDH subunit, mitochondrial precursor (complex I-SGDH) 1 beta subcomplex, 5, 16kDa	NDUFB5	1	5' ATGGATATTARAAGGGAAAGT	Intron	62	398	NDUFB5#3	SNPlex
NADH-ubiquinone oxido-reductase SGDH subunit, mitochondrial precursor (complex I-SGDH) 1 beta subcomplex, 5, 16kDa	NDUFB5	1	5' TGGGTTCTGGYGGTTATTTAT	Intron	62	398	NDUFB5#4	SNPlex
NADH-ubiquinone oxido-reductase SGDH subunit, mitochondrial precursor (complex I-SGDH) 1 beta subcomplex, 5, 16kDa	NDUFB5	1	5' CATAGCAGCARTTTTACTTTT	Intron	62	398	NDUFB5#1	SNPlex

Name of the Gene	Symbol	BTA	SNP Sequence context	SNP location	Position in Mb on chromosome	Sire	SNPs used for genotyping	Method of genotyping
NADH-ubiquinone oxido-reductase SGDH subunit, mitochondrial precursor (complex I-SGDH) 1 beta subcomplex, 5, 16kDa	NDUFB5	1	5' ATACTTCACAYATATATAAAA	Intron	62	398	NDUFB5#5	SNPlex
NADH-ubiquinone oxido-reductase SGDH subunit, mitochondrial precursor (complex I-SGDH) 1 beta subcomplex, 5, 16kDa	NDUFB5	1	5' AGTTAAAAATKTGTAGAATAT	Intron	62	398	NDUFB5#6	SNPlex
NADH-ubiquinone oxido-reductase SGDH subunit, mitochondrial precursor (complex I-SGDH) 1 beta subcomplex, 5, 16kDa	NDUFB5	1	5' AAGTAGTAGTRACATGAATAT	Intron	62	398	NDUFB5#2	SNPlex
Interleukin 12 A	IL12A	1	5' CCAGAGAGACMTCTTTTATAA	exon 5 (silent SNP)	67.4	398	IL12A#1	SNPlex
Sucrase-isomaltase, intestinal	SI	1	5' ACTAAAGAACKCTGCGAAGAA	Exon (Ala-Pro)	68	398	SI1	SNPlex
Sucrase-isomaltase, intestinal	SI	1	5' CAGCATACAARCTAAATTCAT	Intron	68	398	SI2	SNPlex
Sucrase-isomaltase, intestinal	SI	1	5' AATTTCAATTYCTATTCCTAG	Intron	68	398	SI3	SNPlex
Sucrase-isomaltase, intestinal	SI	1	5' TTAGTGAGCCRTCAACAATTG	Intron	68	398	SI4	SNPlex
Angiotensin receptor 1	AGTR1	1	5' ACAGCTTGGTRGTGATTGTCA	Exon 2 (Silent)	74.3	368	AGTR1#1	Primer extention
Angiotensin receptor 1	AGTR1	1	5' TCCACCGCAAYGTATTTTTCA	Exon 2 (Silent)	74.3	398	AGTR1#2	Primer extention
Glycogenin-1	GYG1	1	5' CAGGGGGTGYGGTTCATATT	Intron	75.9	368		

Name of the Gene	Symbol	BTA	SNP Sequence context	SNP location	Position in Mb on chromosome	Sire	SNPs used for genotyping	Method of genotyping
Glycogenin-1	GYG1	1	5' TTCTGTTTTCYTTGTTTTAAG	Intron	75.9	398	GYG1#1	SNPlex
Glycogenin-1	GYG1	1	5' CATCACCTCCSCTGTTTCTAG	Intron	75.9	398	GYG1#2	SNPlex
Glycogenin-1	GYG1	1	5' GGGTGATCCARGTGAGTGATT	Intron	75.9	398		
Glycogenin-1	GYG1	1	5' TAAAAACTTGRTATACGAGTA	Intron	75.9	398		
Neprilysin (Neutral endopeptidase) (NEP) (Enkephalinase) Neutral endopeptidase	MME	1	5' GAAGGGTCTAMTGTCTATCAA	3' region	67	361		
Neprilysin (Neutral endopeptidase) (NEP) (Enkephalinase) Neutral endopeptidase	MME	1	5' CTAATGAAACRGAGAAAGAAA	3' region	67	361		
G Protein -coupled receptor kinase GRK7	GPCRK	1	5' TCTTCTTTTCYTCCCTACCTT	3'	NA	361		
Epidermal Growth factor	EGF	6	5' ATCCTTTTTTWTTATTCACAA	Intron	NA	361,		
Epidermal Growth factor	EGF	6	5' TCCTGAAACCYCCCCCTGCAA	Intron	NA	368		
Epidermal Growth factor	EGF	6	5' ACTCCTAATAYTTATGTAGTC	Homozygous intron	NA	(C)368, (T) 361, 398		
Epidermal Growth factor	EGF	6	5' TAAAGAGCAGYGAACCATTAA	Homozygous intron	NA	(C)368, (T) 361, 398		
Epidermal Growth factor	EGF	6	5' GAGACTCCCAGRGAACTGGGGG	Intron	NA	361		
Epidermal Growth factor	EGF	6	5' TGGGTGGTTAYAAGCCATGAA	Intron	NA	(C)368, (T) 361, 398		

Name of the Gene	Symbol	BTA	SNP Sequence context	SNP location	Position in Mb on chromosome	Sire	SNPs used for genotyping	Method of genotyping
Epidermal Growth factor	EGF	6	5' TATACTTTATRTCAAATAGTG	Intron	NA	(A) 361, 398		
Bone Sialoprotein	SIAL	6	5' TGGCCTTAAAYTTTATGTTTT	Intron	15	368, 398		
Bone Sialoprotein	SIAL	6	5' GACGGTGAAGRAGAAAGTGTC	Intron	15	398		
Microsomal triglyceride transfer protein	MTP	6	5' CTATGTTTAAYGGAAATTTAA	Intron	NA	368, 398		
Osteopontin-k	SPP1	6	5' TTTAGTAAAAMGAGACAATAT	Exon	NA	398		
Alpha –s1-casein	CSN 1	6	5' TGAGTTTACAYATTATATAAT	Exon	NA	398		
Alpha –s1-casein	CSN 1	6	5' TCAGGTACCCYAGAAAAGCC	Exon	NA	368, 398		
Alpha –s1-casein	CSN 1	6	5' AAGCCCTTTCYAAAATTTCCT	Exon	NA	398		
Alpha –s1-casein	CSN 1	6	5' CATGTCTGAAWTGAAKGCAATG	Exon	NA	368, 398		
Alpha –s1-casein	CSN 1	6	5' TCTGAAWTGAAKGCAATGATTC	Exon	NA	368, 398		
Alpha –s1-casein	CSN 1	6	5' TTCTCATACASTGTTGCTTTT	Exon	NA	368, 398		
Alpha –s1-casein	CSN 1	6	5' GAGAACAGTGRAAAGACTACT	Intron	NA	368, 398		
Alpha –s1-casein	CSN 1	6	5' TGAAATGGAARATTGATGATA	Exon	NA	398		
Cathepsin B	CSTB	8	5' TTCAGTCCATRTGCAGTCCTT	Intron	1	398	CSTB3	SNPlex

Name of the Gene	Symbol	BTA	SNP Sequence context	SNP location	Position in Mb on chromosome	Sire	SNPs used for genotyping	Method of genotyping
Cathepsin B	CSTB	8	5' CGCCTCTGTCYGATGAGCTGG	Intron	1	398	CSTB4	SNPlex
Cathepsin B	CSTB	8	5' GCCACCCTCARCTGCCTGCTG	Exon 2	1	361,368, 398	CSTB2	Primer extention
Cathepsin B	CSTB	8	5' TGTACCTTTTSCAATCACTGC	3'UTR	1	368		
Cathepsin B	CSTB	8	5' GGCCCTCCAGYGTTGCAGCTG	3'UTR	1	368,398	CSTB1	Primer extention
Nociceptin	PNOC	8	5' GCACCAAGGTMATGGCCAGGG	Exon	5	361, 368, 398	PNOC#1	Primer extention and SNPlex
Nociceptin	PNOC	8	5' GGGCTCCTGGMGCTMGCCCTG	Exon	5	398	PNOC#2	SNPlex
Nociceptin	PNOC	8	5' TCCTGGMGCTMGCCCTGCTGA	Exon	5	398	PNOC#3	SNPlex
Tyrosine kinase, endothelial	TEK	8	5' CTGTAATGCAYAACTCATTGT	Intron	10.3	398	TEK3"#3	SNPlex
Tyrosine kinase, endothelial	TEK	8	5' TTCTAACCGGRCATGGATTTA	3'	10.3	398	TEK3"#1	Primer extention
Tyrosine kinase, endothelial	TEK	8	5' ATTCCTTAGAWGCCTAAGAAC	3'	10.3	398,361	TEK3"#2	Primer extention
Tyrosine kinase, endothelial	TEK	8	5' ACCAACCTGASGTGCTACAGG	Intron	10.3	398	TEK3"#4	SNPlex
Lipoprotein Lipase	LPL	8	5' AGTCTAAATAYAGGAAGTAAG	Exon 10 (silent)	35	368,398	LPL#1	Primer extention
Lipoprotein Lipase	LPL	8	5' CCGTTTACCTRTCAATCAAAA	Exon	35	368,398	LPL#2	Primer extention
Lipoprotein Lipase	LPL	8	5' GCTTAAAACCRTTGTGGACAA	Exon	35	368,398	LPL#4_2	SNPlex

Name of the Gene	Symbol	BTA	SNP Sequence context	SNP location	Position in Mb on chromosome	Sire	SNPs used for genotyping	Method of genotyping
Lipoprotein Lipase	LPL	8	5' GAAACAGAAARGTTAMAGTCAG	Exon	35	368,398	LPL#3	SNPlex
Lipoprotein Lipase	LPL	8	5' CAGAAARGTTAMAGTCAGTCAT	Exon (Thr-Cys)	35	368,398	LPL#4_1	SNPlex
Lipoprotein Lipase	LPL	8	5' ATTTATTTATMAACTAGATCT	Exon	35	368	LPL#5	SNPlex
Neurofilament M subunit	NEFM	8	5' AAAGAAGGGCRGTGATAAAAG	3' UTR	NA	368, 361	NEFM#1	SNPlex
Neurofilament M subunit	NEFM	8	5' GGCTCCAAAGSAGGAGCTGGC	3' UTR	NA	398		SNPlex didn't work
Elongation protein 3 homolog	ELP3	8	5' CATTCCGTTTYGAATTGGTTG	Exon	NA	398	ELP3#1	SNPlex
Elongation protein 3 homolog	ELP3	8	5' GGAAGAGGAARGGAGAAAGGA	Intron	NA	398	ELP3#2	SNPlex
Elongation protein 3 homolog	ELP3	8	5' TCAGGCAAAGRGACAAAAAGC	3' UTR	NA	398	ELP3#3	SNPlex
Fructose-1,6-bisphosphatase isozyme 2	FBP2	8	5' TCTCCTCAGCYGTGCGTAAGG	Exon	NA	398	FBP2#1	SNPlex
Fructose-1,6-bisphosphatase isozyme 2	FBP2	8	5' TCAACCACCAMCTGGAAAACA	Exon	NA	398		SNPlex didn't work
SHC transforming protein 3 (SH2 domain protein C3)	SHC3	8	5' AGCAAGGCAGYCTCCATGGAA	Exon	NA	398	SHC3#2	SNPlex didn't work
SHC transforming protein 3 (SH2 domain protein C3)	SHC3	8	5' TCAACCACCAMCTGGAAAACA	Intron	NA	398	SHC3#1	SNPlex
Clusterin	CLU	8	5' TGGAGCTGCARCCAGAGCCCA	Intron	NA	398	CLU1	SNPlex
Clusterin	CLU	8	5' TCCCCACGATRGAATTCACAG	Intron	NA	361, 368, 398	CLU2	SNPlex

Name of the Gene	Symbol	BTA	SNP Sequence context	SNP location	Position in Mb on chromosome	Sire	SNPs used for genotyping	Method of genotyping
Clusterin	CLU	8	5' TTAACCCAGTYAAACAGGCTG	Intron	NA	398		
Clusterin	CLU	8	5' GCATGGCCACSCTCTCACCAC	Intron	NA	398		
Clusterin	CLU	8	5' AGTGAGTGTGYGCCCCCTGCC	Intron	NA	398		
ATPase, H+ transporting, lysosomal 31kDa, V1 subunit E isoform 2	ATP6V1E2	11	5' GTGGAGCTCCRGAAACACACC	Intron	23	361	ATP6V1E2#1	SNPlex
Follicle stimulating hormone receptor	FSHR	11	5' AGGTCAGAAASCTCATCCACT	Exon10 (Asn-Lys)	24	361	FSHR#1	Primer extention
Follicle stimulating hormone receptor	FSHR	11	5' ATCCAAGGAAYGGCCACTGCC	Exon 10 (Trp-Arg)	24	361	FSHR#2	Primer extention
Follicle stimulating hormone receptor	FSHR	11	5' AAGGCCCGACYAAGGTGAATG	Intron	24	361	FSHR#3	SNPlex
Follicle stimulating hormone receptor	FSHR	11	5' GGTGAATGGARAGGTTTGGTA	Intron	24	361	FSHR#4	SNPlex
Follicle stimulating hormone receptor	FSHR	11	5' AGAGATGTAASAGACTGCATG	Intron	24	361	FSHR#5	SNPlex
Interleukin 1beta	IL1B	11	5' GGTACCTAATRAGAGCTGAGG	Intron	31	368		
Interleukin 1beta	IL1B	11	5' GGGAGTCCACKTGGGCTGAAT	Intron	31	361	IL1B#2	Primer extention
Interleukin 1beta	IL1B	11	5' GAATAACCCCRAGGACTGGCA	Intron	31	361	IL1B #3	SNPlex
Interleukin 1beta	IL1B	11	5' TGCCTGCAAAYGCAAGAGATT	Intron	31	361		
Interleukin 1beta	IL1B	11	5' AGACCTCTGCRTCGGGAAGAA	Intron	31	361	IL1B #4	SNPlex

Name of the Gene	Symbol	BTA	SNP Sequence context	SNP location	Position in Mb on chromosome	Sire	SNPs used for genotyping	Method of genotyping
Interleukin 1beta	IL1B	11	5' ACATAAGAGTYGGACACTTCT	Intron	31	368		
Interleukin 1beta	IL1B	11	5' CCAACTTGAARTCATTCTAGC	Intron	31	368		
Interleukin 1beta	IL1B	11	5'AGGGTAGAATRTCTTTGCCCT	Intron	31	361,368		
Interleukin 1beta	IL1B	11	5'AAATCAAGAAYACAGTTGAAT	Exon	31	361,368	IL1B #1	Primer extention
Interleukin 1beta	IL1B	11	5'TTTTCCCACCMGTTTTCCCAG	Intron	31	361,368		
Proopiomelanocortin	POMC	11	5' AAGAATTGAAAYATAGTTGAGGGG	Intron	53	368	POMC-I1RC#7	SNPlex
Proopiomelanocortin	POMC	11	5' GGCGAGGACCRGCCTCTCTGG	Intron	53	368		
Proopiomelanocortin	POMC	11	5' AAGTGAAAAGYGAAAGTGAAG	Intron	53	368	POMC-I1RC#8	SNPlex
Proopiomelanocortin	POMC	11	5' TTACTTTCTTYTCTGCTGCTG	Intron 1-2	53	368	POMC#2	Primer extention
Proopiomelanocortin	POMC	11	5' CTGACTCTGTKCGACCCCATA	Intron 1-2	53	368	POMC#1	Primer extention
Proopiomelanocortin	POMC	11	5' CTTCCCTGGTSATCCAGTGGT	Homozygous Intron	53	(G)368,398		
Proopiomelanocortin	POMC	11	5' CGCCCCTTGTYACGCTGTTCA	Exon (silent)	53	368	POMC-Ex3#3	SNPlex
Proopiomelanocortin	POMC	11	5' CTGGCTAGGCYGCAGTCCATG	5'	53	368	POMC-5'B#4	SNPlex
Proopiomelanocortin	POMC	11	5' AGAGTCGAACWTGACTGAGCG	5'	53	368	POMC-5'B#5	SNPlex

Name of the Gene	Symbol	BTA	SNP Sequence context	SNP location	Position in Mb on chromosome	Sire	SNPs used for genotyping	Method of genotyping
Proopiomelanocortin	POMC	11	5' CTGACTTGTGSCCTCTTGTTC	5'	53	368	POMC-5'B#6	SNPlex
Trifunctional enzyme alpha subunit, mitochondrial precursor (TP-alpha) (78 kDa gastrin-binding protein)	HADHA	11	5' CAAAAAGGAAMGAGGGCCGCT	3' region	54	361	HADHA#2	SNPlex
Trifunctional enzyme alpha subunit, mitochondrial precursor (TP-alpha) (78 kDa gastrin-binding protein)	HADHA	11	5' AAATTATGTTSAAACATTAAT	3' region	54	361	HADHA#1	SNPlex
Ribonucleoside-diphosphate reductase M2 chain	RRM1	11	5' TTGACTTAACYGTTTATACTT	Intron	66	361,368	RRM1#1	SNPlex
Ribonucleoside-diphosphate reductase M2 chain	RRM1	11	5' TAACCTGGGTRTGCGGGAGGG	Intron	66	398		
Ribonucleoside-diphosphate reductase M2 chain	RRM1	11	5' CAGCCTCAGGYRAGCCACCTC	3' region	66	361, 368	RRM1#2	SNPlex
Ribonucleoside-diphosphate reductase M2 chain	RRM1	11	5' CAGCCTCAGGYRGAGCCACCTC	3' region	66	361, 368	RRM1#3	SNPlex
Ribonucleoside-diphosphate reductase M2 chain	RRM1	11	5' TGAAAGTGAARTYGCTCAGTCAG	3' region	66	361, 368	RRM1#4	SNPlex
Ribonucleoside-diphosphate reductase M2 chain	RRM1	11	5' TGAAAGTGAARTYGCTCAGTCAG	3' region	66	361, 368	RRM1#5	SNPlex
NADH-ubiquinone oxidoreductase 19 kDa subunit	NDUFA8	11	5' ATCGATTACTMCGGCCTGCAG	Exon 3 (Tyr-Ser)	73	361	NDUFA8	SNPlex
Argininosuccinate synthase	ASS	11	5' TTCCTCTTTAYACTTTCCCAC	3' Intron	81	361	ASS#1	Primer extention
Argininosuccinate synthase	ASS	11	5' ATTTGATTACRATAGGCCTTG	Intron	81	361	ASS#2	Primer extention
Presenilin 2	PSN2	16	5' GCTTCCACTGYGCTGAAGGCT	Intron	1	361		

Name of the Gene	Symbol	BTA	SNP Sequence context	SNP location	Position in Mb on chromosome	Sire	SNPs used for genotyping	Method of genotyping
Presenilin 2	PSN2	16	5' GAGGAGTGAGRGAGTTTAATT	Intron	1	361, 398		
Presenilin 2	PSN2	16	5' CTTTAAAAAGSAAACAAAGCA	Intron	1	398		
Presenilin 2	PSN2	16	5' TCAGCACCTTRCCTAATGCTT	Intron	1	361, 398		
Presenilin 2	PSN2	16	5' CCTAATGCTTYGGGAAGATGT	Intron	1	361		
Presenilin 2	PSN2	16	5' GTTCCTGATTWAAAACAAAGA	Intron	1	361, 368, 398		
Presenilin 2	PSN2	16	5' GGACATCAGCYTAACCCAGGG	Intron	1	398		
Presenilin 2	PSN2	16	5' CGCTTCACCCRCAGGAAACCC	Intron	1	368, 398		
Presenilin 2	PSN2	16	5' TTCTTGCCTGSAAAATTCCTT	Intron	1	361, 398		
Myogenin	MYOG	16	5' CAGAACCCCTSATTCAAGGCC	Intron	0.4	F60G/C 61, (368-C,398-C)		
Myogenin	MYOG	16	5' GCAGAGTGTCYGGCTCAACTA	Intron	0.4	F60G/C 61,(368-C,398-C)		
Myogenin	MYOG	16	5' TACTTTGACTSAAATCACACA	Intron	0.4	F60G/C 61,(368-C,398-C)		
Interleukin 10	IL10	16	5' CCAGAAGCCGYGGAACCTATG	Intron	4	368		
Interleukin 10	IL10	16	5' AACACGTCTTRTCTCCCCACA	Intron	4	368, 398		
Fibromodulin	FMOD	16	5' AACCACCTTASGAAGGTACCT	Exon Homozygous	2	(G) 368, 398 (C) 361		

Name of the Gene	Symbol	BTA	SNP Sequence context	SNP location	Position in Mb on chromosome	Sire	SNPs used for genotyping	Method of genotyping
Fibromodulin	FMOD	16	5' TCCCTGATACYGTGTATGCTT	Exon	2	361		
Glutamine synthetase	GLUP	16	5' CCCCAAGGTCYCTACTACTGT	3' region	NA	368, 398		
Glutamine synthetase	GLUP	16	5' CATCAAGATCRGGAGGCAGGA	3' region	NA	361, 368, 398		
6-Phosphofructo-2-kinase	PFKFB2	16	5' NNNNNNWCGTGTCCAGA	Intron	3	368,398	PFK-In4#1	SNPlex
6-Phosphofructo-2-kinase	PFKFB2	16	5' CCTGGTTTACYGGCTTTATTC	Intron	3	398		
6-Phosphofructo-2-kinase	PFKFB2	16	5' AGTCAGATAAYTTAAGACTTG	Intron	3	398	PFK-In4#2	SNPlex
6-Phosphofructo-2-kinase	PFKFB2	16	5' CCCTTGGCCAYTCTGACATTA	Intron	3	398		
6-Phosphofructo-2-kinase	PFKFB2	16	5' CCGAGAAGGCYGCTTTGGGAC	Intron	3	398		
6-Phosphofructo-2-kinase	PFKFB2	16	5' GTGTAAGTTAYCCACTGGGCG	Intron	3	398		
C4BP beta chain	C4BPB	16	5' CAGATTCTTTRCCGCTGAACC	Homozygous intron	3	(G) 398, (A) 368, 361		
C4BP beta chain	C4BPB	16	5' AAAAACACATRTTTAGAATTT	Homozygous intron	3	(A) 398, (C) 368, 361		
C4BP beta chain	C4BPB	16	5' TTCCTCCATAYCTTACATGCT	Homozygous intron	3	(C)398, (T) 368, 361		
C4BP beta chain	C4BPB	16	5' TATGATTGTTRTGTGATACTG	Homozygous intron	3	(A)398, (C) 368, 361		
P selectin	SELP	16	5' CACCCAATTCYTTTCCATTCT	Intron	25.3	368, 398		

Name of the Gene	Symbol	BTA	SNP Sequence context	SNP location	Position in Mb on chromosome	Sire	SNPs used for genotyping	Method of genotyping
P selectin	SELP	16	5' GAGGAGTGAGRGAGTTTAATT	Intron	25.3	368, 361		
P-selectin	SELP	16	5' CTTTAAAAAGSAAACAAAGCA	Intron	25.3	368		
P selectin	SELP	16	5' TCAGCACCTTRCCTAATGCTT	Intron	25.3	368, 361		
P selectin	SELP	16	5' CCTAATGCTTYGGGAAGATGT	Intron	25.3	368, 361		
P selectin	SELP	16	5' AGATGTAGCASCTATTGCTGG	Intron	25.3	368		
P selectin	SELP	16	5' TTCTTGCCTGSAAAATTTCTT	Intron	25.3	368		
P selectin	SELP	16	5' TTCCCCTCTASTGGCTTGKTGT	Intron	25.3	368		
P selectin	SELP	16	5' TCTASTGGCTTGKTGTAACTACT	Intron	25.3	368		
Complement factor H 1	CFH	16	5' ATCATTTTGTRCCTCCTTCAC	Intron	4	361, 368, 398		
Complement factor H 1	CFH	16	5' TCCTGGGACCWCCTGACTTGC	Intron	4	361, 368, 398		
Complement factor H 1	CFH	16	5' TTAAGTGTTAYGTAACAACAG	Intron	4	361		
Complement factor H 1	CFH	16	5' TAACAACAGTRAGGCCACGGG	Intron	4	368		
Complement factor H 1	CFH	16	5' AGAGATACAGRGACTTTACAA	Intron	4	361, 368, 398		
Complement factor H 1	CFH	16	5' TATATTTGAAYACTAATGCAT	Intron	4	361, 368, 398		

Name of the Gene	Symbol	BTA	SNP Sequence context	SNP location	Position in Mb on chromosome	Sire	SNPs used for genotyping	Method of genotyping
Complement factor H 1	CFH	16	5' AATGGACATAMCCMACATCSTG	Intron	4	368		
Complement factor H 1	CFH	16	5' GGACATAMCCMACATCSTGAAGA	Intron	4	368		
Complement factor H 1	CFH	16	5' ATAMCCMACATCSTGAAGAAAAA	Intron	4	361,368		
Complement factor H 1	CFH	16	5' GTAAGAGTTCRCTGCYATGAA	Intron	4	361		
Complement factor H 1	CFH	16	5' AGTTCRCTGCYATGAAGGCTA	Intron	4	368		
Complement factor H 1	CFH	16	5' ACAATGAGGTYGTGGAATATG	Intron	4	368		
Complement factor H 1	CFH	16	5' TGCAACCCCARATTTCTGATG	Intron	4	361,368, 398		
Complement factor H 1	CFH	16	5' GTAATGTATTRAAAGTAGTAA	Intron	4	361, 398		
Complement factor H 1	CFH	16	5' GATTTATCACYGTGTATTAGT	Intron	4	368		
ATPase, Ca++ transporting, plasma membrane 4	ATP2B4	16	5' TTTCTTTGCTRACAGCCCTTT	3' region	2	361	ATP2B4-3'-2	SNPlex
ATPase, Ca++ transporting, plasma membrane 4	ATP2B4	16	5' GTAGTTTTCAMCTGAAGCCTG	3' region	2	361	ATP2B4-3'-3	SNPlex
ATPase, Ca++ transporting, plasma membrane 4	ATP2B4	16	5' GTAGTTTTCAMCYGAAGCCTGAG	3' region	2	398		
ATPase, Ca++ transporting, plasma membrane 4	ATP2B4	16	5' GTAGTTTTCAMCYGAAGCCTGAG	3' region	2	398		
ATPase, Ca++ transporting, plasma membrane 4	ATP2B4	16	5' GTAGTTTTCAMCYGAAGCCTGAG	3' region Deletion of C nucleotide	2	398		

Name of the Gene	Symbol	BTA	SNP Sequence context	SNP location	Position in Mb on chromosome	Sire	SNPs used for genotyping	Method of genotyping
ATPase, Ca++ transporting, plasma membrane 4	ATP2B4	16	5' GTGAACTTCTWCTCTGCTCCC	3' UTR	2	361, 398	ATP2B4-3'-1	SNPlex
Microtubule-associated protein -1B	MAP1B	20	5' AGACCGGAGAYTATGAAGAGA	exon 5 (silent SNP)	6.3	361	SNP1	Primer extention
Mitogen-activated protein kinase kinase kinase 1	MAP3K1	20	5' TTCTGTGAGTWTTTTAAATCA	3' region	12	368,361	MAP3K1#1	SNPlex
Mitogen-activated protein kinase kinase kinase 1	MAP3K1	20	5' ATAGACTGCTRTTGGAATTTC	3' region	12	398	MAP3K1#2	SNPlex
Follistatin precursor	FST	20	5' GGAGATTTGGRTAGGGAATGC	Intron	13	368,398	FST#1	Primer extention
Follistatin precursor	FST	20	5' GCTTGAGGTARACCGCTGCA	Intron Homozygous SNP	13	(G)361, 368 (A)398		
Follistatin precursor	FST	20	5' AATAATAATARTATCAATAAG	Intron	13	398	FST#6	SNPlex
Follistatin precursor	FST	20	5' AATAATAATARTATCAAATAA	intron	13	398	FST#5	SNPlex
Follistatin precursor	FST	20	5' TTTTGAGTATRTGTGTGTGTG	Intron	13	368	FST#7	SNPlex
Follistatin precursor	FST	20	5' TGAGCTGTGCSCTGAGAGTAA	Exon 5 (Ala-Pro)	13	368	FST#2	Primer extention
Follistatin precursor	FST	20	5' AGCAAGACACRGGAAACAATT	Intron	13	398	FST#4	SNPlex
Follistatin precursor	FST	20	5' ACATATTGAARTGCCAGCAAG	Intron	13	398	FST#3	SNPlex
Follistatin precursor	FST	20	5' TGTGCCAGTGMCAATGCCACC	Intron	13	361,368, 398	FST#8	SNPlex
Integrin alpha 2	ITGA2	20	5' ACAAGCAATTYGCCTTRGAAAA	Intron	14.4	361		

Name of the Gene	Symbol	BTA	SNP Sequence context	SNP location	Position in Mb on chromosome	Sire	SNPs used for genotyping	Method of genotyping
Integrin alpha 2	ITGA2	20	5' GCAATTYGCCTTRGAAAAAGCAG	Intron	14.4	368		
Integrin alpha 2	ITGA2	20	5' GGCTCAGCAGMACATTTAAGT	Intron	14.4	398		
Integrin alpha 2	ITGA2	20	5' ATATTTCAGCWGCCTCTGCCA	Intron homozygous SNP	14.4	398A		
Integrin alpha 2	ITGA2	20	5' ACATGACTGTRTTTCTCCAAA	Intron homozygous SNP	14.4	398 A		
Integrin alpha 2	ITGA2	20	5' AAGTCAATACYGTAAGTGGTA	Intron homozygous SNP	14.4	398T		
Integrin alpha 2	ITGA2	20	5' TGGTAGTCTTRCATCAATTTG	Intron homozygous SNP	14.4	398A		
Integrin alpha 2	ITGA2	20	5' AGTCTCCAATRTGTCTGTTCG	Intron homozygous SNP	14.4	398G		
Integrin alpha 2	ITGA2	20	5' TTTTGAGCACMTCCTATGGGA	Intron homozygous SNP	14.4	398C		
Integrin alpha 2	ITGA2	20	5' CCTTTGAAGGSAGKACTACTAT	Intron homozygous SNP	14.4	398C		
Integrin alpha 2	ITGA2	20	5' GAAGGSAGKACTACTATCC	Intron homozygous SNP	14.4	398T		
Integrin alpha 2	ITGA2	20	5' GGTTAATTACYTGCTCAAAGA	Intron homozygous SNP	14.4	398T		
Integrin alpha 2	ITGA2	20	5' CTCAAAGATAMAAAACTTAAC	Intron homozygous SNP	14.4	398A		
Integrin alpha 2	ITGA2	20	5' AACCCCTTCTYTCCTAGGTTA	Intron homozygous SNP	14.4	398C		
Integrin alpha 2	ITGA2	20	5' ATCTGGCCAARATRTTCAACAG	Intron homozygous SNP	14.4	398G		

Name of the Gene	Symbol	BTA	SNP Sequence context	SNP location	Position in Mb on chromosome	Sire	SNPs used for genotyping	Method of genotyping
Integrin alpha 2	ITGA2	20	5' CTGGCCAARATRTTCAACAGCA	Intron homozygous SNP	14.4	398A		
Integrin alpha 2	ITGA2	20	5' TCTACAATGGYCATGAGGGCA	Exon 14 Homozygous SNP	14.4	398C		
Integrin alpha 2	ITGA2	20	5' GGTGATATGTRTACATGTGAG	Intron homozygous SNP	14.4	398G		
Integrin alpha 2	ITGA2	20	5' TACATGTGAGYATCATTGTGT	Intron homozygous SNP	14.4	398C		
Integrin alpha 2	ITGA2	20	5' CCAATCCATCYCTCTTACTTT	Intron homozygous SNP	14.4	398C		
Integrin alpha 2	ITGA2	20	5' ACTTTATAACYTAATTCACTT	Intron homozygous SNP	14.4	398C		
Integrin alpha 2	ITGA2	20	5' ATGGGTCTTTMATTCTTGTGA	Intron homozygous SNP	14.4	398C		
Integrin alpha 2	ITGA2	20	5' AGGAATTTTTWAAAAAAACTA	Intron homozygous SNP	14.4	398A		
Integrin alpha 2	ITGA2	20	5' ACTCAGAAGCRGCTTTTGAGT	Intron homozygous SNP	14.4	398G		
Integrin alpha 2	ITGA2	20	5' AAATGAGCTARGAGAGGAGTC	Intron homozygous SNP	14.4	398G		
Integrin alpha 2	ITGA2	20	5' AAGAGACACTSATGTATAGAA	Intron	14.4	361		
Integrin alpha 2	ITGA2	20	5' GCAGATTGCTYTGCTAGTATT	Intron homozygous SNP	14.4	398T		
Integrin alpha 2	ITGA2	20	5' AGGAAGGAGTRTGTTTTTCCT	Intron homozygous SNP	14.4	398A		
Integrin alpha 2	ITGA2	20	5' TCTATAAAATRAGGAGAAAAA	Intron homozygous SNP	14.4	398A		

Name of the Gene	Symbol	BTA	SNP Sequence context	SNP location	Position in Mb on chromosome	Sire	SNPs used for genotyping	Method of genotyping
Integrin alpha 2	ITGA2	20	5' AAAAGTGTATWGAAAAGCTAA	Intron homozygous SNP	14.4	398A		
Integrin alpha 2	ITGA2	20	5' TAAAGCTCTTKAAATGGTATT	Intron	14.4	368		
Integrin alpha 2	ITGA2	20	5' AGGCCACACAWGTGAAGTACA	Intron homozygous SNP	14.4	398T		
Integrin alpha 2	ITGA2	20	5' CTGAGCATTCYATCAGGAGTC	Intron homozygous SNP	14.4	398C		
Integrin alpha 2	ITGA2	20	5' TGAAGAGCAGRGGGGAACAAT	Intron	14.4	368		
Integrin alpha 2	ITGA2	20	5' CTTTACTGTCRTCTGTCTGTG/TAA	Intron homozygous SNP	14.4	398G		
Integrin alpha 2	ITGA2	20	5' TCG/ATCTGTCTGTKAAGCTAGGT	Intron	14.4	361		
Integrin alpha 2	ITGA2	20	5' GGACTCAAATSCATATTTTGA	Intron homozygous SNP	14.4	398G		
Integrin alpha 2	ITGA2	20	5' TTTAAGATAGMCCATGATGGC	Intron homozygous SNP	14.4	398A		
Integrin alpha 2	ITGA2	20	5' TATACTGTGAYGTTCCCTTTT	Intron homozygous SNP	14.4	398C		
Integrin alpha 2	ITGA2	20	5' GTAGACCTCARACATGCTAGG	Intron homozygous SNP	14.4	398G		
Integrin alpha 2	ITGA2	20	5' TAGGTTATAAAGCATCTGCCTGCAATGTGG	10 nucleotides deleted	14.4	398		
Integrin alpha 2	ITGA2	20	5' GGAAAAAAAAATGCTTGCTTA	1 nucleotide deleted	14.4	398		
Growth hormone receptor	GHR	20	5' ATCGTGGACAMCGCTTACTTC	Exon	18	361, 398	GHR#8	SNPlex

Name of the Gene	Symbol	BTA	SNP Sequence context	SNP location	Position in Mb on chromosome	Sire	SNPs used for genotyping	Method of genotyping
Growth hormone receptor	GHR	20	5' CGAGGTAGACRCCAAAAAGTA	Exon 10 (Ala-Thr)	18	398	GHR#1	Primer extention
Growth hormone receptor	GHR	20	5' TGGCCCCTCAYGTCGAGGCTG	Exon	18	361	GHR#9	SNPlex
Growth hormone receptor	GHR	20	5' CGTAGAGCCARGCTTTAACCA	Exon	18	361, 398	GHR#10	SNPlex
Growth hormone receptor	GHR	20	5' CAGCAGGAAAYGTGGTCCTTT	Exon	18	398	GHR#7	SNPlex
Growth hormone receptor	GHR	20	5' TTTGATTTCCYATGAGCTACC	Exon	18	361, 398	GHR#11	SNPlex
Growth Hormone receptor	GHR	20	5' AACTTTCTTCYTCACCACATC	3' region	18	398	GHR#5	SNPlex
Growth Hormone receptor	GHR	20	5' GAGTTTCATCRTTTTTTACCT	3' region	18	361, 398	GHR#2	Primer extention
Growth Hormone Receptor	GHR	20	5' GAGGCAATGCRTTGTGTGCTC	promoter	18	361, 368, 398	GHR#6	SNPlex
Growth Hormone Receptor	GHR	20	5' TGCTTCAGCCRTATTTAAACA	Intron	18	361		
Growth Hormone Receptor	GHR	20	5' CTGCTTCAGCYGTATTTAAAC	Intron	18	368		
Growth Hormone Receptor	GHR	20	GATAAGCTGGYGAACAAGAAA	Intron	18	398	GHR#4	SNPlex
Growth Hormone Receptor	GHR	20	TGAGAATGAGKAACTTACATC	intron	18	361,398		
Growth Hormone Receptor	GHR	20	GGAGAATGAGMTATAACACTT	Intron	18	361, 368, 398		
Growth Hormone Receptor	GHR	20	5' TGAGAATGAGKAACTTACATC	Intron	18	361,398		

Name of the Gene	Symbol	BTA	SNP Sequence context	SNP location	Position in Mb on chromosome	Sire	SNPs used for genotyping	Method of genotyping
Growth Hormone Receptor	GHR	20	5' GGAGAATGAGMTATAACACTT	Intron	18	361, 368, 398		
Growth Hormone Receptor	GHR	20	5' CCAGATCAATRTACATTAGCC	Intron	18	361,368		
Growth Hormone Receptor	GHR	20	5' CTGATATGTTYTGCCAGTTAT	Intron	18	368		
Growth Hormone Receptor	GHR	20	5' GAGGCAATGCRTTGTGTGCTC	Exon	18	361, 368, 398	GHR#3	SNPlex
5'-AMP-activated protein kinase, catalytic alpha-1 chain	PRKAA1	20	5' TGATTAATTARTTGACTCTTA	Exon 6	19.9	398	PRKAA1#1	Primer extention
5'-AMP-activated protein kinase, catalytic alpha-1 chain	PRKAA1	20	5' AACGTATTTAYTGGATTTCCG	Exon	19.9	368		Primer extention?
5'-AMP-activated protein kinase, catalytic alpha-1 chain	PRKAA1	20	5' CCTGTGATATRCCATGAACCC	Promoter	19.9	368	PRKAA15'#6	
5'-AMP-activated protein kinase, catalytic alpha-1 chain	PRKAA1	20	5' TTTTTTTTTTYTCGTTATTTT	5' UTR	19.9	368	PRKAA15'#7	Primer extention?
5'-AMP-activated protein kinase, catalytic alpha-1 chain	PRKAA1	20	5' TTTTAAAAAGSACTGAAGGAA	5' UTR	19.9	398	PRKAA1#3	SNPlex didn't work
5'-AMP-activated protein kinase, catalytic alpha-1 chain	PRKAA1	20	5' TGAATGTCAARGTTTCATCAC	3' UTR	19.9	368	PRKAA13'#8	SNPlex
5'-AMP-activated protein kinase, catalytic alpha-1 chain	PRKAA1	20	5' CAGAGACTTTWAGAGGTGATT	3' UTR	19.9	361	PRKAA1#4_2	SNPlex
5'-AMP-activated protein kinase, catalytic alpha-1 chain	PRKAA1	20	5' ATCCCTGGTARGGGAACTCAG	3' UTR	19.9	368	PRKAA1#4_1	SNPlex
Prolactin receptor precursor	PRLR	20	5' AGCCTGGCAGKCTACAGTCCA	Intron	27.9	368	PRLR#3	SNPlex
Prolactin receptor precursor	PRLR	20	5' CAGTCCATAGRGTCGCAAGGA	Intron 8-9	27.9	368, 398	PRLR#2	Primer extention

Name of the Gene	Symbol	BTA	SNP Sequence context	SNP location	Position in Mb on chromosome	Sire	SNPs used for genotyping	Method of genotyping
Prolactin receptor precursor	PRLR	20	5' ACTGGGTCCCRCAGGTTTTATGC	Intron 9- 10	27.9	398	PRLR#1	Primer extention
Cocaine- and amphetamine-regulated transcript protein precursor	CARTPT	20	5' TGTACAAAGTRTTCTATTCTT	Intron	48	368	CARTPT#1	SNPlex
Phosphatidylinositol 3-kinase P-85 -alpha subunit	PIK3R1	20	5' TAGAACATACYGGCGTTTGTT	Intron	NA	368	PIK3R1#1	Primer extention
Phosphatidylinositol 3-kinase P-85 -alpha subunit	PIK3R1	20	5' AATTAATCAARATATTTCACC	Exon (silent SNP)	NA	368	PIK3R1#2	Primer extention
Phosphatidylinositol 3-kinase P-85 -alpha subunit	PIK3R1	20	5' TAAAATACTTKAACAATAAAA	Intron	NA	368,398		
Phosphatidylinositol 3-kinase P-85 -alpha subunit	PIK3R1	20	5' ACAGCGAGGAMATTTTAAAAG	Intron	NA	368,398		
Phosphatidylinositol 3-kinase P-85 -alpha subunit	PIK3R1	20	5' TTTAAAAGTTSAGAAGGCCTT	Intron	NA	368,398		
Phosphatidylinositol 3-kinase P-85 -alpha subunit	PIK3R1	20	5' AAAACTTTTTSTTTCTCCTCC	Intron	NA	368	PIK3R1#4/PI3KR1-EX17#7	SNPlex
Phosphatidylinositol 3-kinase P-85 -alpha subunit	PIK3R1	20	5' TAAAATACTTKAACAATAAAA	Intron	NA	368,398	PIK3R1#3	SNPlex
Phosphatidylinositol 3-kinase P-85 -alpha subunit	PIK3R1	20	5' TGAAAGTAACMGCTATTGAAG	Exon (silent SNP)	NA	368	PI3KR1-EX11#6	SNPlex
Phosphatidylinositol 3-kinase P-85 -alpha subunit	PIK3R1	20	5' GCCGCCCTCCRGCCTGCTCCT	3' region	NA	368	PIK3R1-3'#5	SNPlex
Transportin	TNP01	20	5' ACACATACTTWGTTTACTGAC	Intron	NA	361, 368		SNPlex didn't work

* Where SNPs are denoted by IUB single letter codes (K = G/T, M = A/C, R = A/G, S = C/G, W = A/T, Y = C/T

Appendix 5.1 Combined MS and MS/MS MASCOT identification of differentially expressed proteins (P<0.05) in liver mitochondria (Angus 2005 cohort)

Spot[@]	Protein Identification	Organism	Accession no	MOSWE score (cut off score)	% seq MS	% seq MS/MS	Observed	Predicted		Average Ratio**
							pI	pI	MW	
266	No match	-	-	-	-	-	6.98	-	-	1.32
274	Albumin	Bos taurus	gi|162648	115 (63)	15.80%	10.40%	4.93	5.82	69293.41	-1.16
297	Heat shock 70 kDa protein 9B(mortalin 2)	Bos taurus	gi|73586960	145 (63)	33.10%	7.80%	5.3	5.79	73741.58	-1.31
298	PREDICTED: similar to Annexin A6 (Annexin VI) (Lipocortin VI) (P68) (P70) (Protein III)	Bos taurus	gi|76623595	99 (63)	32.40%	8.30%	5.47	5.86	84083.7	1.2
299	Heat shock 70 kDa protein 9B(mortalin 2)	Bos taurus	gi|73586960	104 (63)	28.40%	6.20%	5.34	5.79	73741.58	-1.36
300	PREDICTED: similar to Annexin A6 (Annexin VI) (Lipocortin VI) (P68) (P70) (Protein III)*	Bos taurus	gi| 76623595	56 (63)	-		5.43	5.86	84083.7	-1.21
301	ATPase, V1 subunit G2	-	-	-	-	-	5.37	-	-	-1.39
302	Succinate dehydrogenase	-	-	-	-	-	5.89	-	-	-1.32
350	LOC511913 protein (similar to 60 kDa heat shock protein)	Bos taurus	gi|74353880	83 (63)	31.80%	11.30%	5.12	8.9	42163.8	-1.32

Sample	Protein Identification	Organism	Accession no	MOSWE score (cut off score)	% seq MS	% seq MS/MS	Observed	Predicted		Average Ratio
							pI	pI	MW	
354	No match	-	-	-	-	-	5.19	-	-	1.28
355	LOC511913 protein (similar to 60 kDa heat shock protein)	Bos taurus	gil74353880	74 (63)	43.10%	11.30%	5.16	8.9	42163.8	-1.23
356	LOC511913 protein* (similar to 60 kDa heat shock protein)	Bos taurus	gil74353881	41 (63)	-	-	5.22	-	-	1.21
367	NADH dehydrogenase (ubiquinone) 1- alpha subcomplex, 5, 19 kDa	Bos taurus	gi|8039804	64 (63)	31.10%	4.50%	6.28	6.22	35,755.04	-1.28
381	catalase	Bos taurus	gil 229299	204 (63)	46.30%	10.30%	6.67	8.45	57472.75	-1.72
383	catalase	Bos taurus	gil 229299	108 (63)	41.40%	11.70%	6.84	8.45	57472.75	-1.74
420	Chain C, Bovine Mitochondrial F1-ATPase complexed with the peptide antibiotic efrapeptin	Bos taurus	gil 1942370	115 (63)	44.70%	5.70%	6.89	7.87	55234.35	-1.41
	Glutamate dehydrogenase 1	Bos taurus	gil 23306688	90 (63)	30.60%	6.00%		7.04	57666.58	
422	Glutamate dehydrogenase1	Bos taurus	gil 23306689	106 (63)	43.10%	10.20%	6.76	7.04	57666.58	1.35

Sample	Protein Identification	Organism	Accession no	MOSWE score (cut off score)	% seq MS	% seq MS/MS	Observed	Predicted		Average Ratio
							pI	pI	MW	
430	Chain C, Bovine Mitochondrial F1-ATPase complexed with the peptide antibiotic efrapeptin	Bos taurus	gil 1942370	182 (63)	51.00%	8.40%	8.91	7.87	55234.35	-1.31
431	Glutamate dehydrogenase 1, Mitochondrial precursor	Bos taurus	gil 52001466	116 (63)	34.90%	5.90%	6.98	7.25	61511.97	1.31
506	No match	-	-	-	-	-	6.4	-	-	1.6
542	TNF receptor - associated factor 2 isoform 2	-	-	-	-	-	5.85	-	-	-1.27
601	Hypothetical protein LOC515263 (similar to Aldolase B from ovis aries	Bos taurus	gil74354276	96 (63)	36.30%	12.10%	10.26	8.69	39543.1	-1.74
711	No match	-	-	-	-	-	9.93	-	-	-1.33
791	No match	-	-	-	-	-	8.63	-	-	-1.37

* Indicates a tentative protein assignment.
** Average ratio (high:low NFE) of the standerdized log abundance for each protein across the cohort. Negative ratio indicates down-regulation of protein and positive ratio indicates up-regulation of protein in high NFE animals.

Appendix 5.2 Combined MS and MS/MS MASCOT identification of differentially expressed proteins (P<0.05) in muscle mitochondria (Angus 2005 cohort)

Sample	Protein Identification	Organism	Accession no	MOSWE score (cut off score)	% seq MS	% seq MS/MS	Observed pI	Predicted		Average ratio**
								pI	MW	
457	No result	-	-	-	-	-	6.57	-	-	3.75
486	No result	-	-	-	-	-	5.92	-	-	
660	Similar to catalase	Bos taurus	gi|7467820	248/63	38.10%	10.10%	7.07	6.79	59,915.30	-1.74
887	Similar to beta enolase 92-phospho-D-glycerate hydro-lyase) (Muscle-specific enolase)(MSE) (Skeletal muscle enolase) (Enolase 3)	Bos taurus	gi|73587037	339/63	46.80%	17.50%	8.24	7.6	47,096.01	1.27
985	Chain B, crystal structure of bovine mitochondrial Bc1 complex, alpha carbon atoms only	Bos taurus	gi|3891849	420/63	23.40%	16.50%	7.12	6.97	44,974.80	1.38
1064	NDUFA10	Bos taurus	gi|74267974	133/63	22.20%	10.90%	5.58	6.18	37,755.04	1.32
	NADH dehydrogenase (ubiquinone) 1- alpha subcomplex, 10, 42 kDa	Bos taurus	gi|28603782	122/63	21%	10.50%		6.52	39,263.98	
1421	No Match	-	-	-	-	-	6.24	-	-	1.47
1422	Triosephosphate isomerase	Bos taurus	gi|61888856	99/63	43.40%	11.60%	6.83	6.45	26,689.51	1.24

Sample	Protein Identification	Organism	Accession no	MOSWE score (cut off score)	% seq MS	% seq MS/MS	Observed pI	Predicted		Average ratio**
								pI	MW	
1439	H (+)-trasporting ATP synthase	Bos taurus	gil102	69/63	20.10%	3.80%	7.17	9.21	59,719.64	1.22
	Bovine mitochondrial cytochrome Bc1 complex, E chain	Bos taurus	gil30749390	65/63	26.50%	14.80%		6.98	21,609.56	
1503	NADH dehydrogenase (ubiquinone) 1-alpha subcomplex, 10, 22 kDa	Bos taurus	gil73587329	261/63	47.20%	21.60%	10.8	8.74	20,964.84	1.24
1523	Adenylate kinase 1	Bos taurus	gil92097535	95/63	46.40%	12.90%	9.67	8.4	21,663.94	1.58
1757	Myoglobin	Bos taurus	gil127643	120/63	45.80%	28.10%	8.18	7.38	16,922.37	-4.78
2015	NADH dehydrogenase (ubiquinone) 1-alpha subcomplex, 5, 13 kDa	Bos taurus	gil81294272	142/63	27.60%	18.10%	7.92	7.82	13,315.63	1.43

** Average ratio (high:low NFE) of the standerdized log abundance for each protein across the cohort. Negative ratio indicates down-regulation of protein and positive ratio indicates up-regulation of protein in high NFE animals.

Appendix 5.3 Combined MS and MS/MS MASCOT identification of differentially expressed proteins (P<0.05) in liver mitochondria (Angus 2006 cohort)

Sample	Protein identification	Organi-sm	Accession no.	Score/ cut off	%seq. MS	%seq. MS/MS	Predict-ed pI	Observed pI	Predicted MW (Da)	Observed MW (Da)	Average ratio**
439	PREDICTED: similar to C-1-tetrahydrofolate synthase, (C1-THF synthase) isoform 4	*Bos taurus*	gi| 76628078	202/63	29.60%	3.60%	7.08	6.55	101,836	120,000	1.07
740	Chain , Bovine Annexin Vi/ lipocortin VI (Calcium-Bound)	*Bos taurus*	gi| 2914360	112/63	40.90%	4.50%	5.6	5.34	75,902	77,000	1.16
783	PREDICTED: similar to mitochondrial phosphoenolpyruvate carboxykinase 2 isoform 1precursor isoform	*Bos taurus*	gi| 76626830	163/63	44.20%	5%	8.14	6.77	70,650	68,000	1.28
811	PREDICTED: similar to mitochondrial phosphoenolpyruvate carboxykinase 2 isoform 1precursor isoform 1	*Bos taurus*	gi| 76626830	110/63	34.20%	1.70%	8.14	6.44	70,650	66,000	1.24
	PREDICTED: similar to kidney-specific protein (KS), partial	*Bos taurus*	gi| 76694395	110/63	71.50%	11%	#		#		
	Aspartate aminotransferase 1	*Bos taurus*	gi| 59858077	64/63	33.20%	3.10%	6.73		46,382		

Sample	Protein identification	*Organi-sm*	Accession no.	Score/ cut off	%seq. MS	%seq. MS/MS	Predicted pI	Observed pI	Predicted MW (Da)	Observed MW (Da)	Average ratio
849	PREDICTED: similar to 60 kDa heat shock protein, mitochondrial precursor (Hsp60) (60 kDa chaperonin) (CPN60) (Heat shock protein 60)(HSP-60)	*Bos taurus*	gi| 74005074	242/63	35.70%	9.60%	5.47	4.88	57,700	64,000	1.33
904	Protein disulfide-isomerase ER60 precursor / Glucose regulated protein 58KDa/ Carnitine palmitoyltransferase isoenzyme	*Bos taurus*	gi| 1083063	337/63	50.20%	7.80%	6.51	5.48	54,973	61,000	1.54
930	Vimentin	*Bos taurus*	gi| 1353211	114/63	31.80%	6%	5.2	4.41	53,677	60,000	-1.11
1102	PREDICTED: similar to angiomotin like 2	*Bos taurus*	gi| 76608247	65/63	20.20%	1.80%	6.7	5.8	84,727	56,000	1.59
	Integrin beta-2	*Bos taurus*	gi| 53680687	64/63	53.80%	23.10%	7.2		13,006		
1261	Tu translation elongation factor, mitochondrial	*Bos taurus*	gi| 27806367	453/63	48.20%	14.30%	6.72	5.86	49,398	46,000	1.33
1334	hypothetical protein LOC537713 *(similar to GTP-specific succinyl-CoA synthetase)*	*Bos taurus*	gi| 77736229	148/63	26.90%	9%	7.51	5.21	46,691	42,000	1.25
2189	PREDICTED: similar to Glutathione S transferase Mu 1 (GSTM1-1	*Bos taurus*	gi| 76613071	183/63	55%	15.60%	6.45	6.33	25,656	26,000	1.15

Sample	Protein identification	*Organi-sm*	Accession no.	Score/ cut off	%seq. MS	%seq. MS/MS	Predicted pI	Observed pI	Predicted MW (Da)	Observed MW (Da)	Average ratio
2845	No Match	*Bos taurus*	-	-	-	-	-	4.81	-	8,000	1.27
2882	No Match	*Bos taurus*	-	-	-	-	-	9.8	-	8,000	2.56
3128	Heat-shock protein beta-1 (HspB1) (Heat shock 27 kDa protein) (HSP 27)	*Bos taurus*	gi|85542053	346/63	50.20%	20.40%	5.98	5.46	22,393	25,000	1.13

Identified protein represents only a partial sequence, therefore, the pI and MW values of the full length protein are unknown.
* Whilst this value suggestes a high level of sequence coverage by MS/MS analysis, the qualities of the spectra were poor with no discernable sequence tags.
** Average ratio (high:low NFE) of the standerdized log abundance for each protein across the cohort. Negative ratio indicates down-regulation of protein and positive ratio indicates up-regulation of protein in high NFE animals.

Appendix 5.4 Functional significance of differentially expressed mitochondrial proteins (p<0.05)

No	Name	Protein accession number	Average ratio[a]	Molecular weight	pI	BTA position	Function	Reference
Oxidative phosphorylation								
Complex I								
1	NADH dehydrogenase (ubiquinone) 1- alpha subcomplex, 10, 42 kDa	gi|74267974	1.32	37,755.04	6.18	BTA 3, 85 Mb	Involve in electron transfer chain and cellualr energy production	Murray et al 1990
2	NADH dehydrogenase (ubiquinone) 1- alpha subcomplex, 10, 22 kDa	gi|73587329	1.24	20,964.84	8.74	UN	Involve in electron transfer chain and cellualr energy production	Murray et al 1990
3	NADH dehydrogenase (ubiquinone) 1- alpha subcomplex, 5, 13 kDa	gi|81294272	1.43	13,315.63	7.82	UN	Involve in electron transfer chain and cellualr energy production	Murray et al 1990
4	NADH dehydrogenase (ubiquinone) 1- alpha subcomplex, 5, 19 kDa	gi|8039804	-1.28	35,755.04	6.28	BTA 11, 73 Mb	Involve in electron transfer chain and cellualr energy production	Murray et al 1990
Complex V								
5	ATPase, V1 subunit G2		-1.39		5.37	BTA 23? BTA11?	Involve in electron transfer chain and cellualr energy production	Murray et al 1990

No.	Name	Protein accession number	Average ratio[a]	Molecular weight	pI	BTA position	Function	Reference
6	Chain C, Bovine Mitochondrial F1-ATPase complexed with the peptide antibiotic efrapeptin	gi|1942370	-1.41	55234.35	7.87	UN	Involve in electron transfer chain and cellualr energy production	Murray et al 1990
Complex III								
7	Chain B, crystal structure of bovine mitochondrial Bc1 complex, alpha carbon atoms only	gi|3891849	1.38	44,974.80	6.97	BTA 10?	Involve in electron transfer chain and cellualr energy production	Murray et al 1990
Complex II								
8	Succinate dehydrogenase		-1.32		5.89	BTA 2, 86 Mb	Involve in electron transfer chain and cellualr energy production	Murray et al 1990
Stress related proteins								
9	Catalase	gi|7467820	-1.74	59,915.30	7.07	BTA 15, 39 Mb	Strong antioxidant, which reduces the level of hydrogen peroxide developed from fatty acid oxidation, and thus, is involved in the ROS metabolic pathway.	Suttorp 1986

No.	Name	Protein accession number	Average ratio[a]	Molecular weight	pI	BTA position	Function	Reference
10	Glutathione S transferase Mu 1 (GSTM1-1) (GST class-mu 1) (GSTM1a-1a) (GSTM1b-1b) (HB subunit 4) (GTH4) isoform 1	gi|76613071	1.15	25,656	6.45	BTA 3, 25 Mb	Glutathione-s-transferases (GSTs) conjugate GSH to free-radicals or xenobiotics. GST activity depletes GSH levels and may either detoxify or enhance the toxicity of a compound.	Bekris et al 2005
11	Heat shock 70 kDa protein 9B (mortalin 2)	gi|73586960	-1.36	73741.58	5.34	UN	Expression is substantial during stressful conditions, such as heat shock, inhibition of energy metabolism, exposure to heavy metals, oxidative stress, and inflammation	Zylicz et al, 2001; Jolly et al 2000
12	60 kDa heat shock protein, mitochondrial precursor (Hsp60) (60 kDa chaperonin) (CPN60) (Heat shock protein 60)(HSP-60)	gi|74005074	-1.32!	57,700	5.47	BTA 19, 28 Mb		
13	Heat-shock protein beta-1 (HspB1) (Heat shock 27 kDa protein) (HSP 27)	gi|85542053	1.13	22,393	5.98	BTA 25, 31 Mb		
14	Albumin	gi|162648	-1.16	69293.41	5.82	BTA 28, 25Mb	Binds fatty acids and is involved in oxidative stress in mitochondria.	Bito R, 2005

No.	Name	Protein accession number	Average ratio[a]	Molecular weight	pI	BTA position	Function	Reference
Energy production, glucose turnover								
15	Mitochondrial phosphoenolpyruvate carboxykinase 2 isoform 1 precursor isoform	gi|76626830	1.28	70,650	8.14	BTA 10, 12Mb	Involved in anaplerotic biochemical pathways, gluconeogenesis, enzymatic reactions that replenish TCA cycle intermediates	Croniger , 2002
16	Carnitine palmitoyltransferase isoenzyme / Glucose regulated protein 58 kDa / protein disulfide-isomerase ER60 precursor	gi|1083063	1.52	54,973	6.51	UN	Involve in AMPK pathway and LCFA-CoA oxidation	Obici and Rossetti, 2003
17	Aldolase B	gi|74354276	-1.74	39543.1	8.69	BTA 8 48 Mb	Involve in fructose metabolism and gluconeogenesis	Cox (1988)

No.	Name	Protein accession number	Average ratio[a]	Molecular weight	pI	BTA position	Function	Reference
18	Similar to beta enolase 92-phospho-D-glycerate hydro-lyase) (Muscle-specific enolase)(MSE) (Skeletal muscle enolase) (Enolase 3)	gi|73587037	1.27	47,096.01	7.6	BTA 19, 14 Mb	Involved in the glycolytic activity of muscle catalyse the reversible dehydration of 2-phospho-D-glycerate to phosphoenolpyruvate as part of the glycolytic and gluconeogenesis pathways	Pancholi 2001, Horecker, 1972
19	TNF receptor - associated factor 2 isoform 2		-1.27		5.85	UN	Play partial role in development of insulin resistance	Robinson, et al 2000
20	Adenylate kinase 1	gi|92097535	1.58	21,663.94	8.4	BTA 11, 77 Mb	Maintenance of cellular energetic economy, enabling skeletal muscle to perform at the lowest metabolic cost. Defficiency develops higher ATP turnover rate and larger amounts of ATP consumed per contraction	Janssen 2000
21	Triosephosphate isomerase	gi|61888856	1.24	26,689.51	6.45	BTA 5, 60Mb	Glycolytic enzyme that catalyzes the reversible interconversion of glyceraldehyde 3-phosphate and dihydroxyacetone phosphate, plays important role in glycolysis and is essential for efficient energy production	Lolis et al 1990

No.	Name	Protein accession number	Average ratio[a]	Molecular weight	pI	BTA position	Function	Reference
Protein turnover and nitrogen balance								
22	Glutamate dehydrogenase 1	gi|23306689	1.35	57666.58	7.04	BTA 28?	Rate-limiting enzyme in amino acid degradation and also is a marker for TCA and OX-PHOS activities, also involve in protein turnover and N balance	Miller et al, 1990
Miochondrial DNA and protein biosynthesis								
23	Tu translation elongation factor, mitochondrial	gi|27806367	1.33	49,398	6.72	BTA 25, 24Mb	Protein biosynthesis, Maintenance of mitochondrial deoxyribonucleoside triphosphate (dNTP) pools or replication of mtDNA	Chiron et al 2005
24	Succinyl-CoA synthetase	gi|77736229	1.25	46,691	7.51	BTA 11, 37Mb	Generates high-energy phosphate at the substarte level, during TCA cycle, Maintenance of mitochondrial deoxyribonucleoside triphosphate (dNTP) pools or replication of mtDNA.	Orly et al 2005

No.	Name	Protein accession number	Average ratio[a]	Molecular weight	pI	BTA position	Function	Reference
25	C-1-tetrahydrofolate synthase, isoform 4 (C1-THF synthase)	gi| 76628078	1.07	120,000	6.55	UN	Interconverts folic acid derivatives between various oxidation states, purine biosynthesis	Howard et al 2003
Cytoskeleton								
26	Vimentin	gi|1353211	-1.11	60,000	4.41	BTA 13	Control the transport of low density lipoprotein, LDL,-derived cholesterol from a lysosome to the site of esterification	Sarria et al 1992
27	Lipocortin VI (Annexin VI)	gi| 76623595	1.2	84,083	5.47	UN	Structural proein regulated by calcium	Grewal et al 2000
Identity not confirmed								
1	Angiomotin like 2	gi| 76608247	1.59	56,000	5.8	BTA 1	Motility regulator of vascular endothelial cells	Jiang et al 2006
2	Integrin beta-2 or leukocyte cell adhesion molecule CD18	gi| 53680687	1.59	56,000	5.8	BTA 1	Regulates immunity of the body	Hynes 1992
3	Aspartate aminotransferase 1	gi| 59858077	1.24	46,382	6.73	BTA 18, 23 Mb	Protein turnover and trasamination reaction	Barron et al 1998
4	H (+)-trasporting ATP synthase	gi|102	1.22	59,719.64	7.17	UN	Involve in electron transfer chain and cellualr energy production	Murray et al 1990
5	Bc1 complex, E chain	gi|30749390	1.22	21,609.56	7.17	UN	Involve in electron transfer chain and cellualr energy production	Murray et al 1990

a: average ratio (high:low NFE) of the standardised log abundance for each protein across cohort. Negative ratio indicates down-regulation of proteins and positive ratio indicates up-regulation of proteins; UN: unknown

Appendix 6.1 Mitochondrial genes involved in oxidative phosphorylation (identified in the QTL and 2-D DIGE proteomic experiments).

GENE NAME	Gene identified in following experiment
NADH-ubiquinone oxidoreductase B15 subunit (Complex I-B15) (CI-B15)	QTL experiment
NADH-ubiquinone oxido-reductase SGDH subunit, mitochondrial precursor (Complex I-SGDH) 75 kDa	QTL experiment, 2-D experiment
NADH-ubiquinone oxidoreductase 19 kDa subunit (Complex I-19KD)	QTL experiment, 2-D experiment
NADH-ubiquinone oxidoreductase 22 kDa beta subunit (Complex I)	2-D experiment
NADH-ubiquinone oxidoreductase 13 kDa alpha subunit (Complex I)	2-D experiment
NADH-ubiquinone oxidoreductase 42 kDa alpha subunit (Complex I)	2-D experiment
NADH-ubiquinone oxidoreductase 18 kDa alpha subunit (Complex I)	QTL experiment
NADH-ubiquinone oxidoreductase 16 kDa alpha subunit (Complex I)	QTL experiment
Cytochrome c oxidase subunit VIIa-related protein, mitochondrial precursor (COX7a-related protein) (EB1).	QTL experiment
V-ATPase V1, G2 subunit	2-D experiment, QTL
V-ATPase B2 subunit	QTL experiment
Vacuolar ATP synthase subunit G 1 (V-ATPase G subunit 1) (Vacuolar proton pump G subunit 1 (V-ATPase 13 kDa subunit 1) (Vacuolar ATP synthase subunit M16).	QTL experiment
Chain C, Bovine Mitochondrial F1- ATPase complexed with the peptide antibiotic efrapeptin	2-D experiment
Vacuolar ATP synthase catalytic subunit a, ubiquitous isoform (V-ATPase a subunit 1) (vacuolar proton pump alpha subunit 1) (v-atpase 69 KDa subunit 1) (isoform Va68)	QTL experiment
Complex III, chain B	2-D experiment
Complex III, chain E	2-D experiment
Succinate dehydrogenase (Complex II)	2-D experiment

Appendix 6.2 Genes involved in GHR-IRS-PI3K pathway (found within NFE-QTL)

Name of gene	BTA chromosome
Phosphoinositide-3-kinase, regulatory subunit 4, p150; phosphatidylinositol 3-kinase-associated p150	1
IGF-II mRNA-binding protein 2	1
Mitogen-activated protein kinase 10 (EC 2.7.1.37) (Stress-activated protein kinase JNK3) (c-Jun N-terminal kinase 3) (MAP kinase p49 3F12).	6
Mitogen-activated protein kinase kinase 1 interacting protein 1 (MEK binding partner 1) (Mp1).	6
Pro-epidermal growth factor precursor (EGF) [Contains: Epidermal growth factor (Urogastrone)].	6
Orexigenic neuropeptide QRFP receptor (G-protein coupled receptor 103) (SP9155) (AQ27).	6
Tyrosine kinase, endothelial TEK	8
Docking protein 2(p56(dok-2) (Downstream of tyrosine kinase 2)	8
Mitogen-activated protein kinase phosphatase 2 (MAP kinase phosphatase 2) (MKP-2) (Dual specificity protein phosphatase hVH2).	8
Insulin-like growth factor binding protein-like 1	8
Tyrosine-protein kinase (Janus kinase 2) (JAK-2).	8
Orexigenic neuropeptide QRFP precursor (P518)	8
SH2 domain containing 3C isoform 2	8
SHB (Src homology 2 domain containing) adaptor protein B	8
SHC transforming protein 3 (SH2 domain protein C3) (Src homology 2 domain containing transforming protein C3)	8
Insulin-like growth factor 2 receptor	9
Insulin receptor substrate 1 (IRS-1).	11
Corticotropin-lipotropin precursor (Pro-opiomelanocortin) (POMC) [Contains: NPP; Melanotropin gamma (Gamma-MSH); Potential peptide; Corticotropin (Adrenocorticotropic hormone) (ACTH); Melanotropin alpha (Alpha-MSH); Corticotropin-like intermediary peptide	11

Appendix 6.2 Genes involved in IRS-PI3K pathway (found within NFE-QTL) (continuation)

Name of gene	BTA chromosome
Mitogen-activated protein kinase kinase kinase kinase 3 (MAPK/ERK kinase kinase kinase 3) (MEK kinase kinase 3) (MEKKK 3) (Germinal center kinase-related protein kinase) (GLK).	11
Cytokine inducible SH2-containing protein 5 (Suppressor of cytokine signalling 5) (SOCS-5) (Cytokine-inducible SH2 protein 6) (CIS-6).	11
Mitogen-activated protein kinase kinase kinase 1 (MAPK/ERK kinase kinase 1) (MEK kinase 1) (MAPKK 1) (fragment).	20
Insulin gene enhancer protein ISL-1 (ISLET-1).	20
Growth hormone receptor precursor (GHR)	20
AMPK alpha-1 chain	20
Prolactin receptor	20
Cocaine and amphetamine regulated transcript	20
Phosphatidylinositol 3-kinase regulatory alpha subunit (PI3-kinase P85-alpha subunit) (ptdins-3-kinase P85-alpha) (PI3k).	20

References

REFERENCES

Adams, MW. and Belyra, RL. (1987) Nutritional and energetic differences of dairy cows varying in milk yield. *Journal of Animal Science*, **70**:182 (Supplement 1).

Adeola, OLG., Young, BW., McBride, BW., and Ball, RO. (1989) *In vitro* Na^+K^+ATPase (EC 3.6.1.3)-dependent repiration and protein synthesis in skeletal muscle of pigs fed at three dietary protein levels. *The British Journal of Nutrition*, **61**:453-465.

Ait-Si-Ali, S., Ramirez, S., Robin, P., Trouche, D., and Harel-Bellan, A. (1998) A rapid and sensitive assay for histone acetyl-transferase activity. *Nucleic Acids Res.* **26**:3869–3870.

Alban, A., David, S., Bjorkesten, L., Andersson, C., Sloge, E., Lewis, S. and Currie, I. (2003) A novel experimental design for comparative two-dimensional gel analysis: Two-dimensional difference gel electrophoresis incorporating a pooled internal standard. *Proteomics,* **3**:36-44.

Alfanso, P., Nunez, A., Madoz-Gurpide, J., Lombardia, L., Sanchez, L. and Casal, I. (2005) Proteomic expression analysis of colorectal cancer by two-dimensional differential gel electrophoresis. *Proteomics,* **5**:202-2611.

Allen, DL., Weber, JN., Sycuro, LK. and Leinwand, LA. (2005) Myocyte enhancer factor-2 and serum response factor binding elements regulate fast myosin heavy chain transcription in vivo. *Journal of Biological Chemistry*, **280**:17126–34.

Amthor, H., Nicholas, G., McKinnell, I., Kemp, CF., Sharma, M., Kambadur, R., Patel, K. (2004) Follistatin complexes myostatinand antagonises mysostatin-mediated inhibition of myogenesis. *Dev Biol.* **270**:19-30.

Ana, RN. , Ana, R., Marta, CN. , Michiel K. , Jeroen H. , Willem, M. de V., Jonas, A. and Helena S. (2000) *In vivo* nuclear magnetic resonance studies of glycolytic kinetics in Lactococcus lactis. *Biotechnology and Bioengineering,* **64**: 200 – 212.

Andersson, U., Filipsson, K., Abbott, C., Woods, A., Smith, K., Bloom, S., Carling, D., and Small, C. (2004) AMP-activated protein kinase plays a role in the control of food intake. The Journal of Biological Chemistry, 279:12005-12008.

Angus Society of Australia, 2002. Trial breed plan EBVs for net feed intake (NFI). The Angus Society of Australia, Armidale, Australia.

Ankra-Badu, GA. and Aggrey, SE. (2005) Identification of candidate genes at quantitative trait loci on chicken chromosome Z using orthologous comparison of chicken, mouse, and human genomes In Silico. *Biology,* **5**:53-362.

Archer, JA., Arthur, PF., Herd, RM., Parnell, PF. and Pitchford, WS. (1997) Optimum postweaning test for measurement of growth rate, feed intake, and feed efficiency in British breed cattle. *Journal of Animal Science,* **75**:2024-2032.

Archer, JA., Arthur, PF., Herd, RA. and Richardson, EC. (1998) Genetic variation in feed efficiency and its component traits. In: *Proc. 6th World Cong. Genet. Appl. Livest. Prod. Armidale, NSW, Australia.* **25**:81-84.

Archer, JA. and Barwick, SA. (2001) An analysis of investment in advanced breeding program designs for beef cattle. In: *Proc. 14th Conf. Assoc. Advmt. Anim. Breed. Genet., Queenstown, New Zealand,* Pages 465–468.

Archer, JA., Barwick, SA. and Graser, HU. (2004) Economic evaluation of beef cattle breeding schemes incorporating performance testing of young bulls for feed intake. *Australian Journal of Experimental Agriculture,* **44**:393-404.

Archer, JA. and Pitchford, WS. (1996) Phenotypic variation in residual food intake of mice at different ages and its relationship with efficiency of growth, maintenance and body composition. *Animal Science*, (Penicuik, Scotland), **63**:149-157.

Archer, JA., Pitchford, WS. Hughes, TE. and Parnell, PF. (1998) Genetic and phenotypic relationship between food intake, growth, effieicny and body composition of mice post waening and at maturity. Animal Science (Penicuik, Scotland), **67**:171-182.

Archer, JA., Richardson, EC., Herd, RM., and Arthur, PF. (1999) Potential for selection to improve efficiency of feed use in beef cattle: a review, *Australian Journal of Experimental Agriculture,* **50**:147-161.

Armsby, HP. and Fries, JA. (1911) The influence of type and of age upon the utilization of feed by cattle. Bull. No. 128. Washington, D.C., U.S. Department of Agriculture, Bureau of Animal Industry.

Arthur, PF., Archer, JA. and Herd, RM., (2004) Feed intake and efficiency in beef cattle: overview of recent Australian research and challenges for the future. *Australian Journal of Experimental Agriculture,* **44**:361-369.

Arthur, PF., Archer, JA., Herd, RM., and Melville, GJ. (2001a) Response to selection for net feed intake in beef cattle. In *Proc. 14th Conf. Assoc. Advancement Anim. Breed. Genet.,* Queenstown, New Zealand Pages (135-138)

Arthur, PF., Archer, JA., Johnston, DJ., Herd, RM., Richardson, EC. and Parnell, PF. (2001b) Genetic and phenotypic variance and covariance components for feed intake, feed efficiency and other postweaning traits in Angus cattle. *J. Anim. Sci.,* **79**:2805–2811.

Arthur, PF., Archer, JA., Herd, RM., Johnston, DJ., Richardson, EC. and Parnell PF. (2001c) Genetic and phenotypic variance and co-variance components of feed intake, feed efficiency and other postweaning traits in angus cattle. *Journal of Animal Science,* **79**:2805-2811.

Arthur, PF., Arthur, JA., Herd, RM., and Richardson, EC. (1999) Relationship between postweaning growth, net feed intake and cow performance. *In Proc. 13th Conf. Assoc. Advancement Anim. Breed. Genet.*, Mandurah, Australia 484-487.

Arthur, PF., Herd, RM., Wright, J., Xu, G., Dibley, K. and Richardson, EC. (1996) Net feed conversion efficiency and its relationship with other traits in beef cattle. *Proceedings of the Australian Society of Animal Production,* **21**: 107-110.

Arthur, PF., Renand, G. and Krauss, D. (2001d) Genetic and phenotypic relationships among different measures of growth and feed efficiency in young charolais bulls. *Livestock Production Science,* **668**:131-139.

Asakawa, A., Inui, A., Ueno, N., Fujimiya, M., Fujino, MA., and Kasuga, M. (1999) Mouse pancreatic polypeptide modulates food intake, while not influencing anxiety in mice. *Peptides*, **20**:1445-1448.

Asakawa, A., Inui, A., Ueno, N., Makino, S., Fujino, MA., and Kasuga. M. (1999). Urocortin reduces food intake and gastric emptying in lean and ob/ob obese mice. *Gastroenterology,* **116**:1287–1292.

Aubert, JO., Champigny, P., Saint-Marc, P., Negrel, R., Collins, S., Ricquier, D., and Ailhaud, G. (1997) Up-regulation of UCP-2 gene expression by PPAR agonists in preadipocytes and adipose cells. *Biochem. Biophys. Res. Commun.* **238**:606-611.

Audero, E., Cascone. I., Maniero, F., Napione, L., Arese, M., Lanfrancone, L.and Bussolino, F. (2004) Adaptor ShcA protein binds tyrosine kinase Tie2 receptor and regulates migration and sprouting but not survival of endothelial cells. *J. Biol. Chem.,* **26**:13224-33.

Avendaño, A., Deluna, A., Olivera, H., Valenzuela, L., and Gonzalez, A. (1997) GDH3 encodes a glutamate dehydrogenase isozyme, a previously unrecognized route for glutamate biosynthesis in Saccharomyces cerevisiae. *J. Bacteriol.,* **179**:5594–5597.

Bado, A., Levasseur, S., Attoub, S., Kermorgant, S., Laigneau, JP., Bortoluzzi, MN., Moizo, L., Lehy, T., Guerre-Millo, M., Marchand-Brustel, Y., and Lewin, MJ. (1998) The stomach is a source of leptin. *Nature,* **394**: 790–793.

Baile, C. and Della-Fera, MA. (2001) The future of feed intake regulation research. *J. of Animal Science*, **79**:1-9.

Baker, J., Liu, J-P., Robertson, EJ. and Efstratiadis, A. (1993) Role of insulin-like growth factors in embryonic and postnatal growth. *Cell,* **75**:73–82.

Baldwin, G. (1994) Antiproliferative gastrin/cholecystokinin receptor antagonists target the 78-kDa gastrin-binding protein (autocrine loop/colorectal carduoma/gastrin receptor). *Proc. Natl. Acad. Sci. USA,* **91**:7593-7597.

Baracos, VE., Devivo, C., Hoyle, DHR., and Goldberg, AL. (1995) Activation of different proteolytic systems in skeletal muscles of cachexic rats bearing a hepatome. *Am. J. Physiology,* **268**:E996-E1006.

Barkan, AL., Dimaraki, EV., Jessup, SK., Symons, KV., Ermolenko, M., Jaffe, CA. (2003) Ghrelin secretion in humans is sexually dimorphic, suppressed by somatostatin, and not affected by the ambient growth hormone levels. *J. Clin. Endocrinol. Metab.,* **88**:2180-2184.

Barron, J.T., Gu, L., and Parrillo, J.E. (1998) Malate-aspartate shuttle, cytoplasmic NADH redox potential, and energetics in vascular smooth muscle. *J Mol Cell Cardiol.* **30**:1571-1579.

Basarab, J. (2003) Net feed efficiency project update. Western Forage/Beef Group and Alberta Agriculture, Food and Rural Development. (October issue).

Basarab, JA., Price, MA., Aalhus, JA., Okine, EK., Snelling, WM. and Lyle, KL. (2003) Residual feed intake and body composition in young growing cattle. *Can. J. Anim. Sci.* **83**:189-204.

Basarab, JA., Ramsey, P., French, N., Crews, D., Okine, KLE. Moore, S. and Price, M. (2005). Commercialization of Net Feed Efficiency (NFE): Olds College NFE Test Facility - 2002 to 2005. *Net feed Efficiency Bull Test Results Meeting, Olds College, Olds, Alberta, Canada (Agriculture, food and rural development).*

Beaudry, G., Zekki, H., Rouillard, C. and Leyesque, D. (2004). Clozapine and dopamine d[3] receptor antisense reduce cocaine- and amphetamine-regulated transcript expression in the rat nucleus accumbens shell. *Synapse,* **51**:233-240.

Bekris, L., Shephard, C., Peterson, M., Hoehna, J., Yserloo, B., Rutledge, E., Farin, F., Kavanagh, T. and Lernmark, A. (2005) Glutathione-s-transferase M1 and T1 polymorphisms and associations with type 1 diabetes age-at-onset. *Autoimmunity,* **38**:567 – 575.

Belmont, JW., Reid, B., Taylor, W., Baker S., Moore, W., Morriss, MC., Podrebarac, SM., Glass, N., and Schwartz D (2002). Congenital sucrase-isomaltase deficiency presenting with failure to thrive, hypercalcemia, and nephrocalcinosis. *BMC Pediatrics,* **2**: 4.

Benomar, Y., Roy, A., Aubourg, A., Djiane, J., and Taouis, M. (2005) Cross down-regulation of leptin and insulin receptor expression and signalling in a human neuronal cell line, *Biochem J.,* **15**: 929–939.

Berkelman, T., Brubacher, M., Chang, H., CrosS, T., and Strong, W. (2005) Tips to prevent streaking on 2-D gels. *American Biotechnology Laboratory,* **28**:8-10.

Berner, HS., Lyngstadaas, SP., Spahr, A., Monjo, M., Thommesen, L., Drevon, CA., Syversen, U. and Reseland, J.E. (2004) Adiponectin and its receptors are expressed in bone-forming cells. *Bone,* **35**: 842–9.

Bernier, JF. (1986) Maintenance energy requirement and net energetic efficiency in mice with a major gene for rapid postweaning gain. *J. Nutr.,* **116**: 419-428.

Bishop, SC. and Hill, WG. (1985) Effects of selection on growth, body composition, and food intake in mice. III. Correlated responses: growth, body compostion, food intake, efficiency and metabolism. *Genetical Research*, **46**:57-74.

Bito, R., Hino, S., Baba, A., Tanaka, M., Watabe, H. and Kawabata, H. (2005) Degradation of oxidative stress-induced denatured albumin in rat liver endothelial cells. *Am J Physiol Cell Physiol.* **289**:C531-C542.

Bizeau, M., Willis, W. and Hazel, J. (1998) Differential responses to endurance training in subsarcolemmal and intermyofibrillar mitochondria. *Journal of Applied Physiology*, **85**:1279-1284.

Bole-Fesot, C., Goffin, V., Edery, M., Binart, N., and. Kelly, P. (1999) Prolactin (PRL) and Its Receptor: Actions, Signal Transduction Pathways and Phenotypes Observed in PRL Receptor Knockout Mice. *Endocrine reviews*, **19**:225-268.

Bordas, A., Tixier-Boichard, M., and Merat, P. (1992) Direct and correlated responces to divergent selection for residual food intake in Rhode Island Red laying hens. *British Poultry Science*, **33**:741-754.

Botma, G., Verhoeven, A.J. and Jansen, H. (2001) Hepatic lipase promoter activity is reduced by the C-480G and G-216A substitutions present in the common *LIPC* variant and is increased by upstream stimulatory factor. *Atherosclerosis,* **154**: 625–32.

Bottje, W., Iqbal, M., Pumford, N. R., Ojano-Dirain, C. and Lessiter, K. (2004) Role of mitochondria in the phenotypic expression of feed efficiency. *Poultry Science,* **13**:94-105.

Bottje, W., Iqbal, M., Pumford, N. R., Ojano-Dirain, C. and Lessiter, K. (2006) Invited Review: Feed efficiency and mitochondrial function. *Poultry Science,* **85**:8-14.

Bottje, W., Tang, X., Cawthon, D., Okimoto, R., Wing, T. and Cooper, M. (2002) Association of mitochondrial function with feed efficiency within a single genetic line of male broilers. *Poultry Science,* **81**:546-555.

Bourges, I., Ramus, C., Mousson de Camaret, B., Beugnot, R., Remacle, C., Cardol, P.,Hofhaus, G. and Issartel, J.-P. (2004) Structural organization of mitochondrial human complex I: role of the ND4 and ND5 mitochondria-encoded subunits and interaction with prohibitin. *Biochem. J.*, **383**:491-499.

Brameld, JM., Buttery, PJ., Dawson, JM. and Harper Jane, M. (1998) Nutritional and hormonal control of skeletal muscle cell growth and differentiation. *Proc. Nutr. Soc.*, **57**:207-217.

Brand, MD., Affourtit, C., Esteves, TC., Green, K., Lambert, AJ., Miwa, S., Pakay, JL. and Parker, N. (2004) *Free Radical Biol. Med.*, **37**:755–767.

Bray, GA. (2000) Afferent signals regulating food intake. *Proc. Nutr. Soc.*, **59**:373-384.

Bray, GA., Fisler, J., and York, DA. (1990) Neuroendocrine control of the development of obesity: understanding gained from studies of experimental animal models. *Front. Neuroendocrinol.*, **11**:128-181.

Breitbart, RE., Liang, C., Smoot, B., Laheru, DA., Mahdavi, V., Nadal-Ginard, B. (1993) A fourth human MEF2 transcription factor, hMEF2D, is an early marker of the myogenic lineage. *Development,* **118**: 1095-1106.

Brelin, B. and Brannang, E. (1982) Phenotypic and genetic variation in feed efficiency of growing cattle and their relationship with growth rate, carcass traits and metabolic efficiency. *Swedish Journal of Agricultural Research*, **12**:29-34.

Broberger, C. (2000) Cocain- and amphetamine-regulated transcript (CART) and food iintake:behaviour in search of anatomy, *Drug Development Research*, **51**:124-142.

Brockmann, GA. and Bevova, MR. (2002) Using mouse models to dissect the genetics of obesity. *Trends in Genetics*, **18**:367-376.

Brockmann, GA., Hayley, C., Renne, U., Knott, S., and Schwerin, M. (1998) Qunatitative trait loci affecting body weight and fatness from a mouse line selected for extreme high growth. *Genetics,* **150**:369-381.

Brooks, H. and Krahenbuhl, S. (2000) Development of a new assay for complex I of the respiratory chain. *Clinical Chemistry,* **46**:345-350.

Brown, GC. (1992) Control of respiration and ATP synthesis in mammalian mitochondria and cells. *Biochem. J.,* **284**: 1–13.

Buchanan, FC., Fitzsimmons, CJ., Van Kessel, AG., Thue, TD., Sim, DCW. and Schmutz, SM. (2002) Association of a missense mutation in the bovine leptin gene with carcass fat content and leptin mRNA levels. *Genet. Sel. Evol.,* **34**:105–116.

Bunger, L., MacLeod, MG., Wallace, CA. and Hill, WG. (1998) Direct and correlated effects of selection for food intake correlated for liveweight in the adult mouse. In '*Proceedings of the 6th World*

Congress on Genetics Applied to Livestock Production'. Vol 26. (Ed. L Piper) pp. 97-100. (University of New England, Armidale).

Burrin, DG., Ferrell, CL., Britton, RA., and Bauer, M. (1990) Level of nutrition and visceral organ size and metabolic efficiency. *Swedish Journal of Agricultural Research*, **12**:29-34.

Burrow, HM. and Bindon, BM. (2005) Genetics research in cooperative research centre for cattle and beef quality. *Australian Journal of Experimental Agriculture,* **45**:941-657.

Butler, AA., Marks, DL., Fan, W., Kuhn, CM., Bartolome, M., and Cone, RD. (2001) Melanocortin-4 receptor is required for acute homeostatic responses to increased dietary fat. *Nat Neurosci.*, **4**:605-611.

Cai, A. and Hyde, JF. (1999) The human growth hormone-releasing hormone transgenic mouse as a model of modest obesity: differential changes in leptin receptor (OBR) gene expression in the anterior pituitary and hypothalamus after fasting and OBR localization in somatotrophs. *Endocrinology,* **140**: 3609-3614.

Cai, L., Taylor, J., Smyth, K., Findeisen, B., Lehn, C., and Davis, S. (2004) *Quantitative Trait Loci and Somatostatin.* United States Patent Application no 20040018511 Available at http://appft1.uspto.gov/netahtml/PTO/srchnum.html [accessed 12 October 2006].

Calo G., Guerrini, R., Rizzi, A., Salvadori, S., and Regoli, D. (2000) Pharmacology of nociceptin and its receptor: a novel therapeutic target. *British Journal of Pharmacology,* **129**:1261–1283.

Cameron, ND. (1998) Across species comparisons in selection for efficiency. *Proceedings 6th World Congress on Genetics Applied to Livestock Production*, Armidale, Australia **25**:73-80.

Campbell, and Fabbraio (2001) Effect of ovarian hormones on mitochondrial enzyme activity in the fat oxidation pathway of skeletal muscle. *Am. J. Physiol. Endocrinol. Metab.,* **281**:E803-E808.

Carstens, GE., Johnson, DE., Bourdon,M., Richardson, GV, and Johnson, KA (1987b) Metabolic rate comparisons in monozygous beef calves. *Proc. West. Sect. J. Anim. Sci.* 3833.

Carstens, GE., Johnson, DE., Johnson, KA., Hotovy, SK., and Szymanski, TJ. (1989) Genetic variation in energy expenditures of monozygous twin beef cattle at 9 and 20 months of age. *In Energy Metabolism of Farm Animals.. Proceedings 11th Symposium, Luteren, Netherlands*, EAAP Publication No. 43. (Eds Y. Van der Honing and W. H. Close.) (Pudoc: Wageningen.)

Casado, M., Vallet, VS., Kahn, A. and Vaulont, S. (1999) Essential role in vivo of upstream stimulatory factors for a normal dietary response of the *fatty acid synthase* gene in the liver. *Journal of Biological Chemistry,* **274**:2009–13.

Chandran, M., Phillips, SA., Ciaraldi, T. and Henry, RR. (2003) Adiponectin: more than just another fat cell hormone? *Diabetes Care,* **26**:2442–50.

Chanseaume, E., Malpuech-Brugère, C., Patrac, V., Bielicki, G., Rousset, P., Couturier, K., Salles, J., Renou, J.P., Boirie, Y. and Morio, B. (2006) Diets High in Sugar, Fat, and Energy Induce Muscle Type–Specific Adaptations in Mitochondrial Functions in Rats. *J. Nutr,*. **136**:2194-2200.

Chaudhuri, AR., De Waal, EM., Pierce, A. and Van Remmen, H. (2006) Detection of protein carbonyls in aging liver tissue: a fluorescence-based proteomic approach. *Mech. Ageing Dev.*, **127**:849-61.

Cheatham, B. and Kahn, B. (1995) Insulin action and the insulin signalling network. *Endocr. Rev.*, **16**:117-142.

Chen, X., Levine, L., and Kwok, P-Y. (1999) Fluorescence polarization in homogeneous nucleic acid analysis. *Genome Res.,* **9**:492-498.

Choi, BR. and Palmquist, DL. (1996) High fat diets increase plasma cholecystokinin and pancreatic polypeptide, and decrease plasma insulin and feed intake in lactating cows. *J. Nutr.,* **126**: 2913–2919.

Choi, BR., Palmquist DL. and Allen MS. (2000) Cholecystokinin mediates depression of feed intake in dairy cattle fed high fat diets. **19**:159-175.

Christen, P., Graf-Hausner, U., Bossa, F., Doonan, S., *Trans-aminases.* John Wiley and Sons, New York, 1985, pp. 173–185.

Christensen, A. (1971) Frozen thin sections of fresh tissue for electron microscopy, with a description of liver and pancreas. *The Journal of Cell Biology*, **51**:772-804.

Clop, A., Marcq, F., Takeda, H., Pirottin, D., Tordoir, X., Bibe, B., Bouix, J., Caiment, F., Elsen, JM., Eychenne, F., Larzul, C., Laville, E., Meish, F., Milenkovic D., Tobin, J., Charlier, C., and Georges, M. (2006). A mutation creating a potential illegitimate microRNA target site in the myostatin gene affects muscularity in sheep. *Nature Genetics*, **38**:813-818.

Comi, G.P., Fortunato, F., Lucchiari, S., Bordoni, A., Prelle, A., Jann, S., Keller, A., Ciscato, P., Galbiati, S., Chiveri, L., Torrente, Y., Scarlato, G. and Bresolin, N. (2001) Beta-enolase deficiency, a new metabolic myopathy of distal glycolysis. *Ann. Neurol.,* **50**:202-207.

Considine, R. (2002) Regulation of energy intake, Endotext.com.

Corva, P. and Medrano, J. (2000) Diet effects on weight gain and body composition in high growth (*hg/hg*) mice. *Physiol. Genomics*, **3**:17-23.

Cota, D., Proulx, K., Smith, KA., Kozma, SC., Thomas, G., Woods, SC. and Seeley, RJ. (2006) Hypothalamic mTOR signaling regulates food intake. *Science,* **312**:927–930.

Cowley, MA., Smart, JL., Rubinstein, M., Cerdan, MG., Diano, S., Horvath, TL., Cone, RD., Low, MJ. (2001). Leptin activates anorexigenic POMC neurons through a neural network in the arcuate nucleus. *Nature,* **411**:480-484.

Cox, T.M. (1988) Hereditary Fructose Intolerance. *Quart. J. Med. New Ser.*, **68**:585-594.

Crews, DH., Nkrumah, JD., Yu, J., and Moore, SS. (2004) Association of single nucleotide polymorphisms in the bovine leptin gene with feedlot and carcass characteristics of crossbred steers. *Can. J. Anim. Sci.* **84**:749–750. (Abstr.).

Croniger, C., Olswang, Y., Reshef, L., Kalhan, S., Tilghman, S. and Hanson, R. (2002) Phosphoenolpyruvate carboxykinase revisited: insights into Its metabolic role. *Biochemistry and*
Csaba, Z., and Dournaud, P. (2001) Cellular biology of somatostatin receptors *Neuropeptides,* **35**:1-23.

Cuervo, AM. and Dice, JF. (2000a) When lysosomes get old. *Exp Gerontol.*, **35**:119–131.

Cummings, DE. and Overduin, J. (2007) Gastrointetsinal regulation of food intake. *The journal of Clinical Investigation*, **117**:13-23.

Cundiff, LV., Gregory, KE., Koch, RM., and Dickerson, GE. (1986) Genetic diversity amoung cattle breeds and its use to increase beef production efficiency in a temperate environment. In: *Proc. 3^{d} World Cong. Genet. Appl. Livest. Prod.*, **9**:271-282.

Curzon, G., Gibson, EL., and Oluyomi, AO. (1997). Appetite suppression by commonly used drugs depends on 5-HT receptors but not on 5-HT availability. *Trends Pharmacol. Sci.,* **18**:21-25.

Daryl, LD, Sacha, TK., John, JW., Brian, FK., Ronald LA., Cheng X., Jiang, HY., Hui, S., Li, Z., Xiang-Qun, H., Volodya, H., David, ML. and Tina, KM. (2006) Effects of Ethanol on Adenosine 5'-Triphosphate–Gated Purinergic and 5-Hydroxytryptamine$_3$ Receptors. *Alcoholism Clinical and Experimental Research*, **30**:349 – 359.

Davey, GP., and Clark, JB. (1996) Threshold effects and control of oxidative phosphorylation in nonsynaptic rat brain mitochondria. *J Neurochem.,* **66**:1617–1624.

Davies, SP., Carling, D. and Hardie, DG. (1989) Tissue distribution of the AMP-activated protein kinase, and lack of activation of cyclic-AMP-dependant protein kinase, studied using a specific and sensitive peptide assay. *European Journal of Biochemistry,* **186**:123-128.

De Koning, DJ., Windsor, D., Hocking, PM., Burt, DW., Law, A., Haley, CS., Morris, A., Vincent, J., and Griffin, H. (2003) Quantitative trait locus detection in commercial broiler lines using candidate regions. *J. Anim. Sci.,* **81**:1158-1165.

de Lecea, L. Kilduff, TS., Peyron, C., Gao, XB., Foye, PE., Danielson, PE., Fukuhara, C., Battenberg, ELF., Gautvik, VT., Bartlett, FS., Frankel, WN., van den Pol, AN., Bloom, FE., Gautvik, KM., and Sutcliffe, JG. (1998) The hypocretins:hypothalamus-specific peptides with neuroexcitarory activity. *Proc. Natl. Acad. Sci.*, **95**: 322-327.

Della-Fera, MA. and Baile, CA. (1981) Cholecystokinin octapeptide (CCK-OP) injected in cerebrospinal fluid (CSF) decreased plasma insulin concentration in sheep. *Soc. Neurosci. Abstr.*, **7**: 33 (abs.).

Denborough, M. (1998) Malignant hyperthermia. *Lancet,* **352**:1131-1136.

Denice, PB. (2001) *Science*, **294**:1102:2001.

Dhillion, H., Zigman, JM., Ye, C., Lee, CE., McGovern, RA., Tang, V., Kenny, CD., Christiansen, LM., White, RD., Edelstein, EA., Coppari, R., Balthasar, N., Cowley, MA., Chua, S. Jr., Elmquist, JK., and Lowell, BB. (2006) Leptin directly activates SF1 neurons in the VMH, and this action by leptin is required for normal body-weight homeostasis. *Neuron*, **49**:191-203.

DiCostanzo, A., Meiske, JC., Plegge, SD., Peters, TM., and Goodrich, RD. (1990) Within-herd variation in energy utilization for maintenance and gain in beef cows. *J. Anim. Sci.*, **68**:2156.

Diez, JJ. and Iglesias, P. (2003) The role of the novel adipocyte-derived hormone adiponectin in human disease. *European Journal of Endocrinology,* **148**:293–300.

Dobrzyn, P., Dobrzyn, A., Miyazaki, M., Cohen, P., Asilmaz, E., Hardie, G., Friedman, J., and Ntambi, J. (2004) Stearoyl-CoA desaturase 1 deficiency increases fatty acid oxidation by activating AMP-activated protein kinase in liver. *PNAS*, **101**:6409-6414.

Domonoci, FP. and Turyn, D. (2002) Minireview: Growth hormone – induced alterations in the insulin signalling system. *Experimental Biology and Medicine,* **227**:149-157.

Donahue, LR. and Beamer, WG. (1993) Growth hormone deficiency in 'little' mice results in aberrant body composition, reduced insulin-like growth factor-I and insulin-like growth factor-binding protein-3 (IGFBP-3), but does not affect IGFBP-2, -1 or -4. *J. Endocrinol.,* **136**: 91– 104.

Drucker, DJ. (2002) Biological actions and therapeutic potential of the glucagon-like peptides. *Gastroenterology*, **122**:531-544.

Dudek H., Datta SR, and Franke TF. (1997) Regulation of neuronal survival by the serine–threonine protein kinase Akt. *Science,* **275**:661–665.

Dudkina, N., Heinemeyer, J., Sunderhaus, S., Boekema, E., and Braun, HP. (2006) Respiratory chain supercomplexes in the plant mitochondrial membrane. *Trends in Plant Science*, **11**: No.5

Dunn-Meynell, AA., Routh, VH., Kang, L., Gaspers, L., and Levin, BE. (2002) Glucokinase is the likely mediator of glucosensing in both glucose-excited and glucose-inhibited central neurons. *Diabetes*, **51**:2056–2065.

Early, RJ., McBride, BW., and Ball, RO. (1990) Growth and metabolism in somatotropin-treated steers: III Protein synthesis and tissue energy expenditures. *Journal of Animal Science*, **68**:4153-4166.

Echtay, KS., Murphy, MP., Smith, RA., Talbot, DA., and Brand, MD. (2002) Superoxide activates mitochondrial uncoupling protein 2 from the matrix side. Studies using targeted antioxidants. *J. Biol. Chem.*, **277**:47129-47135.

Edwards, CM., Stanley, SA., Davis, R., Brynes, AE., Frost, GS., Seal, LJ., Ghatei, MA., Bloom, SR. (2001) Exendin-4 reduces fasting and postprandial glucose and decreases energy intake in healthy volunteers. *Am. J. Physiol. Endocrinol. Metab.*, **281**:E155-E161.

Eizirik, DL., Welsh, M., Strandell, E., Welsh, N., and Sandler, S. (1990) Interleukin-1 beta depletes insulin messenger ribonucleic acid and increases the heat shock protein hsp70 in mouse pancreatic islets without impairing the glucose metabolism *Endocrinology*, **127**:2290-2297.

Elias, CF., Aschkenasi, C., Lee, C., Kelly, J., Ahima, RS., Bjorbæk, C., Flier, JS., Saper, CB., and Elmquist, JK. (1999) Leptin differentially regulates NPY and POMC neurons projecting to the lateral hypothalamic area. *Neuron*, **23**:775–786.

Elias, CF., Lee, C., Kelly, J., Aschkenasi, C., Ahima, RS., Couceyro, PR., Kuhar, MJ., Saper, CB., Elmquist, JK. (1998) Leptin activates hypothalamic CART neurons projecting to the spinal cord. *Neuron*, **21**:1375-1385.

Elliott, RM., Southon, S., and Archer, DB. (1999) Oxidative insult specifically decreases levels of a mitochondrial transcript. *Free. Radic. Biol. Med.*, **26**:646-655.

Elmquist, JK. (2001) Hypothalamic pathways underlying the endocrine, autonomic, and behavioral effects of leptin. *Int J Obes Relat Metab Disord.*, **25**:S78-82.

Elmquist, JK., Elias, CF., and Saper CB. (1999) From lesions to leptin: hypothalamic control of food intake and body weight. *Neuron*, **22**:221-232.

Elo, K., (2003) Towards integrated genomic approaches-lessons from energy metabolism studies. *Nordic Association of Agricultural Scientists 22nd Congress report, July 1-4, Finland.*

Elo, K., Wesolowski, M., Nilesen MK., Van Vleck, LD., and Pomp, D. (2002) Fine mapping of genes regulating heat loss in mice. *Proceedings of the 7th world congress on genetics applied to livestock production, Montpelier, France.*

Elpeleg, O., Miller, C., Hershkovitz, E., Bitner-Glindzicz, M., Bondi-Rubinstein, G., Rahman, S., Pagnamenta, A., Eshhar, S., and Saada, A. (2005) Deficiency of the ADP-Forming Succinyl-CoA Synthase Activity Is Associated with Encephalomyopathy and Mitochondrial DNA Depletion. *Am. J. Hum. Genet.*, **76**:1081–1086.

Entelis, N., Brandina, I., Kamenski, P., Krasheninnikov, I., Martin, R. and Tarassov, I. (2006). A glycolytic enzyme, enolase, is recruited as a cofactor of tRNA targeting toward mitochondria in *Saccharomyces cerevisiae. Genes and Development*, **20**:1609-1620.

Erwin, RA., Kirken, RA., Malabarba, MG., Farrar, WL., and Rui, H. (1996) Prolactin activates ras via signalling proteins Shc, growth factor receptor bound 2, and Son of Sevenless, *Endocrinology*, **136**:3512-3518.

Esposito, LA., Melov, S., Panov, A., Cottrell, BA., and Wallace, DC. (1999) Mitochondrial disease in mouse results in increased oxidative stress. *Proc. Natl Acad. Sci.*, **96**: 4820–4825.

Estany, J., Villalba, D., Tibau, J., Soler, J., Babot, D., and Noguera, JL. (2002) Correlated response to selection for litter size in pigs: I. Growth, fat deposition, and feeding behaviour traits. *Journal of Animal Science*, **80**:2256-2565.

Evan, JL. (2001) Genetic prediction of mature weight and mature cow maintenance energy requirements in cattle. Ph.D. Colorado State University, Fort Collins.

Falconer, DS. (1981) *Introduction to Quantitative Genetics, 2nd ed. Longman, London, U.K.*

Fan, W., Boston, BA., Kesterson, RA., Hruby, VJ., and Cone, RD. (1997) Role of melanocortinergic neurons in feeding and the agouti obesity syndrome. *Nature*, **385**:165-168.

Fan, W., Dinulescu, D., Butler, A., Zhou, J., Marks, D., and Cone, R. (2000) The Central melanocortin system can directly regulate serum insulin levels. *Endocrinology*, **141**:3072-3079.

Favre, H., Benhamou, A., Finidori, J., Kelly, PA., and Edery, M. (1999) Dual effects of suppressor of cytokine signalling (SOCS-2) on growth hormone signal transduction. *FEBS lett.*, **453**:63-66.

Fenton, ML. (2004) Genomics of feed efficiency for livestock. *PhD thesis.* (The University of Adelaide).

Fernandez, X., Hocquette, JF., and Geay, Y. (1997) Glycolytic metabolismin different muscles of normal and double-muscled calves. In: *Book of Abstracts of the 48th Annual Meeting of the European Association for Animal Production, Wageningen Pers, Wageningen, The Netherland, van Arendonk, J.A.M. (Ed.).*

Ferrell, C.L. and Jenkins, T.G. (1984) Energy utilization by mature, non-pregnant, non-lactating cows of different types. *Journal of Animal Science,* **58:** 234-243.

Ferrell, CL. and Jenkins, TG. (1985) Cow type and the nutritional environment: nutritional aspects. *Journal of Animal Science*, **61**:725-741.

Finck, B., Gropler, M., Chen, Z., Leone, T., Croce, M., Harris, T., Lawrence, J., and Kelly, D. (2006) Lipin 1 is an inducible amplifier of the hepatic PGC-1α/PPARα regulatory pathway. *Cell Metabolism*, **4**:199-210.

Finck, B., Matthew C. Gropler, M., Chen, Z., Leone, T., Croce, M., Harris, T., Lawrence Jr., J., and Kelly, D. (2006) Lipin 1 is an inducible amplifier of the hepatic PGC-1α/PPARα regulatory pathway. *Cell Metabolism*, **4**:199-210.

Fitzsimmons, CJ., Schmutz, SM., Bergen, RD. and McKinnon, JJ. (1998) A potential association between the BM1500 microsatellite and fat deposition in beef cattle. *Mamm. Genome,* **9**:432–434.

Fleury, C., Neverova, M., Collins, S., Raimbault, S., Champigny, O., Levi-Meyrueis, C., Bouillaud, F., Seldin, MF., Surwit, RS., Ricquier, D., and Warden, CH. (1997) Uncoupling protein-2: a novel gene linked to obesity and hyperinsulinemia. *Nature Genetics*, **15**:269-272.

Flier, JS. (2004) Obesity wars: molecular progress confronts an expanding epidemic. *Cell,* **116**:337-350.

Flier, JS. and Maratos-Flier, E. (1998) Obesity and the Hypothalmus. Novel Peptides for New Pathways. *Cell*:437-440.

Fonnum, F. (1984) Glutamate: A neurotransmitter in mammalian brain. *J. Neurochem.* **42**:1–11.

Fox-Orenstein, A., Camilleri, M., Stephens, D., and Burton, D. (2003) Effect of somatostatin analog on gastric motor and sensory functions in healthy humans. *Gut,* **52**: 1555-1561.

Fredriksson, K., Radell, P., Eriksson, L., Hultenby, K. and Rooyackers, O. (2005) Effect of prolonged mechanical ventilation on diaphragm muscle mitochondria in piglets. *Acta Anaesthesiol. Scand.* **10**:1-7.

Freeman, BD., Buchman, TG., McGrath, S., Tabrizi, AR., and Zehnbauer, BA (2002) Template-directed dye-terminator incorporation with fluorescence polarization detection for analysis of single nucleotide polymorphisms implicated in Sepsis. *Journal of Molecular Diagnostics,* **4**:209-215.

Fruebis J, Tsao T, Javorschi S, Ebbets-Reed D, Erickson M, Yen F, Bihain B, and Lodish H Proteolytic cleavge product of 30-kDA (2001) Adipocyte comlement- related protein increases fatty acid oxidation in muscle and causes weight loss in mice, *PNAS*, **98**:2005-2010.

Gabarrou, JF., Geraert, PA., Picard, M., and Bordas, A. (1997) Diet-induced thermogenesis in cockerels is modulated by genetic selection for high or low residual feed intake. *The Journal of Nutrition*, **127**: 2371-2376.

Gardner, AF. and Jack, WE. (2002) Acyclic and dideoxy terminator preferences denote divergent sugar recognition by archaeon and *Taq* DNA polymerases *Nucleic Acids Res.*, **30:**605-613.

Garfinkel, AS., Baker, N. and Schotz, MC. (2000) Relationship of lipoprotein lipase activity to triglyceride uptake in adipose tissue. *British Journal of Pharmacology,* **129**:1261–1283.

Gautier, M., Hayes, H. and Eggen, A. (2003) A comprehensive radiation hybrid map of bovine chromosome 26 (BTA26): comparative chromosomal organization between HSA10q and BTA26 and BTA28. *Mamm. Genome,* **14:** 711–721.

Gaytan, F., Morales, C., Barreiro, ML., Jeffery, P., Chopin, lk., Herington, AC., Casanueva, FF., Aguilar, E., Dieguez, C. and Tena-sempere, M. (2005) Expression of growth hormone secretagogue receptor type 1a, the functional ghrelin receptor, in human ovarian surface epithelium, mullerian duct derivatives, and ovarian tumours. *J. Clin. Endocrinol. Metab.*, **90**:1798-1804.

Gazzola, C. (1993) α_2-aderenoceptor-mediated effects on resting energy expenditure. *International Journal of Obesity*, **17**:637:641.

Gazzola, C., Magner, T., Lisle, AT. and Hunter, RA. (1995) Effect of α-aderenoceptor agonists and antagonists on metabolic rate in cattle. *Comparative Biochemistry and Physiology*, **111A**:73-77.

Geary, TW., McFadin, EL., MacNeil, DM., Grings, EE., Short, RE., Funston, RN., and Keisler, DH. (2003) Leptin as a predictor of carcass composition in beef cattle. *J. Anim. Sci.*, **81**:1–8.

Genova, ML., Pich, MM., Biondi, A., Bernacchia, A., Falasca, A., Bovina, C., Formiggini, G., Castelli, GP., and Lenaz, G. (2003) Mitochondrial Production of Oxygen Radical Species and the Role of Coenzyme Q as an Antioxidant. *Experimental Biology and Medicine,* **228**:506-513.

Gerich, J.E., Lorenzi, M. and Bier, D.M. (1976) Effects of physiologic levels of glucagon and growth hormone on human carbohydrate and lipid metabolism: studies involving administration of exogenous

hormone during suppression of endogenous hormone secretion with somatostatin. *Journal of Clinical Investigation*, **57**:875–84.

German, M. (1993). Glucose sensing in pancreatic islet beta cells: a key role of glucokinase and glycolytic intermediates. *Proc. Natl. Acad. Sci. USA.*, **90**:1781-1785.

Ghijsen, WE., Leenders, AGM., and Wiegant VM. (2001) Regulation of cholecystokinin release from central nerve terminals. *Peptides,* **22**:1213-1221.

Gibbs, J., Young, RC., and Smith, GP. (1973) Cholycystokinin elicits satiety in rats with open gastric fistulas. *Nature*, **245**:323–325.

Gilmour, AR., Thompson, R., Cullis, BR. and Welham, SJ. (1999) ASREML reference manual, *NSW Agriculture Biometric Bulletin*, **3**.

Goddard, M., Hulett, D., McPartlan, H., Hayes, B., and Krishnan, L. (2006) Personal communication, Department of Primary Industries, Victoria, Australia.

Goudriaan, JR., Tacken, PJ., Dahlmans, V., Gijbels, MJ., van Dijk, KW, Havekes, LM., Jong, MC. (2001) Protection From Obesity in Mice Lacking the VLDL Receptor, *Arteriosclerosis,Thrombosis, and Vascular Biology,* **21**:1488.

Green, P., Falls, K. and Crooks, S. (1990) Documentation for CRIMAP Version 2.4., Washington University School of Medicine, St Louis, MO, USA.

Gregory, KE (1972) Beef cattle type for maximum efficiency "Pulling it all together." J. *Anim. Sci.,* **34**:881.

Grewal, T., Heeren, J., Mewawala, D., Schnitgerhans, T., Wendt, D., Salomon, G., Enrich, C., Beisiegel, U., and Jackle, S. (2000) Annexin VI stimulates endocytosis and is involved in the trafficking of low density lipoprotein to the prelysosomal compartment. *J. Biol. Chem.* **275:**33806-33813.

Grubb, BR. (1981) Blood flow and oxygen consumption in avian skeletal muscle during hypoxia. *J. Appl. Physiol.,* **50,** 450-455.

Halatchev, IG. (2004) Peptide YY3-36 inhibits food intake in mice through a melanocortin-4 receptor-independent mechanism. *Endocrinology,* **145**: 2585-2590.

Hand, SC. and Hardewig, I. (1996) Down regulation of cellular metabolism during environmental stress: Mechanisms and implications. *Annual Reviews Physiology,* **58**:539-563.

Hansen C., Yi NJ., Zhang YM., Xu SZ., Gavora, J., and Cheng, HH. (2005) Identification of QTL for production traits in chickens. *Animal Biotechnology,* **16**:67–79.

Hardie, DG., Scott, JW., Pan, DA. and Hudson, ER. (2003) Management of cellular energy by the AMP-activated protein kinase system. *FEBS Letters,* **546:**113-120.

Harmon, J. (1982) Isolation of totally inverted submitochondrial particles by sonication of beef heart mitochondria, *Journal of Bioenergeties and Biomembranes,* **14**:377-386.

Hartman, ML., Faria, ACS. and Vance, ML. (1991) Temporal sequence of in vivo growth hormone secretory events in man. *American Journal of Physiology*, **260**:E101–10.

Hastings, JM., Moruppa, SM., Bunger, L., and Hill, WG. (1997) Effects of selection on fod intake in the adult mouse. Journal of Animal Breeding and Genetics, **114**:419-434.

Hawley, SA., Davison, M., Woods, A., Davies, SP., Beri, RK., Carling, D. and Hardie, DG. (1996) Characterization of the AMP-activated protein kinase from rat liver and identification of threonine 172 as the major site at which it phosphorylates AMP-activated protein kinase. *Journal of Biological Chemistry,* **271**:7879-27887.

Hayes, B and Goddard, M. (2006). *The Meat Livestock of Australia Report 2006*, unpublished.
Hayley, C. and Knott, S. (1992) A simple regression method for mapping quantitative trait loci in line crosses using flanking markers. *Heredity,* **69**:312-324.

Hayley, C., Knott, S., Smith, C., Gavora, J., Benkel, B., Chesnais, J., Fairfull W., Gibson, J., Kenedy, B. and Burnside, E. (1994) Interval mapping. *Proceedings, Vth World congress on genetics applied to livestock production, Guelph: Canada, International committee for world congresses on genetics applied to livestock production.*

Heart, E., Choi, WS., and Sung, CK. (2000) Glucosamine-induced insulin resistance in 3t3-L1 adipocytes. *Am. J. Physiol*, **278**:E103-140.

Heisler, LK., Jobst, EE., Gregory M Sutton, GM., Zhou, L., Borok, E., Thornton-Jones, Z., Liu, H., Zigman, J., Balthasar, N., Kishi, T., Lee, C., Aschkenasi, C., Zhang, CY., Yu, J., Boss, O., Mountjoy, K., Clifton, P., Lowell, B., Friedman, J., Horvath, T., Butler, A., Elmquist, J., Cowley., E. (2006) Serotonin Reciprocally Regulates Melanocortin Neurons to Modulate Food Intake. *Neuron* **51**: 239-249.

Helmbrecht, K., Zeise, E. and Rensing, L. (2000) Chaperones in cell cycle regulation and mitogenic signal transduction: a review. *Cell Prolif.,* **33**:341-365.

Herd, RM., Archer, JA., and Arthur, PF. (2003) Reducing the cost of beef production through genetic improvement in residual feed intake: Opportunity and challenges to application. *Journal of Animal Science,* **81**:(E. Suppl. 1) E9-E17.

Herd, RM., Archer, JA., Arthur, PF., Richardson, EC., Wright, JH., Dibley, KCP. and Burton, DA. (1997) Performance of progeny of High *vs* Low net feed conversion efficiency cattle. *Proceeding Association Advancement Animal Breeding Genetics,* **12**:742-745.

Herd, RM., and Bishop, SC. (2000) Genetic variation in residual feed intake and its association with other production traits in British Hereford cattle. *Livestock Production Science,* **63**:111-119.

Herd, RM., Oddy, VH., and Lee, GJ. (1993) Effect of divergent selection for weaning weight on liveweight and wool growth responses to feed intake in Merino ewes. *Australian Journal of Experimental Agriculture*, **33**:699-705.

Herd, RM., Richardson, EC., Hegarty, RS., Woodgate, RT., Archer, JA. And Arthur, PF. (1998) Pasture intake by high versus low net feed efficient Angus cows. *Anim. Prod. Aust.*, **22**:137-140.

Herd, RM., Williams, TMJ., Woodgate, R., Ellis, KJ., and Oddy, VH. (1996) Using alkane technology to measure intake of a barley diet by cattle. *Proceedings of the Nutrition Society of Australia,* **20**:106.

Herrington, J. and Carter-Su, C. (2001) Signaling pathways activated by the growth hormone receptor, *Trend in Endocrinology and Metabolism*, **12**:252-257.

Higginbotham, G.E., Torabi, M. and Huber, J.T. (1989b) Influence of dietary protein concentration and degradability on performance of lactating cows during hot environmental temperature. *Jour. Dairy Sci.*, **72**: 2554-2564.

Hillar, M. (1974) Glutamate dehydrogenase. *Journal of Bioenergetics and Biomembranes,* **6**:89-123.
Himms-Hagen J. (1989) Brown adipose tissue thermogenesis and obesity. *Prog. Lipid Res.,* **28**:67-115.

Hjalmarson, A., Isaakson, O. and Ahmed, K. (1969) Effects of growth hormone and insulin on amino acid transport in perfused rat heart. *American Journal of Physiology*, **217**:1795–802.

Hocquette, JF., Ortigues, Marty I., Pethick, D., Herpin, P., Fernandez, X., (1998) Nutritional and hormonal regulation of energy metabolism in skeletal muscles of meat producing animals. *Livestock Production Science,* **56**:115-143.

Horecker, B., Tsola, O. and Lai, C. (1972) Aldolaes. In: *The Enzyme , Boyer PD ed, Academic Press* , **7**:213–258.

Horvath, TL., Diano, S., Sotonyi, P., Heiman, M., and Tschop, M. (2001) Minireview: Ghrelin and the regulation of energy balance- A hypothalamic perspective. *Endocrino.l,* **142**:4163-4169.

Hotovy, SK., Johnson, KA., Johnson, DE., Carstens, GE., Bourdon, RM. and Seidel, GE. Jr. (1991) Variation among twin beef caltle in maintenance energy requirements'. *J. Anim. Sci.* **69**:940-946.

Howard, KM., Muga, SJ., Zhang, L., Thigpen, AE. and Appling, DR. (2003) Characterization of the rat cytoplasmic C1-tetrahydrofolate synthase gene and analysis of its expression in liver regeneration and fetal development. *Gene,* **319**:85-97.

Hsu, TM., Chen, X., Duan, S., Miller, RD., and Kwok, P-Y. (2001) Universal SNP genotyping assay with fluorescence polarization detection. *BioTechniques,* **31**:560-570.

Huang, H., Stasyk, T., Morandell, S., Dieplinger, H., Falkensammer, G., Griesmacher, A., Mogg, M., Schreiber, M., Feuerstein, I., Huck, C., Stecher, G., Bonn, G., and Huber, L. (2006). Biomarker discovery in breast cancer serum using 2-D differential gel electrophoresis/MALDI-TOF/TOF and data validation by routine clinical assays. *Electrophoresis,* **27**:1641-1650.

Huber, JT., Higginbotham, G., Gomez-Alarcon, RA., Taylor, RB., Chen, KH., Chan, SC., and Wu, Z. (1994) Heat stress interactions with protein, supplemental fat, and fungal cultures. *Jour. Dairy Sci.*, **77**: 2080-2090.

Hue, L., and Rider, MH. (1987). Role of fructose 2,6-bisphosphate in the control of glycolysis in mammalian tissues. *Biochem. J.,* **15**:313–324.

Hughes, T. (2003). Direct and correlated responses to seven generations of divergent selection for post-weaning net feed intake in mice. Department of Animal Science, Adelaide, South Australia, University of Adelaide.

Hughes, TE., Archer, JA. and Pitchford, WS. (1997) Response to selection for high and low net feed intake in mice. *Proceedings of the Association for the Advancement of Animal Breeding and Genetics,* **12**:230-233.

Hughes, TE. and Pitchford, WS. (2004a) Direct response to selection for post-weaning net feed intake in mice, and correlated responses in post-weaning growth, intake, gross digestibility and body composition. *Australian Journal of Experimental Agriculture Beef CRC special edition,* **44**:489-500.

Hughes, TE. and Pitchford, WS. (2004b) How does pregnancy and lactation affect efficiency of female mice divergently selected for post-weaning net feed intake? *Australian Journal of Experimental Agriculture,* **44**:501-152.

Huntington, GB. and Prior, RL. (1985) Net absorption of amino acids by portal-drained viscera and hind half of beef cattle fed a high concentrate diet. *J. Anim. Sci.*, **60**:1491-1499.

Huszar, D., Lynch, CA., Fairchild-Huntress, V., Dunmore, JH., Fang, Q., Berkemeier, LR., Gu, W., Kesterson, RA., Boston, BA., Cone, RD., Smith, FJ., Ampfield, LA., Burn, P., and Lee, F. (1997) Targeted disruption of the melanocortin-4 receptor results in obesity in mice. *Cell,* **88**:131–141.

Hynes, RO. (1992) Integrins: versatility, modulation and signalling in cell adhesion. *Cell,* **69**:11-25.

Ibrahim, N., Bosch, M., Smart, J., Qiu, J., Rubinstein, M., Ronnekleiv, O., Low, M., and Kelly, M. (2003) Hypothalamic Proopiomelanocortin neurons are glucose responsive and express K_{ATP} channels. *Endocrinology,* **144**:1331-1340.

Iqbal, M., Pumford, N. R., Lassiter, K., Wing, T., Cooper, M., and Bottje, W. (2004) Low feed efficient broilers within a single genetic line exhibit higher oxidative stress and protein expression in breast muscle with lower mitochondrial complex activity. *Poultry Science,* **83**:474-484.

Ishibashi, O., Oka, T., and Yahyu, H. (2000) Targeted disruption of hormone-sesitive lipase results in male sterility and adipocyte hypertrophy, but not in obesity. *Proceedings of the National Academy of Sciences of the United States of America*, **97**:787-792.

Jacobi, SK., Ajunwon, KM., Weber TE., Kuske, JL. and Dyer, CJ. (2004) Cloning and expression of porcine adiponectin, and its relationship to adiposity, lipogenesis and the acute phase response. *Journal of Endocrinology*, **182**:133–44.

Jakobsen, JH., Madsen, P., Jensen, J., Pedersen, GA.,and Petersen, PH (2000) Genetic prameters for average daily gain, area of M. longissimus dorsi, feed efficiency and feed intake capacity in young bulls of dairy populations. *Acta Agriculturae Scandinavica Section A – Animal Science*, **50**: 146-152.

Janssen, E., Dzeja, P., Oerlemans, F., Simonetti, A., Heerschap, A., Haan, A., Rush, P., Terjung, R., Wieringa, B. and Terzic, A. (2000) Adenylate kinase 1 gene deletion disrupts muscle energetic economy despite metabolic rearrangement. *The EMBO Journal*, **19**:6371–6381.

Janssen, E., Groof Ad DE., Wijers M., Fransen, J., Dzeja P., Terzic, A.and Wieringa, Bé (2003) Adenylate kinase 1 deficiency induces molecular and structural adaptations to support muscle energy metabolism. *The Journal of Biological Chemistry*, **278**:12937-12945.

Jennings, RB. and Ganote, CE. (1976) Mitochondrial structure and function in acute myocardial ischemic injury. *Circ. Res.* 38: I-80–I-91.

Jensen, J., Mao, IL., Andersen, BB., and Madsen, P. (1992) Phenotypic and genetic relationships between residual energy intake and growth, feed intake, and carcass traits of young bulls. *Journal of Animal Science,* **70**:386-395.

Jezek, P., Engstová, H., Zácková, M., Vercesi, AE., Costa, ADT., Arruda, P. and Garlid, KD. (1998) Fatty acid cycling mechanism and mitochondrial uncoupling proteins. *Biochim. Biophys. Acta.,* **1365**: 319 -327.

Jiang, Z. and Michal, JJ. (2003) Linking porcine microsatellite markers to known genome regions by identifying their human orthologs. *Genome,* **46**: 798-808.

John, WB., Barbara, R., William, T., Susan, SB., Warren, HM. Michael, CM., Susan, MP., Nancy, G. and David, IS. (2002) Congenital sucrase-isomaltase deficiency presenting with failure to thrive, hypercalcemia, and nephrocalcinosis. *BMC Paediatrics*, **2**:4.

Johnston, D. (2003) Genetic prediction of efficiency in the future: an Australian perspective. *Proceedings from the 34th BIF Conference,* Lexington, KY.

Johnston, DJ., Herd, RM., Kadel, MJ., Graser, H-U., Arthur, PF. and Archer, JA. (2002). Evidence of IGF-1 as a genetic predictor of feed efficiency traits in beef cattle. *Proc. 7th World Congr. Genet. Appl. Livest. Prod., Montpellier, France. Comm. No. 10–16.*

Johnston, DJ., Herd, RM., Reverter, A. and Oddy, VH. (2001). Heitability of IGF-1 in beef cattle and its association with growth and carcase traits. In *Proc. 14th Conf. Assoc. Advancement Anim. Breed. Genet.*, Queenstown, New Zealand, Pages 163–166.

Johnston, DJ., Herd, RM., Kadel, MJ., Graser, H-U., Arthur, PF., and Archer, JA. (2002) Evidence of IGF-1 as a genetic predictor of feed efficiency traits in beef cattle. In '*Proceedings 7th World Congress on Genetics Applied to Livestock Production'. CD-ROM Communication No. 10-16. Institut National de la Recherche Agronomique. Montpellier.*

Jolly, C. and Morimoto, R. (2000) Role of the heat shock response and molecular chaperones in oncogenesis and cell death. *J. Natl. Cancer. Inst.*, **92**:1564-1572.

Jungst, SB., Christian, LL. and Kuhlers, DL. (1981) Response to selection for feed efficiency in individually fed Yorkshire boars. *Journal of Animal Science*, **53**:323-331.

Juszczuk-Kubiak, E., Wyszynska-Koko, J., Wicinska, K., and Rosochacki S. (2007) A novel polymorphisms in intron 12 of the bovine calpastatin gene. *Mol. Biol. Rep., (in press).*

Kaczmarski, RS., and Mufti, GJ. (1991) The cytokine receptor superfamily. *Blood Rev.,* **5**:193-203.

Kaetzel, MA., Pula G., Campos, B., Uhrin, P., Horsemann, N., and J. R. Dedman, J. R. (1994) Annexin VI isoforms are differentially expressed in mammalian tissues. *Biochim. Biophys. Acta.,* **1223**: 368-374.

Kahn, BB. and Myers, MG., Jr. (2006) mTOR tells the brain that the body is hungry. *Nature medicine,* **12**:615- 656.

Kahn, BB., Alquier, T., Carling, D., and Hardie, DG. (2005) AMPK-activated protein kinase: ancient energy gauge provides clues to modern understanding of metabolism. *Cell Metab.,* **1**:15–25.

Kahn, LP., Leng, RA., and Piper, LR. (2000) Rumen microbial yield from sleep genetically different for fleece weight. *Asian-Australasian Journal of Animal Sciences*, **13C**:137.

Karlsson, A., Enfalt, AC., Essen-Gustavsson, B., Lundstrom, K., Rydhmer, L., and Stern, S. (1993) Muscle histochemical and biochemical protperties in relation to meat quality during selection for increased lean tissue growth rate in pigs. *J. Anim. Sci.,* **71**:930-938.

Karlsson, S. and Ahrèn, B. (1992) Cholecystokinin and the regulation of insulin secretion. *Scand. J. Gastroenterol.*, **27**:161–165.

Kearney, GA., Knee, BW., Graham, JF., and Knott., JA. (2004) The length of test required to measure live weight change when testing for feed efficiency in cattle. *Australian Journal of Experimental Agriculture,* **44**:411-414.

Keith, CT. and Schreiber, SL. (1995) PIK-related kinases: DNA repair, recombination, and cell cycle checkpoints. *Science,* **270**:50-51.

Kennedy, BW., van der Werf, JHJ., and Meuwissen, THE. (1993) Genetic and statistical properties of residual feed intake. *Journal of Animal Science,* **71**:3239-3250.

Kennedy, EP., and Lehninger, AL. (1949) Oxidation of fatty acids and tricarboxylic acid cycle intermediates by isolated rat liver mitochondria. *J. Biol. Chem.* **179**: 957–972.

Kim, MS., Pak, Y., Jang, PG., Namkoong, C., Choi, YS., Won, JC., Kim, KS., Kim, SW., Kim, HS., Park, JY., Kim' YB., and Lee, KU. (2006) Role of hypothalamic Foxo1 in the regulation of food intake and energy homeostasis, *Nature Neuroscience*, **9**:901-906.

Kissebah, AH., Sonnenberg, GE., and Myklebust, J. (2000) Quantitative trait loci on chromosomes 3 and 17 influence phenotypes of the metabolic syndrome. *Proceedings of the National Academy of Sciences of the United States of America,* **97**:14478–83.

Knott, S., Marklund, L., Hayley, C., Andersson, K., Davies, W., Ellegren, H., Fredholm, M., Hansson, I., Hoyheim, B., Lundstrom, K., Moller, M. and Andersson, L. (1998) Multiple marker mapping of quantitative trait loci in a cross between outbred wild boar and large white pigs. *Genetics,* **149**:1069-1080.

Koch, RM., Swiger, LA., Chambers, D., and Gregory, KE. (1963) Efficiency of feed use in beef cattle. *Journal of Animal Science,* **22**:486-494.

Kolath, WH., Kerley, MS., Golden, JW., and Keisler, DH., (2006) The relationship between mitochondrial function and residual feed intake in Angus steers, *Journal of Animal Science*, **84**:861-865.

Kolath, WH., Kerley, MS., Golden, JW., Shahid, SA., and Johnson, GS. (2006) The relationships among mitochondrial uncoupling protein 2 and 3 expression, mitochondrial deoxyribonucleic acid

single nucleotide polymorphisms, and residual feed intake in Angus steers, *Journal of Animal Science*, **84**:1761-1766.

Konig S., Luger, TA., and Scholzen, TE. (2006) Monitoring neuropeptide-epcific proteases: processing of the proopiomelanocortin peptides adrenocoticotropin and alpha-melanocyte-stimulating hormone in the skin. *Exp. Dermatol.*, **15**:751-761.

Koo, SH., Flechner, L., Qi, L., Zhang, X., Screaton, RA., and Jeffries, S. (2005) The CREB coactivator TORC2 is a key regulator of fasting glucose metabolism. *Nature*, **437**:1109–1114.

Kopchick, JJ. and Cioffi, JA. (1991) Exogenous and endogenous effects of growth hormone in animals. *Livest. Prod. Sci.*, **27**:61-75.

Korver, S. (1988) Genetic aspects of feed intake and feed efficiency in dairy cattle: A review. *Livestock Production Science*, **20**:1-13.

Korver, S., Van Eekelen, EAM., Vos, H., Nieuwhof, GJ., and Van Arendonk, JAM. (1991) Genetic parameters for feed intake and feed efficiency in growing dairy heifers. *Livestock Production Science*, **29**:49-59.

Kow, L., and Pfaff, D. (1991) The effects of TRH-metabolic cyclo (His-Pro) and its analogs on feeding. *Pharmacol. Biochem. Behav.*, **38**:359-364.

Kowald, A. (1999) The mitochondrial theory of aging: Do damaged mitochondria accumulate by delayed degeneration? *Exp. Gerontol.* **34**:605–612.

Krauss, S., Zhang, C. and Lowell, B. (2005) The mitochondrial uncoupling-protein homologues. *Molecular Cell Biology*, **6**:249-261.

Krude, H., Biebermann, H., Luck, W., Horn, R., Brabant, G., and Grüters, A. (1998) Severe early-onset obesity, adrenal insufficiency and red hair pigmentation caused by *POMC* mutations in humans. *Nature Genetics*, **19**:155 -157.

Kuo, DY. (2002) Co-administration of dopamine D1 and D2 agonists additively decreases daily food intake, body weight and hypothalamic neuropeptide Y level in rats. *J Biomed Sci.*, **9**:126-32.

Kussmaul L. and Hirst J. (2006) The mechanism of superoxide production by NADH:ubiquinone oxidoreductase (complex I) from bovine heart mitochondria. *PNAS*, **103**, 7607-7612.

Kwong, LK and Sohal RS. (1998) Substrate and site specificity of hydrogen peroxide generation in mouse mitochondria. *Arch. Biochem. Biophys.*, **350**:118-126.

Lagonigro, R., Wiener, P., Pilla, F., Woolliams, JA., and Williams, JL. (2003) A new mutation in the coding region of the bovine leptin gene associated with feed intake. *Anim. Genet.*, **34**:371–374.

Lambert, AJ. and Brand, MD. (2004) Superoxide production by NADH:ubiquinone oxidoreductase (complex I) depends on the pH gradient across the mitochondrial inner membrane *J. Biol. Chem.* **279**:39414–39420.

Lander, E., and Kruglyak, L. (1995) Genetic dissection of complex traits: guidelines for interpreting and reporting linkage results. *Nature Genetics,* **11**:241-247.

Larkin, D., Everts-van der Wind, A., Rebeiz, M., Schweitzer, P., Bachman, S., Green, C., Wright, C., Campos, E., Benson, L., Edwards, J., Liu, L., Osoegawa, K., Womack, J., de Jong, P and Lewin, H. (2003) A Cattle–Human Comparative Map Built with Cattle BAC-Ends and Human Genome Sequence. *Genome Research,* **13**:1966-1972.

Larsen, PR., Kronenberg, HM., Melmed, S. and Polonsky, KS. (2003) *Williams Textbook of Endocrinology, 10th edn. The Curtis Center, Independence Square West, Philadelphia, PA*

Lee, CF. (2003) Feeding management and stategies for lactating dairy cows under heat stress. *Food and Fertiliser Technology Center Publications, Taiwan.*

Lee, H. and Yei, Y. (2001) Mitochondrial alterations, cellular response to oxidative stress and defective degradation of proteins in aging. *Biogerontology* **2**:231-244.

Lee, S. (2005) Net feed intake in beef cattle: the role of AMP activated protein kinase, Honours thesis, Department of Animal Science, University of Adelaide, Adelaide, South Australia.

Lee, YS., Challis, BG., Thompson, DA., Yeo, GS., Keogh, JM., Madonna, ME., Wraight, V., Sims, M., Vatin, V., Meyre, D., Shield, J., Burren, C., Ibrahim, Z., Cheetham, T., Swift, P., Blackwood, A., Hung, CC., Wareham, NJ., Froguel, P., Millhauser, GL., O'Rahilly, S., Farooqi, IS. (2006) A POMC variant implicates beta-melanocyte-stimulating homone in the control of human energy balance. *Cell Metab.* **3**:135-40.

Lehninger, AL., Nelson, DL., and Cox, MM. (1993) In: *Principles of Biochemistry. 2nd ed. Worth Publishers, New York, p. 558.*

Leibowitz, S., Roossin, P. and Rosenn, M. (1984) Chronic norepinephrine injection into the hypothalamic paraventricular ncleus produeces hyperphagia and increased body weight in the rat. *Pharmacol. Biochem. Behav.*, **21**:801-808.

Leibowitz, SF. and Hoebel, BG. Behavioral neuroscience of obesity. In: *Handbook of Obesity, Bray GA, Bouchard C, James WPT, eds., Marcel Dekker, Inc., New York, 1998, pp 313-358.*

Levine, AS., Billington, CJ. (1989) Opioids: are they regulators of feeding? *Ann. NY. Acad. Sci.*, **575**:209–219.

Liang, L. (1999). Insulin receptor substrate-1 enhances growth hormone-induced proliferation. *Endocrinology,* **140**:1972-83.

Liddle, RA., Gertz, BJ., Kanayama, S., Beccaria, L., Gettys, TW., Taylor, IL., Rushakoff, RJ. , Williams VC. and Coker, LD. (1990) Regulation of pancreatic endocrine function by cholecystokinin. Studies with MK-329, a nonpeptide cholecystokinin receptor antagonist. *J Clin Endocrinol Metab,*. **70**:1312–1318.

Li, Y., D'Aurelio, M., Deng, JH., Park, JS., Manfredi, G., Hu, P., Lu, J., and Bai, Y. (2007) An Assembled Complex IV Maintains the Stability and Activity of Complex I in Mammalian Mitochondria. *J. Biol. Chem.,* **282**:17557-17562.

Liu, L., Gong, G., Liu, Y., Natarajan, S., Larkin D., Everts-van der Wind A., Rebeiz, M., and Beever, J. (2004) Multi-species comparative mapping *in silico* using the COMPASS strategy. *Bioinformatics,* **20:**148-154.

Liu, L. Karkanias, G., Morales, J., Hawkins, M., Barzilai, N., Wang, J., and Rossetti, L. (1998) Intracerebroventricular (ICV) leptin regulates hepatic but not peripheral glucose fluxes. *J. Biol. Chem.*, **27**:31160-31167.

Lloyd, TL., Oxana, KP., Amy, CP., Andreas, R., Elaine, MH., Jena, MG., Lauren,MA., Hong Z., Davis RE., Mohan, S., Larry, MW., Eric, DH., Judy, A., Anne, PM., Melinda, GH., Edward, AS., and Louis, MS. (2001) Genomic-scale measurement of mRNA turnover and the mechanisms of action of the anti-cancer drug flavopiridol. *Genome Biology*, **2**:41.1-41.11.

Lobley, GE. (1991) Organ and tissue metabolism: present status and future trends. In: *Energy Metabolism of Farm Animals, Institut fur Nutztierwissenschraften, Zurich, pp. 80-87 Wenk, C., Boessinger, M. (Eds).*

Lohrke, B., Jentsch, W., and Derno, M. (2003) Regulation of the energy metabolism: nutritional, environmental and meolceular aspects. In: *Progress in research on energy and protein metabolism, EAAP publication, Germany, 317-330.*

Lolis, E., Alber, T., Davenport, RC., Rose, D., Hartman, FC. and Petsko, GA. (1990) Structure of yeast triosephosphate isomerase at 1.9-A resolution. *Biochemistry,* **29**:6609-6618.

Lord, E., Ledoux, S., Murphy, BD., Beaudry, D. and Palin, MF. (2005) Expression of adiponectin and its receptors in swine. *Journal of Animal Science,* **83**:565–78.

Lovatto, P., Sauvant, D., Noblet, J., Dubois, S., and Milgen, J. (2006) Effects of feed restriction and subsequent refeeding on energy utilization in growing pigs. *J. Anim Sci.*, **84**:3329-3336.

Lowell, BB., and Spiegelman, BM. (2000) Towards a molecular understanding of adaptive thermogenesis. *Nature*, **404**:652-660.

Lowry, OH., Rosebrough, NJ., Farr, AL., and Randall, RJ. (1951) Protein measurement with the folin phenol reagent. *Journal of Biological Chemistry,* **193**:265-275.

Lui, M., Doi, T., Shen, L., Woods, SC., Seeley, RJ., Zheng, S., Jackman, A., and Tso, P. (2001) Intestinal satiety protein apolipoprotein AIV is synthesized and regulated in rat hypothalamus. *Am. J. Physiol.,* **280**:R1382-R1387.

Lui, M., Shen, L., and Tso, P. (1999) The role of enterstatin and apolipoprotein AIV on the control of food intake. *Neuropeptides,* **33**:425-433.

Luiting, P. (1990) Genetic variation of energy partitioning in laying hens: causes of variation in residual feed consumption. *World Poultry Science Journal*, **46**:133-151.

Luiting, P. (1991) The value of feed consumption data for breeding in laying hens. *PhD. Thesis, Wageningen Agricultural University, The Netherlands.*

Luiting, P. and Urff, EM. (1991) Residual feed consumption in laying hens. 2. Genetic variation and correlations. *Poultry Science*, **70**:1663-1672.

Luiting, P., Urff, EM., and Verstegen, WA. (1994) Between-animal variation in biological efficiency as related to residual feed consumption. *Netherlands Journal of Agricultural Science*, **42**: 59-67.

MacKenzie, SJ., Yarwood, SJ., Peden, AH., Bolger, GB., Vernon, RG., and Houslay, MD. (1998) Stimulation of p70S6 kinase via a growth hormone-controlled phosphatidylinositol 3-kinase pathway leads to the activation of a PDE4A cyclic AMP-specific phosphodiesterase in 3T3-F442A Preadipocytes. *Proc. Natl. Acad. Sci.,* **95**:3549-3554.

Madapallimattam, AG., Law, L. and Jeejeebhoy, KN. (2002) Effect of hypoenergetic feeding on muscle oxidative phosphorylation and mitochondrial complex I – IV activities in rats. *American Journal of Clinical Nutrition* **76**:1031-1039.

Mainieri, D., Montani, JP., Seydoux, J., Giacobino, JP., Boss, O., and Dulloo, AG. (2007) beta-Adrenergic control of stearoyl-CoA desaturase 1 repression in relation to sympathoadrenal regulation of thermogenesis. *Int. J. Obes.,* **31**:378-381.

Mainieri, D., Summermatter, S., Seydoux, J., Montani, JP., Rusconi, S., Russell, A., Boss, O., Buchala, A., Dulloo, A. (2006) A role for skeletal muscle stearoyl-CoA desaturase 1 in control of thermogenesis. *FASEB J.* **20**:1751-1753.

Mal, A., and Harter, ML. (2003) MyoD is functionally linked to the silencing of a muscle-specific regulatory gene prior to skeletal myogenesis. *Proc. Nat. Acad. Sci.*, **100**: 1735-1739.

Malgat, M., Letellier, T., and Rossignol, R. (2000) Metabolic control analysis and threshold effect in oxidative phosphorylation: study in an intermediate state of respiration. *Conference Program of the 9th International BioTheroKinetics Meeting, Stellenbosch, South Aafrica.*125-134.

Masuzaki, H., Ogawa, Y., Sagawa, N., Hosoda, K., Matsumoto, T., Mise, H., Nishimura, H., Yoshimasa, Y., Tanaka, I., Mori, T., and Nakao, K. (1997) Nonadipose tissue production of leptin: leptin as a novel placenta-derived hormone in humans. *Nat. Med.*, **3**:1029–1033.

Mather, K., and Jinks, JL. (1971) *Biometrical Genetics*, Chapman and Hall ed., London.

Mathews, S., Singh, G., Ranalletta, M., Cintron, V., Qiang, X., Goustin, A., Jen, KL., Charron, M., Jahnen-Dechent, W., and Grunberger, G. (2002) Improved Insulin Sensitivity and Resistance to Weight Gain in Mice Null for the *Ahsg* Gene. *Diabetes* **51**:2450-2458.

McBride, BW., and Kelly, JM. (1990) Energy costs of absoption and metabolism in the ruminant gastrointestinal tract and liver: a review. *Journal of Animal Science*, **68**:2997-3010.

McDonagh, MB., Herd, RM., Richardson, EC., Oddy, VH., Archer, JA., and Arthur, PF. (2001) Meat quality and the calpain system of feedlot steers following a single generation of divergent selection for residual feed intake. *Australian Journal of Experimental Agriculture*, **41**: 1013-1021.

Melmed, S., Yamashita, S. and Yamasaki, H. (1996) IGF-1 receptor signalling: lessons from the somatotroph. *Hormone Research,* **51**: 189–215.

Melov, S., Coskun, P., Patel, M,, Tuinstra, R., Cottrell, B., Jun, AS., Zastawny, TH., Dizdaroglu, M., Goodman, SI., Huang, TT., Miziorko, H., Epstein, CJ.. and Wallace, DC. (1999) Mitochondrial disease in superoxide dismutase 2 mutant mice. *Proc. Natl. Acad. Sci.,* **96**: 846–851.

Merali, Z., McIntosh, J. and Anisman. H. (1999) Role of bombesin-related peptides in the control of food intake. *Neuropeptides,* **33**:376-386.

Miller, SM. and Magasanik, B. (1990) Role of NAD-linked glutamate dehydrogenase in nitrogen metabolism in Saccharomyces cerevisiae. *J Bacteriol.* **172**:4927–4935.

Minchenko, J., Williams, A. and Christodoulou, J. (2003) Adaptation of a Mitochondrial Complex III Assay for Automation: Examination of Reproducibility and Precision. *Clinical Chemistry,* **49**:330-332.

Minivielle, F., Kayang, BB., Inoue-Murayama, M., Miwa, M., Vignal, A., Gourichon, D., Neau, A., Monvoisin, L., and Shin'ichi, I. (2005) Microsatellite mapping of QTL affecting growth, feed consumption, egg production, tonic immobility and body temperature of Japanese quail. *BMC Genomics*, **6**:87.

Minokoshi, Y., Alquier, T., Furukawa, N., Kim, YB., Lee, A., Xue, B., Mu, J., Foufelle, F., Ferré, P., Birnbaum, M., Stuck' B., and Kahn B., (2004) AMP-kinase regulates food intake by responding to hormonal and nutrient signals in the hypothalamus. *Nature*, **428**:569-574.

Minokoshi, Y., Kim, YB., Peroni, OD., Fryer, LGD., Muller, C., Carling, D., and Kahn, BB, (2002) Leptin stimulates fatty-acid oxidation by activating AMP-activated protein kinase. *Nature*, **415**:339–343.

Minton, JE., Bindel, DJ., Droullard, JS., Titgemeyer, EC., Grieger, DM., and Hill, CM. (1998) Serum leptin is associated with carcass traits in finishing cattle. *J. Anim. Sci.*, 76 (Suppl.), **231** (Abstr.).

Miwa, T., Boxer, LM., and Kedes, L. (1987) CArG boxes in the human cardiac alpha-actin gene are core binding sites for positive trans-acting regulatory factors. *Proc. Natl. Acad. Sci. U S A.*, **84**: 6702–6706.

Montaldo-Bermudez, M., Nielsen, MK., and Deutscher, GH. (1990) Energy requirements for maintenance of crossbred beef cattle with different genetic potential for milk. *J. Anim Sci.* **68**:2279-2288.

Moody, DE., Pomp, D., and Nielsen, MK. (1998) Isolation of quantitative trait loci (QTL) controlling energy balance in mice. *Proceeding of the 6th World Congress on Genetics Applied to Livestock Production, Armidale, Australia.*

Moody, DE., Pomp, D., Nielsen, MK., and van Vleck, LD. (1999) Identification of quantitative trait loci influencing traits related to energy balance balance in selection and inbred lines of mice. *Genetics*, **152**:699-711.

Moon, A. and Rhead, WJ. (1987). Complementation analysis of fatty acid oxidation orders. *J. Clin. Invest.*, **79**:59–64.

Moore, KL., Johnston, DJ., Graser, HU. and Herd, RM. (2005) Genetic and phenotypic relationships between insulin-like growth factor-I (IGF-I) and net feed intake, fat and growth traits in Angus beef cattle. *Australian Journal of Agricultural Research*, **56**:211-218.

Morely, JE. (1987) Neuropeptide regulation of appetite and weight. *Endocr. Rev.*, **8**:256–287.

Mori, H., Hanada, R., Hanada, T., Aki, D., Mashima, R., Nishinakamura, H., Torisu, T., Chien, KR., Yasukawa, H. and Yoshimura, A. (2004) Socs3 deficiency in the brain elevates leptin sensitivity and confers resistance to diet-induced obesity. *Nature Medicine*, **10**:739–743.

Morris, PN., Dunmore, BJ., Tadros, A., Marchuk, DA., Darland, DC., D'Amore, PA., Brindle, NP. (2005) Functional analysis of a mutant form of the receptor tyrosine kinase Tie2 causing venous malformations. *J. Biol. Chem.*, **83**:58-63.

Morrison, M., Bordas, A., Petit, JM., Jayat-Vignoles, C., Julien, R., and Minivielle, F. (1997). Associated effects of divergent selection for residua feed consumption on reproduction, sperm characteristics, and mitochondria of spermatozoa. *Poultry Science*, **76**:425-431.

Morsci, NS., Schnabel, RD. and Taylor JF. (2006) Association analysis of adiponectin and somatostatin polymorphisms on BTA1 with growth and carcass traits in Angus cattle *Animal Genetics* 37: 554–562.

Morton, GJ., Cummings, DE., Baskins, DG., Barsh, GS., and Schwartz, MW. (2006) Central nervous system control of food intake and body weight. *Nature*, **443**:289-295.

Moruppa, SM. (1990) Energy expenditure and locomotor activity in mice selected for food intake adjusted for body weight, *Theoretical and Applied Genetics*, **79**:131-136.

Mousel, MR. (1998) Daily activity and core body temperature of mice selected for high and low heat loss. *MSc. Thesis, University of Nebraska, Lincoln, NE, USA.*

Moutoussamy, S., Kelly, PA., and Finidori, J. (1998) Growth-hormone-receptor and cytokine-receptor-family singnalling. *Eur. J. Biochem.*, **255**:1-11.

Mrode, RA and Kennedy, BW (1993) Genetic variation in measures of food efficiency in pigs and their genetic relationships with growth rate and backfat. *Animal Production*, **56**:225-232.

Mu, J.., Skurat, AV., and Roach, PJ. (1997) Glycogenin-2, a novel self-glucosylating protein involved in liver glycogen biosynthesis. *J. Biol. Chem.* **272**: 27589-27597.

Murdoch, G., Christopherson, RJ., and Dixon, WT. (2003) Gene expression and energy homeostasis. In*: Progress in Research on Energy and Protein Metabolism, EAAP publication, Germany,* 377-386.

Murray, R., Mayes, P., Granner, D. and Rodell, V. (1996) *Harper's Biochemistry. Prentice Hall International publication, London.*

Naciff, JM., Behbehani,MM., Kaetzel, MA., Dedman, JR. (1996) Annexin VI modulates Ca[2+] and K[+] conductances of spinal cord and dorsal root ganglion neurons. *American Journal of Physiology*, **40**:C2004-C2015.

National Research Council. (1996) *Nutrient Requirement of Beef cattle: 7th revised ed., National Academy Press, Washington, USA.*

Neel, JV. (1999) The "thrifty genotype" in 1998. *Nutr. Rev.*, **57**: S2-S9.

Newsholme, EA. (1980) Sounding Board. A possible metabolic basis for the control of body weight. *N. Engl. J. Med.*, **302**:400-405.

Ngwerume, F. and Mao, IL (1992) Estimation of residual energy intake for lactating cows using an animal model. *Journal of Dairy Science*, **75**:1461-1468.

Nielsen, MK. and McDonald, JM. (2006) Resumed divergent selection for heat loss in mice:selection applied and response in heat loss and feed intake.In 'Proceedings of *8th World Congress on Genetics Applied to Livestock Production, August 13-18, 2006, Belo Horizonte, MG, Brasil'.*

Nielsen, MK., Freking BA., Jones, LD., Nelson, SM., Vorderstrasse, TL., and Hussey, BA (1997b) Divergent selection for heat loss in mice. 2. Correlated responses in feed intake, body mass, body composition, and number born through fifteen generations. *Journal of Animal Science*, **75**: 1469-1476.

Nielsen, MK., Jones, LD., Freking, BA., and DeShazer, JA. (1997a) Divergent selection for heat loss in mice. 1. Selection applied and direct response through fifteen generations. *Journal of Animal Science,* **75**: 1461-1468.

Nkrumah, JD., Li, C., Yu, J., Hansen, C., Keisler, DH. and Moore, SS. (2005) Polymorphisms in the bovine leptin promoter associated with serum leptin concentration, growth, feed intake, feeding behavior, and measures of carcass merit. *J. Anim. Sci.* **83**:20–28.

Obici and Rossetti (2003) Minireview: Malonyl CoA, AMP-activated protein kinase, and adiposity. *Endocrinology*, **144**:5166-5171.

Obici, S. and Rossetti, L. (2003) Minireview: nutrient sensing and the regulation of insulin action and energy balance. *Endocrinology,* **144**:5172-5178.

Obici, S. Wang, J., Chowdury, R., Feng, Z., Siddhanta, U., Morgan, K., and Rossetti, L. (2002) Identification of a biochemical link between energy intake and energy expenditure. *J. Clin. Invest.* **109**:1599-1605.

Obregon, MJ., Calvo., R., Hernandez, A., Escobar, F., and Escobar, GM. (1996) Regulation of uncoupling protein messenger ribonucleic acid and 5' deiodinase activity by thyroid hormones in fetal brown adipose tissue. *Endocrinology,* **137**:4721-4729.

Oddy, VH. (1993) Regulation of muscle protein metabolism in sheep and lambs: nutritional, endocrine and genetic aspects. *Australian Journal of Agricultural Research*, **44**:901-913.

Oddy, VH. (1999). Genetic variation in protein metabolism and implications for variation in efficiency of growth. *Recent Advances in Animal Nutrition*, **12**:23-29.

Oddy, VH. and Owen, PC. (1996). Insulin-like growth factor-1 inhibits degradation and improves retention of protein in hind-limb muscle of lambs. *American Journal of Physiology, Endocrinology and Metabolism,* **271**:E973-E982.

Oddy, VH., Speck, PA., Warren, HM., and Wynn, PC. (1995) Protein metabolism inlambs from lines divergently selected for weaning weight. *J. Agri. Sci. Camb.*, **124**:129-137.

Okine, E. Basarab, J., Goonewardene, L. and Mir, P. (2004) Residual Feed Intake and Feed Efficiency: Differences and Implications. *Florida Ruminant Nutrition Symposium*, 27-38.

Okine, EK., Basarab, JA., Baron, V., and Price, MA. (2001) Net feed efficiency in young growing cattle: III. Relationship to methane and manure production. In *"Abstracts of Presentations and Posters". AIC2001*, University of Guelph, Guelph, Ontario N1G 2W1, July 8-11, 2001, CSAS 01-21.

Ortigues, I. (1991) Adaptation du métabolisme énergétique des ruminants à la sous-alimentation. Quantification au niveau de l'animal entier et de tissus corporels. *Reprod. Nutr. Dev.*, **31**: 593-616.

Oshima, K., Nampei, A., Matsuda, M., Iwaki, M., Fukuhara A., Hashimoto J., Yoshikawa H. and Shimomura I. (2005) Adiponectin increases bone mass by suppressing osteoclast and activating osteoblast. *Biochemical and Biophysical Research Communications,* **331**:520–526.

Pajukanta, P., Lilja, HE., and Sinsheimer, JS. (2004) Familial combined hyperlipidemia is associated with *upstream transcription factor 1 (USF1). Nature Genetics,* **36**: 371–376.

Palaiologos, G., Hertz, L. and Schousboe, A. (1989) Role of aspartate aminotransferase and mitochondrial dicarboxylate transport for release of endogenously and exogenously supplied neurotransmitter in glutamatergic neurons. *Neurochemical Research,* **14**:359-366.

Pancholi, V. (2001) Multifunctional α-enolase: its role in diseases. *Cell. Mol. Life Sci.,* **58**: 902–920.

Pattie, ME. and Kahn, BB. (2004) Nutrient sensor links obesity with diabetes risk. *Nature Medicine,* **10**:1049-1050.

Pedrioli, PG., Eng, JK., Hubley, R., Vogelzang, M., Deutsch, EW., Raught, B., Pratt, B., Nilsson, E., Angeletti, RH., Apweiler, R., Cheung, K., Costello, CE., Hermjakob, H., Huang, S., Julian, RK., Kapp, E., McComb, ME., Oliver, SG., Omenn, G., Paton, NW., Simpson, R., Smith, R., Taylor, CF., Zhu, W., and Aebersold, R. (2004) A common open representation of mass spectrometry data and its application to proteomics research. *Nature Biotechnology,* **22**:1459-1466.

Pell, JM. and Bates, PC. (1987) Colagen and non-collagen protein turnover in skeletal muscle of growth hormone-treated lambs. *J. Endocrinol.*, **115**:R1-R4.

Peng, SY., Wang, WP., Meng, J., Li, T., Zhang, H., Li, YM., Chen, P., Ma, KT. and Zhou, CY. (2005) ISL1 physically interacts with BETA2 to promote insulin gene transcriptional synergy in non-beta cells. *Biochim. Biophys. Acta.,* **1731**:154-159.

Pertsemlidis, A. and Fondon, JW. III (2001) Having a BLAST with bioinformatics (and avoiding BLASTphemy). *Genome Biol. Reviews.,* **2**: 2002.1-2002.10.

Pitchford, WS. (2004) Genetic improvement of feed efficiency of beef cattle: what lessons can be learnt from other species? *Aust. J. Experimental Agriculture. Beef CRC, special edition.* **44**:371-382.

Piwien-Pilipuk, G., Van Mater, D., Ross, SE., MacDougald, OA., Schwartz, J. (2001) Growth hormone regulates phosphorylation and function of CCAAT/enhancer-binding protein-ß by modulating Akt and glycogen synthase kinase-3. *J. Biol. Chem.*, **276**:19664-19671.

Pomp, D., Allan, MF., Jiao, Y., Gu, W., Hanford, KJ., Potts, JK., Ferrell, AD., and Eisen, EJ. Genomic architecture of feed intake and feed efficiency. *8th World Congress on Genetics Applied to Livestock Production, August 13-18, 2006, Belo Horizonte, MG, Brasil.*

Pomp, D., Zou, T., Clutter, AC., and Barendse, W. (1997) Rapid communication: Mapping of leptin to bovine chromosome 4 by linkage analysis of a PCR-based polymorphism. *J. Anim. Sci.*, **75**:1427.

Porte, D. Jr., Baskin, DG., and Schwartz MW. (2002) Leptin and insulin action in the central nervous system. *Nutr Rev.,* **60**: S20–S29.

Price, N., Jackson, V., van der Leij, F., Cameron, J., Travers, M., Bartelds, B., Huijkman, N., and Zammit, V. (2003) Cloning and expression of the liver and muscle isoforms of ovine carnitine palmitoyltransferase 1: residues within the N-terminus of the muscle isoform influence the kinetic properties of the enzyme. *Biochem. J.*, **15**; 372:871–879.

Procaccio, V., Mousson, B., Beugnot, R., Duborjal, H., Feillet, F., Putet, G., Pignot-Paintrand, I., Iombes, A., Coo, R., Smeets, H., Lunardi, J. and Issartel, J. (1999) Nuclear DNA origine of mitochondrial complex I Deficiency in fatal infantile lactic acidosis evidenced by transnuclear complementation of cultured fibroblasts. *The Journal of Clinical Investigation,* **104**:83-92.

Puigserver, P., Adelmant, G., Wu, Z., Fan, M., Xu, J., O'Malley, B., Spiegelman, B. (1999) Activation of PPARγ coactivator-1 through transcription factor docking. *Science,* **286**:1368-1371.

Puigserver, P., Wu, Z., Park, CW., Graves, R., Wright, M. and Spiegelman, BM. (1998) A cold-inducible co-activator of nuclear receptors linked to adaptive thermogenesis. *Cell,* **92**:823-839.

Puller, JD., and Webster, AJF. (1977) The energy cost of fat and protein deposition in the rat. *British Journal of Nutrition,* **12**:355-363.

Pym, RAF. and Tomas, FM. (1990) Protein turnover in chickens selected for different aspects of growth and body composition. In '*Proceedings of the Australian Poultry Science Symposium'. (Ed. D Balnave), p. 116. (University of Sydney, Sydney).*

Rabilloud, T., Strub, J., Carte, N., Luche, S., Dorselaer, AV., Lunardi, J., Giege, R. and Florentz, C. (2002) Comparative proteomics as a new tool for exploring human mitochondrial tRNA disorders. *Biochemistry,* **41**:144-150.

Rabkin, M. and Blum, JJ. (1985) Quantitative analysis of intermediary metabolism in hepatocytes incubated in the presence and absence of glucagon with a substrate mixture containing glucose, ribose, fructose, alanine and acetate. *Biochem. J.*, **225**:761-786.

Radi, R., Turrens, JF., Chang, LY., Bush, KM., Crapo, JD., and Freeman, BA (1991) Detection of catalase in rat heart mitochondria. *J. Biol. Chem.,* **266**: 22028-22034.

Raimbault, S., Dridi, S., Denjean, F., Lachuer, J., Couplan, E., Bouillaud, F., Bordas, A., Duchamp, C., Taouis, M., and Ricquier, D. (2001) An uncoupling protein homologue putatively involved in facultative muscle thermogenesis in birds. *Biochem. J.,* **353:**441–444.

Ramsden, JD., Cocks, HC., Shams, M., Nijjar, S., Watkinson, JC., Sheppard, MC., Ahmed, A., Eggo, MC. (2001) Tie-2 is expressed on thyroid follicular cells, is increased in goiter, and is regulated by thyrotropin through cyclic adenosine 3-prime,5-prime-monophosphate. *J. Clin. Endocr. Metab.,* **86**: 2709-2716.

Rasmussen, U. and Rasmussen, H. (2000) Human quadriceps muscle mitochondria: a functional characterization. *Molecular and Cellular Biochemistry,* **208**:37-44.

Rauw, WM., Luiting P., Bakken, M., Schuurman, T., de Veer, CJM., and Vangen, O. (2000) Behavioural differences in non-reproductive adult females in a long-term selection experiment for litter size in mice. *Applied Animal Behaviour Science,* **66**:249-262.

Ravussin, E. (2002) Cellular sensors of feast and famine. *J. Clin. Invest.* **109**:1537-1540.

Raybould, HE., Glatzle, J., Robin, C., Meyer, JH., Phan, T., Wong, H., and Raybould, HE., Glatzle, J., Robin, C., Meyer, JH., Phan, T., Wong, H., and Sternini, C. (2003) Expression of 5-HT3 receptors by extrinsic duodenal afferents contributes to intestinal inhibition of gastric emptying. *Am. J. Physiol. Gastrointest. Liver Physiol.,* **284**: G367-G372.

Read, ML., Clark, AR. and Docherty, K. (1993) The helix-loop-helix transcription factor USF (upstream stimulating factor) binds to a regulatory sequence of the human insulin gene enhancer. *Biochemical Journal,* **295**:233–237.

Redmond, JB., Towle, HC., and Robertson, RP. (1994) Regulation of human insulin gene transcription by glucose, epinephrine, and somatostatin. *Diabetes*, **43**:546-551.

Reeds, PJ., Burrin, DG., Davis, TA., and Stoll, B. (1998) Amino acid metabolism and the energetics of growth. *Archives of Animal Nutrition*, **51**:187-197.

Reidelberger, RD. (1994) Cholecystokinin and control of feed intake. *J. Nutr.*, **124** :1327S–1333S.

Reidelberger, RD., Arnelo, U., Granqvist, L., Permert, J. (2001) Comparitive effects of amylin and cholecystokinin on food intake and gastric emptying in rats. *Am. J. Physiol.*, **280**:R605-R611.

Reiter, AK., Bolster, DR., Crozier, SJ., Kimball, SR. and Jefferson, LS. (2005) Repression of protein synthesis and mTOR signaling in rat liver mediated by the AMPK activator aminoimidazole carboxamide ribonucleoside. *Am. J. Physiol. Endocrinol. Metab.*, **288**:E980–E988.

Richardson, EC. and Herd, RM. (2004) Biological basis for variation in residual feed intake in beef cattle. 2. Synthesis of results following divergent selection. *Australian Journal of Experimental Agriculture*, **44**:431-440.

Richardson, EC., Herd, RM., Arthur, PF., Wright, J., Xu, G., Dibley, K. and Oddy, H. (1996) Possible physiological indicators for net feed conversion efficiency. *Proceedings of the Australian Society of Animal Production,* **21**:103-106.

Richardson, EC., Herd, RM., Colditz, IG., Archer, JA., and Arthur, PF. (2002) Blood cell profiles of steer progeny from parents selected for and against residual feed intake. *Australian Journal of Experimental Agriculture*, **42**:901-908.

Richardson, EC., Herd, RM., and Oddy, VH. (2000) Variation in body composition, activity and other physiological processes and their associations with feed efficiency. In '*Feed efficiency in beef cattle. Proceedings of the feed efficiency workshop'. (Eds JA Archer, RM Herd, PF Arthur) pp. 46-50. (University of New England: Armidale, NSW).*

Richardson, EC., Herd, RM., Oddy, VH., Thompson, JM., Archer, JA., and Arthur, PF. (2001) Body composition and implications for heat production of Angus steer progeny of parents selected for or against residual feed intake. *Aust. J. Exp. Agric.* **41**:1065–1072.

Ridderstrale, M., Degerman, E. and Tornqvist, H. (1996) Growth hormone stimulates the tyrosine phosphorylation of the insulin receptor substrate-1 and its association with phosphatidylinositol 3-kinase in primary adipocytes. *J. Biol. Chem.*, **270**: 3471-4.

Robinson, DL. and Oddy, VH. (2004) Genetic parameters for feed efficiency, fatness, muscle area and feeding behaviour of feedlot finished beef cattle. *Livestock Production Science,* **90**:255-270.

Robinson, DL.; Oddy, VH.; and Smith, C. (1999) Preliminary genetic parameters for feed intake and efficiency in feedlot cattle. *Proceedings Association Advancement Animal Breeding Genetics*, **13**:492-495.

Robinson, DS., and Wing. DR. (1972) Clearing factor lipase and its role in the regulation of triglyceride utilization. Studies on the enzyme in adipose tissue. *Adv. Exp. BioZ. Med.*, **26**: 71-76.

Robinson, JB., Jr., and Srere, PA. (1985) Organization of Krebs tricarboxylic acid cycle enzymes in mitochondria. *J. Biol. Chem.*, **260**:10800-10805.

Robinson, SW., Dinulescu, DM., and Cone, R., (2000) Genetics models of obesity and energy balance in the mouse. *Annu. Rev. Genet.*, **34**:687-745.

Rolfe, DF., and Brown, GC. (1997) Cellular energy utilization and molecular origin of standard metabolic rate in mammals. *Physiol. Rev.*, **77**:731-758.

Rosenberg, M., Georges, S., Asawachaicharn, A., Analau, E., and Tapscott, S. (2006) MyoD inhibits Fstl1 and Utrn expression by inducing transcription of miR-206. *JCB*, **175**:77-85.

Rossner, S., Barkeling, B., Erlanson-Albertsson, C., Larsson, P., and Wahlin-Boll E. (1995) Intravenous enterostatin does not affect single meal food intake in man. *Appetite*, **24**:37-42.

Roy, A., Sen, S. and Chakraborti, AS. (2004) *In vitro* nonenzymatic glycation enhances the role of myoglobin as a source of oxidative stress. *Free Radic Res.*, **38(2)**:139-46.

Ruderman, N. and Prentki, M. (2004) AMP kinase and malonyl-CoA: targets for therapy of the metabolic syndrome. *Nat. Rev. Drug. Discov.*, **3**:340–351.

Ruderman, N., Saha, A., and Kraegen, E. (2003) Minireview: Malonyl CoA, AMP-activated protein kinase, and adiposity, *Endocrinology*, **144**: 5166-5171.

Ruffolo, RR. Jr. (Ed) (1987) 'The alpha-1 adrenergic receptors'. (Humana:Clifton, NJ).

Ruppert, R., Golden, B., and Hough B. (2002) Maintenance energy EPD update. *ARA magazine*, **2.**
Russell, C. and Lee W. Grotyohann. (1999) Measurement of Mitochondrial Membrane Potential Using Fluorescent Rhodamine Derivatives. *Biophys. J.*, **76**: 469-477.

Russo, D., Damante, G., Foti, D., Costante, G. Filetti, S. (1994). Different molecular mechanisms are involved in the multihormonal control of glucose transport in FRTL5 rat thyroid cells. *J. Endocrinol. Invest.*, **17**:323-327.

Russo, V., Fontanesi, L., Davoli, R., Nanni, L., Costa, Cagnazzo, M., Buttazzoni, L., Virgili R., and Yerle M. (2002) Investigation of candidate genes for meat quality in dry-cured ham production: the porcine cathepsin B (CTSB) and cystatin B (CSTB) genes. *Animal Genetics*, **33**:123.

Sabatini, DM., Erdjument-Bromage, H., Lui, M., Tempst, P., and Snyder, SH. (1994) *Cell*, **78**:35.

Saltiel AR. (2001) You are what you secrete. *Nat Med.*, **7**:887-895.

Sambrook, J., Fritsch, E., and Maniatis. T. (1989) *Molecular cloning: a laboratory manual.* Second edition. Cold Spring Harbor Laboratory Press, Cold Spring Harbor, New York, USA.

Sandelin, B., Brown, A., Brown, M., Ojano-Dirain, C. and Baublits, R. (2005) Association of mitochondrial function with feed efficiency in Angus cattle Arkansas Animal Science Report Research Series 535.

Santos, CD., Essioux, L., Teinturier, C., Tauber, M., Goffin, V., and Bougneres, P. (2004) A common polymorphism of the growth hormone receptor is associated with increased responsiveness to growth hormone. *Nature Genetics*, **36**:720-724.

Sarria, AJ., Panini, SR., and Evans, RM. (1992) *Journal of Biological Chemistry.* **267**:19455-19463.

Schemelzle, T. and Hall, M. (2000) TOR, a central controller of cell growth, *Cell,* **103**:253-262.

Schenkel, FS. , Miller, SP., Ye, X., Moore, SS., Nkrumah, JD., Li, C., Yu, J., Mandell, IB., Wilton, J. W. and Williams, JL. (2005) Association of single nucleotide polymorphisms in the leptin gene with carcass and meat quality traits of beef cattle. *J. Anim. Sci.*, **83**:2009-2020.

Schenkel, FS., Miller, SP. and Wilton, JW. (2004) Genetic parameters and breed differences for feed efficiency, growth, and body composition traits of young beef bulls. *Can. J. Anim. Sci.*, **84**:177-184.

Schmelzle, T. and Hall, MN. (2000) TOR a central controller of cell growth. *Cell,* **103**:253-262

Schwartz, MW., Woods, SC., Porte, JR. D., Seeley, RJ. and Baskin, DG. (2000) Central nervous system control of food intake. *Nature,* **406**:661- 671.

Searle, TW., Murray, JD., and Baker, PJ. (1992) Effect of increased production of growth hormone on body composition in mice: transgenic versus control. *J. Endocrinol.* **132**:285-91.

Seaton, G., Haley, C., Knott, S., Kearsey, M., and Visscher, P. (2001) QTL Express: http://qtl.cap.ed.ac.uk accessed repeatedly during December 2001 and January 2002.

Seaton, G., Hayley, C., Knott, S., and Kearsey M. (2002) QTL express: mapping quantitative trait loci in simple and complex pedigrees. *Bioinformatics*, **18**:339-340.

Shannon, K. and Rabinowitz, J. (1986) Purification and characterization of a mitochondrial isozyme of C1- tetrahydrofolate synthase from *Saccharomyces cerevisiae. J. Biol. Chem.,* **261***:* 12266-12271.

Shearer, J., Wilson, R., Battram, D., Richter, E., Robinson, D., Bakovic, M., and Graham, T. (2005) Increases in glycogenin and glycogenin mRNA accompany glycogen resynthesis in human skeletal muscle, *Am. J. Physiol. Endocrinol. Metab.,* 289: E508-E514.

Shetty, GK., Economides, PA., Horton, ES., Mantzoros, CS. and Veves, A. (2004) Circulating adiponectin and resistin levels in relation to metabolic factors, inflammatory markers, and vascular reactivity in diabetic patients and subjects at risk for diabetes. *Diabetes Care,* **27**:2450–57.

Shintani, M., Ogawa, Y., and Nakao, K. (2000) Insulin resistance, role of leptin and leptin receptor. *Nippon. Rinsho.,* **58**:327-32.

Sidis,Y., Tortoriello, D., Holmes, W., Pan, Y., Keutmann, H., and Schneyer, A. (2002) Follistatin-Related Protein and Follistatin Differentially Neutralize Endogenous Vs. exogenous actvin. *Endocrinology*, **143**:1613-1624.

Siems, W., Muller, M., Dumdey, R., Holzhutter, HG., Rathmann, J., Rapoport, SM. (1982) Quantification of pathways of glucose utilization and balance of energy metabolism of rabbit reticulocytes. *Eur. J. Biochem.,* **124**:567-576.

Simonsen, L., Bülow, J., Madsen, J., and Christensen, NJ. (1992) Thermogenic response to epinephrine in the forearm and abdominal subcutaneous adipose tissue. *Am. J. Physiol.,* **263**: E850-E855.

Sinsuke, Oh-I., Shimazu, H., Satoh, T., Okada, S., Adachi, S., Inoue, K., Eguchi, H., Yamamto, M., Imaki, T., Hashimoto, K., Tsuchiya, T., Monden, T., Horiguchi, K., Yamada, M., and Mori, M. (2006) Identification of nesfatin-1 as a satiety molecule in the hypothalamus. *Nature*, **443**:709-7112.

Smih, F., Rouet, P., Lucas, S., Mairal, A., Sengenes, C., Lafontan, M., Vaulont, S., Casado, M. and Langin, D. (2002) Transcriptional regulation of adipocyte hormone-sensitive lipase by glucose. *Diabetes,* **51**:293–300.

Smith, GP., Jerome, C., Cushin, BJ., Eterno, R., and Simansky, KJ. (1981) Abdominal vagotomy blocks the satiety effect of cholecystokinin in the rat. *Science*, **213**:1036–1037.

Smith, SJ., Cases, S., Jensen, DR., and Chen, HC. (2000) Obesity resistance and multiple mechanisms of triglycerides synthesis in mice lacking Dgat. *Nature Genetics*, **25**:87-90.

Smith, SB. and Crouse, JD. (1984) Relative contributions of acetate, lactate and glucose to lipogenesis in bovine intramuscular and subcutaneous adipose tissue. *J. Nutr.*, **114**:792-800.

Somiari, RI., Somiari, S., Russell, S., and Shriver, CD. (2005) Proteomics of breast carcinoma. *J. Chromatogr. B. Analyt. Technol. Biomed. Life Sci.,* **815**:215-225.

Stanley, S., Wynne, K., McGowan, B., and Bloom, S. (2005) Hormonal regulation of food intake. *Physiol. Rev.*, **85**:1131-1158.

Staubs, PA. (1998) Platelet-derived growth factor inhibits insulin stimulation of insulin receptor substrate-1-associated phosphatidylinositol 3-kinase in 3T3-L1 adipocytes without affecting glucose transport. *J. Biol. Chem.,* **273**: 25139-47.

Steen, H., and Mann, M. (2004) The ABC's (and XYZ's) of peptide sequencing. *Nature Reviews: Molecular Cell Biology*, **5**:699-711.

Stéphane, C., Suleau, A. and Nathalie, B. (2005) Mitochondrial translation: Elongation factor Tu is essential in fission yeast and depends on an exchange factor conserved in humans but not in budding yeast. *Genetics,* **169**:1891-1901.

Steppan, CM., Bailey, ST., Bhat, S., Brown, EJ., Banerjee, RR., Wright, CM., Patel, HR., Aahima, RS., and Lazar, MA. (2001) The hormone resistin links obesity to diabetes. *Nature*, **409**:307-312.

Sternini, C. (2003) Expression of 5-HT3 receptors by extrinsic duodenal afferents contributes to intestinal inhibition of gastric emptying. *Am. J. Physiol. Gastrointest. Liver Physio.,***284**:G367-G372,

Su, X., Burton, MB., and Gebhart, GF. (2001) Effects of octreotide on responses to colorectal distension in the rat. *Gut,* **48**:676-682.

Suttorp, N., Toepfer, W. and Roka, L. (1986) Antioxidant defense mechanisms of endothelial cells: glutathione redox cycle versus catalase. *Am J Physiol Cell Physiol.,* **251**:C671-C680.

Svendsen, M. Skipenes, P. and Mao, IL (1993) Genetic parameters in the feed conversion complex of primiparous cows in the first two trimesters. *Journal of Animal Science*, **71**:1721-1729.

Takayasu, S., Sakurai, T., Iwasaki, S., Teranishi, H., Yamanaka, A. Williams, S., Iguchi, H., Kawasawa, Y., Ikeda, Y. Sakakibara, I., Ohno, K., Ioka, R., Murakami, S., Dohmae, N., Xie, J., Suda, T., Motoike, T., Ohuchi,T., Yanagisawa, M., and Sakai, J. (2006). A neuropeptide ligand of the G protein-coupled receptor GPR103 regulates feeding, behavioural arousal, and blood pressure in mice. *PNAS*, **103**:7438-7443.

Tartaglia, LA. (1997) The leptin receptor. *J. Biol. Chem.*, **272**: 6093-6096.

Tatham, BG., Davis JJ. and Ferrier, GR. (2000) Commercial application of net feed intake assessment, biochemical relationships and economic implications of using tested Angus bulls. *Asian-Australian Journal of Animal Science*, **13** supplement A:327-330.

Taylor, St. CS., Thiessen, RB., and Murray, J. (1986) Inter-breed relationship of maintenance efficiency to milk yield in cattle. *Animal Production,* **43**:37-61.

Tessmann, NJ., Radloff, HD., Kleinmans, J., Dhiman, TR. and Statter LD. (1991) Milk Production response to dietary forage: grain ratio. *Jour. Dairy Sci.*, **74**: 2696-2707.

Thakkar JH., (1977) Oxidative phosphorylation in mitochondria from different fiber types of chicken muscles. *Physiol. Chem and Physics,* **9**:285-295.

Thomas, AW., Morgan, R., Sweeney, M., Rees, A., and Alcolado, J. (1994) The detection of mitochondrial DNA mutations using single stranded conformation polymorphism (SSCP) analysis and heteroduplex analysis, *Human Genetics*, **94**:621-623.

Thomas, MG., Enns, RM., Shirley, KL., Garcia, MD., Garrett, AJ. and Silver, GA. (2007) Associations of DNA polymorphisms in growth hormone and its transcriptional regulators with growth and carcass traits in two populations of Brangus bulls. *Genet. Mol. Res.* **6**:222-237.

Thomas, SA. and Palmiter, RD. (1997) Thermoregulatory and metabolic phenotypes of mice lacking oradrenaline and adrenaline. *Nature,* **387**:94-97.

Tixier-Boichard, M., Boichard, D., Groeneveld, E. and Bordas, A. (1995) Restricted maximum likelihood estimates of genetic parameters of adult male and adult female Rhode Island Red chickens divergently selected for residual feed consumption. *Poultry Science*, **74**:1245-1252.

Tokunaga, C., Yoshino, YI. and Yonezawa, K. (2004) mTOR integrates amino acid- and energy-sensing pathways. *Biochem. Biophys. Res. Commun.,* **313**:443–448.

Tomas, FM., Jones, LM., and Pym, RA. (1988) Rates of muscle protein breakdown in chickens selected for increased growth rate, food consumption, or efficiency of food utilisation as assessed by N-methylhistidine excretion. *British Poultry Science*, **29**:359-370.

Tomas, FM., Pym, RAE., and Johanson RJ (1991) Muscle protein turnover in chickens selected for increased growth rate, food consumption or efficiency of food utilisation: effects of genotype and relationship to plasma IGF1-1 and growth hormone. *British Poultry Science*, **32**:363-376.

Trounce, IA., Kim, YL., AS Jun, AS., and Wallace, DC. (1996) Assessment of mitochondrial oxidative phosphorylation in patient muscle biopsies, lymphoblasts, and transmitochondrial cell lines. *Methods of Enzymology,* **264**: 484-509.

Tryoen-toth, P., Richert, S., Sohm, B., Mine, M., Marsac, C., Dorselaer, AV., Leize, E., and Florentz, C. (2003) Proteiomics as a new tool for exploring human mitochondrial tRNA mutation beyond the frame of mitochondrial translation. *The Journal of Biological Chemistry,* **278**:24314-24323.

Tso, P, Liu, M., Kalogeris, TJ. and Thomson, ABR. (2001) The role of apolipoprotein A-IV in the regulation of food intake. *Ann. Rev. Nutr.*, **21**:231-254.

Tsutomu, H., Mami, H., Nonaka, E., Kasuya, M., Hiroshi, H. and Kenji, K. (2005) Effects of ghrelin on growth hormone secretion *in vivo* in ruminants, **126**:61-65.

Tuiskula-Haavisto, M., Honkatukia, M., Vilkki, J., de Koning, DJ., Schulman, NF., and Maki-Tanila, A. (2002) Mapping of quantitative trait loci affecting quality and production traits in egg layers. *Poult. Sci.*, **81**:919–927.

Turrens, JF. (2003) Mitochondrial formation of reactive oxygen species. *J. Physiol.*, **552**:335–344.

Uhe, AM., Szmukler, GI., Colier, GR., Hansky, J., O'Dea, K., and Young, GP. (1992) Potential regulators of feeding behaviour in anorexia nervosa. *Am. J. Clin. Nutr.* **55**: 28-32.

Uneo, N., Inui, A., Iwamoto, M., Kaga, T., and Asakawa, A. (1999) Decreased food intake and body weight in pancreatic polypeptide-overexpressing mice. *Gastroenterology*, **117**:1427-1432.
Van Arendonk, JAM, Nieuwhof, GJ., Vos, H., and Korver, S (1991) Genetic aspects of feed intake and efficiency in lactating dairy heifers. *Livestock Production Science*, **29**:263-275.

Van Kaam, J., Groenen, MAM., Bovenhuis, H., Veenendaal, A., Vereijken, ALJ., and van Arendonk, JAM (1999) Whole genome scan in chickens for quantitative trait loci affecting growth and feed efficiency. *Poultry Science*, **78(1)**:15-23.

Van, VF., Crabeel, M., Boyen, A., Tricot, C., Stalon, V., Falmagne, P., Nakamura, Y., Baumberg, S., Glansdorff, N. (1990) Sequences of the genes encoding argininosuccinate synthetase in Escherichia coli and Saccharomyces cerevisiae: comparison with methanogenic archaebacteria and mammals. *Genes*, **95**:99-104 .

Veerkamp, RF., Emmans, GC., Cromie, AR. and Simm, G. (1995) Variance components for residual feed intake in dairy cows. *Livestock Production Science*, **41**:111-120.

Verbalis, J., Blackburn, R., Hoffman, G., and Stricker, E. (1995) Establishing behavioural and physiological functions of central oxytocin: insights from studies from oxytocin and ingestive behaviour. *Adv. Exp. Med. Biol.*, **395**:209-225.

Verma, M., Kagan, J., Sidransky, D. and Srivastava, S. (2003) Proteomics analysis of cancer-cell mitochondria. *Nature Reviews,* **3**:789-795.

Vézina, F. and Williams, TD. (2005) Interaction between organ mass and citrate synthase activity as an indicator of tissue maximal oxidative capacity in breeding European Starlings: implications for metabolic rate and organ mass relationships. *Functional Ecology,***19**:119–128.

Vincent, A. and Feldman, E. (2002) Control of cell survival by IGF1 signaling pathways, *Growth Hormone and IGF Research*, **12**:193-197.

Von Felde, A., Roehe, R., Looft, H. and Kalm, E. (1996) Genetic association between feed intake and feed intake behaviour at different stages of growth of group-housed boars. *Livestock Production Science*, **47**:11-22.

Vykoukalová, Z., Knoll, A., Dvořák, J., Čepica, S. (2006) New SNPs in the *IGF2* gene and association between this gene and back fat thickness and lean meat content in Large White pigs. *Journal of Animal Breeding and Genetics*, **123:** 204–207.

Walker, J., Arizmendi, J., Dupuis, A., Fearnley, I., Finel, M., Medd, S., Pilkington, S., Runswick, M., and Skehel, M. (1992) Sequences of 20 subunits of NADH: Ubiquinone oxidoreductase from bovine heart mitochondria: Application of a novel strategy for sequencing proteins using the polymerase chain reaction. *Journal of Molecular Biology*, **226**:1051-1072.

Wang, D. and Sul, HS. (1997) Upstream stimulatory factor binding to the E-box at –65 is required for insulin regulation of the fatty acid synthase promoter. *Journal of Biological Chemistry* , **272**:26367–74.

Wang, J., Liu, R., Hawkins, M., Barzilai, N., and Rossetti, LA. (1998) A nutrient-sensing pathway regulates leptin gene expression in muscle and fat. *Nature*, **393**:684-688.

Watanbe, Y., Tsukada, T., Notake, M., Nankanishi, S., and Numa, S. (1982) Structural analysis of repetitive DNA sequences in the bovine cortico-tropin-beta-lipotropin precursor gene region. *Nucleic Acids Res.*, **10**:1459-1469.

Waterlow, JC. (1984) Protein turnover with special reference to man. *J. Exp. Physiol.*, **69**: 409–438.

Watkins, P., Chen, W., Harris, C., Hoefler, G., Hoefler, S., Blake, D., Balfe, A., Kelley, R., Moser, A. and Beard, M. (1989) Peroxisomal bifunctional enzyme deficiency. *Clin Invest.* **83**:771–777.

Weaver, RF. (2002) General transcription factors in eukaryotes. In: *Molecular Biology (Ed. by R.F. Weaver), McGraw-Hill Education, New York, pp. 308–309.*

Webb, AJ. and King, JWB. (1983) Selection for improved feed conversion ratio on ad libitum group feeding in pigs. *Animal Production*, **37**:375-385.

Webster, AJF. (1980) The energetic efficiency of growth. *Livestock Production Science*, **7**:243-252.

Wei, YH. (1998) Oxidative stress and mitochondrial DNA mutations in human aging. *Proc. Soc. Exp. Biol. Med.*, **217**:53-63.

Weller, JI., Song, JZ., Heyen, DW., Lewin, HA. and Ron, M. (1998) A new approach to the problem of multiple comparisons in the genetic dissection of complex traits. *Genetics,* **150**:1699-1706.

Wen, GJ., Gareth, W., Anthony, DJ., Lars, H., and Robert, EM. (2006) Angiomotin and angiomotin like proteins, their expression and correlation with angiogenesis and clinical outcome in human breast cancer. **6**:16.

West, JW., Haydon, KD., Mullinix, BG., and Sandifer, TG. (1992) Dietary cation-anion balance and cation source effects on production and acid-base status of heat-stressed cows. *Jour. Dairy Sci.*, **75**: 2776-2786.

Wong, A., and Cortopassi, GA. (2002) High-throughput measurement of mitochondrial membrane potential in a neural cell line using a fluorescence plate reader. *Biochem. Biophys. Res. Commun.*, **15**:750-754.

Woods, SC. and Seeley, RJ. (2000) Adiposity signals and the control of energy homeostasis. *Nutr.* **16**:894-902.

Wray-Cahen, D., Bell, AW., Boyd, RD., Ross, DA., Bauman, DE., Krick, BJ., and Harrell, RJ. (1995) Nutrient uptake by the hindlimb of growing pigs treated with porcine somatotropin and insulin. *J. Nutr.*, **125**:125-135.

Wren, AM., Small, CJ., Abbott, CR., Dhillo, WS., Seal, LJ., Cohen, MA., Batterham, RL., Taheri, S., Stanley, SA., Ghatei, MA., Bloom, SR. (2001) Ghrelin causes hyperphagia and obesity in rats. *Diabetes*, **50**:2540-2547.

Wu, X. (2003) Involvement of AMP-activated protein kinase in glucose uptake stimulated by the globular domain of adiponectin in primary rat adipocytes. *Diabetes*, **52**:1355-1363.

Wu, X., Cooper, RS., Borecki, I., Hanis, C., Bray, M., Lewis, CE., Zhu, X., Kan, D., Luke, A. and Curb, D. (2002) A combined analysis of genomewide linkage scans for body mass index from the National Heart, Lung and Blood Institute Family Blood Pressure Program. *American Journal of Human Genetics* **70**:1247–56.

Xu, AW., Kaelin, C.,Takeda, K., Akira, S., Schwartz, M., and Barsh' G. (2005) PI3K integrates the action of insulin and leptin on hypothalamic neurons. *J. Clin. Invest.*, **115**:951-958.

Xue, B. and Kahn, B. (2006) AMPK integrates nutrient and hormonal signals to regulate food intake and energy balance through effects in the hypothalamus and peripheral tissues. *J. Physiol.*, **574.1**:73-83.

Yamauchi, T., Kamo, J., Minokoshi, Y., Ito, Y., Waki, H., and Uchida, S. (2002) Adiponectin stimulates glucose utilization and fatty-acid oxidation by activating AMP-activated protein kinase. *Nat Med,* **8**: 1288–1295.

Yan, L., Levine, R. L. and Sohal, R. S. (1997) Oxidative damage during aging targets mitochondrial aconitase. *Biochemistry,* **94**:11168- 11172.

Yannakoulia, M., Yiannakouris, N., Blüher, S., Matalas, A., Klimis-Zacas, D. and Mantzoros, C.S. (2003) Body fat mass and macronutrient intake in relation to circulating soluble leptin receptor, free leptin index, adiponectin, and resistin concentrations in healthy humans. *Journal of Clinical Endocrinology and Metabolism,* **88**:1730–36.

Yu, YT., Breitbart, RE., Smoot, LB., Lee, Y., Mahdavi, V. and Nadal-Ginard, B. (1992) Human myocyte-specific enhancer factor 2 comprises a group of tissue-restricted MADS box transcription factors. *Genes and Development*, **6**:1783–98.

Zhang, Y., Proenca, R., Maffei, M., Barone, M., Leopold, L., and Friedman, JM. (1994) Positional cloning of the mouse obese gene and its human homologue. *Nature,* **372**: 425–432.

Zhou, YT., Shimabukuru, M., Koyama, Y., Lee, Y., Wang, MY., Trieu, F., Newgard, CB., and Unger, RH. (1997) Induction by leptin of uncoupling protein-2 and enzymes of fatty acid oxidation, *Proc. Nat. Acad. Sci.* **94**:6386-6390.

Zylicz, M., King, FW. and Wawrzynow, A. (2001) Hsp70 interactions with the p53 tumour suppressor protein. *EMBO J.*, **20**:4634-4638.